# Electrochemical Society

# GLC ANODE CUSTOMERS NOW BENEFIT FROM THE RESULTS OF OUR RESEARCH

As suppliers to major chlor-alkali producers here and abroad, it is part of our responsibility to employ the most modern research and development techniques in the constant improvement of GLC anode quality.

Our customers are now reaping the rewards of past explorations in terms of economical performance markedly superior to the standards of yesteryear.

**Electrolytic cell operators, from their own experience, are becoming increasingly aware of the superior performance of GLC custom made anodes—a superiority that becomes even more marked at high current densities.**

Our special anode production and research facilities have as their goal still better quality and higher performance characteristics for the GLC anodes of the future. In this way we hope to merit an increasingly important role in our partnership in your progress.

PRODUCTS YOU CAN TRUST
GLC
DIVISION

**GREAT LAKES CARBON CORPORATION**

18 EAST 48TH STREET, NEW YORK 17, N. Y. OFFICES IN PRINCIPAL CITIES

## EDITORIAL STAFF

**H. H. Uhlig,** Chairman, Publication Committee

**Cecil V. King,** Editor

**Norman Hackerman,** Technical Editor

**Ruth G. Sterns,** Managing Editor

**U. B. Thomas,** News Editor

**H. W. Salzberg,** Book Review Editor

**Natalie Michalski,** Assistant Editor

### DIVISIONAL EDITORS

**W. C. Vosburgh,** Battery

**Milton Stern,** Corrosion, I

**R. T. Foley,** Corrosion, II

**T. D. Callinan,** Electric Insulation

**Seymour Senderoff,** Electrodeposition

**H. C. Froelich,** Electronics, I

**Ephraim Banks,** Electronics, II

**Ernest Paskell,** Electronics—Semiconductors

**Sherlock Swann, Jr.,** Electro-Organic, I

**Stanley Wawzonek,** Electro-Organic, II

**John M. Blocher, Jr.,** Electrothermics and Metallurgy, I

**A. U. Seybolt,** Electrothermics and Metallurgy, II

**N. J. Johnson,** Industrial Electrolytic

**C. W. Tobias,** Theoretical Electrochemistry, I

**A. J. deBethune,** Theoretical Electrochemistry, II

### ADVERTISING OFFICE

**ECS**

1860 Broadway, New York 23, N. Y.

### ECS OFFICERS

**R. A. Schaefer,** President
The Bunting Brass and Bronze Co.,
Toledo, Ohio

**Henry B. Linford,** Vice-President
Columbia University, New York, N. Y.

**F. L. LaQue,** Vice-President
International Nickel Co., Inc.,
New York, N. Y.

**W. J. Hamer,** Vice-President
National Bureau of Standards,
Washington, D. C.

**Lyle I. Gilbertson,** Treasurer
Air Reduction Co., Murray Hill, N. J.

**I. E. Campbell,** Secretary
National Steel Corp., Weirton, W. Va.

**Robert K. Shannon,** Executive Secretary
National Headquarters, The ECS,
1860 Broadway, New York 23, N. Y.


Manuscripts submitted to the Journal should be sent, in triplicate, to the Editorial Office at 1860 Broadway, New York 23, N. Y. They should conform to the Instructions to Authors, last published in the Sept. 1960 issue, pp. 239C-230C. Manuscripts so submitted become the property of The Electrochemical Society and may not be published elsewhere, in whole or in part, unless permission is requested of and granted by the Editor.

Inquiries re positive microfilm copies for volumes should be addressed to University Microfilms, Inc., 313 N. First St., Ann Arbor, Mich.

The Electrochemical Society does not maintain a supply of reprints of papers appearing in its Journal. A photoprint copy of any particular paper, however, may be obtained by corresponding directly with the Engineering Societies Library, 29 W. 39 St., New York 18, N. Y.


# Journal of the Electrochemical Society

**OCTOBER 1960** **VOL. 107 • NO. 10**


## CONTENTS


### Editorial

Federal Aid for School Construction ..... 234C

### Technical Papers

Separation of the Defect Concentration and Diffusion Coefficient in Diffusion-Limited Scaling Reactions. *A. J. Rosenberg* 795

The Electrical Properties of Some Natural Waxes. *T. D. Callinan and A. M. Parks* ..... 799

Factors Influencing the Luminescent Emission States of the Rare Earths. *L. G. Van Uitert* ..... 803

Electroluminescence—A Disorder Phenomenon. *D. W. G. Ballentyne* ..... 807

On the Mechanism of Chemically Etching Germanium and Silicon. *D. R. Turner* ..... 810

Preparation of Boron by Fused Salt Electrolysis. *N. P. Nies* ..... 817

Catalytic Activity and Electronic Structure of Rhodium-Palladium-Hydrogen Cathodes in Acid Solution. *J. P. Hoare* ..... 820

Fused Salt Polarography Using a Dropping Bismuth Cathode. *R. J. Heus and J. J. Egan* ..... 824

Irreversible Thermodynamics in Electrochemistry. *A. J. deBethune* ..... 829

Entropy of the Moving Cuprous Ion in Molten Cuprous Chloride from Thermogalvanic Potentials. *A. R. Nichols, Jr., and C. T. Langford* ..... 842

Cathodic Processes on Passive Zirconium. *R. E. Meyer* ..... 847

### Technical Note

Crystallographic Data on Beta-$Sr_2P_2O_7$. *C. W. W. Hoffman and R. W. Mooney* ..... 854

### Technical Review

The Structure and Relaxation of Dielectrics *C. P. Smyth* ..... 855

**Current Affairs** ..... 239C-246C



Published monthly by The Electrochemical Society, Inc., from Manchester, N. H., **Executive Offices, Editorial Office** and **Circulation Dept.,** and **Advertising Office** at 1860 Broadway, New York 23, N. Y., combining the JOURNAL and TRANSACTIONS OF THE ELECTROCHEMICAL SOCIETY. Statements and opinions given in articles and papers in the JOURNAL OF THE ELECTROCHEMICAL SOCIETY are those of the contributors, and The Electrochemical Society assumes no responsibility for them. Nondeductible subscription to members $5.00; subscription to nonmembers $18.00. Single copies $1.25 to members, $1.75 to nonmembers.


Copyright 1960 by The Electrochemical Society, Inc.


Entered as second-class matter at the Post Office at Manchester, N. H., under the act of August 24, 1912.

One of a series

# New Light on a Compound Semiconductor

**Pictured is a new and unusual transistor . . . made from a *compound* semiconductor. Its electronic properties are greatly affected by *light*. It is a *field-effect* transistor having input impedances up to 100 megohms (versus 1,000 ohms for junction transistors). Its unique combination of properties has enabled it to perform some novel circuit functions not possible with other transistors.**

**Still in the early experimental stage, this phototransistor is a tangible result of the General Motors Research Laboratories' program on semiconductors — particularly the group II-VI compound, cadmium sulfide. Behind its development lies the steady accumulation of (1) know-how in crystal growing, doping, and contact preparation and (2) information about CdS's intriguing solid state properties (red or green luminescence, high photoconductivity, short relaxation times, etc.).**

**For the researcher, this three-terminal device is adding a new dimension to the fundamental understanding of semiconductors. For instance: GM Research scientists have uncovered the important role of photo-generated holes in modulating the conductance of this intrinsic semiconductor and have determined the hole drift mobility through a new theoretical analysis.**

**These semiconductor investigations illustrate the dual aim of GM Research: contributions to the science, advances in the technology of important new subject areas. Such research is the initial step in General Motors' continuing quest for "more and better things for more people."**

## General Motors Research Laboratories

Warren, Michigan

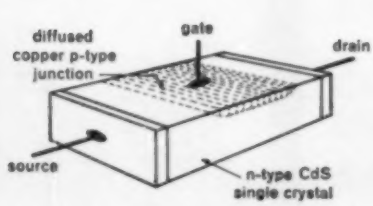


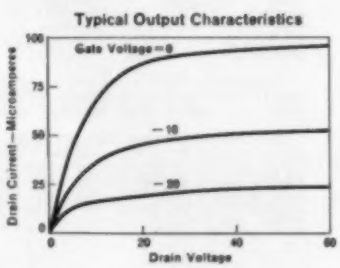

# how do you look at ANODES?

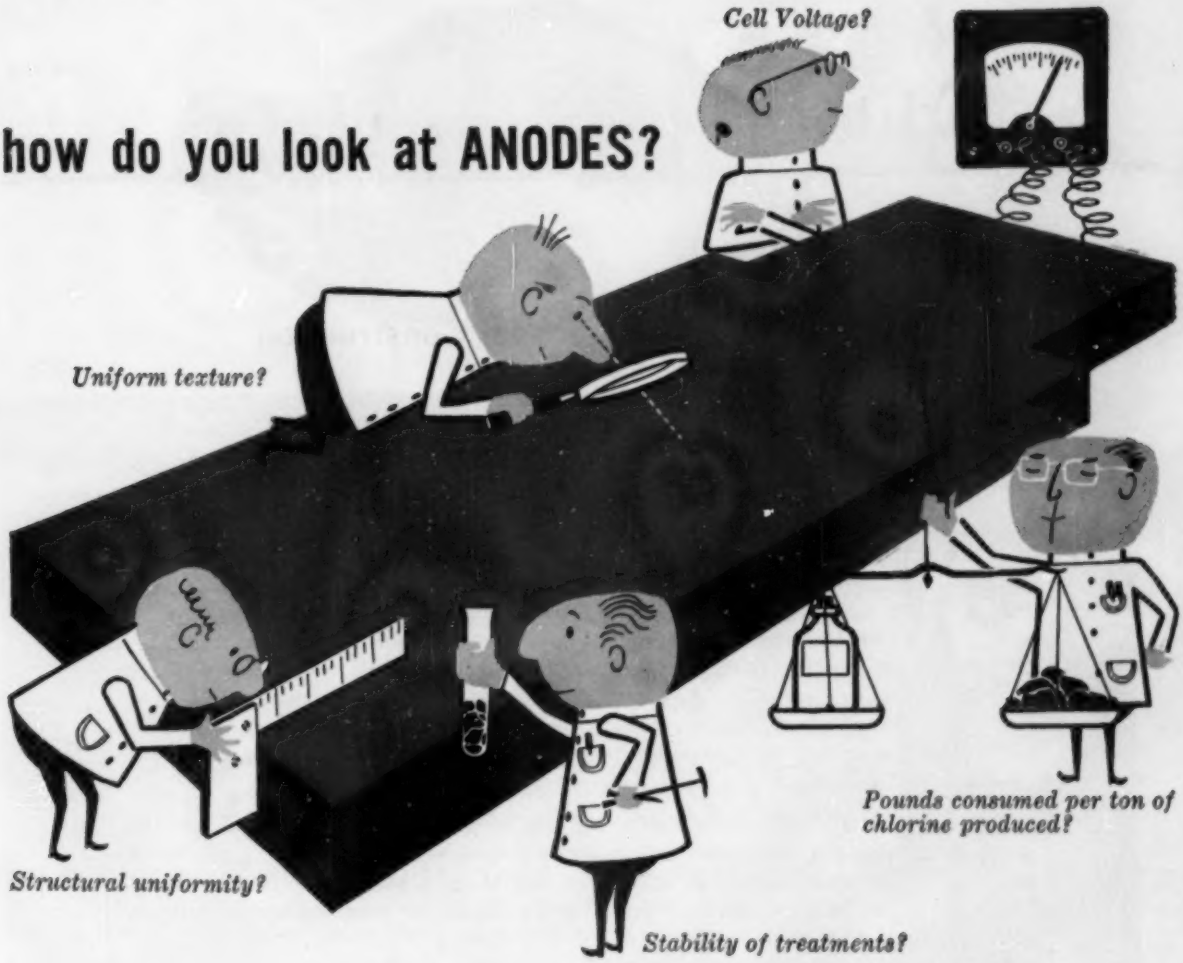


*Judged by Cell Maintenance Costs Alone,*

the highly stable impregnants used in Stackpole GraphAnode reduce diaphragm clogging to a bare minimum. The graphite is consumed slowly and evenly. Because GraphAnode anodes present uniform, low-porosity surfaces to the electrolyte, the graphite does not slough off to clog the diaphragm or to contaminate the cell.

*Judged by Anode Cost and Performance,*

Stackpole GraphAnode proves second to none whether you figure in terms of anode life, or in tons of chlorine produced per pound of graphite consumed. You get maximum anode life . . . and with the added advantage of low cell voltages. Stackpole engineers stand ready to offer a convincing demonstration on your equipment.

Stackpole Carbon Company, St. Marys, Pa.

**STACKPOLE**
**GraphAnode®**

ELECTROCHEMICAL ANODES FOR DIAPHRAGM, MERCURY, MANGANESE DIOXIDE, & SODIUM CHLORATE CELLS. OTHER TYPES FOR CATHODIC PICKLING, ALUMINUM ANODIZING, AND OTHER USES.

CATHODIC PROTECTION ANODES • FLUXING & DE-GASSING TUBES • SALT BATH RECTIFICATION RODS • ROCKET NOZZLES • RISER RODS • GRAPHITE BEARINGS & SEAL RINGS • ELECTRODES & HEATING ELEMENTS • WELDING CARBONS • VOLTAGE REGULATOR DISCS • "CERAMAGNET"® CERAMIC MAGNETS • ELECTRICAL CONTACTS • BRUSHES for all rotating electrical equipment • and many other carbon, graphite and electronic components.

# Editorial

## Federal Aid for School Construction

*FOR* several years, the National Congress has debated the advisability of appropriating funds to aid in the construction of new schools. Before the July recess, a bill came close to adoption. After Congress reconvened, there was so much unfinished business that the school bill has probably been laid aside until 1961.

The debate has been spurred by the unprecedented number of children and the presumed inability of local communities to finance enough new schools. Everyone agrees that the nation as a whole is wealthy enough to provide excellent education for all its children. In fact, in these days of international competition and threats, it is almost imperative that all young people receive as much schooling as possible, and that the most capable ones continue with higher education with a view to entering professional careers. The Federal Government is already supporting higher education in various ways. Should it now collect taxes and feed them back to the States to aid the elementary and secondary school system, or can the States and local communities do better without such paternal aide?

One editor says: Adequate money for new schools . . . can only come from Washington. Someone else estimates: There is now a nation-wide shortage of 140,000 classrooms. On the other hand, an official of the U. S. Chamber of Commerce says: Throughout the 1950's, classrooms have been built almost twice as fast as enrollment has increased; during the 1960's enrollment will drop. Evidently, there is much disagreement as to actual needs. We all know cases of inadequate, over-age, dilapidated schools, over-crowded classes, double sessions. Is this because of a real shortage of ability and wealth in the community, or is it because the officials, and the taxpayers, are reluctant and unwilling?

Let us cite the case of one rapidly growing community. During the last 20 years, taxes (in dollars) have been increased as much as 650% on residential properties (which received only normal maintenance). Much of the increase has been for schools; in fact 11 tax points out of 15 are, at present, for the school budget. The community still does not have its own high school. and must build, equip, and staff one soon. Should Federal funds be made available, for the construction at least?—Actually, the residents are well able to find the necessary funds themselves; true, a few more elderly people may be forced out of the homes where they have spent most of their lives. There are, no doubt, many communities in much less favorable positions.

Many people would favor federal financing of new schools and even of teachers' salaries, if they could be assured that this would be no entering wedge for Federal control or enforced standardization in any form. On the other hand, the Government has been accused of far too lax control in handing out funds for worthy purposes, recently and notably in the present long-range highway construction program.

If Government *must* become entangled in the financing of the public school system, it would seem more realistic to undertake a much less ambitious program of making small grants and low-interest loans to needy communities, after careful investigation by a committee of truly high standards, such as the Conant Committee.

—CVK

Sylvania CR-407 phosphor, a totally new phosphor, offers outstanding characteristics in adherence, contamination, and ion burn resistance, and brightness that promise to put a new glitter in your TV picture tube quality.

One long-sought-after characteristic, superior adherence during the rewetting cycle, has been developed into this new phosphor. Sylvania CR-407 phosphor offers up to 20% better adherence than any phosphor now commercially available.

Another reason: Sylvania CR-407 phosphor provides greater contamination resistance than phosphors available in production quantities.

Advances like these are common at Sylvania. The Chemical & Metallurgical Division is fully equipped to provide extensive engineering research in a wide variety of technological areas. We are continually seeking new and better materials to help you make a better, more stable and salable product. For additional information on Sylvania CR-407 phosphor, write Chemical & Metallurgical Division, Sylvania Electric Products Inc., Towanda, Pennsylvania.

# SYLVANIA

*Subsidiary of* **GENERAL TELEPHONE & ELECTRONICS**

# The SARGENT Model XV
# RECORDING POLAROGRAPH®

*offers you—*

- **FULL 10 INCH CHART**
- **1/10% ACCURACY OF MEASUREMENT**
- **TEN STANDARDIZED POLARIZING RANGES**

This new Sargent Polarograph gives you a large 250 mm (10 inches) chart and the highest accuracy and current sensitivity at the lowest price of any pen writing polarographic instrument on the market.

It offers you optimum specifications based on over twenty years of leadership in design, manufacture and service in this specialized field of analysis.

The polarographic method is capable of reproducibility to 1/10% and analytical accuracy to ½%. To make use of this facility, the instrument must be accurate to 1/10% and chart space must be provided for recording large steps to achieve measuring precision. We strongly advise against the purchase of any polarographic instrument using miniature (5 inch) charts and low gain balancing systems in the 1% order of precision.

This Model XV is adaptable to $10^{-4}$ M determinations with the S-29315 Micro Range Extender

®Registered Trade Mark (Pat. No. 2,931,964)

| | |
|---|---|
| **Current Ranges:** | 19, from .003 to 1.0 μA/mm. |
| **Current Sensitivity:** | standard specifications, $10^{-2}$μA/mm. |
| **Polarizing Ranges, volts:** | 0 to −1; −1 to −2; −2 to −3; −3 to −4; +.5 to −5; 0 to −2; −2 to −4; +1 to −1; 0 to −3; +1.5 to −1.5. |
| **Balancing Speed:** | standard, 10 seconds; 1 second or 4 seconds optional. |
| **Bridge Drive:** | synchronous, continuous repeating, reversible; rotation time, 10 minutes. |
| **Chart Scale:** | current axis, 250 mm; voltage axis, 10 inches equals one bridge revolution. |
| **Current Accuracy:** | 1/10% |
| **Voltage Accuracy:** | ¼% |
| **Chart Drive:** | synchronous, 1 inch per minute standard; other speeds optional. |
| **Writing Plate:** | 10½ x 12½ inches; angle of slope, 30°. |
| **Standardization:** | manual against internal cadmium sulfate standard cell for both current and voltage. |
| **Damping:** | RC, four stage. |
| **Pen:** | ball point; Leroy type optional. |
| **Suppression:** | zero displacement control, mercury cell powered, 6 times chart width, upscale or downscale. |
| **Potentiometric Range:** | 2.5 millivolts, usable as general potentiometric recorder. |
| **Finish:** | case, enameled steel; panels, anodized aluminum; writing plate, polished stainless steel; knobs and dials, chromium plated and buffed. |
| **Dimensions:** | 23 x 17 x 10. |
| **Net Weight:** | 65 pounds. |

Catalog number **S-29310** with accessories and supplies. . . . **$1585.00**

***For complete information write for Sargent Bulletin P***

**SARGENT** *SCIENTIFIC LABORATORY INSTRUMENTS • APPARATUS • SUPPLIES • CHEMICALS*

E. H. SARGENT & CO., 4647 W. FOSTER, CHICAGO 30, ILLINOIS
DETROIT 4, MICH. • DALLAS 35, TEXAS • BIRMINGHAM 4, ALA. • SPRINGFIELD, N.J.

# FUTURE MEETINGS OF
# The Electrochemical Society

**Houston, Texas, October 9, 10, 11, 12, and 13, 1960**

**Headquarters at the Shamrock Hilton Hotel**
**Sessions will be held on**
**Batteries, Corrosion, Electrodeposition,**
**Electrodeposition—Electrothermics & Metallurgy**
**Joint Symposium on Vapor Deposited Coatings,**
**Electronics (Semiconductors),**
**and Electrothermics and Metallurgy**

★ ★ ★

**Indianapolis, Ind., April 30, May 1, 2, 3, and 4, 1961**

**Headquarters at the Claypool Hotel**
**Sessions probably will be scheduled on**
**Electric Insulation, Electronics (including Luminescence and Semiconductors), Electrothermics and Metallurgy,**
**Industrial Electrolytics, and Theoretical Electrochemistry**

★ ★ ★

**Detroit, Mich., October 1, 2, 3, 4, and 5, 1961**

**Headquarters at the Statler Hotel**

★ ★ ★

**Los Angeles, Calif., May 6, 7, 8, 9, and 10, 1962**

**Headquarters at the Statler Hilton Hotel**

★ ★ ★

**Boston, Mass., September 16, 17, 18, 19, and 20, 1962**

**Headquarters at the Statler Hilton Hotel**

Papers are now being solicited for the meeting to be held in Indianapolis, Ind., April 30-May 4, 1961. Triplicate copies of each abstract *(not exceeding 75 words in length)* are due at Society Headquarters, 1860 Broadway, New York 23, N. Y., *not later than January 2, 1961* in order to be included in the program. *Please indicate on abstract for which Division's symposium the paper is to be scheduled, and underline the name of the author who will present the paper.* Complete manuscripts should be sent in triplicate to the Managing Editor of the JOURNAL at 1860 Broadway, New York 23, N. Y.

Presentation of a paper at a technical meeting of the Society does not guarantee publication in the JOURNAL. However, all papers so presented become the property of The Electrochemical Society, and may not be published elsewhere, either in whole or in part, unless permission for release is requested of and granted by the Editor. Papers already published elsewhere, or submitted for publication elsewhere, are not acceptable for oral presentation except on invitation by a Divisional program Chairman.

# ANACONDA "PLUS-4"

phosphorized copper anodes

in a new form

# CURVED ANODES

## for plating cylinders faster and more uniformly

To make anode surfaces parallel the rotogravure cylinder being plated, and to fit the curve of the current-carrying slings, Anaconda "Plus-4" phosphorized copper anodes are now extruded to precisely curved shapes.

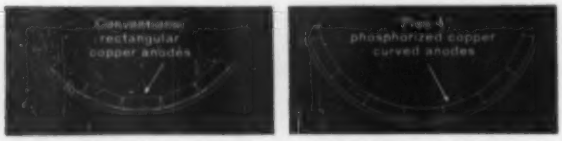


This design offers possible cost savings and improved cylinder quality.

It is reported that very uniform deposits are obtained from these specially shaped anodes, thus helping to cut finishing costs. The solution of the anode is also more uniform, thereby reducing the scrap.

**For more information,** write: Anaconda American Brass Company, Waterbury 20, Conn. In Canada: Anaconda American Brass Ltd., New Toronto, Ont. 6610B

**NO EXTRA DIE COST**
Simply specify inside radius of anode.

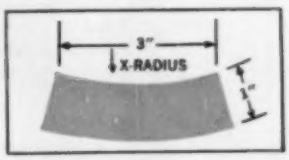


"Plus-4"® phosphorized copper anodes

**ANACONDA®**

Anaconda American Brass Company

# Separation of the Defect Concentration and Diffusion Coefficient in Diffusion-Limited Scaling Reactions[1]

**Arthur J. Rosenburg**[2]

*Lincoln Laboratory, Massachusetts Institute of Technology, Lexington, Massachusetts*

ABSTRACT

In diffusion-limited scaling reactions the rate constant is proportional to the quantity $DC_o$, where $D$ and $C_o$ are the diffusion coefficient and the solubility of the defect whose motion through the growing scale is essential to continued reaction. In order to separate $D$ and $C_o$, recourse is usually made to an independent measurement of one or the other, which is a difficult and frequently unreliable procedure. A new technique is proposed which permits the accurate and simultaneous determination of $D$ and $C_o$ from reaction rates alone. The method is based on the controlled interruption of a scaling reaction and possesses a rigorous internal check. It is applicable in principle to any such reaction, and the necessary mathematical formulation is presented in a convenient analytical form. Conventional experimental techniques can be used when $C_o >> 10^{17}$ cm$^{-3}$. The treatment is illustrated for the oxidation of InSb.

In diffusion-limited scaling reactions, of which the oxidation of metals provides the most familiar examples, direct contact of the reactants is prevented by the formation of a protective scale at the reaction interface. Once such a scale is formed, continued reaction is made possible by the motion of atomic defects through it. Thus, in the oxidation of a metal surface

$$yM + \frac{z}{2} O_2 = M_yO_z \qquad [1]$$

the formation of a nonporous film of $M_yO_z$ on the surface prevents direct access of the oxygen to the underlying metal, but the diffusion of metal or oxygen defects, interstitial atoms or lattice vacancies, charged or uncharged, through the film lets the reaction proceed. One such defect predominates in a given oxide, and the rate at which the film continues to grow is given by (1, 2)

$$dX/dt = k\,X^{-s} \quad k = \Omega D(C_o - C_i) \qquad [2]$$

where $C_o$ is the equilibrium concentration of the defect at the interface where it originates, and $C_i$ is the equilibrium concentration at the interface where the reaction is completed. $D$ is the diffusion coefficient of the defect and is assumed to be independent of concentration. $X$ is the film thickness, and $\Omega$ is the increase in the volume of the film which occurs when one defect completes its reaction.[3] Equation [2] assumes that space-charge effects at the boundaries of the oxide can be neglected. This is always the case for uncharged defects, and holds for charged defects when $X >> (\kappa\, kT/8\pi e^2 C_o)^{1/2}$ where $\kappa$ is the dielectric constant of the oxide (usually $\sim 10$), $e$ is the electronic charge, and the other symbols have their usual meanings.

Upon integration Eq. [2] gives the familiar parabolic growth law

$$X^2 = 2kt \qquad [3]$$

It applies in principle to all reactions which are controlled by the diffusion of defects through a scale which deposits at the interface between the reactants. The reactants may be solids, liquids, or gases, and the scale may be solid or liquid, but solid scales at gas-solid, gas-liquid, liquid-solid, or liquid-liquid interfaces are most frequently encountered.

Since $C_o$ is generally much larger than $C_i$, and $\Omega$ is usually known, measurements of the parabolic rate constant $k$ give the product $DC_o$ directly. By itself, however, this quantity is of little theoretical value. In order to separate $D$ and $C_o$, which have fundamental significance, independent measurements of $D$ or $C_o$ are required. These measurements are not only very difficult to make but are inconclusive unless differences in sample structure and purity are demonstrably negligible.

It is the purpose of this article to discuss a simple experimental method for simultaneously determining the quantities $D$ and $C_o$. The method uses reaction rate measurements only and is applicable in principle to any scaling reaction described by Eq. [2].

## Theory of Interrupted Kinetics of Diffusion-Controlled Scale Formation

We shall consider the generalized reaction

$$aA + bB = S \qquad [4]$$

where the product S forms a flat, nonporous scale which separates the reservoirs containing A and B. It is assumed that a defect enters the A/S interface ($x = 0$) and diffuses to the S/B interface ($x = X$) where it completes the reaction with B causing an increase, $\Omega$, in the volume of the scale. Since the

[1] The work reported in this paper was performed at Lincoln Laboratory, a center for research operated by Massachusetts Institute of Technology with the joint support of the U. S. Army, Navy, and Air Force.

[2] Present address: Materials Research Division, TYCO Incorporated, Waltham, Mass.

[3] If, for instance, the defect is a metal atom, $\Omega$ is $1/y$ times the volume of an $M_yO_z$ molecule.

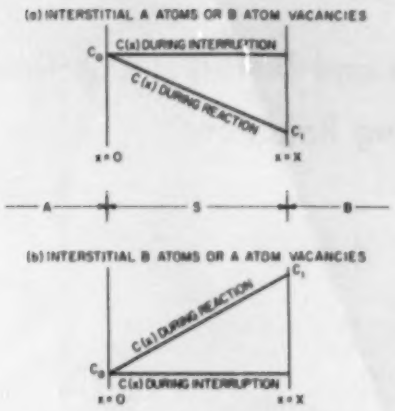


Fig. 1. Concentration of defects in a scale (S) interposed between A and B during the reaction $aA + bB = S$. In each case it is assumed that the supply of B can be interrupted while that of A is held constant.

diffusion of the defect controls the over-all rate, the reaction at each surface goes to equilibrium. The equilibrium concentration of the defect at $x = 0$ is $C_0$ while that at $x = X$ is $C_1$ (Fig. 1a). At intermediate positions in the scale the concentration is $C(x)$; if the diffusion coefficient of the defects is independent of $C(x)$, the latter is a linear function of $x$ as shown in Fig. 1a.

Assume that the film has reached a thickness, $X$, and that its rate of growth is given by Eq. [2]. Let the concentration of B in its reservoir be reduced to a concentration which puts reaction [4] at equilibrium. (In a metal oxidation this would correspond to reducing the oxygen pressure to the dissociation pressure of the oxide.) The defects continue to enter the film at $x = 0$ but are no longer removed at $x = X$. Their concentration approaches $C_0$ throughout the film, and the reaction stops (Fig. 1a).

If the concentration of B is now suddenly raised to its value prior to the interruption, the flow of defects is resumed and the original concentration distribution is re-established. If $C_0X$ is large enough, the restoration of the concentration gradient should resolve itself as a relatively fast initial uptake of B followed by a gradual return to the rate observed prior to the interruption.

Mathematically, the rate after the interruption can be treated as follows. In addition to requiring that $D$ is independent of $C(x)$ and that the surface is flat, it is assumed that $X >> \Omega C_0$ (so the increase of $X$ during this phase of reaction is negligible), and that defects can be created or destroyed only at $x = 0$ and $x = X$. Then at a given temperature,

$$\frac{\partial C(x)}{\partial t} = D\frac{\partial^2 C(x)}{\partial x^2} \qquad [5]$$

with the boundary conditions that

$$\left.\begin{aligned} &C(x) = C_0 \text{ for all } x && \text{when } t = 0 \\ &C(x) = C_0 \text{ at } x = 0 \\ \text{and} \quad &C(x) = C_1 \text{ at } x = X \end{aligned}\right\} \quad \text{when } t > 0 \qquad [6]$$

where $t$ is measured from the readmission of B to the system. The equation is readily solved by standard techniques (3) giving

$$C(x) = C_0 - \frac{(C_0 - C_1)x}{X} + \frac{2}{\pi}\sum_1^\infty \frac{C_1\cos n\pi - C_0}{n} \sin\frac{n\pi x}{X} e^{-D'n^2t} + \frac{4C_0}{\pi}\sum_0^\infty \frac{1}{2m+1}\sin(2m+1)\pi\frac{x}{X} e^{-D'(2m+1)^2t} \qquad [7]$$

where $D' = D\pi^2/X^2$.

By taking the derivative of $C(x)$ with respect to $x$, evaluating it at $x = X$, and integrating from $t = 0$ to $t = t$, one obtains an expression for $\Delta$, the number of defects crossing unit area at $x = X$ in time $t$.

$$\Delta = D\int_0^t \left(\frac{\partial C}{\partial x}\right)_{x=X} dt = \frac{D(C_1 - C_0)t}{X} - \frac{2X}{\pi^2}\sum_1^\infty [C_1 - C_0(-1)^n]\left[\frac{1}{n^2}\right][e^{-D'n^2t} - 1] + \frac{4C_0X}{\pi^2}\sum_0^\infty \frac{1}{(2m+1)^2}[e^{-D'(2m+1)^2t} - 1] \qquad [8]$$

For most practical purposes $C_1 >> C_0$ and Eq. [8] reduces to

$$\frac{\pi^2\Delta}{XC_0} = 2\sum_1^\infty \frac{(-1)^n}{n^2} - 4\sum_0^\infty \frac{1}{(2m+1)^2} - D't + 2\sum_1^\infty \frac{(-1)^n}{n^2} e^{-n^2D't} + 4\sum_0^\infty \frac{1}{(2m+1)^2} e^{-(2m+1)^2D't} \qquad [9]$$

Equation [9] has been solved numerically with the results given in Table I. The equation has two simple limiting forms. At the beginning of the reaction

$$\Delta = Bt^{1/2} \quad (t << X^2/D) \qquad [10]$$

where

$$B = 1.12\, D^{1/2} C_0 \qquad [10a]$$

Later in the reaction

$$\Delta = Q + Rt \quad (t > X^2/2D) \qquad [11]$$

where

$$Q = XC_0/3 \qquad [11a]$$

and

$$R = DC_0/X \qquad [11b]$$

Therefore, while direct rate measurements can at best give the product $DC_0/X$ (Eq. [2] or [11b]) the

**Table I. Numerical solution for the diffusion equation of interrupted kinetics, Eq. [9]**

$$\frac{\Delta}{XC_0} = \frac{2}{\pi^2}\sum_{1}^{\infty}\frac{(-1)^n}{n^2} + \frac{4}{\pi^2}\sum_{0}^{\infty}\frac{1}{(2m+1)^2} + \frac{Dt}{X^2} - \frac{2}{\pi^2}\sum_{1}^{\infty}\frac{(-1)^n}{n^2}e^{-n^2\pi^2Dt/X^2} - \frac{4}{\pi^2}\sum_{0}^{\infty}\frac{1}{(2m+1)^2}e^{-(2m+1)^2\pi^2Dt/X^2}$$

| $Dt/X^2$ | $(Dt/X^2)^{1/2}$ | $\Delta/XC_0$ |
|---|---|---|
| 0.02026 | 0.1422 | 0.159 |
| 0.03040 | 0.1744 | 0.195 |
| 0.04053 | 0.2011 | 0.226 |
| 0.05066 | 0.2250 | 0.253 |
| 0.06079 | 0.2466 | 0.276 |
| 0.07092 | 0.2664 | 0.299 |
| 0.08115 | 0.2845 | 0.320 |
| 0.09118 | 0.3020 | 0.339 |
| 0.1013 | 0.3183 | 0.357 |
| 0.1114 | 0.3338 | 0.375 |
| 0.1216 | 0.3485 | 0.392 |
| 0.1317 | 0.3629 | 0.408 |
| 0.1418 | 0.3765 | 0.423 |
| 0.1621 | 0.4026 | 0.453 |
| 0.1824 | 0.4272 | 0.480 |
| 0.2026 | 0.4501 | 0.507 |
| 0.2229 | 0.4720 | 0.532 |
| 0.2432 | 0.4930 | 0.556 |
| 0.2837 | 0.5325 | 0.603 |
| 0.3242 | 0.5694 | 0.647 |
| 0.3647 | 0.6038 | 0.691 |
| 0.4053 | 0.6366 | 0.733 |
| 0.5066 | 0.7117 | 0.837 |
| 0.6079 | 0.7795 | 0.939 |
| 0.7092 | 0.8422 | 1.041 |
| 0.8105 | 0.9002 | 1.142 |
| 0.9118 | 0.9549 | 1.243 |
| 1.0132 | 1.0065 | 1.344 |

interrupted rate measurements give additional expressions for $D^{1/2}C_0$ (Eq. [10a]) and $XC_0$ (Eq. [11a]). A separation of $D$ and $C_0$ is thus effected; in terms of the parameters in Eq. [10] and [11] one obtains

$$C_0 = \frac{0.8}{X}\frac{B^2}{R} \qquad [12]$$

$$C_0 = 3Q/X \qquad [13]$$

$$D = 1.25\left(\frac{RX}{B}\right)^2 \qquad [14]$$

It is clear from Eq. [12] and [13] that the parent Eq. [9] is overdetermined, since three independently measurable experimental quantities, $B$, $Q$, and $R$, must be quantitatively described with only two adjustable parameters, $D/X^2$ and $XC_0$. The entire formalism thus possesses the rare and wondrous quality of a rigorous internal check.

### *Experimental Procedure*

The use of interruption kinetics depends on the feasibility (i) of reducing the concentration of B to its equilibrium value, and (ii) of measuring the arrival of defects at the S/B interface. Both are quite easily accomplished.

(i) The supply of B to the B reservoir can simply be cut off. The reaction then automatically proceeds to equilibrium, the scale acting as a sink for the residual B. If the reservoir is large, it may be evacuated or flushed with inert gas or liquid (depending on the system) and then closed off. The scale then acts as a source of B (by partial decomposition) and the concentration again adjusts to the equilibrium value. In most cases the latter is small enough so that the required decomposition is negligible.

(ii) When a defect reaches the outer interface it immediately reacts with a stoichiometric number of B atoms. The two kinds of atomic defects which can originate at $x = 0$ are interstitial A atoms or B atom vacancies. When the former reach $x = X$ they will combine with $\frac{b}{a}$ atoms (cf. Eq. [4]) while the latter will combine with one B atom. In either case the depletion of B atoms from the freshly filled B reservoir gives a direct measure of the arrival of defects at $x = X$. $\Delta_B$, the total depletion of B atoms from the B reservoir after time, $t$, thus gives a direct measure of $\Delta$, the quantity in Eq. [9]-[11]. It should be noted that one may determine $\Delta$ by measuring the increase in $X$, but this will generally be very difficult.

The question naturally arises as to what procedure should be used to measure $\Delta$ if the defects originate at the S/B surface, but, as before, the B concentration is the only quantity which can be varied and measured. The defects which can arise at the S/B interface are B interstitial atoms or A atom vacancies. Their concentration distribution before and after the interruption of the supply of B is compared in Fig. 1 with the case where the defects originate at the A/S interface. The obvious difference lies in the relative magnitudes of $C_0$ and $C_1$.

It turns out, however, that Eq. [9] is completely symmetrical and, with suitable changes in sign, describes each of the four cases equally well. Procedures (i) and (ii) are thus applicable regardless of the defect type, and the measurement of $\Delta_B$ again gives a direct measure of $\Delta$. In order to make the treatment entirely general we shall redefine $C_0$ in Eq. [9]-[13] to mean the equilibrium concentration of the mobile defect at the interface where it originates when the reaction is proceeding normally. This may or may not correspond to the concentration during the interruption.

Since $\Delta_B$ is the quantity which is actually measured, it is convenient to use it directly. If $\Delta_B$ is substituted for $\Delta$ in Eq. [9], [10], and [11], then, instead of obtaining $C_0$ from Eq. [12] and [13], one obtains $C_0^B$ whose relation to $C_0$ is summarized in Table II. The value of $D$ is entirely independent of the units of $\Delta$.

### Use of Eq. [9]-[14]

The most convenient way to use Eq. [9]-[14] will be illustrated with recent data obtained on the oxidation of the intermetallic compound InSb where a thin protective scale of $In_2O_3$ is formed (4). A monocrystalline specimen exposing 4.0 $cm^2$ of flat surfaces was oxidized at 342°C and 0.3 mm oxygen until the total oxygen uptake was $5.76 \times 10^{17}$ atoms $cm^{-2}$. The sample enclosure was evacuated and

Table II. Relation between $C_o$ and $C_o^B$ in the reaction $aA + bB = S$

| | |
|---|---|
| Defects originating at A/S interface | |
| 1. Interstitial A atoms | $C_o = \frac{a}{b} C_o^B$ |
| 2. B atom vacancies | $C_o = C_o^B$ |
| Defects originating at S/B interface | |
| 3. Interstitial B atoms | $C_o = C_o^B$ |
| 4. A atom vacancies | $C_o = \frac{a}{b} C_o^B$ |

closed off for 15 hr without changing the temperature. Oxygen was then readmitted and the uptake measured by following the small pressure change at constant volume with a thermistor manometer. The results are plotted vs. $t^{1/2}$ and $t$ in Fig. 2a and 2b.

As expected Fig. 2a is linear at small times, while Fig. 2b becomes linear at the longer times, and the rate approaches the value observed just prior to the interruption. The intercept of Fig. 2a is not zero. The value of the intercept, designated Z, can be treated as an additive constant for which a correction must be made in any expression containing $\Delta_B$.

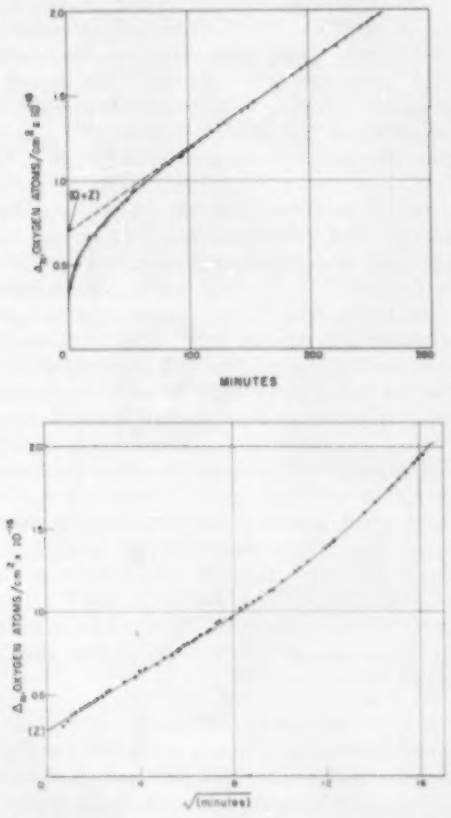


Fig. 2a (top), Fig. 2b (bottom). Interrupted oxidation of InSb. The uptake of oxygen was measured after a 15-hr interruption of the reaction at 342°C, $p_{O_2}$ = 0.3 mm, and X ~1.24 x $10^{-5}$ cm. The time is measured from readmission of oxygen. The solid curves represent the solution of Eq. [9], modified by the inclusion of the additive constant, Z (see text).

From Fig. 2a and 2b one finds B, the slope of Fig. 2a to be 8.60 x $10^{14}$ oxygen atoms $cm^{-2}$ $min^{-1/2}$; R, the slope of Fig. 2b to be 4.92 x $10^{15}$ oxygen atoms $cm^{-2}$ $min^{-1}$, and Q, the intercept of Fig. 2b minus Z, to be 4.04 x $10^{15}$ oxygen atoms $cm^{-2}$. From Eq. [14] one obtains $D/X^2$ = 4.09 x $10^{-4}$ $min^{-1}$. From Eq. [13] one obtains $XC_o^B$ = 1.212 x $10^{16}$ oxygen atoms $cm^{-3}$. From Eq. [12] one obtains $XC_o^B$ = 1.202 x $10^{16}$ oxygen atoms $cm^{-3}$. The close agreement of the two independent values of $XC_o^B$ provides the most important confirmation of the diffusion mechanism, and presages an excellent over-all description of the data by Eq. [9].

Substituting the value of $D/X^2$ and the average value of $XC_o^B$ into the column headings of Table I, one obtains values of $\Delta_B$ vs. $t$ and $t^{1/2}$ for the entire range of $t$. Adding Z to these values of $\Delta_B$, plotting the results, and drawing a smooth curve through the points, gives the solid curves in Fig. 2a and 2b. The applicability of Eq. [9] is clearly verified in this case.

Values of $D/X^2$ and $XC_o^B$ are thus obtained without reference to the chemistry or the thickness of the scale. Knowing $X$, one can obtain $D$ directly. In order to determine $C_o$ however, one must know both $X$ and the identity of the defect. The quantity $X$ may be determined independently, or by using the total oxygen uptake combined with the stoichiometry of the scale and its molecular volume. For $In_2O_3$ the uptake of 5.8 x $10^{17}$ oxygen atoms $cm^{-2}$ corresponds accordingly to *ca.* 1.24 x $10^{-5}$ cm.[4]

For reasons which are described elsewhere (4) it is believed that the mobile defects are interstitial $In^{+3}$ cations arising at the InSb/$In_2O_3$ interface. Thus $C_o = \frac{2}{3} C_o^B$. One obtains, accordingly[5] $D$ = 1.04 x $10^{-14}$ $cm^2$ $sec^{-1}$, $C_o^B$ = 1.22 x $10^{21}$ oxygen atoms $cm^{-3}$, $C_o$ = 8.1 x $10^{20}$ $In^{+3}$ ions $cm^{-3}$.

## Practical Considerations

(i) The length of time for which the reaction is interrupted must exceed $X^2/D$ if the equilibrium concentration is to be attained throughout the film.

(ii) The quantity $Q^B = XC_o^B/3$ must be considerably larger than the sensitivity limit of the analytical technique. For gaseous reactions the sensitivity of microgravimetric methods is usually about $10^{15}$ atoms, while standard low-pressure manometric techniques (thermistor or Pirani gauge) permit measurements of $10^{14}$ atoms. For practical film thicknesses ($< 10$ $\mu$) and surface areas ($< 10$ $cm^2$), $C_o^B$ must exceed *ca.* $10^{17}$ $cm^{-3}$. The use of larger areas, thicker films, or very low-pressure techniques, although less convenient, would extend the practical limit of $C_o^B$ to substantially lower values. For practical reasons it is also evident that $DC_o^B t_{min}$ must be smaller than $XC_o^B/3$ where $t_{min}$ is the minimum time before which a measurement can be made after the readmission of B to the system.

(iii) When $XC_o^B/3$ is less than $10^{15}$ atoms $cm^{-2}$,

[4] The geometric surface area to which the data is normalized is a factor, $F$, ("roughness factor") less than the true area. If $F \simeq 1.3$ as is believed to be the case for chemically polished InSb, the corrected values of $X$, $D$, $C_o^B$, and $C_o$ are 9.5 x $10^{-6}$ cm, 6.15 x $10^{-15}$ $cm^2$ $sec^{-1}$, 1.57 x $10^{21}$ $cm^{-3}$, and 1.05 x $10^{21}$ $cm^{-3}$, respectively.

one may encounter spurious effects due to chemisorption. Since chemisorption usually proceeds much more rapidly than the diffusion reaction described by Eq. [9], it will contribute an additive constant to $\Delta_n$ in a manner analogous to that observed in Fig. 2a.[5]

[5] In the case of InSb the effect is not thought to be associated with simple chemisorption of oxygen (4).

Manuscript received Feb. 26, 1960.

Any discussion of this paper will appear in a Discussion Section to be published in the June 1961 JOURNAL.

REFERENCES

1. C. Wagner, *Z. Phys. Chem.*, **B21**, 25 (1933).
2. N. Cabrera and N. F. Mott, *Rep. Prog. Phys.*, **12**, 163 (1948).
3. J. Crank, "The Mathematics of Diffusion," p. 42 ff, Oxford (1956).
4. A. J. Rosenberg, *J. Phys. Chem.* (in press).

# The Electrical Properties of Some Natural Waxes

**Thomas D. Callinan and Ann M. Parks**

*International Business Machines Corporation, Yorktown Heights, New York*

ABSTRACT

The dielectric constants and dielectric loss factors of Carnauba, Ouricuri, and American Montan wax determined over a temperature range of —60° to 90°C and at frequencies of 0.1, 1, 10, and 100 kc, indicate that the component omega-hydroxy acid esters rotate in the solid state in the temperature region 25°-70°. Furthermore, from dipole measurements, the molecules were found to possess a trans-trans configuration.

Recent advances in dielectric spectroscopy (1) suggested that this might prove a valuable tool in the determination of the nature of waxes. By dielectric spectroscopy is meant the elucidation of certain properties of materials in terms of their molecular and atomic constituents through an analysis of their dielectric constants and dielectric losses over a broad temperature (—100° to 200°C) and broad frequency (dc to $10^{10}$ cps) range. From the discipline as it now stands, it is possible to establish the presence and magnitude of permanent electric moments in the component molecules and to determine whether association exists. Certain peaks and troughs in the loss spectra may also be related directly to the molecular structure.

Using this technique, it has been found possible to establish the essential molecular structure of such naturally occurring waxes as Carnauba, Ouricuri, and Montan wax and to suggest why they behave the way they do in certain circumstances. In each case, the dielectric constant and dielectric loss factor were determined at frequencies between 100 and 100,000 cps at temperatures in the range —60° to 98°C, and the dipole moments of each were calculated from measurements made on benzene solutions of the waxes.

## Materials

The Carnauba wax used in these tests was derived from a genus of palm known as *Copernicia Cerifera Martius*. The wax was obtained from mature leaves and bears the commercial designation "North Country No. 3" and the provincial name "Gordierosa." The solid was a hard, brown material which melted abruptly at 79°C. It has a specific gravity at 25°C of 0.9988. Chemically, Carnauba wax is a mixture of alkyl esters (85%) and uncombined acids, alcohols, lactides, and hydrocarbons. Approximately 40% of the wax consists of omega-hydroxy acid esters having the formula:

$$HO—C_nH_nC(O)O\,C_mH_{m+1}$$

where $n$ and $m$ may be 18, 20, 22, or 28, (2). No effort was made to separate the components of Carnauba wax as it was the purpose of the work to study the material as a mixture.

Ouricuri wax is derived from the undersurface of the leaves of the palm tree known as *Attalea Excelsa Martisu*. It is a hard, dark brown solid, having a specific gravity at 25°C of 1.06661 and melts at 69°C. The wax is considered to have the following composition: alkyl esters (myricyl cerotate) and hydroxy esters total 61%, free wax acids 11%, resin acids 4%, resinols 15%, hydrocarbons 7%, and residue 2% (2).

Montan wax is a brown-black solid extracted from a California lignite. It has a specific gravity of 1.020 at 25°C and melts at 77°C. It is considered to be composed of esters of wax acids (53%) including hydroxy acids. It resembles, therefore, the Carnauba and Ouricuri waxes, (2).

Some of the properties of these waxes are tabulated in Table I.

## Experimental Methods

Each wax was melted and poured into an Elliott cell (3) previously heated in an air oven to 100°C. In actual practice the cell was modified by drilling holes in the base so that dry nitrogen gas could be passed around the electrodes and sample during measurement. This effectively eliminated interference by moisture condensation in the 0°C region. The assembled and filled cell was removed from the oven and allowed to cool to room temperature. Dielectric properties were then determined from

Table I. Select properties of waxes

| Chemistry | Montan | Ouricuri | Carnauba |
|---|---|---|---|
| (A) Alkyl esters, % | 53 | 61 | 85 |
| (1) Hydroxy acid esters, % | 12-14 | — | 55 |
| (B) Hydrocarbons, % | 3 | 7 | 3 |
| Specific gravity | 1.020 | 1.0661 | 0.9988 |
| Penetration, 150 g/ 5 sec/25°C | 0.06 | 0.10 | 0.08 |
| Melting point, °C | 77 | 69 | 79 |
| Acid value | 50-55 | 21-24 | 3 |

measurements on the General Radio 1610-A capacitance bridge network. Measurements were made as the samples slowly cooled from 95° to 25°C and as they warmed from −60° to 25°C.

The resistance of each wax sample was measured in the Elliott cell on a General Radio Type 544-B megohm bridge in the temperature range of 25°-95°C. Results are expressed in terms of the volume resistivity of the sample in order to correct for the resistance in the cell itself.

Dipole moments were calculated from measurements on dilute benzene solutions of the waxes. The density of each solution was measured on a Seederer-Kohlbusch density balance and the refractive index measured on a Spencer Refractometer at 24°C. The dielectric constant was measured in a two terminal Balsbaugh cell with a volume of 75 cc, at 24°C and 10,000 cps frequency. This frequency is believed to be above the range of ionic vibrations in the molecules, and the polarization calculated is a result of induced and orientation polarizations. The molar polarization and refraction were calculated according to the Clausius-Mosotti (4) and Debye (5) equations. This method involves use of the relationships

$$P = \frac{\epsilon' - 1}{\epsilon' - 2} \cdot \frac{M_1N_1 + M_2N_2}{d}$$

$$\text{and } R = \frac{n^2 - 1}{n^2 + 2} \cdot \frac{M_1N_1 + M_2N_2}{d}$$

where $P$ is the molar polarization, $\epsilon'$ the dielectric constant, $d$ the density, $M$ and $N$ refer to the molecular weights and mole fractions of solute and solvent, $R$ is the molar refraction, and $n$ is the refractive index.

By linear extrapolation of the molar polarization to infinite dilution the dipole moment of the molecules is calculated from the relationship $M = 0.0128 \sqrt{(P-R)\,T}$, where $T$ is expressed in absolute degrees.

### Dielectric Properties of Carnauba Wax

The dielectric constants $\epsilon'$ and dielectric loss factors $\epsilon''$ of Carnauba wax are listed in Table II and are shown graphically in Fig. 1. At very low temperature, the dielectric constant of Carnauba wax is low (2.16-2.29) and differs only slightly at different frequencies. As the temperature rises the dielectric constant increases at first slowly (0.006/degree) and then more rapidly (0.02/degree) until a temperature is reached at which the dielectric constant passes through a maximum and decreases with further increases in temperature. Concomitant with these changes in dielectric constant, there are changes in dielectric loss factor. All pass through a maximum at different temperatures depending on the frequency.

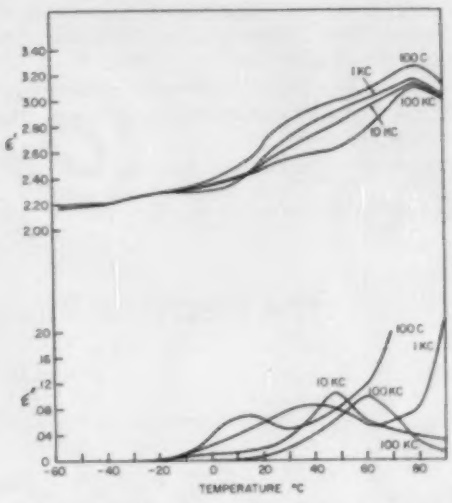


Fig. 1. Variation of dielectric constant $\epsilon'$ and dielectric loss factor $\epsilon''$ of Carnauba wax with temperature at 100, 1,000, 10,000, and 100,000 cps.

Table II. Carnauba wax

| Frequency (cps), temp, °C | 100 $\epsilon'$ | 100 $\epsilon''$ | 1000 $\epsilon'$ | 1000 $\epsilon''$ | 10,000 $\epsilon'$ | 10,000 $\epsilon''$ | 100,000 $\epsilon'$ | 100,000 $\epsilon''$ |
|---|---|---|---|---|---|---|---|---|
| −58 | 2.17 | 0.000 | 2.16 | 0.000 | 2.19 | 0.000 | 2.19 | 0.000 |
| −50 | 2.18 | 0.000 | 2.18 | 0.000 | 2.20 | 0.000 | 2.20 | 0.000 |
| −20 | 2.30 | 0.000 | 2.29 | 0.000 | 2.28 | 0.000 | 2.28 | 0.000 |
| −5 | 2.34 | 0.010 | 2.29 | 0.000 | 2.33 | 0.000 | 2.33 | 0.000 |
| 18 | 2.59 | 0.066 | 2.48 | 0.004 | 2.46 | 0.016 | 2.44 | 0.016 |
| 21 | 2.69 | 0.060 | 2.57 | 0.061 | 2.52 | 0.023 | 2.49 | 0.019 |
| 31 | 2.84 | 0.050 | 2.72 | 0.080 | 2.64 | 0.040 | 2.55 | 0.020 |
| 40 | 2.94 | 0.060 | 2.85 | 0.081 | 2.72 | 0.070 | 2.58 | 0.040 |
| 48 | 2.98 | 0.080 | 2.91 | 0.080 | 2.79 | 0.105 | 2.62 | 0.060 |
| 60 | 3.07 | 0.120 | 3.00 | 0.055 | 2.94 | 0.060 | 2.76 | 0.100 |
| 79 | 3.26 | 0.435 | 3.16 | 0.080 | 3.13 | 0.060 | 3.10 | 0.030 |
| 95 | 3.13 | 1.90 | 3.04 | 0.217 | 3.03 | 0.029 | 3.02 | 0.014 |

At higher temperatures the dielectric loss factors show runaway tendencies at low frequencies reaching values greater than the maxima obtained at lower temperatures.

### Dielectric Properties of Ouricuri Wax

The dielectric constant $\epsilon'$ and dielectric loss factor $\epsilon''$ of Ouricuri wax as a function of frequency and temperature is shown graphically in Fig. 2 based on the data listed in Table III. At low temperatures and all frequencies the dielectric constants and dielectric loss factors are again low.

As was observed above the temperature coefficient of change in dielectric constant changes markedly at about 25°C from 0.003/degree to 0.02/degree. It then passes through a maximum in the vicinity of the melting point of the wax, when determined at frequencies higher than 1 kc. Runaway characteristics are observed above 50°C, but below this temperature the dielectric loss factor curves pass through a maximum at a characteristic temperature for each frequency.

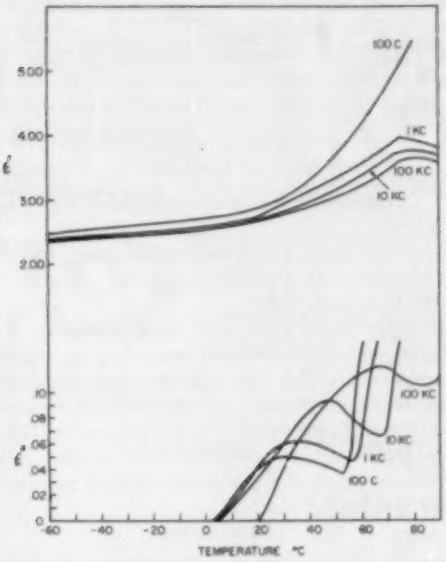


Fig. 2. Variation of dielectric constant $\epsilon'$ and dielectric loss factor $\epsilon''$ of Ouricuri wax with temperature at 100, 1,000, 10,000, and 100,000 cps.

**Table III. Ouricuri wax**

| Frequency (cps), temp, °C | 100 $\epsilon'$ | 100 $\epsilon''$ | 1000 $\epsilon'$ | 1000 $\epsilon''$ | 10,000 $\epsilon'$ | 10,000 $\epsilon''$ | 100,000 $\epsilon'$ | 100,000 $\epsilon''$ |
|---|---|---|---|---|---|---|---|---|
| −60 | 2.47 | 0.000 | 2.40 | 0.000 | 2.38 | 0.000 | 2.39 | 0.000 |
| −50 | 2.54 | 0.000 | 2.43 | 0.000 | 2.40 | 0.000 | 2.40 | 0.000 |
| −5 | 2.68 | 0.000 | 2.56 | 0.000 | 2.52 | 0.000 | 2.52 | 0.000 |
| 18 | 2.84 | 0.036 | 2.71 | 0.046 | 2.66 | 0.030 | 2.64 | 0.000 |
| 22 | 2.90 | 0.044 | 2.76 | 0.053 | 2.70 | 0.040 | 2.68 | 0.008 |
| 42 | 3.37 | 0.043 | 3.19 | 0.060 | 3.05 | 0.089 | 2.95 | 0.080 |
| 48 | 3.44 | 0.040 | 3.28 | 0.056 | 3.14 | 0.093 | 3.00 | 0.100 |
| 68 | 4.54 | 1.70 | 3.63 | 0.290 | 3.55 | 0.067 | 3.36 | 0.120 |
| 75 | 5.15 | 7.30 | 3.96 | 1.17 | 3.74 | 0.180 | 3.62 | 0.112 |
| 80 | 5.43 | 11.50 | 3.92 | 1.40 | 3.74 | 0.209 | 3.63 | 0.108 |
| 93 | 6.58 | 19.48 | 3.88 | 2.11 | 3.69 | 0.274 | 3.58 | 0.110 |

## Dielectric Properties of Montan Wax

The dielectric constant $\epsilon'$ and dielectric loss factor $\epsilon''$ of American Montan wax are listed in Table IV and are shown graphically in Fig. 3. The dielectric constant remains low and increases only slowly (0.008/°C) on passing from −60° to 25°C. Above this temperature there is a rapid increase resulting in an apparent dielectric constant of 16 at 98°C; this is accompanied by and attributable to very high losses. These losses are so high that they swamp the usual maxima in the dielectric constant at the melting point; the only suggestion of it existing comes from the definite plateau which occurs at 100,000 cps. Again, however, each loss curve passes through a maximum at a definite temperature.

## Comparison of Electrical Properties

For the sake of comparison and to interpret the dielectric loss spectra the volume resistivity of each wax as a function of temperature is shown in Fig. 4. In each case the resistance remains constant until the wax begins to melt. At this point the resistance decreases rapidly and levels out again in the liquid.

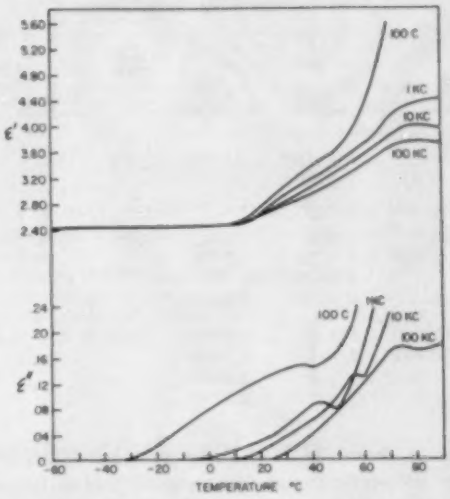


Fig. 3. Variation of the dielectric constant $\epsilon'$ and dielectric loss factor $\epsilon''$ of American Montan wax with temperature at 100, 1,000, 10,000, and 100,000 cps.

**Table IV. American No. 16 Montan wax**

| Frequency (cps), temp, °C | 100 $\epsilon'$ | 100 $\epsilon''$ | 1000 $\epsilon'$ | 1000 $\epsilon''$ | 10,000 $\epsilon'$ | 10,000 $\epsilon''$ | 100,000 $\epsilon'$ | 100,000 $\epsilon''$ |
|---|---|---|---|---|---|---|---|---|
| −60 | 2.44 | 0.000 | 2.42 | 0.000 | 2.43 | 0.000 | 2.43 | 0.000 |
| −40 | 2.44 | 0.000 | 2.43 | 0.000 | 2.45 | 0.000 | 2.43 | 0.000 |
| −10 | 2.44 | 0.052 | 2.43 | 0.000 | 2.43 | 0.000 | 2.43 | 0.000 |
| 0 | 2.44 | 0.080 | 2.43 | 0.006 | 2.43 | 0.000 | 2.43 | 0.000 |
| 5 | 2.44 | 0.092 | 2.43 | 0.010 | 2.43 | 0.000 | 2.43 | 0.000 |
| 18 | 2.66 | 0.122 | 2.57 | 0.027 | 2.55 | 0.009 | 2.55 | 0.000 |
| 24 | 2.90 | 0.134 | 2.80 | 0.036 | 2.67 | 0.025 | 2.79 | 0.000 |
| 35 | 3.20 | 0.144 | 3.04 | 0.070 | 2.77 | 0.050 | 2.86 | 0.024 |
| 42 | 3.40 | 0.148 | 3.20 | 0.088 | 3.10 | 0.068 | 3.00 | 0.048 |
| 50 | 3.62 | 0.17 | 3.44 | 0.080 | 3.28 | 0.100 | 3.15 | 0.080 |
| 60 | 4.23 | 1.15 | 3.68 | 0.18 | 3.54 | 0.13 | 3.37 | 0.12 |
| 70 | 5.58 | 6.10 | 4.12 | 0.82 | 3.84 | 0.23 | 3.66 | 0.17 |
| 80 | — | — | 4.36 | 2.32 | 3.99 | 0.38 | 3.75 | 0.17 |
| 90 | — | — | 4.42 | 3.70 | 3.96 | 0.52 | 3.72 | 0.18 |

As expected from this data since Carnauba shows the lowest conductivity in the liquid form it also has the lowest dielectric losses. In the same manner

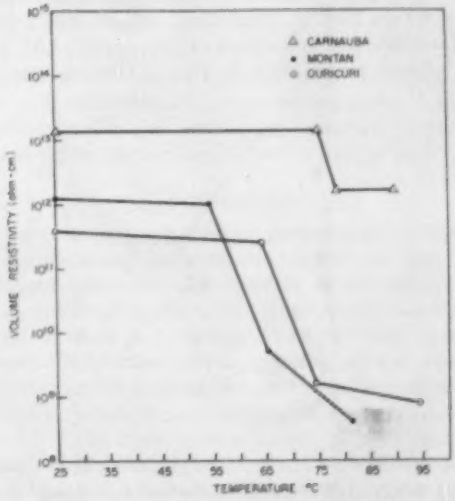


Fig. 4. Volume resistivity vs. temperature of the waxes

**Table V. Dipole moments of the waxes**

| Wax | Mole fraction | $\epsilon'$, at 10,000 cps | Extrapolated polarization, $P$, cc | Molar refraction | Dipole moment, esu-cm, $\times 10^{-18}$ |
|---|---|---|---|---|---|
| Carnauba | $5 \times 10^{-6}$ | 2.2768 | 2040 | 1568 | 4.8 |
| $M = 920$ | $1 \times 10^{-5}$ | 2.2772 | | | |
| | $5 \times 10^{-5}$ | 2.2780 | | | |
| Ouricuri | $4 \times 10^{-6}$ | 2.2811 | 4200 | 3037 | 7.5 |
| $M = 848$ | $9 \times 10^{-6}$ | 2.2803 | | | |
| | $4 \times 10^{-5}$ | 2.2839 | | | |
| | $9 \times 10^{-5}$ | 2.2855 | | | |
| Montan | $1 \times 10^{-5}$ | 2.2763 | 885 | 472 | 4.5 |
| $M = 834$ | $2 \times 10^{-5}$ | 2.2780 | | | |
| | $1 \times 10^{-4}$ | 2.2800 | | | |
| | $2 \times 10^{-4}$ | 2.2833 | | | |

Ouricuri shows less conductivity than Montan and lower dielectric losses. In the solid waxes, however, the order of increasing conductivity is Carnauba, Montan, Ouricuri, but Ouricuri generally shows the lowest losses. Correlation in this region is difficult, however, due to the presence of maxima in the loss curves.

Because of the temperature and frequency dependence of the dielectric constants of the waxes, relatively high dipole moments are indicated. The results of these measurements are shown in Table V. Montan and Carnauba have essentially the same dipole moments, but that of Ouricuri is considerably higher. As was shown above Ouricuri also has the highest dielectric constant at 24°C followed by Montan and Carnauba. Calculation of the theoretical dipole moment for various configurations of a planar omega-hydroxy acid ester such as is present in the waxes leads to the conclusion that these esters must be arranged predominately in a trans-trans configuration. This arrangement is shown in Fig. 5 and predicts a moment of 4. 3D on the basis of known bond moments and angles (6a). The opposite configuration, the cis-cis form in which the hydroxyl hydrogen and the alkyl group of the esters are on the same side of the chain as the carbonyl predicts a moment of only 0.25D. Combination of the *cis* and *trans* forms lead to theoretical moments of 2.65D.

The dielectric properties of the waxes at 25°C are reproduced graphically in Fig. 6. The Ouricuri wax

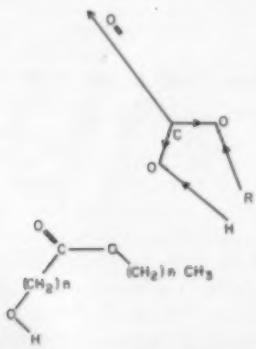


Fig. 5. Vectoral representation of trans-trans omega-hydroxy acid ester.

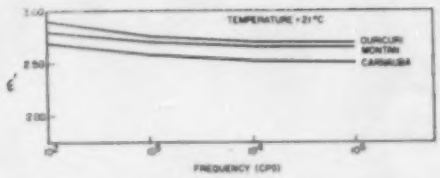


Fig. 6. Comparison of the dielectric constants $\epsilon'$ of the waxes

shows the highest $\epsilon'$ throughout the frequency range with Montan wax and Carnauba wax placing second and third in that order.

All three natural waxes were found to possess dielectric constants which were highly dependent on temperature and two discrete regions where the temperature coefficient of dielectric constant differed. Both Fitzgerald (7) and Stempel (8) have shown that the waxes remain crystalline to within six degrees of their respective melting points.

## Conclusions

In view of the fact that the change in the temperature coefficient of the dielectric constant being discussed occurs well below the melting points of the waxes, a mechanism analogous to that observed on abrupt melting of organic crystals does not apply. This leaves us with the explanation of molecular rotation similar to that found in water and some organic crystals.

Molecular rotation has been also reported to occur in a number of long-chain compounds such as primary alcohols. These compounds are known to exist in alpha and beta forms, and rotation takes place about the axis of the chain in the alpha or high-temperature form (9). That this mechanism also applies to the three waxes under consideration is confirmed by the similarity of their dielectric behavior to that observed in 1-docosanol, a material previously shown to exhibit molecular rotation (6b). In this case the dielectric constant is strongly temperature dependent and shows a fivefold increase in the temperature coefficient of change in dielectric constant at about 26°C, a temperature well below its melting point.

Since the three waxes are composed largely of omega-hydroxy acid esters, the mechanisms of the effects determined dielectrically are interpreted to be as shown in Fig. 7. The molecules tend to align themselves in an orderly fashion. At very low temperatures there is high cohesion between parallel chains and strong head-to-head attraction between hydroxyl groups. As the temperature rises the hydrogen bonding between hydroxyl groups is reduced so that the molecules can rotate around the molecular

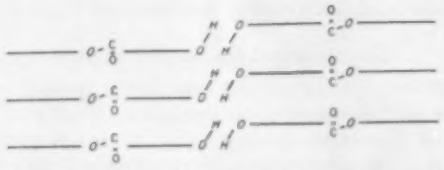

Fig. 7. Molecular arrangement of omega-hydroxy acid esters in wax crystals.

axis but remain in an orderly bundle. At elevated temperatures the cohesion between chains is reduced and the material melts. The noted differences between the three waxes are believed to be caused by differences in the relative amounts of esters and other materials present.

Manuscript received Feb. 15, 1960. This paper was prepared for delivery before the Philadelphia Meeting, May 3-7, 1959.

Any discussion of this paper will appear in a Discussion Section to be published in the June 1961 JOURNAL.

REFERENCES

1. A. R. V. Hippel, "Dielectric Materials & Applications," John Wiley & Sons, Inc., New York (1954).
2. A. H. Warth, "The Chemistry & Technology of Waxes," Reinhold Publishing Co., New York (1956).
3. M. A. Elliott, A. R. Jones, and L. B. Lockhart, *Ind. Eng. Chem., Anal. Ed.*, **19**, 10 (1947).
4. O. F. Mosotti, *Mem. Soc. Ital. Sc. (Modena)*, **14**, 49 (1850); R. Clausius, "Die Mechanische Warmetheorie," Vol. II, p. 94, Vieweg, Verlag, Brunswick, Germany (1879).
5. P. Debye, "Polar Molecules," Chemical Catalog, New York (1929).
6. C. P. Smyth, "Dielectric Behavior and Structure," McGraw-Hill Book Co., Inc., New York (1955) a, Chap IX; b, Chap. V.
7. E. Fitzgerald, Private communication.
8. N. Stempel, Private communication.
9. S. Glasstone, "Textbook of Physical Chemistry," 2nd ed., p. 424, D. VanNostrand & Co., New York (1946).

# Factors Influencing the Luminescent Emission States of the Rare Earths

**L. G. Van Uitert**

*Bell Telephone Laboratories, Incorporated, Murray Hill, New Jersey*

ABSTRACT

The number of electronic states from which luminescent emission by rare earth ions can be observed is dependent on the extent to which the host lattice perturbs their *f*-orbital electrons. Among others, perturbing influences may stem from the following sources: (*a*) coulombic affinities of the ions or molecules surrounding the rare earth ions for the electrons they share with the latter; (*b*) concentration effects, i.e., exchange coupling; (*c*) thermal effects, i.e., vibronic interactions.

Results obtained on metal organic complexes, hydrates, fluorides, and tungstates are compared. The effects on emission of the rare earth ion concentration in the tungstates are compared for europium, terbium, dysprosium, and erbium at room temperature, and the influences of thermally excited interactions on the emission of erbium are demonstrated.

In principle, emission should be observable from all of the excited states of the rare earth ions when they are not influenced by their surroundings. Of course, this condition cannot be fully realized in the solid state. However, different environments have markedly different influences on the rare earths. In the case of europium, for example, the number of states from which emission is observed varies from one in its chelate compounds to four in its oxides (1-3). Even in a given structure, the number of states from which emission is observed can be quite dependent on the rare earth concentration (4, 5) and thermal effects (6). In this paper, the influences of a number of environments on the luminescent emission of several of the rare earths are compared, and the factors which appear to be responsible for the relationships observed are discussed.

## Materials

Members of the series $Ca_{1-2x}Na_xRE_xWO_4$, where RE = europium with $x = 3 \times 10^{-4}$, $10^{-4}$, $5 \times 10^{-4}$, $10^{-3}$, $10^{-1}$, and 0.50; RE = terbium with $x = 10^{-4}$, $10^{-3}$, $10^{-2}$, $5 \times 10^{-2}$, 0.2, and 0.5; RE = dysprosium with $x = 5 \times 10^{-4}$, $10^{-4}$, $10^{-3}$, $5 \times 10^{-3}$, $10^{-2}$, $10^{-1}$, 0.25, and 0.50; and RE = erbium with $x = 10^{-5}$, $3 \times 10^{-5}$, $10^{-4}$, $10^{-3}$, $3 \times 10^{-3}$, $10^{-2}$, 0.25, and 0.50, were prepared by crystallization from a $Na_2W_2O_7$ flux, as previously described (7). The crystals obtained by this method are nearly perfect in structure compared to those obtained by sintering techniques and therefore are suitable for making emission intensity comparisons. Emission from samples of a given composition grown at various rates, and hence of quite different crystallite size, compares in intensity to within a few per cent of one another under the measuring conditions employed.

### *Measurements*

Measurements were made employing a Gaertner high dispersion spectrometer with an AMINCO photomultiplier microphotometer which employed a 1P22 photomultiplier tube. The system was calibrated against a tungsten lamp to give relative values of brightness of the emitting surface in units of power per unit wave-length range. Emission was excited by illuminating a sample 1 in. long by ½ in. wide by ¼ in. deep with a 3660Å rich H4 spotlight through a Corning 5874 filter. All of the intensity measurements are relative to 100 for the 5450Å peak of a comparable sample of $Na_{.5}Tb_{.5}WO_4$.

Table I

| Process | Ionization potential, ev | Reference |
|---|---|---|
| $La \rightarrow La^{+}$ | 5.61 | (10) p. 137 |
| $La^{+} \rightarrow La^{2+}$ | 11.4 | (10) p. 138 |
| $La^{2+} \rightarrow La^{3+}$ | 19.2 | (10) p. 139 |
| $H_2O \rightarrow H_2O^{+}$ | 12.6 | (11) p. 265 |
| Organic-O → Organic-$O^{+}$ | >10 | (11) p. 265 |

Table II

| Process | Electron affinity, ev | Reference |
|---|---|---|
| $F \rightarrow F^{-}$ | 4.27 | (12) p. 161 |
| $O \rightarrow O^{-}$ | 3.1 | (11) p. 40 |
| $O \rightarrow O^{=}$ | −7.28 | (12) p. 161 |

## Discussion

The number of electronic states from which luminescent emission by rare earth ions can be observed may be expected to depend on the extent to which the host lattice perturbs their electron envelopes. The number of emitting states observed does not appear to be as critically dependent on geometric considerations as the crystal field splitting or the relative strengths of the emission lines. Among others, the perturbing influences may stem from the following sources: (a) the coulombic affinities of the ions or molecules surrounding the rare earth ions for the electrons they share with the latter; (b) concentration effects, i.e., exchange coupling; (c) thermal effects, i.e., vibronic interactions.

### *Coulombic Affinities*

There is considerable evidence that bond strength, which may be expected to bear directly on perturbing influences, increases with an increase in the affinity of one or both of the bonded atoms for the electrons shared (8, 9). As a first approximation one may consider the electron affinities or ionization potentials of the ions or molecules surrounding the rare earth ions in the several host lattices to provide a measure of the extent to which these surroundings may perturb the f-orbital electrons of the rare earths. A comparison of the values given in Tables I and II shows that the third ionization potential of lanthanum, which may be considered to be representative of the rare earths, is larger than the ionization potentials of $H_2O$ or organic oxygen and is much larger than the electron affinities of fluorine or oxygen. Hence, one cannot ascribe full possession of the electrons about these molecules and ions to themselves when they are bonded to trivalent rare earth ions. Electron diffraction work carried out on beryl ($Be_3Al_2Si_6O_{18}$) by Bragg and West (13) has shown that in the silicates the silicon and oxygen atoms are closer to the $Si^{+}$ and $O^{-}$ ionic states than to the $Si^{4+}$ and $O^{2-}$ states. Hence, one may expect the ionization potential of oxygen to depend on the central cation when it is part of an anionic group such as $WO_4^{=}$.

In a similar manner, the electron affinity of an organic oxygen atom is dependent on the nature of the molecule of which it is part. Coulson (14) has shown that for carbon-carbon bonding one may expect an increase in the electron affinities of the carbon entities as the s-character of their $\sigma$ bonds increases in the order $sp^3$ (single bonding), $sp^2$ (double bonding), and sp (triple bonding). This is a consequence of the fact that the s-orbital lies lower energetically than do the p-orbitals. It may be expected that a similar increase in the multiple bond character of isoelectronic oxygen would result in its having an increased electron affinity. Hence, one may expect a stronger bonding of ketonic oxygen (double bonded to carbon) to the rare earth ions than occurs with ethers or alcohols. Further, one might expect an additional increase in bonding strength to the rare earths through the oxygen atoms of chelating agents such as acetylacetone by the development of resonance structures and a reduction in entropy.

The above considerations, in conjunction with the observations given below, suggest that the following environments diminish in perturbing influence in the order: O—O chelates, ketones and hydrates, fluorides, high central charge anionic groups ($WO_4^{=}$), less covalent oxides. In the case of europium, one emission state (17,300 $cm^{-1}$) is active in the chelate (1, 15), and an additional state (19,000 $cm^{-1}$) is observed in the hydrate (1); a third (21,500 $cm^{-1}$) is apparent in the fluoride (3), and a fourth (24,200 $cm^{-1}$) in the tungstate (5) and calcium oxide (16). In a like manner, one emission state (20,700 $cm^{-1}$) is observed for terbium in the chelate, hydrate (1), and fluoride (3); a second is found in the tungstate (4); and there are possibly three or more when terbium is combined with aluminum oxide (4, 17). Erbium does not luminesce in the chelate or hydrate but exhibits two main emission states (15,300 and 18,400 $cm^{-1}$) in the fluoride (3) and a third (24,500 $cm^{-1}$) in the tungstates (6) and calcium oxide (16). Parallel patterns are observed for a number of the other rare earths.

### *Concentration Effects*

Increasing the rare earth concentration can produce effects quite comparable to those found on changing the host environments. This is readily observed by comparing members of the series $Ca_{1-3x}Na_xRE_xWO_4$. Figure 1 shows the dependencies of the intensities of emission from the 26,500 and 20,700 $cm^{-1}$ states of terbium on the concentration of terbium in the above tungstates and of the 20,700 $cm^{-1}$ state of terbium when it is substituted totally or in part for yttrium in yttrium hexa-antipyrene tri-iodide (4). These values are represented

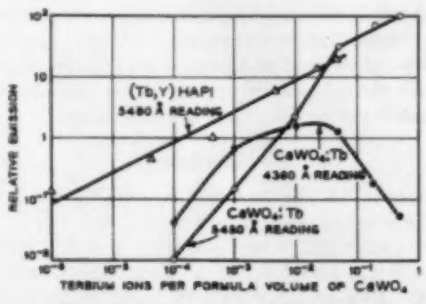


Fig. 1. Relative emission vs. the concentration of terbium

by the intensities measured for the emission peaks at 4360 and 5450Å in the tungstates and 5480Å in the antipyrene complexes, respectively. The metal ions are separated by 14Å in the antipyrene complexes; hence, they can be considered to be isolated from each other. Therefore, it is reasonable to employ the curve for the antipyrene complexes as a reference for the dependence of emission intensity on concentration for strongly bonded terbium ions.

In the dilute materials, the emission from the tungstates is much weaker than that from the antipyrene complexes. However, at high terbium concentrations, the tungstates compare favorably to terbium hexa-antipyrene tri-iodide and take on the emission characteristics of its yttrium substitution series in its intensity dependence on concentration and number of emission states. This is equivalent to a change from a relatively ionic to a more covalent or stronger bonding environment and appears to be related to the development of exchange coupling between the paramagnetic rare earth ions.

Figure 2 shows the dependencies of the intensities of emission from the 24,200, 21,500, 19,000, and 17,000 $cm^{-1}$ states of trivalent europium (represented by the values measured for the peaks at 4312, 5105, 5545, and 6140Å, respectively) on europium concentration. The relationships shown suggest that the emission from 24,200 $cm^{-1}$ is quenched by the pairing of europium ions (they occur in neighboring calcium sites) and emission from 21,500 and 19,000 $cm^{-1}$ is quenched by the association of three or more europium ions (5).

In contrast to the behavior exhibited by europium, the intensities of emission from 24,500, 18,400, and 15,300 $cm^{-1}$ exhibited by erbium vary uniformly (as shown in Fig. 3 which is discussed below) instead of quenching sequentially with increasing concentration. This provides supporting evidence that the quenching observed for terbium and europium is not due to an emission and reabsorption process.

The spectrum of dysprosium in calcium tungstate which is observed in the visible range is due to emission from an electronic state (2, 3) at 21,000 $cm^{-1}$. The dependence of the intensity of emission from this state (represented by the values measured for the strongest peak which is at 5750Å) on dysprosium content is shown as part of Fig. 4. Dysprosium luminesces a bright yellow at a 1% concentration but is completely quenched in $Na_{0.5}Dy_{0.5}WO_4$. The quenching observed in this case also appears to be due to exchange coupling.

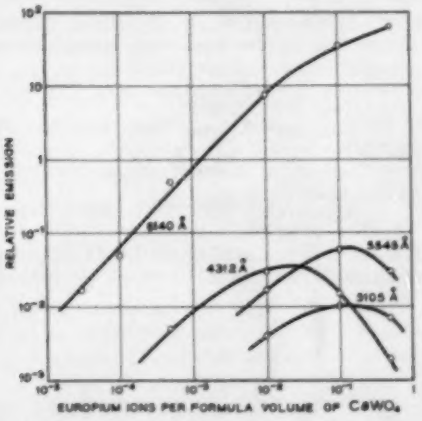


Fig. 2. Relative emission vs. the concentration of europium

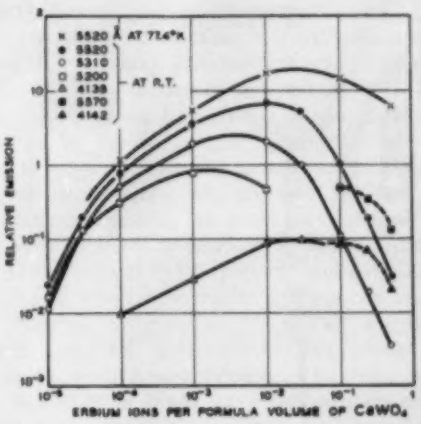


Fig. 3. Relative emission vs. the concentration of erbium

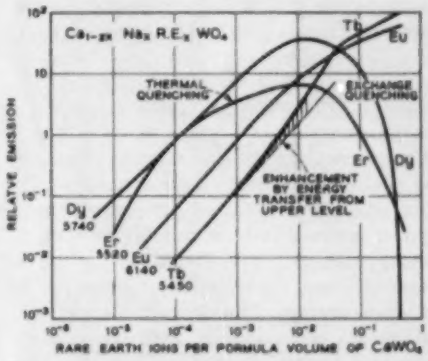


Fig. 4. Relative emission vs. rare earth concentration

### *Thermal Effects*

Thermal effects play an important role in the emission spectra of erbium in the scheelite structure. Besides the three main emission states at 15,300, 18,400, and 24,500 $cm^{-1}$, erbium shows strong emission from thermally excited levels at 18,830, 19,080, and 19,200 $cm^{-1}$ at room temperature (6). In $Na_{0.5}Er_{0.5}WO_4$, emission from the above states is quenched at room temperature, thus allowing emission from states that are probably just below those at 18,400 and 19,200 $cm^{-1}$ to be seen. At 77°K emission from the thermally excited states is no longer observed, but emission from the high erbium content samples is again very bright (6). Figure 3 shows the dependencies of the intensities of emission from the 18,400, 24,500, 18,830, and 19,200 $cm^{-1}$ levels of erbium (represented by the values measured for the peaks at 5520, 4138, 5310, and 5200Å, respectively) on erbium concentration at room temperature. It also shows the comparable data for levels which are presumed to lie just below those

at 18,400 and 19,200 $cm^{-1}$ (represented by the values measured for the peaks at 5570 and 4142Å, respectively). The comparable data for the peak at 5520Å at 77°K are also given.

The relationships observed show that emission from the thermally excited states of erbium is quenched by increasing the concentration of erbium as well as by lowering the temperature. However, while the emission from the principal excited states is also quenched by increasing the concentration of erbium at room temperature, lowering the temperature reduces the effectiveness of this quenching mechanism and bright emission is obtained from these levels. The effects noted are quite probably due to vibronic interactions and their dependence on temperature. Since the peaks at 5570 and 4142Å do not show the same concentration or thermal dependencies as their close neighbors, they may originate from levels which, while only a few wave numbers below the dominant levels, do not couple thermally to the lattice in the same way.

### *Comparisons*

Figure 4 presents a comparison of the dependencies of emission at room temperature on rare earth concentration for the dominant excited states of the several rare earth ions discussed. The curve for the emission measured for the 6140Å peak of europium appears to be a reliable reference for the following reasons: (*A*) The dilute materials show an almost linear dependence of emission on europium concentration. The deviation observed at high concentration is consistent with the change in environmental conditions discussed in the case of terbium. (*B*) The aggregate emission from the excited states, other than that at 17,000 $cm^{-1}$, is never more than a few per cent of the latter. Thus, possible emission enhancement due to energy transfer from higher levels as a result of changing environmental conditions would not be significant. (*C*) Emission from the 17,000 $cm^{-1}$ level of europium does not appear to be quenched by concentration or thermal effects in these compositions.

The curve for dysprosium shows the same linear dependence as the one for europium at low concentrations. The rapid decrease in emission as the dysprosium concentration increased above $10^{-2}$ provides an excellent example of concentration quenching. This effect, as well as the quenching of emission from the higher energy states of terbium and europium, is not altered by reducing the temperature to 77°K.

Concentration quenching of emission from the higher of two energy states can occur so as to permit energy transfer to the lower, thus enhancing emission from it. The data for terbium provide an example of such a transfer. Figure 1 shows that at low terbium concentrations the emission from 26,500 $cm^{-1}$ (as indicated by the data for the peak at 4360Å) is about three times as bright as that from 20,700 $cm^{-1}$ (represented by the data for the peak at 5450Å). As the terbium concentration is increased from $10^{-6}$ to $5 \times 10^{-5}$, both curves deviate from linearity, the curve for the peak at 4360Å in a direction which indicates a relative loss in brightness and the curve for the peak at 5450Å in a direction which indicates a relative gain in brightness. The latter curve is readily compared to the curve for the 6140Å peak of europium in Fig. 4. The arithmetic sum of the two terbium emission curves provides a resultant curve that is symmetrical with that for the 6140Å peak of europium.

The curve in Fig. 4 for the emission at room temperature for the erbium peak at 5520Å shows the effects of a quenching process which has a strong thermal dependence. This curve deviates strongly from linearity at concentrations of erbium as low as $10^{-4}$, in addition to showing strong quenching effects above $10^{-3}$, as do the curves for dysprosium and the higher emitting states of terbium and europium.

### Acknowledgments

The author is indebted to C. G. B. Garrett, D. L. Wood, A. D. Liehr, K. Nassau, and J. H. Scaff of these Laboratories for helpful discussions and comments.

Manuscript received April 4, 1960. This paper was prepared for delivery before the Chicago Meeting, May 1-5, 1960.

Any discussion of this paper will appear in a Discussion Section to be published in the June 1961 JOURNAL.

### REFERENCES

1. O. Deutchbein and R. Tomaschek, *Ann. Phys.*, (5) **29S**, 311 (1937).
2. H. Gobrecht, *ibid.*, (5) **28S**, 673 (1937).
3. N. Chatterjee, *Z. Phys.*, **113**, 96 (1939).
4. L. G. Van Uitert and R. R. Soden, *J. Chem. Phys.*, **32**, 1161 (1960).
5. L. G. Van Uitert and R. R. Soden, *ibid.*, **32**, 1687 (1960).
6. L. G. Van Uitert and R. R. Soden, *ibid.*, in press (1960).
7. L. G. Van Uitert and R. R. Soden, *J. Appl. Phys.*, in press (1960).
8. W. Gordy, *J. Chem. Phys.*, **14**, 305 (1946).
9. A. D. Walsh, *J. Chem. Soc., London*, **1948**, 398.
10. C. E. Moore, "Atomic Energy Levels," National Bureau of Standards, V3 (1958).
11. Y. K. Syrkin and M. E. Dyatkina, "Structure of Molecules in the Chemical Bond," Interscience Publishers, New York (1950).
12. T. Moeller, "Inorganic Chemistry," J. Wiley & Sons, Inc., New York (1955).
13. W. L. Bragg and J. West, *Proc. Roy Soc*, **A111**, 691 (1926).
14. C. A. Coulson, V. Henri Memorial Volume, Desuer, Liege (1948).
15. V. V. Kuznetsoug and A. N. Sevchenko, *Akad. Nauk. Izv.*, **23**, No. 1, 2 (1959).
16. G. Urbain, *Ann. Chim. Phys.*, [8] **18**, 222 (1902).
17. M. Ch. de Rohden, *Ann. Chem.*, **3**, 338 (1915).

# Electroluminescence—A Disorder Phenomenon

**D. W. G. Ballentyne**

*Harlow Research Laboratories, Associated Electrical Industries Limited, Harlow, Essex, England*

ABSTRACT

In general, electroluminescence is considered to occur at a junction between a semiconducting crystal and a metal or electron rich material. The present work indicates that electroluminescence only occurs in zinc sulfide powders containing both sphalerite and wurtzite. This observation suggests that electroluminescence is a disorder phenomenon associated with stacking faults in the crystal.

Two types of electroluminescence have been observed. Certain substances (e.g., SiC, GaP, etc.) (1) emit light when subjected to a direct electric field applied between electrodes in contact with the surface of the crystal. This emission, carrier injection electroluminescence, is simply explained by the recombination of injected carriers at p-n junctions. The second type of electroluminescence, intrinsic electroluminescence (2), gives rise to the sustained emission of light on the application of an alternating field to the phosphor suspended in a dielectric. In this case, carrier injection is not possible, and the effect has been explained by the acceleration of carriers in an exhaustion barrier in the phosphor, say zinc sulfide activated with copper, at an interface with an electron rich layer of copper sulfide. Such a mechanism does not explain fully certain observations. Many workers have observed that light can be emitted internally from a crystal (2, 3). Steward, *et al.* (4) showed that the electroluminescent emission from a ZnS platelet occurred in bands parallel to birefringent-colorless bands denoting regions of wurtzite and sphalerite. Ultraviolet emission occurred throughout the crystal, and it was concluded that the emission in this case was associated with stacking faults in the c-direction. McKeag and Steward (5) reported a new method of preparing a zinc sulfide phosphor, which consisted of prefiring ZnS at 1200°C, activating with copper at 700°C. The material was electroluminescent throughout the body of the crystal. The copper necessary for the activation entered the crystal most effectively at the refiring stage which was the temperature where the transformation from the hexagonal to cubic zinc sulfide occurred most readily. There existed a correlation between electroluminescence and disorder.

In the present work (6) it is intended to show that in all cases investigated electroluminescent phosphors consist of mixtures of sphalerite and wurtzite. This structure is associated with a redistribution of trapping levels with the removal of the deep traps. An electroluminescent phosphor has been prepared without the addition of a substance capable of forming an electron rich layer. This phosphor also has a disordered structure.

## Experimental Results

Two types of general electroluminescent phosphors were prepared. One type of phosphor was prepared according to the Froelich (7) method at 1100°C, while the other group was prepared according to the Butler (8) method at 800°C. Various activators, copper, silver, and manganese, and various coactivators, aluminum, gallium, indium, and thallium, were added. The crystal structure of the phosphors was determined using a 9 cm Unican Powder camera in conjunction with a Raymax 60 x-ray set.

In Fig. 1 the diffraction photographs of a series of phosphors fired at 1100°C in wet $H_2S$ are given. The phosphors A, B, and C containing less than $10^{-4}$ g Cu/1 g ZnS are totally hexagonal in structure and are not electroluminescent. Phosphors D and E containing copper in excess of $10^{-4}$ g Cu/1 g ZnS contain both cubic and hexagonal zinc sulfide. These phosphors are electroluminescent. In the actual case

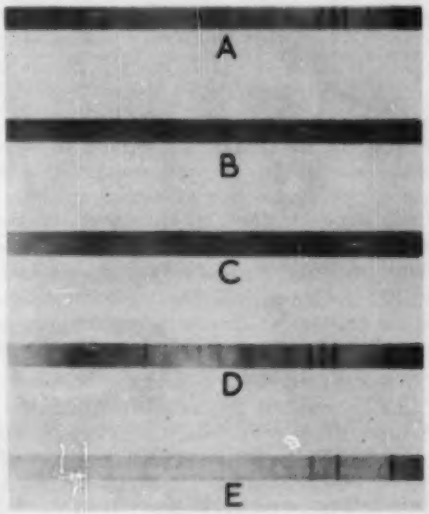


Fig. 1. X-ray powder photograph of a series of phosphors fired at 1100°C in wet $H_2S$. A, 1 g ZnS 1 x $10^{-4}$ g Cu 1 x $10^{-4}$ g Al; B, 1 g ZnS 1 x $10^{-5}$ g Cu 1 x $10^{-4}$ g Al; C, 1 g ZnS 1 x $10^{-4}$ g Cu 1 x $10^{-4}$ g Al; D, 1 g ZnS 1 x $10^{-6}$ g Cu 1 x $10^{-4}$ g Al; E, 1 g ZnS 1 x $10^{-6}$ g Cu 1 x $10^{-4}$ g Al.

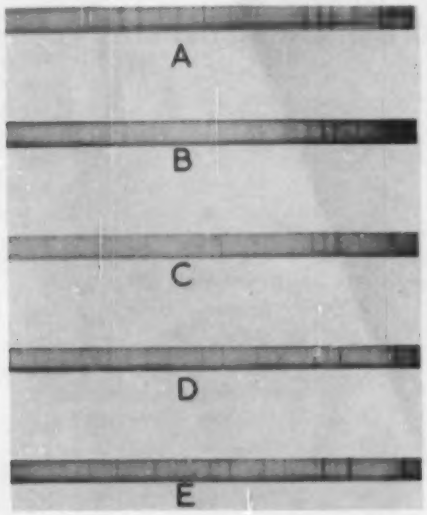


Fig. 2. X-ray powder photograph of a series of phosphors fired at 1100°C in wet $H_2S$. A, 1 g ZnS $2 \times 10^{-4}$ g Cu $1 \times 10^{-4}$ g Al; B, 1 g ZnS $4 \times 10^{-4}$ g Cu $1 \times 10^{-4}$ g Al; C, 1 g ZnS $6 \times 10^{-4}$ g Cu $1 \times 10^{-4}$ g Al; D, 1 g ZnS $8 \times 10^{-4}$ g Cu $1 \times 10^{-4}$ g Al; E, 1 g ZnS $1 \times 10^{-6}$ g Cu $1 \times 10^{-4}$ g Al.

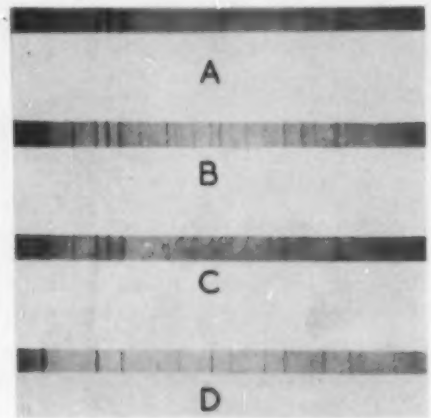


Fig. 3. X-ray powder photograph of a series of phosphors fired at 1100°C in wet $H_2S$. A, 1 g ZnS $1 \times 10^{-5}$ g Ag $1 \times 10^{-4}$ g Al; B, 1 g ZnS $1 \times 10^{-4}$ g Ag $1 \times 10^{-4}$ g Al; C, 1 g ZnS $1 \times 10^{-6}$ g Ag $1 \times 10^{-4}$ g Al; D, 1 g ZnS $1 \times 10^{-7}$ g Ag $1 \times 10^{-4}$ g Al.

given the concentration of aluminum coactivator was $10^{-4}$ g Al/1 g ZnS. The same result is obtained for aluminum concentrations varying between $10^{-5}$ g Al to $10^{-4}$ g Al/1 g ZnS. The replacement of aluminum by gallium or indium gives similar results. In Fig. 2 the diffraction photographs for a series of phosphors with copper concentrations between C and D in Fig. 1 are given. Up to a concentration of $6 \times 10^{-4}$ g Cu/1 g ZnS the material is hexagonal, above this concentration it consists of a mixture of two phases and only in these cases are the phosphors electroluminescent. It was thought that the correlation between electroluminescence and crystal structure might be fortuitous as copper sulfide precipitation onto the crystallites occurs at approximately the same concentrations. A study of silver phosphors indicates that this is not the case. The

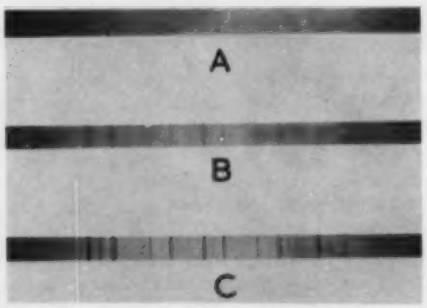


Fig. 4. X-ray powder diffraction photograph of a series of phosphors fired in argon at 800°C. A, 1 g ZnS $1 \times 10^{-6}$ g Cu $1 \times 10^{-6}$ g KCl; B, 1 g ZnS $1 \times 10^{-6}$ g Cu $1 \times 10^{-6}$ g $NH_4Cl$; C, 1 g ZnS $1 \times 10^{-6}$ g Cu $1 \times 10^{-6}$ g $NH_4Cl$ $1 \times 10^{-4}$ g Pb.

body color of a series of phosphors whose diffraction patterns are shown in Fig. 3 indicates that silver precipitation occurs at $10^{-4}$ g Ag/1 g ZnS. The mixed phases only occur in the phosphor containing $10^{-5}$ g Ag/1 g ZnS, and only this phosphor is electroluminescent. There was a further possibility that electroluminescence was a property of cubic zinc sulfide, and that it was the appearance of this phase rather than the formation of a mixture which caused the emission in the cases considered above.

Figure 4 shows the diffraction photographs of three typical so-called cubic zinc sulfide electroluminescent phosphors prepared below the transition point (1024°C). The best of these phosphors is C, and inspection shows that this phosphor has the most clearly defined hexagonal phase. It may be concluded, therefore, that in the so-called cubic electroluminescent zinc sulfide phosphors two phases are necessary for the emission, and the addition of the various substances during the preparation facilitates the growth of the hexagonal phase in the sphalerite temperature range.

Thermoluminescence experiments show that the appearance of electroluminescence and disorder in zinc sulfide is accompanied by a major change in the trapping states in the phosphor. Figure 5A gives the glow curves for the phosphors whose diffraction patterns are given in Fig. 1. It can be seen that the nonelectroluminescent phosphors containing less than $10^{-4}$ g Cu/1 g ZnS have trapping levels which cause a maximum in the glow curve at −100°C and a "tail" which extends to room temperature. The electroluminescent phosphors, on the other hand, have much shallower traps and the deeper traps have disappeared or no longer give rise to radiative transitions. This trend is shown more clearly in Fig. 5B for phosphors containing the same copper concentration ($10^{-4}$ g-$10^{-5}$ g) but with $10^{-6}$ g Al instead of $10^{-4}$ g Al/1 g ZnS. In this case the photoluminescent phosphors have a glow curve consisting of two peaks, one at −100°C, and one nearer room temperature at approximately −40°C. The electroluminescent phosphors again have a much narrower glow curve peak with a maximum between −120°C and −140°C.

Similar results have been obtained for all the other phosphors investigated, although the position

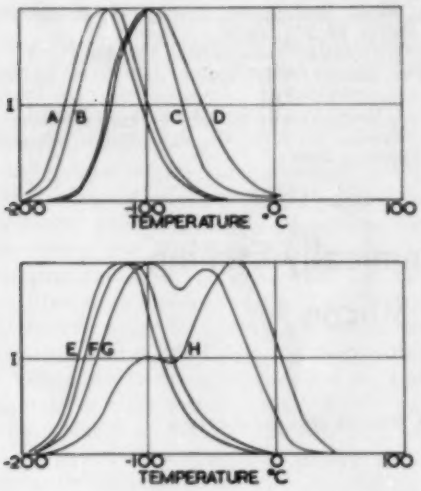


Fig. 5. Thermoluminescence curves of phosphors containing between $10^{-5}$ and $10^{-6}$ g Cu (D→A and H→E) with $10^{-4}$ and $10^{-6}$ g Al, respectively.

of the glow curve maximum does not appear to be so important as the absence of traps which extend the glow curve to room temperature.

These results appear to indicate, therefore, that electroluminescence occurs in crystals in which there are regions of both wurtzite and sphalerite. It may, therefore, be a property of the disordered region between the two types of crystal. If this is the case, then it should be possible to prepare an electroluminescent phosphor by disordering zinc sulfide by some other means than adding excess copper sulfide. Such a phosphor is described below.

During investigations into thallium-activated phosphors 10% TlCl was added to zinc sulfide and the phosphor was fired at 800°C in a stream of wet $H_2S$. The resulting phosphors were shown by spectroscopic means to contain no thallium ion; at the temperature of the experiment it had all sublimed. This phosphor was brilliantly photoluminescent and moderately electroluminescent in the green due presumably to vacancies. Exhaustive analysis did not indicate the presence of copper or thallium. The body color, off-white, also showed that an excess of electron-rich material which hitherto had been thought to be necessary for electroluminescence was not present. Figure 6 shows that the crystals of phosphor consisted of a mixture of hexagonal and cubic zinc sulfide. That this phosphor is electroluminescent is shown by the brightness against voltage and frequency curves. The brightness variation may be expressed by the usual relation

$$B = A_s \sqrt{F} \exp\left(-b/\sqrt{v}\right)$$

## Discussion

Conventional electroluminescent phosphors have been shown to consist in all cases of the two phases of zinc sulfide, wurtzite, and sphalerite. It would appear possible that electroluminescence can occur without the addition to the phosphor of a material that could act as an electron source.

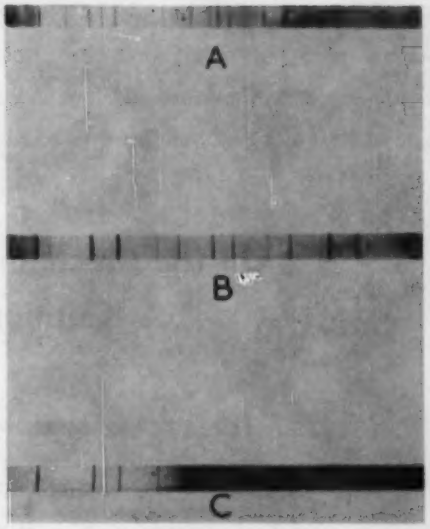


Fig. 6. X-ray powder photograph of: A, hexagonal zinc sulfide; B, 0.9 g ZnS 0.1 g TlCl fired at 800°C in $H_2S$; C, cubic zinc sulfide.

It is difficult to see, however, where the field for the acceleration of the electrons sufficient to ionize the luminescent centers can arise in such a system. The band gap energy between the two forms of zinc sulfide is small (0.01 ev), but Merz considers that the impurities may cause the band gap to widen to 0.1 ev. The observation of high photovoltages in zinc sulfide single crystals (9) shows experimentally that high fields must exist in these crystals, although the mechanism is obscure. In view, however, of these results, it may not be amiss to suggest the possibility that electroluminescence is a recombination effect at what is essentially a p-n junction. The original objections to this approach, the low threshold and the minority carrier being a hole, is not now important. The threshold of electroluminescence has been shown to depend on the method of detection of the light emitted, and Destriau has been able to go down to levels 0.01 of that visible to the dark adapted eye and still detect light. Wood's (10) observation of p-type conduction in cadmium sulfide doped with copper shows that p-type conduction in the II-VI compounds is not so unlikely as has been hitherto thought.

However, it must be admitted that no explanation of the biphase effect in electroluminescence is satisfactory, and at present the experimental results only are reported.

## Acknowledgments

The author would like to thank Dr. M. E. Haine and the A.E.I. (Woolwich) Research Laboratories for permission to publish these results. Further, he would like to acknowledge with gratitude the help of his colleagues during the course of this work.

Manuscript received March 7, 1960.

Any discussion of this paper will appear in a Discussion Section to be published in the June 1961 JOURNAL.

## REFERENCES

1. See, for example, G. Destriau and H. Ivey, *Proc. I.R.E.*, **44**, 1911 (1956).

2. G. Destriau, *Phil. Mag.*, **38**, 700 (1947); P. Zalm, *Philips Research Reports*, **11**, 353 (1956).
3. See, however, D. Frankl, *Phys. Rev.*, **100**, 1105 (1956).
4. M. A. Short, E. G. Steward, and T. B. Tomlinson, *Nature*, **177**, 240 (1956).
5. A. H. McKeag and E. G. Steward, *This Journal*, **104**, 41 (1957).
6. D. W. G. Ballentyne, *J. Physics & Chemistry of Solids*, **10**, 272 (1959).
7. H. C. Froelich, *This Journal*, **100**, 496 (1953).
8. H. H. Homer, R. M. Rulon, and K. H. Butler, ibid., 100, 566 (1953).
9. W. J. Merz, *Helv. Phys. Acta*, **31**, 6 (1958).
10. J. Woods, Birmingham Symposium on Dielectric Devices, 1959.

# On the Mechanism of Chemically Etching Germanium and Silicon

**D. R. Turner**

*Bell Telephone Laboratories, Incorporated, Murray Hill, New Jersey*

ABSTRACT

The electrode potential of germanium or silicon in a chemical etching solution is a function of solution pH, rate of etching, physical condition of the surface, conductivity type, and resistivity. The results suggest that excess holes and electrons are produced at the surface of the semiconductor during chemical etching. Holes are injected at cathode sites, but only a portion of these holes are consumed at anode sites since the anode reaction involves current multiplication.

Semiconductors such as Ge or Si are chemically etched in aqueous solutions containing an oxidizing agent such as nitric acid and an anion such as $F^-$ which is capable of forming water-soluble complexes with the semiconductor. The etching process is actually electrochemical in its action, that is, there are anode and cathode sites on the surface of the semiconductor with local cell currents flowing between them. Semiconductor material goes into solution at the anodic sites while the oxidizing agent is reduced at the cathodic areas. The rate of chemical etching is determined by the magnitude of the corrosion current. If the etching process is nonpreferential and material is removed uniformly, any given area on the surface of the semiconductor must continually alternate between being anode and cathode. When one spot is anodic much more than it is cathodic, an etch pit will form at that point. Experience has shown that this is most likely to occur at grain boundaries and dislocations at the surface of the single crystal. Conversely, hillocks are formed on areas that are cathodic more than they are anodic.

The average current density between local anode and cathode areas during chemical etching can be estimated from the rate of etching. Assuming that the surface while etching is half anode and half cathode and that Ge or Si goes into solution with a valence of 4, the average corrosion current density in amp/cm$^2$ is given by:

$$i = 2\Delta\epsilon d \qquad [1]$$

where $\Delta$ is the etch rate in cm/sec, $\epsilon$ is the electrochemical equivalent in coulombs/g, and $d$ is the density of the semiconductor in g/cm$^3$. The rate of chemically etching n-type Si in HF-$HNO_3$ mixtures has been determined by Robbins and Schwartz (1). A plot of some of their data along with the equivalent corrosion current density derived from Eq. [1] is shown in Fig. 1. Similar results should be obtained for p-type Si specimens. The etch rate can be converted into inches per minute by multiplying by the factor $2.36 \times 10^{-5}$. The maximum rate of etching occurs when the ratio of $HNO_3$ to HF in the solution is 1 to 4.5. Klein (2) has studied the rate of chemically etching silicon in $HNO_3$-HF mixtures under carefully controlled conditions of temperature and stirring. He also found that maximum etching rate occurred when the $HNO_3$/HF mole ratio was about 1 to 4.5. The significance of this ratio will be discussed later. The maximum Si etch rate is about 28 $\mu$/sec which corresponds to about 190 amp/cm$^2$ average corrosion c.d. This is a tremendous current density, but even more amazing is the fact that an n-type silicon electrode biased anodically in a suitable electroetching solution will pass just a few $\mu$a/

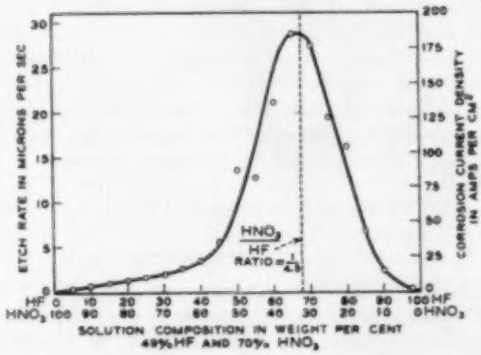
ETCH RATE IN MICRONS PER SEC
CORROSION CURRENT DENSITY IN AMPS PER CM²
HNO₃/HF RATIO = 1/4.5
HF 0 10 20 30 40 50 60 70 80 90 100 HF
HNO₃ 100 90 80 70 60 50 40 30 20 10 0 HNO₃
SOLUTION COMPOSITION IN WEIGHT PER CENT
49% HF AND 70% HNO₃

Fig. 1. Rate of chemical etching Si and equivalent corrosion C.D. vs. solution composition, HF + $HNO_3$ mixtures. Etch rate vs. solution composition data from Robbins and Schwartz (1).

cm². This means the maximum chemical etch rate is higher by a factor of $10^6$ than the maximum electrolytic etch rate. In order to obtain a better understanding of this phenomenon, potential measurements were made on Ge and Si electrodes in etching and nonetching solutions.

Potential measurements always require two electrodes. If the second electrode is a standard reference electrode, i.e., its potential is known and is constant during the experiment, then the single electrode potential of a semiconductor can be determined from the measured cell voltage. Semiconductor electrodes differ from metal electrodes in that an appreciable part of the single electrode potential may be located inside the semiconductor. In analyzing the potential measurements made on Ge and Si it will be necessary to consider the potential within the semiconductor as well as that at the semiconductor-solution interface.

### Experimental Studies on Electrode Potentials

Bars of n- and p-type Ge and Si were used as electrodes. The size, geometry, and surface orientation of the electrodes did not affect the measured potentials within the limit of experimental reproducibility—about ± 0.005 v. Ohmic contacts were made to the Ge by abrading one end, tinning and soft soldering it to a Cu wire. The Si electrodes were abraded at one end and then coated with nickel by the "electroless process" (3) before soldering to the Cu wire. Prior to the potential measurement, each electrode was bright etched in C.P.-4 etching solution (for Si the bromine is omitted), rinsed in deionized water, and blotted dry with filter paper. The electrodes were held vertically during a measurement so that only the tip end of the semiconductor was immersed. Unless otherwise indicated, the solutions were unstirred and initially at room temperature. All potential measurements were made against a saturated KCl calomel reference electrode, hereafter referred to as S.C.E.

Since many of the electrolytes used contained HF or strong alkali, polyethylene containers were used instead of glass. The electrolyte was separated from the saturated KCl solution and the reference electrode by a polyethylene syphon fitted with a filter paper plug. Electrode potential measurements were made with either a Millivac Type MV-17C d-c voltmeter, a L&N X-Y recorder, or a Sanborn Type 151 recorder depending on the experiment and the kind of data desired.

Single electrode potential measurements were made in a variety of solutions, some etching and others nonetching. The results of potential measurements in some of the solutions are shown in Fig. 2. The solutions listed are arranged in their approximate order of increasing pH from left to right: (A) conc. (16*N*) $HNO_3$, (B) CP-4 without Br, (C) 32% conc. $HNO_3$ + 68% (48%) HF, (D) Landgren's etch (4) — 3% $KMnO_4$ + 97% conc. $HNO_3$,[1] (E) 48% HF, (F) sat. KCl, and (G) 1N KOH. All per cent compositions in this paper are weight per cent values. The potentials of n- and p-type Ge electrodes are indicated by the small letters while the capital letters are for Si electrodes. These are average values of measurements made on 3 to 5 different electrodes. The spread of the data is indicated where it is more than ±0.02 v. Whenever the electrode potential was photosensitive, the cell was shielded from room light.

[1] Solution rapidly etches p-type portions of a silicon single crystal containing p- and n-regions with little effect on n-type regions.

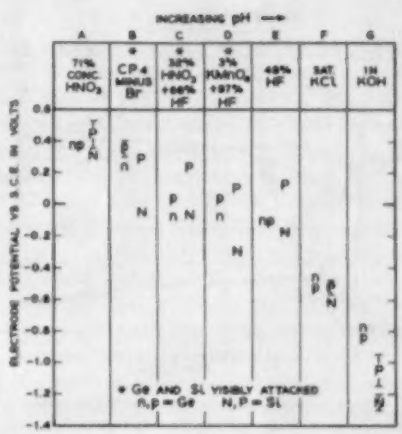


Fig. 2. Electrode potentials of n- and p-type Ge and Si in various etching and non-etching solutions. Unstirred at room temperature.

Figure 2 shows three things: (*a*) increasing pH shifts the electrode potential in the negative direction; (*b*) an appreciable potential difference is observed between n and p-type Ge and Si when the solution rapidly corrodes the semiconductor; and (*c*) p-type Ge or Si is always positive in potential with respect to n-type when a potential difference does exist. The effect of pH on the electrode potential of Ge has been observed many times before (5, 6). Cretella and Gatos (7) have observed n-type Ge to be positive in potential with respect to p-type Ge in nitric acid solutions more dilute than 6*N*. This effect cannot always be duplicated. The surface pretreatment appears to be more of a factor than the nitric acid solution. In rapidly etching solutions, however, the results are reproducible and p-type Ge is positive relative to n-type Ge. In etching solutions where the rate of corrosion is controlled by the mass transfer of one of the reacting species to or from the surface stirring increases the etch rate and it also may shift the electrode potential. The effect of stirring on the electrode potentials of Ge and Si are discussed later. If the solution does not attack the semiconductor at an appreciable rate, there is no potential difference between n- and p-type electrodes of either Ge or Si. Electrolytes B, C, and D in Fig. 2 visibly attack both Ge and Si, as evidenced by gas evolution and rapid electrode dissolution. The potential difference between n- and p-type Si in 48% HF is attributed to a slow corrosion process which is made possible by dissolved oxygen. Solution G (1*N* KOH) also attacks Si but only slowly at room temperature. When the electrolyte corrodes the semiconductor at a sufficiently rapid rate, light has no effect on the measured electrode potentials. The potential of Ge and Si in etching solutions is

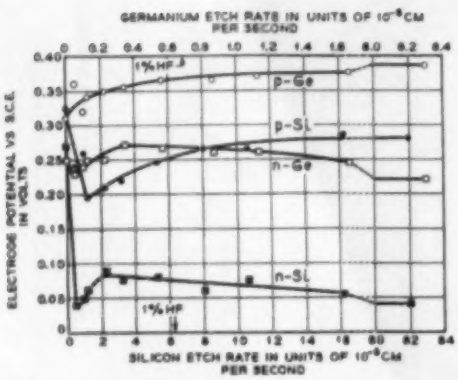


Fig. 3. Effect of etch rate on the electrode potentials of n- and p-type Ge and Si in HF-$HNO_3$ mixtures. Rate of etching increased by adding HF to $HNO_3$.

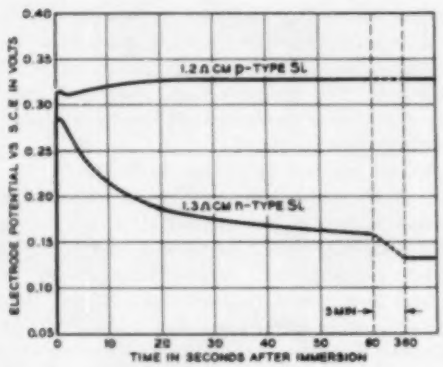


Fig. 4. Electrode potential-time curves for lapped n- and p-type Si immersed in 10% HF + 90% $HNO_3$.

also a function of the equilibrium hole density in the semiconductor, as is shown later.

A fresh solution of concentrated $HNO_3$ does not chemically etch Ge or Si at an appreciable rate. The etch rates increase rapidly with additions of HF as shown by Cretella and Gatos (7) for Ge and Robbins and Schwartz' for Si (see Fig. 1). It is of interest to observe the change in the single electrode potential of a semiconductor when the electrolyte changes from an essentially nonetching solution to an etching one. This experiment was carried out by measuring the electrode potentials of 0.8 ohm cm n- and 3.5 ohm cm p-type Ge and 0.7 ohm cm n- and 1.2 ohm cm p-type Si first in concentrated $HNO_3$ and then with various additions of HF. In concentrated $HNO_3$ alone the electrode potentials are extremely light-sensitive. For this reason, all light was excluded from the cell. Instead of plotting electrode potential against the amount of HF added, it is more meaningful to show the relation between the electrode potential and the rate of etching as given in Fig. 3. The etch rate for a solution composition 1% (49%) HF + 99% concentrated $HNO_3$ is indicated for both Ge and Si. The etch rate for Ge in conc. $HNO_3$ solutions containing from 0 to 10% (49%) HF was determined experimentally from weight loss measurements with four specimens, two n-type and two p-type. Robbins and Schwartz's[1] data, Fig. 1, was used for Si. Note that Si etches about ten times faster than Ge in comparable HF-$HNO_3$ mixtures. One drop (~ 0.04 cc) of 49% HF produces a large shift in the potential of n- and p-type Si and n-type Ge toward the negative direction. p-Type Ge changes slightly in the positive direction. As the etch rate increases with more HF, the electrode potentials of n-type Ge and Si rise and then decrease again while the potentials of p-type Ge and Si increase. The electrode potentials of all the electrodes reach relatively stable values in solutions containing about 10% HF + 90% $HNO_3$, where the etch rate is 63 x $10^{-5}$ cm/sec on Si and 6.7 x $10^{-5}$ cm/sec on Ge. At this rate of etching the photovoltaic effect is completely absent.

Another interesting experiment was to abrade the surface of semiconductor electrodes and record the change in potential with time as the damaged surface layer was chemically etched away. This was done with 1.3 ohm cm n- and 1.2 ohm cm p-type Si electrodes. The surfaces were abraded by lapping on a glass plate with No. 600 silicon carbide and water. Typical electrode potential-time curves after immersion in 10% (49%) HF + 90% concentrated $HNO_3$ are shown in Fig. 4. Initially the electrode potentials of abraded n- and p-type Si are about the same. As the damaged surface layer is etched away, the potentials drift apart. The largest potential change occurs with the n-type Si electrode. p-Type Si reaches a stable potential in about 30 sec while the potential of n-type Si becomes stable after 6 min. A potential measurement of this kind may be useful in determining when all the abraded surface material has been removed by etching.

Single electrode potentials of n- and p-type Ge and Si in $HNO_3$ + HF acid mixtures were also measured as a function of material resistivity. To get reproducible results it was necessary to use freshly prepared solutions. The electrode potentials against the resistivity, $\rho$, and the equilibrium bulk hole density, p, at 300°K, are shown on a semilog plot in Fig. 5 and 6. The p values were determined from the resistivities using the relation:

$$\frac{1}{\rho} = q\mu_n n + q\mu_p p$$

where $q$ is the charge on the electron, $\mu_n$ is the electron mobility, $n$ is the equilibrium bulk electron

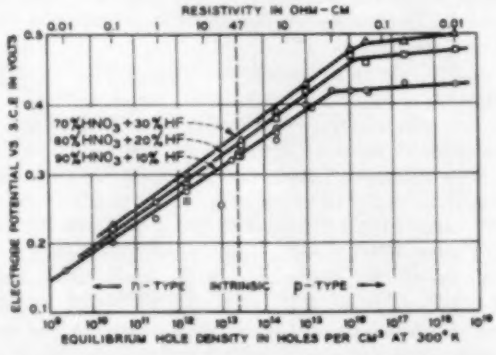
RESISTIVITY IN OHM-CM
ELECTRODE POTENTIAL VS S.C.E. IN VOLTS
70% HNO3 + 30% HF
80% HNO3 + 20% HF
90% HNO3 + 10% HF
n-TYPE
INTRINSIC
p-TYPE
EQUILIBRIUM HOLE DENSITY IN HOLES PER CM³ AT 300° K

Fig. 5. Electrode potentials of Ge in $HNO_3$-HF mixtures vs. resistivity and equilibrium hole density.

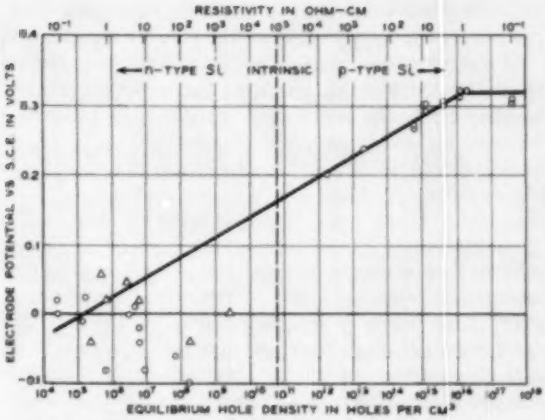


Fig. 6. Electrode potentials of Si in 90% conc. $HNO_3$ + 10% conc. HF vs. resistivity and equilibrium hole density.

density, and $\mu_p$ is the hole mobility. Electron and hole mobilities were obtained from Prince's (8) data and $n$ was derived from the relations: $np = 6.25 \times 10^{26}/cm^6$ at 300°K for Ge and $np = 4.6 \times 10^{26}/cm^6$ at 300°K for Si.

Electrode potentials of Ge were measured in 90% $HNO_3$ + 10% HF, 80% $HNO_3$ + 20% HF, and 70% $HNO_3$ + 30% HF. The measured potentials were fairly stable in freshly prepared 90% $HNO_3$ + 10% HF, but in the other solutions, where the rate of etching was more rapid, the potentials fluctuated probably because of the stirring effect produced by a greater rate of gas evolution. Most of the data show a linear relation between the electrode potential and the logarithm of the equilibrium hole density with a slope of 0.04 up to about $p \sim 10^{16}$ holes/$cm^3$. Above $10^{16}$ holes/$cm^3$, the electrode potential becomes almost constant. The reason for this limiting potential effect is discussed later. Although there is some difficulty in obtaining a reasonably accurate potential measurement at the higher etching rates, it is clear that at a given equilibrium hole density the electrode potential increases with the etching rate. The difference is most apparent in the region where the potential levels off.

The variation of the electrode potential of Si with $p$ in 90% $HNO_3$ + 10% HF is different from the Ge results in some respects, as can be seen in Fig. 6. The data obtained with p-type Si electrodes have the same form as p-type Ge except that the slope of the best straight line through the points is about 0.03 instead of 0.04. The results with n-type Si are quite different from those of n-type Ge. The points are widely scattered and there does not appear to be a consistent relation between $E_{III}$ and $p$. It was thought at first that perhaps minority carrier lifetime was an important factor. Several uncompensated Si specimens were obtained with reasonably good lifetimes for the resistivity. These results are the triangular points in Fig. 6 and are also widely scattered. An extrapolation of the line from the p-side to the n-side shows the extent of deviation and that there are a few points near the line.

## Discussion

An interpretation of the electrode potential measurements on Ge and Si in etching and nonetching solutions should aid in elaborating the mechanism of chemical etching Ge and Si. It will be convenient to discuss the three parts of the measured electrode potentials: (*a*) the contact potential between the copper wire attached to the semiconductor by means of an ohmic contact and the semiconductor bulk ($E_I$), (the contact potential is defined as the potential difference in the work functions of the metal and the semiconductor), (*b*) the potential drop across the space-charge layer between the semiconductor bulk and the surface ($E_{II}$) (this is called the surface potential, $\Psi_s$, by physicists), and (*c*) the potential across the semiconductor-electrolyte interface ($E_{III}$).

The contact potential $E_I$ between the copper and the semiconductor varies with the position of the Fermi level in the semiconductor bulk; that is, the nature of the doping. The contact potential can be considered to be constant in the electrode potential measurements on a given semiconductor specimen at room temperature. In nonetching solutions, that is, when there is essentially no charge transfer across the semiconductor-electrolyte interface and the semiconductor is at equilibrium, $E_I + E_{II}$ is also a constant regardless of the conductivity type and semiconductor resistivity. This is due to the fact that the Fermi level at the surface of a semiconductor in solutions is determined not by the bulk charge carrier density but by the charge density at the surface. This is illustrated in Fig. 7. The Fermi level at the surface is at a fixed position relative to the valence and conduction bands, that is, $\Phi_s$ is independent of the bulk properties of the semiconductor (9, 10). This means that the potential difference $\Delta E_{II}$ between n- and p-type material is exactly equal but opposite in sign to the contact potential difference $\Delta E_I$. In nonetching solutions, therefore, changes in the measured electrode poten-

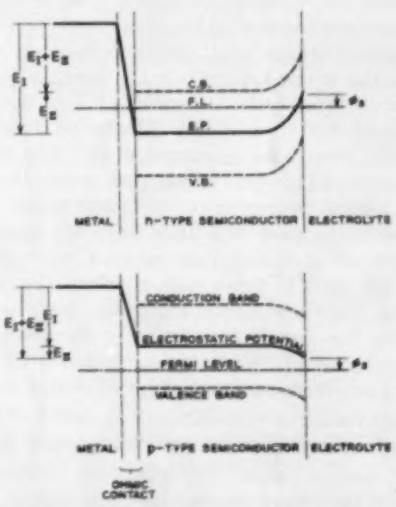


Fig. 7. Energy level diagrams for an n- and p-type semiconductor in contact with a metal and an electrolyte.

tial can be due only to changes in the interfacial potential ($E_{III}$).

Potential differences between n- and p-type Ge or n- and p-type Si are observed when the electrodes immersed in a nonetching electrolyte are illuminated with light or when they are immersed in a chemical etching solution without light. Under these conditions the surface region of the semiconductor is not at equilibrium. The photovoltaic effect of semiconductor electrodes in solutions has been observed many times (11, 12). It is attributed to hole-electron pairs produced by light energy in the surface region. These extra hole-electron pairs change the Fermi level at the surface of the semiconductor with respect to that of the bulk, that is, $E_{II}$ changes. The measured electrode potential of semiconductors changes when illuminated with light (11, 13). The sign and magnitude of the potential differences between n- and p-type electrodes in etching solutions as shown in Fig. 5 and 6 are essentially the same as those obtained in the photovoltaic effect. This suggests that holes and electrons are produced at the surface of the semiconductor during chemical etching. Several other observations tend to support this interpretation: (*a*) the photovoltaic effect disappears even at moderate rates of chemical etching; (*b*) the rectifying characteristic of a broad-area p-n junction is completely eliminated if either side of the junction is exposed to an etching solution; (*c*) a Ge or Si diode, with masked leads, generates a considerable amount of power (~ 0.3 milliwatt/cm of exposed junction length) when immersed in C.P.-4 solution; and (*d*) the saturation current density of n-type Ge or Si made anodic in a chemical etching solution increases in proportion to the rate of etching (14). These effects can be explained satisfactorily only by assuming that large numbers of holes and electrons are produced at the surface of semiconductors during chemical etching.

The mechanism of chemically etching Ge and Si must include a source of excess holes and electrons. As stated earlier, chemical etching of semiconductors is an electrochemical process with local anode and cathode areas. Semiconductor dissolution takes place at the anode sites, while the oxidizing agent is reduced at the cathode areas. It has been well established that the anodic dissolution reaction at Ge and Si electrodes consumes holes (11). Brattain and Garrett (11) also found that when they anodically biased an n-type Ge electrode to the saturation current region and then injected holes with light, the total dissolution current increased between 1.4 to 1.8 times the current due to hole injection. Turner (15) has suggested that the mechanism for the anodic dissolution of Ge involves the diffusion of two holes to the surface with a return flow of two electrons for each atom dissolving. This would give a current multiplication factor of 2. Beck and Gerischer (9), however, have found that the current multiplication factor is near 2 only when holes are consumed as fast as they arrive at the anode surface. If holes can diffuse to the surface or holes are injected into the surface region faster than they are consumed in the anode reaction, then the current multiplication factor may be less than 2.

If a semiconductor such as Si is chemically etched in a $HNO_3$-HF acid mixture, the reaction at the anode sites is the dissolution of silicon as follows:

$$Si + 2H_2O + ne^+ \rightarrow SiO_2 + 4H^+ + (4-n)\,e^- \qquad \xrightarrow{6HF} \quad H_2SiF_6 + 2H_2O \quad [2]$$

where $e^+$ represents a hole and $n$ is the average number of holes required to dissolve 1 Si atom; $n$ may range from 2 to 4 depending on the current multiplication factor. A Si dissolution valence of four is assumed for the process which is probably correct for $HNO_3$-rich solutions. In HF-rich solutions, there is evidence that Si dissolution is divalent (12, 16, 17). It is also assumed that Si dissolves by first forming an oxide which then reacts with HF to form the water-soluble silicofluoride complex.

The main function of the oxidizing agent in the chemical etching solution is not to oxidize the semiconductor as is sometimes proposed (1) (Ge and Si are readily oxidized in most oxygen-containing systems) but to provide an easily reduced material for the cathode reaction. In the absence of an oxidizing agent (including oxygen) and metal ions more noble than the semiconductor, the only cathode reaction possible is the discharge of hydrogen ions. The hydrogen discharge reaction can only proceed at a very slow rate, however, because of hydrogen overvoltage. This limits the chemical etching rate to a negligible value.

Oxidizing agents do more than provide an easily reduced material at semiconductor electrodes. They modify the distribution of mobile charge carriers in the surface region so that the Fermi level at the surface is nearer the valence band than it is the conduction band. This is illustrated in Fig. 7. The electron transfer process in the reduction of the oxidizing agent involves the transfer of an electron from the valence band to the ion being reduced. It is equivalent to hole injection. This concept was formulated independently by Gerischer and Beck (9, 18) and Dewald (10). Both have obtained experimental evidence in support of this mechanism. Pleskov (19), using a novel technique of working both sides of a Ge electrode electrochemically, has confirmed their observations.

The reduction of $HNO_3$ is a complicated reaction involving several steps (20, 21). Cretella and Gatos (7) have shown that the mechanism proposed by Vetter (20) for the cathodic reduction of $HNO_3$ on a Pt electrode also applies to Ge. The over-all reaction can be written as follows:

$$HNO_3 + 2H^+ \rightarrow HNO_2 + H_2O + 2e^+ \qquad [3]$$

Holes injected into the semiconductor by the cathodic reduction of the oxidizing agent supply the holes required for the anodic dissolution part of the chemical etching process. Combining Eq. [2] with two times Eq. [3] (for charge balance) gives the following over-all reaction for chemically etching silicon in $HNO_3$-HF mixtures:

$$Si + 2HNO_3 + 6HF \rightarrow H_2SiF_6 + 2HNO_2 + 2H_2O + (4-n)e^+ + (4-n)e^- \quad [4]$$

Each atom of Si dissolving uses up to 2 molecules of $HNO_3$ and six of HF. The activation energy (~ 4 kcal/mole) (2, 22) for the over-all reaction indicates that the kinetics of the process is diffusion-controlled. Therefore, if the rates of diffusion and convection of $HNO_3$ and HF from the solution bulk to the Si surface are approximately equal, the maximum etching rate should occur when the mole ratio of $HNO_3$ to HF is 1/3 [solution composition: 42% by wt (70%) $HNO_3$ + 58% by wt (49%)HF].

Schmid and Spahn (21, 23) found that $HNO_3$ reduces beyond nitrous acid, $HNO_2$, to nitric oxide, NO, when copper is chemically etched in $HNO_3$. For this mechanism, the over-all cathodic reduction of nitric acid is

$$HNO_3 + 3H^+ \rightarrow NO + 2H_2O + 3e^+ \quad [5]$$

Robbins and Schwartz (1, 24) have assumed that $HNO_3$ reduces to NO as in Eq. [5] when Si is chemically etched in $HNO_3$-HF mixtures. However, they also propose that the anode reaction product is $SiF_4$. As a result, their over-all anode-cathode reaction for etching silicon in $HNO_3$-HF mixtures gives a 1/3 mole ratio as in Eq. [4] which is only fair in agreement with the results shown in Fig. 1. An excellent agreement is obtained, however, if $H_2SiF_6$ is assumed to be the anode reaction product instead of $SiF_4$. The over-all etching reaction obtained by combining Eq. [2] and [5] (Eq. [2] is multiplied by 3 and Eq. [5] by 4 for the necessary charge balance) is as follows:

$$3Si + 4HNO_3 + 18HF \rightarrow 3H_2SiF_6 + 4NO + 8H_2O + 3(4-n)e^+ + 3(4-n)e^- \quad [6]$$

The mole ratio of $HNO_3$ to HF for this reaction is 4/18 or 1/4.5. This agrees very well with the $HNO_3$-HF composition which gives the maximum rate of etching shown in Fig. 1 [33% by wt (70%)$HNO_3$ + 67% by wt (49%)HF]. Klein (2) obtained a maximum etching rate on Si at about the same solution composition. Robbins and Schwartz (1) have properly concluded that to the left of the maximum, where the HF concentration is relatively low, the rate of etching is controlled by the diffusion and convection of HF to the Si surface. The arrival of $HNO_3$ at the Si surface becomes rate determining in solutions with compositions to the right side of the maximum in Fig. 1.

The number of excess holes and electrons produced in chemically etching Si, as shown in Eq. [4] and [6], depends on the rate of etching and the current multiplication factor $\left(\alpha = \frac{4}{n}\right)$ in the anode reaction. If $n$ is 2, then $\alpha = 2$; but if 4 holes are consumed in dissolving 1 Si atom, then $\alpha = 1$ and no excess holes and electrons are produced. Potential measurements on Ge and Si electrodes in chemical etching solutions indicate that $\alpha > 1$, since the potential is a function of the conductivity type and resistivity as shown in Fig. 5 and 6. The measured electrode potential, except for n-type Si, is shown to be a logarithmic function of the equilibrium hole density. At present, the author does not have a satisfactory interpretation of the results obtained with n-type Si. The material lifetime or the total impurity density were found not to be a factor. Dewald (10) has shown that holes are the potential-determining carriers at semiconductor electrodes in etching solutions. The hole density just inside the space-charge layer ($p_s$) is large on n-type as well as p-type electrodes. For very strongly p-type samples (equilibrium hole densities $p > \sim 10^{16}$ holes $cm^{-3}$), $p_s$ is not appreciably different from the equilibrium hole density and the measured electrode potential becomes almost constant. The limiting potential effect should occur at higher p values if the rate of hole generation at the surface increases. This is confirmed by the results shown in Fig. 5 since the etch rate increases with larger amounts of HF.

The potential ($E_{III}$) at the semiconductor-electrolyte interface can best be illustrated with typical anode and cathode potential-current curves as shown in Fig. 8. In order to simplify the diagram, the *IR* drops in the local corrosion circuits were not included. In $HNO_3$-HF mixtures the cathode reaction is the reduction of $HNO_3$ according to Eq. [5], while the anode reaction is the dissolution of the semiconductor, Eq. [2]. The case illustrated in Fig. 8 is the condition where the etching rate is determined by the mass transfer of HF to the surface. The intersection of the anode and cathode curves determines the etching or corrosion current, and the measured potential of the electrode. In concentrated $HNO_3$ without HF, the corrosion current is essentially zero and the measured potential is the open-circuit potential of the cathode reaction—the reduction of nitric acid on the semiconductor. When HF is added, the anode reaction proceeds at a much higher rate before polarization sets in, curve $A_2$. The etching rate on Ge or Si increases markedly and the measured electrode potential changes in the negative direction. When the measured electrode potential is appreciably far from the open-circuit anode or cathode potential it is often called a mixed corrosion potential. The large initial poten-

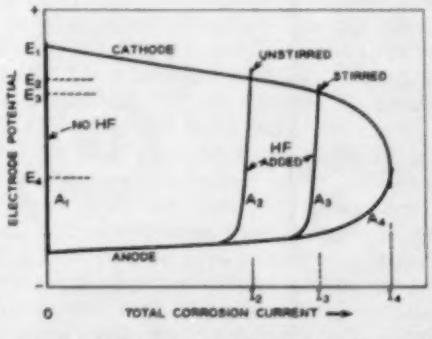


Fig. 8. Typical electrochemical polarization curves for local anodes and cathodes on Ge or Si in $HNO_3$ with and without HF additions.

tial change in Fig. 3 which occurred when a small amount of HF was added to $HNO_3$ is attributed to a large change in the mixed interfacial potential. Subsequent changes in the electrode potential at higher etch rates with more HF as shown in Fig. 3 are complicated by changes in $E_{ii}$ (inside the semiconductor) due to the excess holes and electrons produced. Stirring increases the supply of the rate-determining material to the surface of the semiconductor. This increases the corrosion current and shifts the electrode potential, as shown in Fig. 8. The potential change with stirring is easily demonstrated by simply jiggling the electrode. When HF is the rate-determining material the potentials of both n- and p-type Ge (or Si) always shift in the negative direction and when $HNO_3$ is the controlling factor, the potentials become more positive with stirring. Current $I_s$ and potential $E_s$ represent the values obtained when the mass transfer of $HNO_3$ and HF are equally rate determining. As previously mentioned, this occurs on Si at the maximum rate of etching when the $HNO_3$/HF ratio is about 1-4.5.

## Summary and Conclusions

The chemical etching of semiconductors is really an electrochemical process. Semiconductor dissolution takes place at local anode sites while the oxidizing agent is reduced at local cathode areas. The total anodic current always equals the total cathodic current. The average anode and cathode current density calculated from rates of etching data is in the order of amperes per square centimeter. The rate of etching is controlled by the mass transfer of an ionic or molecular species in the electrolyte to the surface of the semiconductor. It is not limited by the supply of holes or electrons in the semiconductor surface. In fact an excess of holes and electrons are produced at the surface. The large number of holes required to maintain the semiconductor dissolution reaction rate at amperes per square centimeter are supplied by hole injection at nearby cathodic areas. Due to a current multiplication effect in the anode reaction, an equal number of excess holes and electrons are produced at the semiconductor surface. These excess holes and electrons modify that part of the measured electrode potential which is just inside the surface of the semiconductor.

## Acknowledgments

The author is grateful to Miss A. D. Mills and D. D. Bacon for their help in obtaining the germanium and silicon electrode material used in this work. He is also indebted to U. B. Thomas, J. F. Dewald, and D. L. Klein for their aid in interpreting the data and suggestions as to the best way to present the material.

Manuscript received March 30, 1960. This paper was prepared for delivery before the Chicago Meeting, May 1-5, 1960.

Any discussion of this paper will appear in a Discussion Section to be published in the June 1961 JOURNAL.

## REFERENCES

1. H. Robbins and B. Schwartz, *This Journal*, **106**, 505 (1959).
2. D. L. Klein, Recent News Paper, Electrochem. Soc. Meeting, Chicago (1960).
3. M. V. Sullivan and J. H. Eigler, *This Journal*, **104**, 226 (1957).
4. C. R. Landgren, U. S. Pat. 2,847,287, Aug. 12, 1958.
5. M. L. Nichols and S. R. Cooper, *Ind. and Eng. Chem. Anal. Ed.*, **7**, 350 (1935).
6. W. W. Harvey and H. C. Gatos, *This Journal*, **107**, 65 (1960).
7. M. C. Cretella and H. C. Gatos, *ibid.*, **105**, 487 (1958).
8. M. B. Prince, *Phys. Rev.*, **92**, 681 (1953); **93**, 1204 (1954).
9. F. Beck and H. Gerischer, *Z. Elektrochem.*, **63**, 943 (1959).
10. J. F. Dewald, "Semiconductors," Chap. 17, Reinhold Publishing Corp., New York (1959).
11. W. H. Brattain and C. G. B. Garrett, *Bell System Tech. J.*, **34**, 129 (1955).
12. A. Uhlir, *ibid.*, **35**, 333 (1956).
13. W. W. Harvey and H. C. Gatos, *J. Appl. Phys.*, **29**, 1267 (1958).
14. D. R. Turner, To be published.
15. D. R. Turner, *This Journal*, **103**, 252 (1956).
16. D. R. Turner, "Surface Chemistry of Metals and Semiconductors," H. C. Gatos, Editor, John Wiley & Sons, Inc., New York (1960).
17. R. J. Archer, *J. Phys. Chem. Solids*, In press.
18. H. Gerischer and F. Beck, *Z. Phys. Chem.*, **13**, 389 (1957).
19. Iu. V. Pleskov, *Akad. Nauk. SSSR, Doklady*, **126**, 111 (1959).
20. K. Vetter, *Z. Phys. Chem.*, **194**, 199 (1950).
21. G. Schmid, *Z. Elektrochem.*, **63**, 1183 (1959).
22. H. Robbins and B. Schwartz, Electrochemical Society Meeting, Oct. (1960).
23. G. Schmid and H. Spahn, *Z. Metallkunde*, **46**, 128 (1955).
24. H. Robbins and B. Schwartz, *This Journal*, **107**, 108 (1960).

# Preparation of Boron by Fused Salt Electrolysis

**Nelson P. Nies**

*U. S. Borax Research Corporation, Anaheim, California*

ABSTRACT

The preparation of elemental boron by fused salt electrolysis was investigated using various electrolytes composed of $B_2O_3$ dissolved in mixtures of alkali metal and magnesium chlorides, fluorides and oxides, with a graphite crucible anode and a steel cathode at about 850°C. The best product purity, 97.5%, was obtained with a bath containing KCl, KF, and $B_2O_3$, treated with HCl gas. This electrolyte has the advantage that it is not as volatile as previously used baths containing $KBF_4$. Lower purities were obtained with baths containing sodium or magnesium salts. An approximate phase equilibrium diagram is given of the liquid system KCl-KF-$B_2O_3$.

Elemental boron has been prepared by (*a*) thermal reduction of boric oxide with metals (1, 2), (*b*) thermal reduction of boron halides or fluoborates with metals or hydrogen (2-5), (*c*) thermal dissociation of boron halides or hydrides (5-8), and (*d*) fused salt electrolysis. In the first of these methods the highest purity has been obtained by the use of magnesium powder (Moissan process); most commercial boron has been produced by this means. However, the purity of Moissan boron (without further treatment) is usually less than 92%, and this method is limited economically by the cost of the magnesium and the excess $B_2O_3$ used. Methods (*b*) and (*c*) are capable of producing higher purity boron but also have been limited economically by the cost of raw materials. The electrolytic method is not so limited by raw material costs and was believed worthy of further investigation.

Early work on the electrolysis of alkali borates, reviewed by Andrieux (9), resulted in impure products and low yields. Kahlenberg (10) electrolyzed fused $KBF_4$ and stated that operation was satisfactory except for contamination of the product with copper from oxidation of the cathode. He also attempted the electrolysis of a KF-$B_2O_3$ bath but was unsuccessful because of attack on his containers. He reported a product analyzing 100% B from a nonfluoride bath containing KCl, $K_2O$, and $B_2O_3$, but, as will be shown, this result could not be confirmed in the present work.

Andrieux (11) reported that in the electrolysis of borates, the product of highest purity, about 85% B, was obtained when the cation present was magnesium. Cooper (12) reported a maximum purity of 96.7% B by electrolysis of a KF-$KBF_4$-$B_2O_3$ bath and 99.5% B with KCl-$KBF_4$ and KCl-$KBF_4$-$B_2O_3$ baths. Cooper's electrolytes containing $B_2O_3$ are analogous to those used in aluminum production. Andrieux and Deiss (13), Ellis (14), Miller (15), Murphy, Tinsley, and Meenaghan (16), Fullam (17), and Stern and McKenna (18) have also electrolyzed baths containing $KBF_4$. These investigators also obtained their maximum purity by using $KBF_4$. In most cases they did not reach the maximum purity reported by Cooper.

The use of $KBF_4$ leads to appreciable loss of boron and fluoride by volatilization, because of its tendency to decompose on heating [v.p. 182 mm at 800°C(19)]. The purpose of the present work was to find, if possible, a bath which would be more stable than those containing fluoborates and which would produce a comparable product.

## Experimental

A graphite crucible, of inside diameter 254 mm, inside depth 380 mm, with walls 76 mm thick and with a close-fitting shell of 6.4 mm (¼ in.) Inconel was used as a bath container and as the anode. This was enclosed in a brick furnace heated with a gas burner. The cathodes used were either cylindrical or flat. The flat cathodes were made by welding 5 mm x 127 mm or 152 mm Armco iron plates together with ⅜ in. spacers between them, to form a hollow cathode which could be cooled by blowing compressed air into it. The cylindrical cathodes were made from mild steel pipe closed at the bottom, with a tube inside the cathode extending almost to the bottom for cooling with compressed air at the end of a run. It was found helpful in preventing attack on the cathodes to have tubes for air cooling welded to the cathode above the bath level. A layer of frozen electrolyte was put on the upper part of the cathode, above the bath level, by momentarily dipping the cathode in the bath before bolting it in place for the electrolysis, and this layer was maintained during electrolysis by passing a current of air through these tubes. To start a run, the crucible was filled with about 35 kg of the mixed ingredients (technical grade) and heated until fused and the desired temperature was reached. The cathode was then bolted to a water-cooled copper cathode holder and lowered into the bath. The bath was not covered and no protective atmosphere was used. The current was supplied by Edison batteries. In some experiments the potential was applied to the cathode before placing it in the

bath; this procedure usually resulted in a layer of electrolyte between the black deposit and the cathode. In most experiments, therefore, the current was not turned on until a few minutes after lowering the cathode into the bath, in order to permit melting of the layer of frozen salt which formed at first on the surface of the cathode. Any black scum on the surface of the bath was removed by skimming at frequent intervals. It was found desirable at the end of a run to decrease the current to about 25-40 amp and cool the cathode by passing compressed air through it for a few minutes before raising the cathode from the bath, in order to increase adherence of the deposit to the cathode. The product generally formed on the surface of the cathode as a smooth black deposit (occasionally rough in places) containing about 25% elemental boron and 75% electrolyte. The deposit often showed a tendency to ignite in spots just after removal of the cathode from the bath. If this occurred it was quickly extinguished by covering with granular sodium chloride. On soaking the cathode in water the deposit disintegrated and was easily removed from the cathode. In some cases, the deposit was removed by hammer and chisel, in order to separate the smooth parts of the deposit from the rough. Any parts which appeared different, such as the deposits on the edges and sides of a flat cathode, were separated also. These portions of the crude deposit were extracted with boiling water, digested overnight with hot concentrated HCl, washed and dried at 110°C. The products were practically amorphous to x-rays.

For analysis, a freshly dried 0.2-g sample, was either fused with 10 g of sodium carbonate (20) or dissolved in mixed acids (21); $B_2O_3$ was determined by titration by the usual method, using mannite.

Data on selected runs with various electrolytes are given in Table I.

## Discussion

One of the first bath compositions investigated (Run 1) was the KCl-$K_2O$-$B_2O_3$ bath, which had been stated by Kahlenberg (10) to give pure boron. In this nonfluoride bath some alkalinity is necessary to dissolve the $B_2O_3$. Only a very low yield of 65% boron could be obtained with this bath.

Replacement of KCl partially (Run 2) or completely (Run 3) by KF in these alkaline baths gave a somewhat better but still unsatisfactory purity, 78-79% B. If the alkalinity was increased to 32.5% (Run 4), no deposit at all was obtained. These poor results with alkaline baths may have been due to oxidation of the deposit by carbonate, which was present in alkaline baths in higher concentrations than in nonalkaline baths (Runs 3, 4, 6).

Better results were obtained with electrolytes not containing added alkalinity. Electrolytes com-

Table I. Summary of experiments on the electrolytic production of elemental boron

| Run No. | Bath components, wt % | | | | pH of 0.33% solution | Hr | Avg temp, °C | Volts | Amp | Average cathodic current density, amp·dm$^{-2}$ | Current efficiency, % | Product purity, % B |
|---|---|---|---|---|---|---|---|---|---|---|---|---|
| | KCl | KF | $K_2O$ | $B_2O_3$ | | | | | | | | |
| 1 | 59 | 0 | 21 | 20 | — | 2 | 882 | 4.3-5.4 | 560-780 | 87 | 1 | 65.0 |
| 2 | 23.5 | 31.5 | 21.5 | 23.5 | — | 3 | 857 | 4.2-5.3 | 570-800 | 98 | 31 | 79.3 |
| 3[a] | 0 | 50 | 20 | 30 | — | 3 | 849 | 4.5-5.5 | 495-775 | 96 | 55 | 78.0 |
| 4[b] | 0 | 43 | 32.5 | 24.5 | — | 3 | 882 | 3.5-4.6 | 500-775 | 81 | 0 | — |
| 5[c] | 56 | 36 | | 8 | — | 1.3 | 810 | 5.3-5.7 | 580-605 | 135 | 34 | 80.4 |
| 6[d] | 11.5 | 73.5 | | 15 | — | 2.0 | 850 | 3.8-4.7 | 600-740 | 99 | 81 | 87.8 |
| 7 | 71 | 21.5 | | 7.5 | — | 1.5 | 845 | 3.9-4.7 | 505-650 | 81 | 40 | 83.5 |
| 8 | 44 | 33 | | 23 | 7.6 | 1.5 | 860 | 3.6-3.8 | 255-300 | 74 | 67 | 87.0 |
| 9[e] | 43.5 | 32 | | 24.5 | 4.7-4.9 | 1.5 | 860 | 3.5-3.7 | 280-300 | 79 | 58 | 93.3 |
| 10[e,f] | 91 | 7.2 | | 1.8 | 3.4 | 1.5 | 840 | 4.0-4.2 | 285-310 | 82 | 62 | 90.4 |
| 11[e] | 46.5 | 30.0 | | 23.5 | 4.9 | 1.5 | 871 | 3.6-3.8 | 290-300 | 79 | 47 | 96.0 |
| 12[e] | 44 | 41 | | 15 | 7.1-7.2 | 2.0 | 812 | 3.1-3.2 | 310-370 | 87 | 57 | 94.7 |
| 13 | 0 | 92.5 | | 7.5 | — | 3.0 | 896 | 3.4-4.1 | 595-940 | 107 | 58 | 84.0 |
| 14 | 0 | 69.5 | | 30.5 | — | 3.0 | 802 | 4.9-5.6 | 515-710 | 92 | 67 | 86.5 |
| 15[g] | 0 | 85 | | 15 | 5.6-5.7 | 2.5 | 877 | 2.6-3.2 | 310-355 | 87 | 28 | 90.7 |
| | | $KBF_4$ | | | | | | | | | | |
| 16[h] | 70 | 22 | | 8 | 3.8 | 2.0 | 827 | 3.5-3.7 | 295-360 | 84 | 79 | 95.0 |
| | | NaCl | NaF | | | | | | | | | |
| 17[e] | 20.5 | 32 | 27.5 | 20 | 8.1 | 2.0 | 909 | 2.7-3.4 | 295-340 | 84 | 56 | 85.9 |
| 18[e] | 0 | 39 | 36 | 25 | 7.7-7.9 | 1.0 | 836 | 3.7-3.9 | 340-370 | 93 | 27 | 79.4 |
| | $MgF_2$ | KF | | | | | | | | | | |
| 19[i] | 11 | 79 | | 10 | | 4 | 906 | 2.5-3.2 | 315-360 | 48 | 18 | 84.3 |

[a] Run 3: Analysis of electrolyte for $CO_2$: before run, 0.42%; after run, 0.19% $CO_2$.
[b] Run 4: Analysis of electrolyte for $CO_2$: before run, 0.43%; after run, 0.23% $CO_2$.
[c] Run 5: KCl-KF eutectic (m.p. 605°C) + $B_2O_3$.
[d] Run 6: $CO_2$ content of electrolyte at start of run, 0.012%.
[e] Runs 9-12; 17 and 18: Electrolyte acidified with gaseous HCl before electrolysis.
[f] Run 10: HCl was passed into this bath for 2½ hr, causing a second liquid of composition 21% KCl, 31% KF and 48% $B_2O_3$ to form at the bottom of the crucible.
[g] Run 15: Gaseous HF passed into bath before electrolysis.
[h] Run 16: Cooper (12) electrolyte.
[i] Run 19: Product contained 3.3% Mg.
Note: Cathode dimensions: Runs 1-4, 6, 7, 13, 14, 19: flat, 12 × 2 cm, immersed 23 cm; Run 5: cylindrical, 9 cm diameter, immersed 12 cm; Runs 8-12, 15-18: cylindrical, 6 cm diameter, immersed 23-24 cm.

posed of KCl, KF, and $B_2O_3$ (runs 5-8) gave products ranging up to a maximum of 91.6% boron in the coarser fraction of Run 8. In these experiments the + 100 mesh fraction of the product was usually of higher purity than the finer fractions. When a flat cathode was used, the deposit at the edges, where the current density was greater, generally gave a somewhat higher purity than that on the flat sides. This bath composition gave poor results under some conditions such as low temperatures and low KF or $B_2O_3$ concentrations. A KF/KCl ratio equal to that of the eutectic in the system KF-KCl also gave poor results (Run 5).

It is known that fused halides exposed to the atmosphere will gradually become alkaline. Since the above experiments indicated that an increase in electrolyte alkalinity gave a poorer quality product, neutralization with HCl was attempted. It was found that the alkalinity could be eliminated by bubbling HCl gas into the fused salt bath through a graphite tube. A convenient means of controlling the addition of the gas was to determine the pH of a 0.33% solution of the electrolyte. By electrolysis of these acid-treated baths (Runs 9-12) it was possible to produce boron of markedly increased purity. The highest over-all product purity reached was 96% B in Run 11. Coarser fractions of the products were again of higher purity than the finer fractions and reached 97.3-97.5% B in several runs. Boron of good purity was obtained with electrolytes of which the pH of the 0.33% solution ranged from 4.8 to 7.2, and the KCl:KF:$B_2O_3$ proportions by weight were 47:30:23, 57:30:13, 42:38:20, and 45:40:15.

Figure 1 is a phase equilibrium diagram of the liquid system KCl-KF-$B_2O_3$. The numbers shown are examples of the product purity obtained with acid-treated baths of various proportions of these components. In Run 10, the HCl was passed into the fused bath for 2½ hr, which apparently caused a loss of HF from the bath and resulted in separation of the bath into two liquids, represented by the ends of the tie line in Fig. 1.

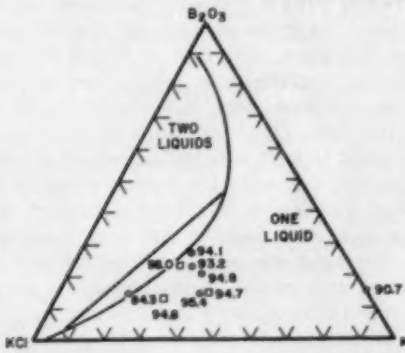


Fig. 1. Phase diagram for the liquid system KCl-KF-$B_2O_3$ at approximately 800°-900°C (wt %), showing the per cent boron in the product obtained by HCl treatment and electrolysis of various electrolyte compositions. Squares represent products in which the +100 mesh fraction consisted of 97.3-97.5% boron.

For reasons not fully understood, lower purities and "blistering" of the deposits were sometimes observed. A cause of this may be the partial burning of the deposit which sometimes occurred in spots just after removal of the cathode from the bath.

Other electrolyte compositions were investigated. Electrolytes of $B_2O_3$ dissolved in KF were tried over a range of $B_2O_3$ concentration up to the composition $B_2O_3$:2KF suggested by Kahlenberg (10). An attempt was made to acidify these baths by passing in gaseous HF. The HF was absorbed, but less readily than HCl. The maximum product purity obtained with this acidified bath was 90.7% (Run 15) compared with 86.5% without addition of acid (Run 14).

Cooper's (12) electrolyte KCl-$KBF_4$-$B_2O_3$ gave typically 93.5-95.5% purity under our conditions. An example is Run 16.

Electrolytes containing sodium salts were tried, HCl being passed in as before (Runs 17, 18). Sodium salts did not absorb either HCl or HF well enough to become acidic. These experiments gave lower product purities than the potassium salts and thus confirm Cooper's (12) statement that sodium salts are detrimental. Metallic sodium was observed in the deposit and on the surface of the bath in some cases, especially where the operating temperature was below the boiling point of sodium, 880°C.

Also, electrolytes composed of KF, $MgF_2$, and $B_2O_3$ were tried (Run 19) but the purities were only 82-84% B and the products contained appreciable amounts of magnesium.

## Acknowledgment

The author wishes to thank Dr. E. W. Fajans for helpful discussions, and Vincent Morgan, L. E. Hiebert, L. L. Thomas, and S. A. Sorenson for their contributions to the experimental work.

Manuscript received March 21, 1960. This paper was prepared for delivery before the New York Meeting, April 27-May 1, 1958.

Any discussion of this paper will appear in a Discussion Section to be published in the June 1961 JOURNAL.

## REFERENCES

1. E. Weintraub, *Trans. Am. Electrochem. Soc.*, **16**, 165 (1909).
2. J. S. Spevack and A. Kurtz, A. E. C. Report A-1246 (1944).
3. H. Haag (to Hermann C. Starck A. G.) U. S. Pat. 2,794,708, June 4, 1957.
4. D. R. Stern and L. Lynds, *This Journal*, **105**, 676 (1958).
5. C. F. Powell, I. E. Campbell, and B. W. Gonser, "Vapor Plating," pp. 106-111, John Wiley & Sons, Inc., New York (1955).
6. H. L. Johnston, H. N. Hersh, and E. C. Kerr, *J. Am. Chem. Soc.*, **73**, 1112 (1951).
7. E. J. Prosen, W. H. Johnson, and F. Y. Pergiel, *J. Res. Nat. Bur. Stds*, **61**, 247 (1958).
8. L. V. McCarty and D. R. Carpenter, *This Journal*, **107**, 38 (1960).
9. J.-L. Andrieux, *Rev. Met.*, **32**, 487 (1935).
10. H. H. Kahlenberg, *Trans. Am. Electrochem Soc.*, **47**, 30 (1925).

11. J.-L. Andrieux, *Ann. Chim.*, **12**, 423 (1929).
12. H. S. Cooper (to Walter M. Weil), U. S. Pat. 2,572,-248 and 2,572, 249, Oct. 23, 1951.
13. J.-L. Andrieux and W. J. Deiss, *Bull. Soc. Chem.*, **1955**, 838.
14. R. B. Ellis (to Callery Chem. Co.), U. S. Pat. 2,810,-683, Oct. 22, 1957.
15. G. T. Miller, *This Journal*, **106**, 815 (1959).
16. H. F. Murphy, R. S. Tinsley, and G. F. Meenaghan, Bull. Virginia Polytech. Inst., Eng. Exp. Sta. Series No. 115 (1957).
17. H. T. Fullam, Doctoral Dissertation Series, Pub. No.: 20,381, pp. 136-7, University Microfilms, Ann Arbor, Mich. (1956).
18. D. R. Stern and Q. H. McKenna (to American Potash & Chemical Corp.) U. S. Pat. 2,892,762, June 30, 1959.
19. J. H. deBoer and J. A. M. van Liempt, *Rec. Trav. Chim.*, **46**, 124 (1957).
20. H. Blumenthal, *Anal. Chem.*, **23**, 992 (1951).
21. C. A. Hampel, "Rare Metals Handbook," p. 81, Reinhold Publishing Co., New York (1954).

# Catalytic Activity and Electronic Structure of Rhodium-Palladium-Hydrogen Cathodes in Acid Solution

James P. Hoare[1]

*Scientific Laboratory, Ford Motor Company, Dearborn, Michigan*

ABSTRACT

Hydrogen overvoltage measurements were made on a series of rhodium-palladium alloy cathode beads. Two phases, $\alpha$ and $\beta$ similar to those in the Pd-H system, are considered in the Rh-Pd-H system. Mechanisms for the hydrogen producing reactions on rhodium, palladium, and rhodium-palladium alloy cathodes are discussed. From low current density measurements the catalytic activity of the cathode surface for the hydrogen reaction was determined. It appears that vacancies in the *d*-band of the catalyst metal are necessary for strong bonds between the absorbed hydrogen and the surface but it is the density of states at the Fermi level that determines how strong the chemisorbed bonds are. The catalytic activity is directly related to the heat of absorption and so to the *d*-band structure.

In recent years much interest has been generated in establishing relationships between the surface properties of metallic catalysts and the electronic structure of the bulk metal (1). It has been suggested that on a metal such as palladium, containing vacancies in the *d*-band, hydrogen is adsorbed with a greater heat of adsorption than on an alloy of palladium and gold in which the number of *d*-band vacancies has been reduced (2).

Hydrogen overvoltage measurements were carried out on a series of Pd-Au (3) and Pd-Ni (4) alloys. The results of these investigations indicated that the surface catalytic activity of the electrode is directly associated with the number of vacancies in the *d*-band of the bulk metal through the heat of adsorption of hydrogen on the metal as pointed out by Conway and Bockris (5). It was, therefore, indicated (2, 3, 5, 6) that for metals on which the slow discharge step or Volmer mechanism (7) is rate determining the catalytic activity should increase (2, 3) as the number of holes is increased. However, for those metals on which an H-atom desorption step is rate controlling, such as the slow combination or Tafel mechanism (8) and the so-called electrochemical or Horiuti mechanism (9), the reverse should be true.

In order to test this theory further and possibly to determine whether the catalytic activity is related to the number of holes or to the density of states in the *d*-band it was desired to find a series of alloys in which the number of holes could be increased. An obvious system is that of Rh-Pd. Although the phase diagram of this system is not available, still the two metals have very similar atomic dimensions and both form face-centered cubic crystals (10). Therefore, it is not unlikely that they are completely miscible in one another. Since Rh has one less electron than Pd, additions of Rh to Pd should form a series of alloys with an increasing number of vacancies in the alloy *d*-band. It is with this system that the present investigation is concerned.

## Experimental Methods

A series of Rh-Pd alloys of the following compositions were made by melting the required amount of Pd, 99.7% pure, with that of Rh, 99.8% pure, in an induction furnace under a hydrogen atmosphere. These compositions are: 1, 2, 5, 10, 15, 20, 50, and 90 atomic per cent (a/o) rhodium. A portion of the alloy, welded to a Pt wire which served as the electrical contact, was melted to form a small bead. The alloy bead and the Pt lead were imbedded in polyethylene in such a manner that only a hemisphere of the alloy bead was exposed. The exposed apparent surface area of the beads, measured geometrically, ranged between 0.09 and 0.04 $cm^2$.

The cylindrical cell, shown in Fig. 1, was made of Teflon and was designed to hold about 25 ml of solution. A large piece of Pt gauze lined three quarters of the inner wall and served as the anode, while a rather small piece of Pt gauze served as the reference electrode. The cell top was fitted with a Teflon tube which provided the hydrogen inlet, a

[1] Present address: Research Labs., General Motors Corp., Warren, Mich.

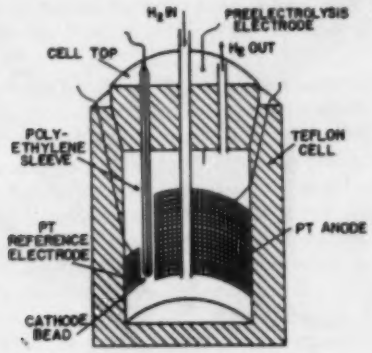


Fig. 1. Teflon cell

short tube for the hydrogen outlet, the polyethylene covered cathode bead and platinum lead, and a hole through which the pre-electrolysis electrode (a Pt wire) could be placed.

The water was triply distilled from an all-quartz still, and all purification techniques were the same as those described before (11, 4). Overvoltage measurements on the alloy beads were carried out with an electronic current interrupter in electrolytically purified 2*N* sulfuric acid solution vigorously stirred with purified hydrogen in the same way as was done in the case of the bright Pd bead (11). Potential measurements were recorded only when the pulse from the current interrupter indicated clean surface (12) conditions (high pseudo-capacitance) (13). The temperature was 25° ± 1°C, and individual points could be reproduced within ± 2.5 mv. The potential $\eta$ (positive in the direction of anodic polarization) is an electrode potential or overpotential measured by reference to a reversible Pt/$H_2$ electrode in the same solution.

## Results and Discussion

Two series of experiments were carried out on the Rh-Pd alloy beads.

*The* $\alpha$-Rh-Pd-H *System.*—In the first series of experiments, the Rh-Pd alloy cathode was anodized at a relatively high current density (0.3 amp/cm²) for about 30 min. The circuit was broken and the open-circuit potential of the bead vs. a Pt/$H_2$ electrode in the same solution was followed as a function of time. When the ternary system, Rh-Pd-H, had reached a steady state and the potential had been constant for at least 12 hr, this steady-state value was recorded. Then by means of a constant current source and a high-value series resistor (20 to 60 megohm), the alloy bead was first slightly cathodized stepwise and the time independent (constant for at least 10 min) values of the potential $\eta$ were recorded for each step. Afterwards, the cathodic current was reduced stepwise to zero and was continued in like manner in the anodic direction. The points on the curves in Fig. 2 are the average values for at least three cycles of increasing and then decreasing the current over the complete current range shown in Fig. 2. These points were reproducible within ± 0.5 mv.

The potential $\eta$ observed at zero current may be interpreted as a mixed potential derived from two

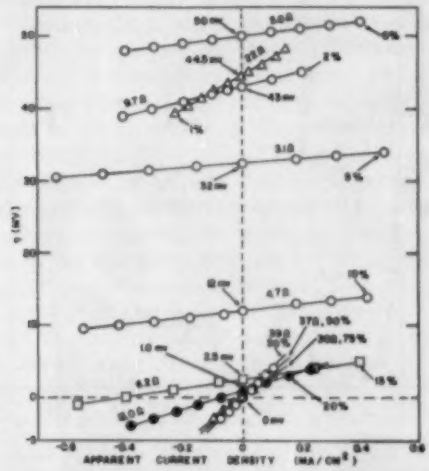


Fig. 2. Apparent current density i vs. electrode potential or overpotential $\eta$ referred to a Pt/$H_2$ electrode in the same solution (2N $H_2SO_4$). Anodic currents to the right, anodic polarizations upward. Linear current density range for Rh-Pd alloys. Atomic per cent Rh indicated on graph together with open-circuit potentials. The slope $d\eta/di$ is given for each alloy in ohm cm² (25° ± 1°C).

phases existing in the Rh-Pd-H system analogous to the $\alpha$ and $\beta$ phases found in the Pd-H system (14). If, in this region, the mixed potential is determined by the $\alpha$-phase analogue of the Rh-Pd-H system (hereafter designated as $\alpha$-Rh-Pd-H), then this steady-state potential is, for practical purposes, identical to the equilibrium potential (15) for the saturated $\alpha$-phase. Since it has been shown (16) that in the Pd-H system a bead-type of electrode similar to that used in this investigation exhibits the potential of a Pd cathode in the $\alpha$-phase of maximum composition for periods of time greater than a week, these electrodes are good approximations to a pure $\alpha$-phase electrode. There may or may not be small amounts of the $\beta$-phase also present, but the electrochemical properties are determined by the dominant $\alpha$-phase.

In the low current density region where a linear relationship between the current density i and electrode potential or overpotential $\eta$ exists, the slope of the i vs. $\eta$ curve may be taken as a measure of the rate of the hydrogen reaction $k$ occurring at the electrode (17), i.e., $k$ will be defined as equal to $di/d\eta$. A plot of the rates of reaction obtained from the reciprocal of the slopes of the curves in Fig. 2 for the hydrogen reaction proceeding on the $\alpha$-Rh-Pd-H cathodes is shown by the triangles in Fig. 3. These experiments were also repeated for a pure Pd bead on which $k$ was observed to be 0.20 mho cm$^{-2}$ in agreement with the value of 0.13 mho cm$^{-2}$ found earlier for $\alpha$-Pd (18).

*The* $\beta$-Rh-Pd-H *System.*—In the second series of experiments, the Rh-Pd beads, after strong anodization, were cathodized at current densities of the order of 300 ma cm$^{-2}$ for about 90 min. This treatment converted the cathodes completely to the $\beta$-Rh-Pd-H phase. Cathodic overvoltage measurements were taken as before (11). Results are shown in Fig. 4. Overvoltage measurements were also

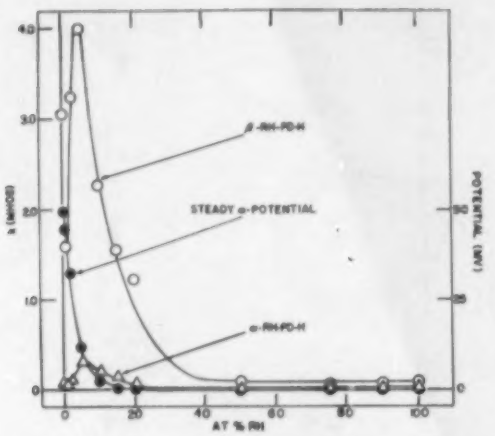


Fig. 3. Rate $k$ (mhos/cm²) of the hydrogen reaction at $\alpha$-Rh-Pd-H (△) and $\beta$-Rh-Pd-H (○) alloy electrodes as a function of atomic per cent Rh in the Rh-Pd alloy. Steady $\alpha$ open-circuit potentials (●) referred to $Pt/H_2$ in the same electrolyte (2N $H_2SO_4$). For $\beta$ open-circuit potentials, see Table I.

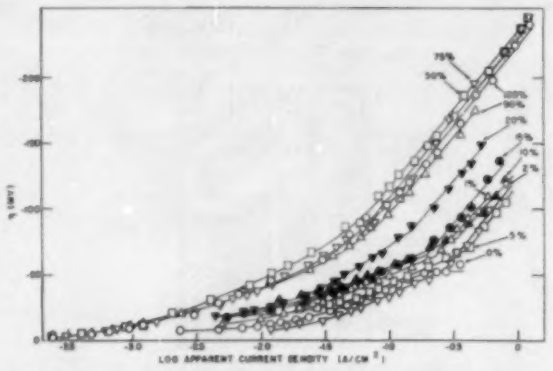

Fig. 4. Log $i$ vs. $\eta$ for cathodic polarization of $\beta$-Rh-Pd-H systems. The atomic per cent Rh in the Rh-Pd alloy is indicated on each curve; 25°±1°C.

made on a pure Pd and pure Rh bead; these results are included in Fig. 4 and are similar to those found in the literature (11, 19).

In general, it is seen that these data may be placed in two groups. In the first group are the data for high Pd-content cathodes up to 15 a/o Rh. The curves are composed of three sections: the low current or non-Tafel region, a Tafel region in which $b$ is about 0.04 v, and a second Tafel region in which $b$ is about 0.12 v. The high Rh content alloys, from 50 to 100 a/o Rh, form the second group. These curves have only one Tafel region whose $b$-slope is 0.12 v in addition to the non-Tafel region. Parsons (20) has discussed the mechanisms of electrochemical kinetics in terms of Tafel $b$-slopes. A slope of 0.04 v found on the high Pd-content alloys as well as on pure Pd (11) is consistent with the electrochemical mechanism on a sparsely covered surface. Although a unique mechanism for a slope of 0.12 v is not available (20), it is felt that the data for high Rh-content cathodes are more easily interpreted in terms of the slow discharge mechanism for the same reasons offered in the case of Pd-Ni alloys (4).

A mixed mechanism is exhibited by the data taken on the 20 a/o Rh cathode shown in Fig. 4. These data seem to correspond to a transition state between the high Rh-content and high Pd-content cathodes. Here a Tafel region with a $b$-value of 0.075 v is observed which could be explained by a mechanism in which both the slow discharge and the electrochemical steps are equally slow and are equally rate determining.

From a plot of $\eta$ vs. $i$ at low current densities, the rate $k$ for the hydrogen reaction proceeding on a $\beta$-Rh-Pd-H cathode was determined in the same way as for the $\alpha$-Rh-Pd-H cathode electrodes above. These linear plots did not pass through zero potential for the high-Pd content cathodes at zero current density. This same behavior was noted in the Pd-H (11), Au-Pd (3), and Ni-Pd-H (4) systems and may be interpreted similarly (11) as due to the partial pressure of the dissolved hydrogen. The curves for the high Rh-content alloys all pass through zero at zero current density. These curves are not shown, but the values for $k$ and for the zero current intercepts $\eta_0$ are given in Table I along with the Tafel $b$-slopes of the high current density regions (Fig. 4).

A plot of $k$ for $\beta$-Rh-Pd-H as a function of atomic % Rh is shown by the circles in Fig. 3. In the case of the high Pd-content cathodes, the rate is considerably higher for the $\beta$ than for the $\alpha$-analogue. However, the rate is approximately the same in the two cases for the high Rh-content cathodes which is to be expected if these alloys dissolve negligible quantities of hydrogen. The smooth curve drawn through these points would indicate, then, that the hydrogen solubility limit occurs at about 30 a/o Rh. Both curves exhibit a pronounced maximum at about 5 a/o Rh.

*Catalytic activity and electronic structure.*—The magnetic susceptibility and the low-temperature specific heat of Pd-Rh alloys have been measured (21). A maximum is found in the susceptibility-composition curve at about 5 a/o Rh. This is interesting since one obtains an alloy with a magnetic susceptibility greater than that of either pure substance. From the specific heat data, the electronic heat coefficient $\gamma$ was determined, and a plot of $\gamma$ as a function of the alloy composition also exhibits a maximum at about 5 a/o Rh. The fact that both quantities have a maximum value for the same

**Table I. Cathodic polarization data for the $\beta$-Rh-Pd-H system in 2N $H_2SO_4$ at 25°C**

| Alloy composition a/o Rh | $k$, mhos/cm² | Zero current intercept, $\eta_0$, mv | $b_1$, v | $b_2$, v |
|---|---|---|---|---|
| 0 | 3.03 | 7.1 | 0.040 | — |
| 1 | 1.59 | 17.8 | 0.040 | 0.117 |
| 2 | 3.24 | 19.9 | 0.041 | 0.122 |
| 5 | 4.00 | 19.5 | 0.042 | 0.119 |
| 10 | 2.26 | 15.4 | 0.040 | 0.122 |
| 15 | 1.67 | 16.2 | 0.042 | 0.119 |
| 20 | 1.23 | 15.4 | 0.075 | 0.116 |
| 50 | 0.093 | 0 | — | 0.118 |
| 75 | 0.080 | 0 | — | 0.120 |
| 90 | 0.083 | 0 | — | 0.122 |
| 100 | 0.095 | 0 | — | 0.120 |

alloy composition suggests that the density of states at the Fermi level for the alloy is at a maximum value.

It has been assumed that the electrode mechanism on the high Pd-content cathodes is electrochemically controlled and, therefore, that a H-atom desorption step is rate determining. As the number of holes in the *d*-band is increased by additions of Rh to Pd, the heat of adsorption of hydrogen should increase and the rate of reaction $k$ should decrease (2). This is observed. The reaction rates are higher for all $\beta$-Rh-Pd-H cathodes where all holes in the *d*-band have been filled with electrons from dissolved hydrogen than for the corresponding $\alpha$-Rh-Pd-H cathodes where all the holes have not been filled as shown in Fig. 3. Apparently this is not the complete picture since each curve in Fig. 3 shows a maximum at an alloy concentration of 5 a/o Rh, suggesting that the rate of the hydrogen reaction on Rh-Pd-H alloy cathodes is also a function of the density of states at the Fermi-level energy of the hydrogen-free Rh-Pd alloys.

Such an interpretation of the data requires that a direct relationship exist between the activation energy and the heat of adsorption of hydrogen, which is not self-evident. By a theoretical analysis of the shape of the energy surfaces involved and by an inspection of the pertinent experimental data, Rüetschi and Delahay (22) were able to show a linear relationship between the hydrogen reaction occurring at Ni, Ag, and Hg cathodes and the heat of adsorption on these metals. However, this gives an expression opposite in sign to that found for Pd-H alloys (2). The rate-determining step on Ni, Ag, and Hg is found to be the slow discharge of a hydrogen ion from the double layer (23). In this case, as the number of holes in the *d*-band are decreased and, consequently, the heat of adsorption of hydrogen decreased, the rate of reaction should decrease (2) as found by Oikawa (24) for a series of Ni-Cu alloy cathodes. This was observed by Rüetschi and Delahay as shown in Fig. 2 of ref. (22).

Recently, from theoretical considerations, Parsons (25) and Gerischer (26) have come to the similar conclusions that the plot of the logarithm of the rate of the hydrogen reaction at equilibrium conditions, (when the overvoltage $\eta$ is zero) i.e., the exchange current density $i_o$, as a function of the energy of adsorption of hydrogen, gives a similar type of curve no matter which step is rate determining. This indicates that the reaction mechanism cannot be determined alone by the sign of the relationship between changes in the rate with changes in the energy of adsorption. This is not held by Conway and Bockris (5). It is to be remembered, though, that Parsons considers a noble metal cathode surface to be highly covered with atomic hydrogen and assumes that the shape of the Morse curve is rigid and does not change as the energy of adsorption changes. Shuldiner and Hoare (3, 4, 11, 27) consider such surfaces to be sparsely covered with atomic hydrogen.

It should also be noted that Parsons, Bockris, and Delahay consider the changes in reaction rate with changes in heat of adsorption obtained from studies of overvoltage on a series of different metal cathodes, while Schuldiner and Hoare (2) observe these changes on continuous series of alloy cathodes. In these latter cases, abrupt changes or even discontinuities in the properties of the cathode surface are less likely.

It is interesting to note that the influence of the density of states on the rate of reaction is such that the activation energy decreases as the density of states in the hydrogen-free Rh-Pd alloys increases. It is not unreasonable to consider that changes in the density of states in the bulk material would change the energy of the surface states which in turn would cause changes in the activation energy of the reaction occurring at the surface.

It is suggested, then, that the presence of holes in the *d*-band of the Rh-Pd alloy cathodes makes possible the formation of strong chemical bonds between the chemisorbed hydrogen atoms and the metallic atoms of the cathode surface (5); that there is a direct correspondence between the heat of adsorption of hydrogen and the activation energy of the hydrogen reaction; and that, once a strong bond is formed, how strong the bond is or how much energy resides in the bond is a function of density of states at the Fermi-level energy in the bulk hydrogen-free alloy in such a manner that, as the density of states increases, the bond becomes less strong.

For the alloys above about 30 a/o Rh there is not any essential difference between the two curves since these alloys do not dissolve significant quantities of hydrogen and, hence, do not form $\alpha$- and $\beta$-type phases but only one single solid Rh-Pd phase. As suggested above, the slow discharge mechanism is rate controlling on these cathodes. As Rh is added and the number of holes increases, the rate on the high Rh-content cathodes should increase since now the slow discharge mechanism is rate determining. The data in column 2 of Table I does show a trend in that direction. Even though this slight increase may be within the limits of experimental error, the amount of the increase for the high-Rh-content cathodes may actually be very small and difficult to detect because of experimental difficulties. This is true since Rh with about two holes in the *d*-band per atom is in such great excess in this range of alloy composition (50 a/o Rh) that the percentage of change in the number of holes in the alloy *d*-band with additions and subtractions of Pd having only 0.6 hole per atom would be very small.

Finally, the initial drop in the rate curves in Fig. 3 from the value for pure Pd is surprising and unexpected. The rate for the 1% Rh cathode was checked twice with new beads, and the value shown was reproduced each time. Although a quantitative explanation for this is not available at this time, a qualitative one may be found in Parsons' work (25). He shows on theoretical grounds that $i_o$ is proportional to $1/p^n$, where p is the partial pressure of molecular hydrogen and $n$ has a value between 0 and 1. If the magnitude of the intercept $\eta_o$ (Table I) is proportional to the excess partial pressure of

dissolved hydrogen above the equilibrium partial pressure, then it is seen that this partial pressure increases in going from pure Pd to 1 a/o Rh in Pd. Therefore, the rate should drop, since $p > 1$. For higher Rh-content alloys there is little or no change in $\eta_o$, and this effect is not observed.

### Acknowledgments

The author wishes to express his gratitude to Dr. A. Arrott and Dr. A. W. Overhauser of the Physics Department for most helpful and interesting discussions and to Dr. J. E. Goldman, Manager of the Chemistry and Physics Departments, for his many well-taken comments and faithful support during the course of this work. The author is also indebted to Dr. F. E. Hoare of Leeds University for his fruitful suggestions, to Dr. G. Parravano of the University of Michigan for his most interesting criticism, to the Metallurgy Department of the Ford Scientific Laboratory for the preparation of the alloys, and to the Analytical Section of the Physics Department for the analysis of the alloys.

Manuscript received Jan. 22, 1960.

Any discussion of this paper will appear in a Discussion Section to be published in the June 1961 JOURNAL.

### REFERENCES

1. O. Beeck, *Discussions Faraday Soc.*, **8**, 118 (1950); A. Couper and D. D. Eley, *ibid.*, **8**, 172 (1950); D. A. Dowden, *J. Chem. Soc.*, **1950**, 242.
2. S. Schuldiner and J. P. Hoare, *J. Phys. Chem.*, **62**, 504 (1958); Electrochemical Mechanisms of Noble-Metal Hydrogen Systems, Part III, Electronic Configuration and Catalytic Activity, NRL Report 5171, July 1958.
3. S. Schuldiner and J. P. Hoare, *J. Phys. Chem.*, **61**, 705 (1957).
4. J. P. Hoare and S. Schuldiner, *ibid.*, **62**, 229 (1958).
5. B. E. Conway and J. O'M. Bockris, *J. Chem. Phys.*, **26**, 532 (1957).
6. J. Horiuti and M. Polanyi, *Acta Physicochem. U.R.S.S.*, **2**, 505 (1935).
7. T. Erdey-Gruz and M. Volmer, *Z. physik Chem.*, **A150**, 203 (1930).
8. J. Tafel, *ibid.*, **50**, 641 (1905).
9. J. Horiuti and G. Okamoto, *Sci. Pap. Inst. Phys. Chem. Res. Tokyo*, **28**, 231 (1936).
10. C. J. Smithels, "Metals Reference Book," 2nd ed., Vol. I, p. 196, Interscience Publishers Inc., New York (1955).
11. J. P. Hoare and S. Schuldiner, *This Journal*, **102**, 485 (1955).
12. S. Schuldiner, *ibid.*, **99**, 488 (1952); S. Schuldiner and J. P. Hoare, *J. Chem. Phys.*, **26**, 1771 (1957).
13. D. C. Grahame, *Chem. Rev.*, **41**, 441 (1947).
14. S. Schuldiner, G. W. Castellan, and J. P. Hoare, *J. Chem. Phys.*, **28**, 16 (1958).
15. J. P. Hoare, G. W. Castellan, and S. Schuldiner, *J. Phys. Chem.*, **62**, 1141 (1958).
16. J. P. Hoare, *This Journal*, **106**, 640 (1959).
17. P. Dolin, B.Ershler, and A. Frumkin, *Acta Physiochem. U.R.S.S.*, **13**, 779 (1940).
18. J. P. Hoare and S. Schuldiner, *This Journal*, **104**, 564 (1957).
19. J. P. Hoare and S. Schuldiner, *J. Chem. Phys.*, **25**, 786 (1956).
20. R. Parsons, *Trans. Faraday Soc.*, **47**, 1332 (1951).
21. F. E. Hoare and J. Preston, *Nature*, **180**, 334 (1957).
22. P. Ruetschi and P. Delahay, *J. Chem. Phys.*, **23**, 195 (1955).
23. I. A. Ammar and S. A. Awad, *J. Phys. Chem.*, **60**, 1290 (1956); J. O'M. Bockris and E. C. Potter, *J. Chem. Phys.*, **20**, 614 (1952); A. N. Frumkin, *Discussion Faraday Soc.*, **1**, 57 (1947).
24. M. Oikawa, *Bull. Chem. Soc. Japan*, **28**, 626 (1955).
25. R. Parsons, *Trans. Faraday Soc.*, **54**, 1053 (1958).
26. H. Gerischer, *Bull. Soc. Chim. Belg.*, **67**, 506 (1958); H. Gerischer and W. Mehl, *Z. Elektrochem.*, **59**, 1049 (1955).
27. S. Schuldiner, *This Journal*, **106**, 891 (1959).

# Fused Salt Polarography Using a Dropping Bismuth Cathode

**Raymond J. Heus and James J. Egan**

*Brookhaven National Laboratory, Upton, New York*

ABSTRACT

An apparatus is described which is suitable to study fused chlorides by the polarographic technique. Dropping bismuth is used in a way analogous to dropping mercury. Polarographic waves are shown for $PbCl_2$, $ZnCl_2$, and $CdCl_2$ in a LiCl-KCl eutectic melt at 450°C. The method serves as an analytical tool at high temperatures, besides yielding physicochemical information such as diffusion coefficients by application of the Ilkovic equation.

Many studies have been made on fused salts using the polarographic technique (1-8). In general solid wire microelectrodes have been used to measure concentrations which were found to be proportional to the limiting current. The dipping platinum microelectrode has been used by Flengas (9), and Chovnyk used derivative polarography at wire microelectrodes (10). Nachtrieb and Steinberg used a dropping mercury electrode to study low melting nitrate melts (11).

The dropping mercury electrode has not been employed at temperatures greater than 220°C, due to the high vapor pressure of mercury. Aside from gallium (12), no metal other than mercury has been employed as a dropping electrode, but dropping electrodes should prove useful since they have been so successful in lower temperature studies.

In order to expand the range of temperatures at which dropping electrodes can be used, the following work was undertaken using molten bismuth at 450°C as the electrode material. Bismuth is an adequate metal for this purpose since its chloride is not too stable, the element is liquid over a large temperature range with a low vapor pressure, and it

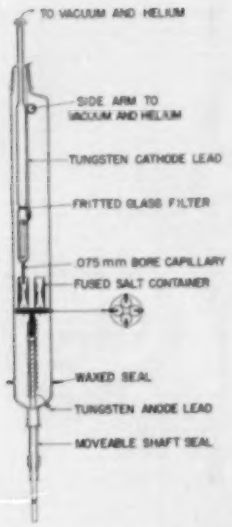


Fig. 1. Dropping bismuth polarographic cell with four fused salt cups.

has a melting point of 271°C. Other metals however can probably be used instead of bismuth depending on the experimental conditions.

Finally, the advantages of the dropping electrode include a constantly renewed surface which is important when ions are being reduced to metals at the electrode, and a shape which enables a mathematical treatment of the mass transport at this electrode (Ilkovic equation). When proper care is taken, the dropping electrode seems to obey these equations better than other electrodes, probably because of the thin diffusion layer which exists at dropping electrodes (13a).

## Experimental Details

The apparatus used for obtaining polarograms is shown in Fig. 1. Since it was imperative to exclude oxygen from both the bismuth (the formation of an oxide causes plugging of the capillary) and the fused salt, the capillary and salt cup were contained in a vacuum-tight Vycor tube 70 cm long and 64 mm in diameter. Ground glass ball joints connected the container and the space above the capillary to separate sources of both helium and high vacuum. This arrangement allows one to regulate the pressure difference across the capillary to any value between 0 and 1 atmosphere.

The capillaries were made by drawing Pyrex tubing to a small bore, care being taken to obtain a thick wall so the end could be cut off at 90° to the bore. The particular capillary to be used was then selected by examination using a microscope. Capillaries with a 0.075-mm bore and a 10-cm length were found best suited for experiments. One could produce a slow drop time with this size, and the bore was large enough not to plug easily. Before the bismuth entered the capillary it was filtered through a coarse Pyrex frit located above the capillary.

The fused salt was held in four Pyrex cups which also contained bismuth pool anodes. A tungsten wire was sealed into the bottom of each cup and cleaned electrolytically to insure good electrical contact. The tungsten wires also served to hold the salt cups on a stand which could be raised and lowered to the desired height by a moveable shaft seal. This shaft seal was constructed from "trubore tubing" which was lubricated with a high vacuum grease to keep the container tight to a vacuum better than $10^{-5}$ mm Hg. Electrical contact to the dropping bismuth cathode was made by sealing a tungsten wire through the inner Pyrex tube as shown. To assure a good electrical contact with the bismuth pool, a tantalum ribbon was spot welded to the tungsten wire.

In an attempt to make the capillary section of use in more than one experiment, a tantalum foil "pillow" was added to this compartment. When the bismuth solidified upon cooling, the pillow would collapse and the glass would not break. Unfortunately, bismuth remaining in the capillary itself would more often than not break the capillary upon expansion.

A wire wound nichrome resistance furnace surrounding the outer Vycor container was used to heat the contents to approximately 450°C. The temperature was measured with a chromel-alumel thermocouple attached to the outside of the Vycor container and was controlled with a recording potentiometer. A sight port through the cylindrical furnace enabled one to view the dropping electrode and the salt cups for manipulation at high temperature.

The current through the cell was measured by recording the voltage drop across a standard resistor (200 or 250 ohm) in series with the cell. A Brown automatic recorder with 25 mv full scale and a pen speed of 3.5 sec full scale was used. The potential applied across the cell varied linearly with time at the rate of 0.3 v/min. This was accomplished by driving a Helipot with a synchronous motor and a Graham variable speed transmission, the source of voltage being a 2-v storage battery.

After each run the entire salt content of the cell was weighed, dissolved, and analyzed for Pb, Cd, or Zn using aqueous polarographic techniques.

The LiCl-KCl eutectic (41 mole % KCl) used as solvent was prepared as follows. The powdered materials, in a weight ratio to form the eutectic mixture, were put above a fine Pyrex frit and attached to a source of high vacuum and purified helium. The contents were heated under vacuum just below the melting point for approximately 24 hr then melted under vacuum for another hour and forced through the frit into capsules by applying an atmosphere of helium pressure over the molten salt. The capsules were then evacuated and sealed off for later use in experiments.

The solute salts were prepared independently. The $PbCl_2$ was used as obtained from the manufacturer. The $CdCl_2$ powder was desiccated for one day under vacuum. The $ZnCl_2$ powder was heated under dry HCl, then melted, and finally evacuated and sealed off in a capsule until used. The bismuth metal was also pretreated before it was loaded into

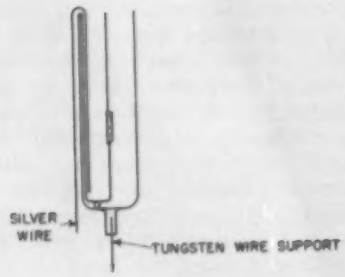


Fig. 2. Fused salt cup using a Ag|AgCl reference electrode

the apparatus by melting and filtering it through a coarse glass frit.

In order to use the half cell Ag|AgCl in LiCl-KCl (eutectic), as a working anode instead of the bismuth pool, the cup shown in Fig. 2 was constructed and replaced the cups shown in Fig. 1. Here a small tube containing a fine Pyrex frit was sealed into one of the ordinary salt cups. A 2 wt % solution of AgCl in KCl-LiCl (eutectic) was added to this tube along with a Ag wire. The remainder of the cup was filled with the solution to be examined. The tungsten wire merely served to hold the cup on its platform and the Ag wire was the anode. Unfortunately, the fine frit would sometimes allow appreciable amounts of AgCl to diffuse through it. The silver chloride would then react with the bismuth pool collected at the bottom of the larger compartment to produce bismuth trichloride. This bismuth trichloride would then be reduced at the dropping electrode and interfere with the shape of the polarograms under investigation. For this reason the bismuth pool anode was used in most experiments.

### Experimental Results

Polarograms obtained with the apparatus are shown in Fig. 3, 4, and 5 and Fig. 8. Figure 3 is a polarogram taken on the solvent salt alone giving a background current of 9 $\mu$a. This current decreases

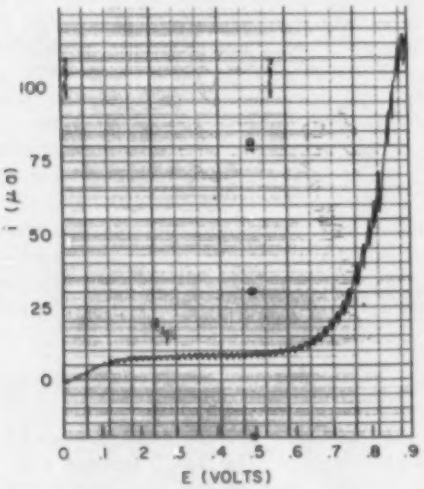


Fig. 3. Polarogram of LiCl-KCl eutectic (blank) using a drop time of 2.7 sec. Potential negative to bismuth pool anode here and in Figs. 4, 5, 8.

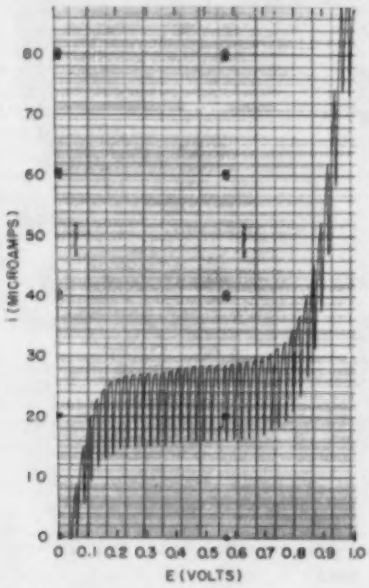


Fig. 4. Polarogram of a 1.8 millimole/liter $PbCl_2$ solution in LiCl-KCl eutectic at a drop time of 4 sec.

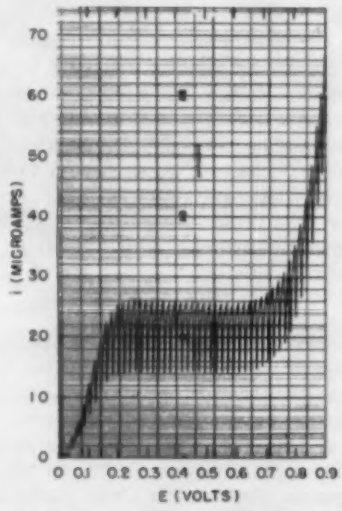


Fig. 5. Polarogram of a 3.4 millimole/liter $CdCl_2$ solution in LiCl-KCl eutectic at a drop time of 3.1 sec.

slightly at larger drop times. An estimate of the reducible impurity content of this salt from the polarogram puts it at about 0.5 millimoles/liter. Figure 4 is a polarogram of $PbCl_2$, whereas Fig. 5 shows a polarogram of $CdCl_2$ in the eutectic mixture. In all of these curves it can be seen that the solvent salt starts to be reduced at around −0.8 v with respect to the bismuth pool.

In the polarogram of $PbCl_2$ there is a small negative current which arises before a voltage is applied to the cell. This is probably due to a mixed potential arising from the reaction

$$2Bi(\text{dropping electrode}) + 3PbCl_2(\text{LiCl-KCl}) = 2BiCl_3(\text{LiCl-KCl}) + 3Pb(Bi)$$

which takes place to a small extent when the fresh bismuth solution comes in contact with the salt

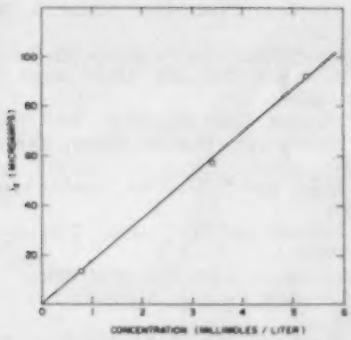

Fig. 6. Concentration dependence of the diffusion current for $PbCl_2$ at a drop time of 4 sec.

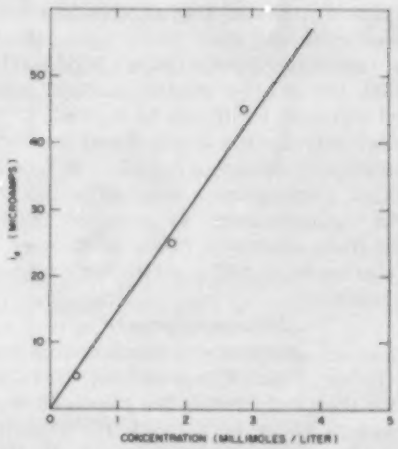

Fig. 7. Concentration dependence of the diffusion current for $CdCl_2$ at a drop time of 3.1 sec.

solution. Since $CdCl_2$ is more stable than $PbCl_2$ (14), this effect is negligible in the $CdCl_2$ polarogram.

The concentration dependence of the diffusion current is shown in Fig. 6 and 7 for $PbCl_2$ and $CdCl_2$ where a correction has been made for the current from the solvent alone. The diffusion current was taken at the maximum current of each drop. Concentrations were calculated using the density data of Van Artsdalen and Yaffe (15). A straight line is obtained within 5% for concentrations from 0.5 to 5 millimolar. This precision can probably be improved by further purification of the solvent salt and the use of more advanced electrical circuitry techniques.

Figure 8 shows a polarogram of $PbCl_2$ and $ZnCl_2$ in the eutectic mixture with a very fast drop time. Here the limiting current is not diffusion controlled (note the large currents obtained in comparison to those using large drop times), the Ilkovic equation fails and one readily obtains maxima as evidence with the $Zn^{++}$ wave. It was found however that the limiting current was proportional to the concentration even at these fast drop times.

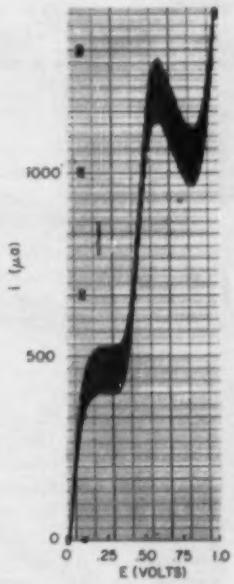


Fig. 8. Polarogram of a solution containing 3.6 millimoles/liter $PbCl_2$ and 8.5 millimoles/liter $ZnCl_2$ in the eutectic mixture at a drop time of 0.8 sec.

## Discussion

The Ilkovic equation for bismuth drops at 450°C is

$$i_d = 880\, n\, D^{1/2} C\, m^{2/3} t^{1/6}$$

where $i_d$ is the diffusion current in microamperes, measured at the maximum current of each drop, $t$ the drop time in seconds, $m$ the mass of the flowing bismuth in mg/sec, $D$ the diffusion coefficient in $cm^2$/sec, and $C$ the concentration in millimoles/liter. This equation is derived using the density of liquid bismuth at 450°C which is 9.8 g/$cm^3$ (16). Since the diffusion current $i_d$ is inversely proportional to the two-thirds power of the density of the flowing metal (13b), the above equation is obtained from the corresponding equation for mercury by multiplication of the mercury constant 706 by the two-thirds power of the density ratio of mercury to bismuth $(13.69/9.8)^{2/3}$.

Diffusion coefficients were calculated from this equation by measuring $m$ and $t$. Knowing the values of $i_d$ and $C$ as shown in Fig. 6 and 7, the values of $D$ were found to be $1.7 \times 10^{-5}$ $cm^2$/sec and $1.8 \times 10^{-5}$ $cm^2$/sec for $PbCl_2$ and $CdCl_2$, respectively, at 450°C.

Since Laitinen and co-workers (17, 18) have obtained the diffusion coefficients for $PbCl_2$ and $CdCl_2$ in this eutectic mixture from chronopotentiometric measurements, a check was available to see that the Ilkovic equation was applicable. These workers obtain values for $D$ of $2.0 \times 10^{-5}$ $cm^2$/sec and $1.7 \times 10^{-5}$ $cm^2$/sec for $PbCl_2$ and $CdCl_2$, respectively. The agreement is considered satisfactory and within the limits expected in light of the assumptions made in obtaining the Ilkovic equation and the experimental accuracy of the measurements reported here.

Other elements may also be examined using dropping bismuth electrodes. Although the LiCl starts to be reduced at −0.8 v with respect to the bismuth pool due to its low activity coefficient in bismuth (19) and its high concentration in the salt

mixture, it is estimated that all chlorides less stable than manganese and more stable than gallium (14) can be investigated with pure dropping bismuth electrodes. Use of alloy electrodes might extend the range of elements which can be studied.

In these experiments it was found that when the concentration of reducible ion exceeds 7 or 8 millimoles/liter, polarographic maxima would interfere with the measurements. As expected the maxima occurred more readily at faster drop times. No attempt was made to find a maximum suppressor for these systems.

### Acknowledgments

The authors would like to thank Mr. L. Bowditch, Dr. K. Rowley, Miss Elinor Norton, and Dr. F. T. Miles, for their help during the course of this work, and especially Dr. R. H. Wiswall, Jr., who originally suggested this problem. They also thank Dr. R. A. Osteryoung for helpful suggestions concerning the importance of drop time in obtaining a diffusion controlled process.

Manuscript received March 31, 1960. Work on this paper was done under the auspices of the U.S.A.E.C.

Any discussion of this paper will appear in a Discussion Section to be published in the June 1961 JOURNAL.

### REFERENCES

1. Y. S. Lyalikov and V. I. Karmazin, *Zavadskaya Lab.*, **14**, 138, 144 (1948).
2. Y. S. Lyalikov, *Zhur. Anal. Khim.*, **5**, 323 (1950); **8**, 38 (1953).
3. Y. K. Delimarski, *Uspekhi Khim.*, **23**, 766 (1954).
4. N. G. Chovnyk, *Doklady Akad. Nauk. SSSR*, **87**, 1033 (1952).
5. N. G. Chovnyk, *Zhur. Fiz. Khim.*, **30**, 277 (1956).
6. I. D. Panchenko, *Ukrain. Khim. Zhur.*, **21**, 468 (1955).
7. E. D. Black and T. DeVries, *Anal. Chem.*, **27**, 906 (1955).
8. H. A. Laitinen and H. C. Gaur, *This Journal*, **104**, 730 (1957).
9. S. N. Flengas, *J. Chem. Soc.*, **1956**, 534.
10. N. G. Chovnyk, *Doklady Akad Nauk. SSSR*, **95**, 599 (1954).
11. N. H. Nachtrieb and M. Steinberg, *J. Am. Chem. Soc.*, **70**, 2613 (1948); **72**, 3558 (1950).
12. P. A. Giguare and D. P. Lamontagne, *Science*, **120**, 390 (1954).
13. I. M. Kolthoff and J. J Lingane, "Polarography," Interscience Publishers, 2nd ed, New York (1952); (a) p. 43-44; (b) p. 40.
14. H. A. Laitinen and C. H. Liu, *J. Am. Chem. Soc.*, **80**, 1015 (1958).
15. E. R. Van Artsdalen and I. S. Yaffe, *J. Phys. Chem.*, **59**, 118 (1955).
16. A. Journiaux, *Bull. Soc. Chim.*, **51**, 677 (1932).
17. H. A. Laitinen and W. S. Ferguson, *Anal. Chem.*, **29**, 4 (1957).
18. H. A. Laitinen and H. C. Gaur, *Anal Chim. Acta*, **18**, 1 (1958).
19. J. J. Egan and R. H. Wiswall, Jr., *Nucleonics*, **15**, 104 (1957).

## Brief Communications

The JOURNAL accepts short technical reports having unusual importance or timely interest, where speed of publication is a consideration. The communication may summarize results of important research justifying announcement before such time as a more detailed manuscript can be published. Consideration also will be given to reports of significant unfinished research which the author cannot pursue further, but the results of which are of potential use to others. Comments on papers already published in the JOURNAL should be reserved for the Discussion Section published biannually.

*Submit communications in triplicate, typewritten double-spaced, to the Editor, Journal of The Electrochemical Society, 1860 Broadway, New York 23, N. Y.*

# Irreversible Thermodynamics in Electrochemistry

**Andre J. deBethune**

*Chemistry Department, Boston College, Chestnut Hill, Massachusetts*

ABSTRACT

The Onsager thermodynamics of irreversible processes provides a unified approach to the study of electrolytic systems out of equilibrium, such as concentration cells with transference, the initial and final emf's of thermal cells, and thermal diffusion (Soret effect) of ions. For concentration cells, the method justifies the classical results obtained by Nernst from equilibrium considerations. For nonisothermal systems, the product $S^*dT$ is the thermodynamic driving force of a process, where $S^*$ is the entropy transported reversibly from the "hot" to the "cold" heat reservoir (in the limiting case of equal temperatures) by the occurrence of a reversible process in the system. The emf of a concentration cell, the initial emf of a thermal cell, and the Soret coefficient, all properties of systems out of equilibrium, are determined, according to the Onsager relations, by the ratios of the reversible fluxes of matter to electricity, of entropy to electricity, and of entropy to matter, respectively, as they occur in systems completely at equilibrium.

The transport entropy $S^*$ can become, according to circumstances, the entropy $S^*_I$ of electrical transport, or the entropy $S^*_D$ of diffusion transport. $S^*_I$ in turn involves the entropies $S^*_E$ of electrochemical transport (for the electrode reactions) and $S^*_M$ of migration transport (for the thermal liquid junction). The contribution of an ion (or electron) to $S^*_E$ and to $S^*_M$ gives rise to the ionic entropies of electrochemical transport $S^*_{Ei}$ and of migration transport $S^*_{Mi}$, respectively. The latter contributes also to $S^*_D$. The sum $\overline{S}_i = S^*_{Ei} + S^*_{Mi}$ is known as the entropy of the moving ion and is measurable for a single ionic species. The initial thermal emf involves the transport entropy $S^*_I$, the Soret coefficient involves $S^*_D$, while the final thermal emf involves $S^*_I \pm t_e S^*_D$ where $t_e$ is the transference number of the ion to which the electrodes are not reversible.

For the hydrogen ion, $S^{*\circ}_E(H^+) = -4.48$ cal/deg, if $S^*_M$ is taken as zero in a saturated potassium chloride salt bridge. For other ions, $S^{*\circ}_{Ei} = S^\circ_i - z_i\,4.48$, and the mass action dependence is normal. For most ions, $S^*_{Mi}$ appears to be small, i.e., about 0-3 cal/deg, and the mass action dependence is abnormal and low. In dilute solutions, $S^*_{Mi}$ shows a Debye dependence on concentration. These facts are consistent with the electrostatic interpretation of $S^*_{Mi}$ as the entropy of depolarization of the solvent dielectric when the ion moves away. For ions transferred by a chain mechanism ($H^+$ and $OH^-$), $S^*_{Mi}$ is significantly larger. The transport of ions across biological membranes plays an important role in life processes. Since living systems are not necessarily uniform in temperature, ionic transport entropies may have a role to play in the function of the biological cell.

The classic application of thermodynamics to a cell out of equilibrium is Nernst's (1) well-known law for the emf of an isothermal concentration cell with transference, derivable from chemical potentials (free energies), and expressible in terms of ionic transference numbers $t_i$ and ionic concentrations $c_i$ (in ideal solutions) or ionic activities $a_i$.

Another example of a cell out of equilibrium is a thermal cell (electrochemical thermocouple) consisting of two identical electrode-electrolyte systems maintained at two different temperatures. A thermal cell develops a measurable emf, usually several tenths of a millivolt per degree, directly proportional to the applied temperature differential over not too wide temperature ranges. Thermal cells have been investigated experimentally, since the pioneering work of Bouty (2), by Richards (3), Kolthoff (4), Sorensen (5), and Lange (6), among others. The subject has been reviewed by Lange (7) and by deBethune, Licht, and Swendeman (8, hereinafter referred to as deBLS). Under usual experimental conditions, the emf developed, known as the *initial thermal emf*, has been found stable whenever free convection maintains constancy of the electrolyte concentration across the temperature gradient.

Thermal cells may be subject to thermal diffusion in the electrolyte (Soret effect) (9). This tends to concentrate strong electrolytes, usually in the cold region (10), by several tenths of one per cent per degree (11). The development of these concentration gradients, if not prevented by convection, further affects the emf, which gradually shifts to a new stationary value, the *final thermal emf*. Such

emf shifts were demonstrated experimentally by Agar and Breck (12) in a cell whose electrolyte was wholly contained within the pores of a sintered Pyrex disk, to prevent convective remixing of the thermally diffused solute. The emf shift, of the order of hundredths of a millivolt per degree, followed a first order law with a half-life of about 10 min in their cell, and was essentially complete in 1-2 hr.

The thermodynamic theory of the *initial emf* of a thermal cell has been given by Eastman (13a) and by Wagner (13b) from Carnot's theorem, in terms of certain transport entropies designated by deBLS (8) as the *ionic entropy of electrochemical transport* $S^*_{ei}$ and the *ionic entropy of migration transport* $S^*_{mi}$.[1] These ionic entropies are not separately determinable (without assumptions) for a single ionic species.

Temkin and Khoroshin (14) combined Eastman's theory (13a) of the Soret effect with Nernst's concentration cell equation to obtain an expression for the *final emf* of a thermal cell. While the *initial thermal emf* depends not only on the ion $r$ to which the electrodes are reversible, but also on the gegenion $g$, Temkin and Khoroshin proved that the *final thermal emf* is independent of the gegenion, [a fact which was experimentally verified by Agar and Breck (12)]. They further proved that the sum $S^*_{ei} + S^*_{mi}$, which they denote as the entropy of the moving ion (Entropiya dvizhushchikhsya Iona) $\overline{\overline{S}}_i$, is an experimentally determinable quantity for a single ionic species, provided a value can be assigned to $\overline{\overline{S}}$ for the electrons.

The thermodynamic relations governing electrolytic systems out of equilibrium, such as concentration cells, thermal cells, and thermal diffusion, can be derived in an elegant manner by the methods of irreversible thermodynamics and the Onsager reciprocal relations (15). Treatments along such lines have already been given by Prigogine (16), deGroot (17a), Holtan (17b), Kirkwood (18), van Rysselberghe (19a), Haase (19b), Harned and Owen (20), and Agar (21).

In the present paper, we shall apply the Onsager thermodynamics from a particularly simple point of view, namely, from a consideration of those fluxes that are macroscopically measurable, the flux $I$ of electricity, $J$ of entropy, and $K$ of solute. These fluxes are measurable, $I$ by an ammeter, $J$ by a calorimeter, and $K$ by chemical analysis. The conjugate driving forces are also measurable, so that the method is a powerful one for expressing theoretical relationships between measurable entities under certain nonequilibrium conditions.

### General Description of Thermodynamic System

Consider an electrolyte containing a single binary solute, one molecule of which dissociates into $\nu = \nu_+ + \nu_-$ ions of valence $z_+$ and $z_-$ (with sign). Electroneutrality demands that $\nu_+z_+ + \nu_-z_- = 0$, while the magnitude of the $\nu_iz_i$ product for either ion will be denoted by $\beta$. The molality of the solute is $m$, its thermodynamic mean ion activity $a_\pm$, and its chemical potential $\mu(\text{salt}) = \nu_+\mu_+ + \nu_-\mu_- = \mu^\circ + \nu RT \ln a_\pm = \mu^\circ + \nu RT \ln \nu_\pm m\gamma_\pm$.

The cell can be represented schematically by

$$\text{Cu}(T_1, V)/\text{Electrode } (T_1)/\text{Electrolyte } (T_1, a)/\text{Electrolyte } (T_2, a + da)/\text{Electrode } (T_2)/(\text{Cu}(T_2)/\text{Cu}(T_1, V + dV) \quad [1]$$

where $T_1$ and $T_2$ denote the temperatures of two large separate heat reservoirs No. 1 and 2 in contact with different portions of the system, and $T_2 = T_1 + dT$ and $dT \geqq 0$. The electrical potentials are $V$ and $V + dV$ in the left and right terminals, respectively. The two ionic species will be denoted by the indeces $i$ and $j$ in general, the ion to which the electrodes are reversible by $r$, the gegenion of $r$ by $g$. Let the current $I$ be positive when it flows through the cell from left to right. The entropy flux $J$ (in calories·deg$^{-1}$·sec$^{-1}$) will be taken positive from the hot ($T_2$) to the cold ($T_1$) heat reservoir. The ionic fluxes $K_i$ (in gram ions·sec$^{-1}$), and the solute flux $K$ (in moles·sec$^{-1}$), defined as $\Sigma K_i/\nu$, will be taken positive through the liquid junction from right to left. The current $I$ at the liquid junction can be expressed by $\mathbf{F}(K_- - K_+)$ for 1,1-salts and by $-\mathbf{F}\Sigma z_iK_i$ in general.

The irreversible rate of production of Clausius' uncompensated entropy (22, 23) from all these fluxes can be expressed by

$$\dot{S} = IX_I + JX_J + \Sigma K_iX_i \geqq 0 \quad [2]$$

where the driving forces are $X_I = -dV/T$, $X_J = dT/T$, $X_i = d\mu_i/T = R\,d\ln a_i$. The two ionic terms are conveniently coalesced to

$$K_+X_+ + K_-X_- = (K_+ + K_-)\,R\,d\ln a_\pm = KX_K \quad [3]$$

where $X_K = d\mu(\text{salt})/T = \nu R\,d\ln a_\pm$. Equation [2] then becomes

$$\dot{S} = IX_I + JX_J + KX_K \geqq 0 \quad [4]$$

The three fluxes may be expressed by phenomenological equations

$$I = L_{II}X_I + L_{IJ}X_J + L_{IK}X_K \quad [5]$$

$$J = L_{JI}X_I + L_{JJ}X_J + L_{JK}X_K \quad [6]$$

$$K = L_{KI}X_I + L_{KJ}X_J + L_{KK}X_K \quad [7]$$

where the $L$'s are generalized admittances (reciprocal resistances). By the Onsager reciprocal relations, the conjugate cross-admittances are equal, i.e., $L_{IJ} = L_{JI}$, $L_{IK} = L_{KI}$ and $L_{JK} = L_{KJ}$.

Apply Eq. [5] to the cell when the temperature and concentration are both uniform ($X_J$ and $X_K = 0$). A current $I$ flowing is then the resultant only of an externally applied emf $-dV = TX_I$, and Ohm's law shows that $L_{II} = T/r$ where $r$ is the total resistance of the circuit, including any "polarization resistances" of the electrodes. In general, however, Eq. [5] shows the current $I$ as the resultant of three emf's: an externally applied emf $dE_{ext} = -dV = L_{II}X_Ir = TX_I$; a thermally induced emf $dE_{th} = L_{IJ}X_Jr = TL_{IJ}X_J/L_{II}$; and a concentration emf $dE_{conc} = L_{IK}X_Kr = TL_{IK}X_K/L_{II}$.

[1] In Eastman's terminology, the absolute ionic entropy, and the entropy of transfer, respectively. See Appendices I and II for nomenclature of transport entropies.

At the potentiometric balance point, $I = 0$, and

$$-TX_I = TL_{II}X_I/L_{II} + TL_{IE}X_E/L_{II} \qquad [8a]$$

or

$$-dE_{ext} = dV = dE_{th} + dE_{conc} \qquad [8b]$$

i.e., we have the ordinary condition for potentiometric balance, in which the observed potential difference $dV$ between the two terminals is a measure of the combined electromotive forces intrinsic to the system. These emf's are to be considered positive, following the Lewis-Stockholm convention (24), whenever they tend to drive positive electricity through the cell from left to right.

### Isothermal Concentration Cells

Take cell [1] at uniform temperature ($X_I = 0$). From Eq. [8],

$$-TX_1 = dV = dE_{conc} = TL_{IE}X_E/L_{II} \qquad [9]$$

By the Onsager relations, this becomes,

$$dE_{conc} = (L_{EI}/L_{II})\nu RT\, d\ln a_{\pm}. \qquad [10]$$

Suppose now that the cell is brought to a state of uniform concentration ($X_E = 0$), and a small external emf applied ($dV$ negative). The current flowing is $I = L_{II}X_I = \beta\mathbf{F}/\tau$ if $\tau$ is the time required for the passage of $\beta$ faradays of positive electricity through the cell from left to right. The simultaneous flux of solute through the cell from right to left is $K = L_{EI}X_I = (K_+ + K_-)/\nu$. The ionic fluxes from right to left are $K_+ = \beta(1 - t_+)/z_+\tau$ for the ion to which the electrodes are reversible, and $K_- = -\beta t_-/z_-\tau$ for the gegenion, where the $t_i$'s are Hittorf transference numbers. Since $t_+ + t_- = 1$, the solute flux becomes

$$K = (\beta t_-/\tau\nu)(1/z_+ - 1/z_-) \qquad [11]$$

Since $\nu_i z_i = \pm\beta$ (for $z_i = \pm$), $1/z_+ - 1/z_-$ is equal to $\pm(\nu_+ + \nu_-)/\beta$ for $z_+ = \pm$, so that

$$K = \pm t_-/\tau \quad (\text{if } z_+ = \pm) \qquad [12]$$

The ratio $L_{EI}/L_{II} = (K/I)_{x_I = x_E = 0} = \pm t_-/\beta\mathbf{F}$. Equation [10] then yields Nernst's expression for the emf of a concentration cell with transference

$$dE_{conc} = \pm t_-(\nu RT/\beta\mathbf{F})\, d\ln a_{\pm} \quad (\text{if } z_+ = \pm) \qquad [13]$$

This equation is derived here as a consequence of the Onsager relations. The emf of an isothermal concentration cell is expressible in terms of the measurable quantities $t_-$ and $a_{\pm}$ and is a fully significant thermodynamic quantity, as discussed by Guggenheim (25).

It is of theoretical interest to decompose the concentration emf [13] into the sum of (*a*) the difference of the electrode potentials $dE_{e1}$; plus (*b*) the liquid junction potential $dE_{lj}$. Neither of these two terms is exactly measurable, and neither is unambiguously calculable from fully significant quantities. Yet both are approximately measurable, e.g., by the use of two saturated potassium chloride calomel electrodes (SCE) immersed in the two electrolyte compartments of the cell, and both can be calculated from any arbitrarily selected definition of single ion activities, such as that implicit in the Debye theory (26).

To clarify the point at issue, postulate an *ideal reference electrode* (IRE), *which can be defined conceptually as an unpolarizable electrode having zero thermal temperature coefficient* (8) *and zero liquid potential at the junction of its salt bridge with any electrolyte*. Two such IRE's are immersed in the two electrolyte compartments of cell [1], and connected by two leads of the same kind of metal to the isothermal potentiometric slide wire to which the two terminals of cell [1] are already connected. The potentials in the two IRE leads are $V'$ and $V' + dV'$, respectively. Then at potentiometric balance for all four electrodes, $dE_{ej} = dV'$, while $dE_{el} = [(V + dV) - (V' + dV')] - [V - V'] = dV - dV'$.

It is convenient to consider the current $I$ and the two ionic fluxes $K_+$ and $K_-$

$$I = L_{II}X_I + L_{I+}X_+ + L_{I-}X_- \qquad [14]$$

$$K_+ = L_{+I}X_I + L_{++}X_+ + L_{+-}X_- \qquad [15]$$

$$K_- = L_{-I}X_I + L_{-+}X_+ + L_{--}X_- \qquad [16]$$

At the balance point, $I = 0$, and

$$-TX_I = dV = dE = TX_+(L_{I+}/L_{II}) + TX_-(L_{I-}/L_{II}) \qquad [17]$$

By the Onsager relations, this becomes

$$dE = TX_+(L_{+I}/L_{II}) + TX_-(L_{-I}/L_{II}) =$$

$$TX_+(K_+/I)_{x_+ = x_- = 0} + TX_-(K_-/I)_{x_+ = x_- = 0} \qquad [18]$$

Consider now a cell at uniform concentration ($X_+ = X_- = 0$). The current $I$ is $\beta\mathbf{F}/\tau$, as before. The two electrode reactions together yield the ionic fluxes $K_+ = \beta/z_+\tau$ and $K_- = 0$. This gives for the difference of the electrode potentials

$$dE_{e1} = TX_+/z_+\mathbf{F} = (RT/z_+\mathbf{F})d\ln a_{\pm} \qquad [19]$$

At the liquid junction, the two ionic fluxes are $K_i = -t_i\beta/z_i\tau$ so that the junction potential becomes

$$dE_{lj} = T\,\Sigma(-t_i/z_i\mathbf{F})X_i = (-RT/\mathbf{F})\cdot \Sigma\,(t_i/z_i)\, d\ln a_i \qquad [20]$$

In contrast to Eq. [13], neither [19] nor [20] are fully thermodynamically significant since they involve nonfully significant single ion activities. They can be made approximately significant by adopting a rule for the definition of single ion activities, either (*a*) Scatchard's practical rule (27) "We will define single ion activities as those measured with the use of a saturated potassium chloride bridge" as in pH or pCl measurements (28, 29) or (*b*) a theoretical rule, consistent with the Debye theory whereby $a_i = \nu_i m\gamma_i$ and $\gamma_{\pm} = \gamma_+^{-\sigma_+/\sigma_j} = \gamma_-^{\sigma_j/\sigma_+}$. Where this latter rule is adopted, [19] becomes

$$dE_{e1} = (RT/z_+\mathbf{F})\, d\ln m[1 + (\nu_-/\nu_+)\cdot (d\ln\gamma_{\pm}/d\ln m)] \qquad [19']$$

and [20] becomes

$$dE_{ij} = (-RT/\mathbf{F})\,\Sigma(t_i/z_i)\,\mathrm{d}\ln m\,.$$

$$[1 + (\nu_j/\nu_i)(\mathrm{d}\ln\gamma\ /\mathrm{d}\ln m)] \qquad [20']$$

where $j = g, \tau$ when $i = \tau, g$. The right hand sides of both [19'] and [20'] now involve only fully significant quantities.

Equations [13], [19], and [20] are identical with the classical expressions derived from chemical potentials by the application of the reversible thermodynamics of isothermal processes to concentration cells with transference, in spite of the fact that these cells are not at equilibrium. The Onsager relations show why the application of reversible relations to a nonequilibrium situation nevertheless yields correct results. The coefficients of the chemical potential gradients $TX_g$, or $TX_\tau$ and $TX_g$, in the emf equations [10], [17] and [18], become, by the Onsager relations, flux ratios of matter to electricity of the form $K/I$. However, these flux ratios are to be taken, in each case, in a cell that is completely at equilibrium ($X_I$ and $X_K$'s all equal to zero). The flux $I$ is therefore a reversible flux of electricity in the strict thermodynamic sense, and the $K$'s are the conjugate reversible fluxes of matter. It is the ratio of the reversible fluxes $K/I$ in an equilibrium cell (whose emf is zero) which determines, together with the actual chemical potential gradients, the observable emf of the actual nonequilibrium concentration cell.

### Initial EMF of Thermal Cells

Take cell [1] at uniform concentration ($X_g = 0$). From Eq. [8],

$$-TX_I = \mathrm{d}V = dE_{th} = TL_{II}X_I/L_{II} \qquad [21]$$

By the Onsager relations, this becomes

$$dE_{th} = (L_{gI}/L_{II})\ dT \qquad [22]$$

Suppose now that the cell is brought to uniform temperature ($dT = 0$) and a small external emf applied ($\mathrm{d}V$ negative). The current flowing is $I = L_{II}X_I = \beta\mathbf{F}/\tau$, as before. At the same time, the entropy flux is $J = L_{gI}X_I = S^*_I/\tau$ if $S^*_I$ is the entropy transported from the right heat reservoir (No. 2) to the left heat reservoir (No. 1), when $\beta$ faradays of positive electricity are transferred through the cell from left to right. $S^*_I$ may be termed the entropy of electrical transport. The ratio $L_{gI}/L_{II} = (J/I)_{X_I=X_K=0} = S^*_I/\beta\mathbf{F}$. From [22], one obtains therefore for the initial thermal emf

$$dE_{th} = (S^*_I/\beta\mathbf{F})\ dT \qquad [23]$$

The ratio $J/I$ is, once again, the ratio of two reversible fluxes occurring in an equilibrium cell (whose emf is zero). This ratio determines, together with the actual temperature gradient, the observable emf of the actual nonequilibrium thermal cell. As defined here, the thermal emf is positive whenever the hot electrode is the (+) terminal of cell [1].

The entropy $S^*_I$ is the entropy transported isothermally and reversibly from one heat reservoir to the other by a reversible flow of electricity, in the absence of a temperature gradient. The transport of entropy occurs by a threefold mechanism. (i) The reaction at the right electrode absorbs a quantity of heat $Q^*_g$ from its heat reservoir (No. 2) while the equal and opposite reaction at the left electrode evolves an equal quantity of heat to its heat reservoir (No. 1). The entropy transported is $S^*_g = Q^*_g/T$ and is denoted as the *entropy of electrochemical transport*. (ii) The migration of ions through the electrolyte is accompanied by the absorption of a quantity of heat $Q^*_M$ (Eastman's "heat of transfer") from the electrolyte in the right compartment, and the evolution of an equal quantity of heat to the electrolyte in the left compartment. An equal amount of heat then enters the right electrolyte from the right heat reservoir (No. 2) and leaves the left electrolyte to the left heat reservoir (No. 1), to keep the temperature constant. The entropy transported is $S^*_M = Q^*_M/T$ and is denoted as the *entropy of migration transport*. (iii) The migration of $\beta$ moles of electrons from the $T_1$ zone to the $T_2$ zone of the right-hand Cu terminal of cell [1] transfers heat from the No. 1 to the No. 2 heat reservoir. Dividing this heat by $T$, one obtains the entropy transported from No. 2 to No. 1 as $-\beta S^*_M$ ($E^-$ in Cu). Thus

$$S^*_I = S^*_g + S^*_M - \beta S^*_M(E^- \text{ in Cu}) \qquad [23a]$$

For the passage of $\beta$ faradays of positive electricity through the cell from left to right, the reaction at the right electrode may be written as $\beta$ times

$$\Sigma\omega_k\mathrm{A}_k + (1/z_\tau)\mathrm{A}_\tau + E^-(\mathrm{Cu}, T_2) = 0 \qquad [24]$$

where $\mathrm{A}_\tau$ is the ion to which the electrode is reversible, and the $\mathrm{A}_k$ denote neutral substances whose stoichiometric coefficients $\omega_k$ may be positive or negative. Thus for Ag/Ag$^+$ electrodes, reaction [24] is: $\mathrm{Ag}^+ - \mathrm{Ag} + \mathrm{E}^- = 0$; for Pb/PbSO$_4$ electrodes: $\frac{1}{2}\mathrm{PbSO_4} - \frac{1}{2}\mathrm{Pb} - \frac{1}{2}\mathrm{SO_4}^= + E^- = 0$. The corresponding *entropy of electrochemical transport* $S^*_g$ is, for $\beta$ faradays,

$$S^*_g = \beta\{-\Sigma\omega_kS_k - (1/z_\tau)S^*_{g,\tau} - S^*_g(E^- \text{ in Cu})\} \qquad [25]$$

where $S_k$ is the partial molal third law of entropy of the neutral species $\mathrm{A}_k$, and $S^*_{g,\tau}$ is the partial molal entropy of electrochemical transport of the ion $\tau$. $S^*_g(E^-$ in Cu) is the electrochemical transport entropy of the electrons in Cu, or in general, in the nonisothermal metallic terminal arm of the cell.

The *entropy of migration transport* can be expressed by

$$S^*_M = \Sigma(-t_i\beta/z_i)S^*_{M,i} \qquad [26]$$

where $S^*_{M,i}$ is the entropy of migration transport of the ion i (also known as its "entropy of transfer," see Appendix II). The total entropy transported by the current becomes

$$S^*_I = -\beta\Sigma\omega_kS_k - (\beta/z_\tau)S^*_{g,\tau} - \Sigma(t_i\beta/z_i)S^*_{M,i} - \beta\overline{S}(E^- \text{ in Cu}) \qquad [27]$$

where $\bar{\bar{S}}$, the entropy of the moving electrons (14), has been written for the sum $S^*_s + S^*_u$ for the electrons in Cu. The only electronic term appearing in the thermal emf is the entropy $\bar{\bar{S}}$ of the moving electrons in the nonisothermal metallic terminal arm of the cell. In Richard's (3) study of the calomel electrode, this was Hg; in Agar and Breck's (12) work, Pt; in the bulk of thermal cell studies, it has been Cu.

Now remove the two electrolyte compartments from cell [1], and allow the two electrodes to touch. Cell [1] becomes the thermocouple: Cu-Electrode. The equivalent value of $S^*_s$ becomes $S^*_s(E^-$ in Electrode$) - S^*_s(E^-$ in Cu) for 1 Faraday. The equivalent of $S^*_u$ becomes $S^*_u(E^-$ in Electrode). Therefore, for the whole thermocouple, Eq.[23] and [23a] yield[9]

$$\mathbf{F}(dE/dT)_{\text{couple}} = \mathbf{F}(dV/dT) = S^*_t = \bar{\bar{S}}(E^- \text{ in Electrode}) - \bar{\bar{S}}(E^- \text{ in Cu}) \qquad [28]$$

A comparison of Eq. [27] and [28] shows that the emf of a thermal cell does not contain a thermocouple emf as such, contrary to earlier statements (3, 8) that it does. But it does contain the entropy $\bar{\bar{S}}$ of the moving electrons in the nonisothermal metallic arm of the cell. No electronic term of the electrode metal itself appears, and the thermoelectric power of the terminal metal relative to the electrode metal makes no direct contribution to the thermal cell emf.

When thermal cells are measured with Cu terminals, and a "thermocouple correction" applied to the data [as in Carr and Bonilla's (30a) study of the Ni electrode], the net effect of the correction, by Eq. [28], is to transform the electronic term in [27] from that of Cu to that of the electrode metal itself. There seems to be no particular advantage to such a procedure, however. The better practice, experimentally and theoretically, would seem to be to *standardize on one metal for the nonisothermal metallic arm of all thermal cells*. In practice, this metal might as well be chosen as Cu.

Equation [28] gives a method for evaluating the entropy $\bar{\bar{S}}$ of moving electrons in different metals, relative to that in a standard metal, usually chosen to be Pb. From the magnitude of thermocouple emf's (microvolts per degree), such entropies amount to microvolt-faradays per degree, i.e., hundredths or tenths of a calorie per degree. Temkin and Khoroshin (14) evaluated the "absolute" value of $\bar{\bar{S}}(E^-)$ in Cu and Pt from the third-law integral

$$\bar{\bar{S}}(E^-) = -\mathbf{F}\int_0^T \sigma dT/T \qquad [29]$$

where $\sigma$ is the "absolute" Thomson coefficient of the metal, i.e., the heat capacity of the unit of positive electricity in the metal (30b). Their results are, in microvolt-faradays per degree,

$$\bar{\bar{S}}(E^- \text{ in Cu}) = -1.95 - 0.005\,(T - 300) \quad (T > 240°\text{K})$$

$$\bar{\bar{S}}(E^- \text{ in Pt}) = 4.54 + 0.044(T - 300) \quad (T > 220°\text{K})$$

Thus, at 298°K, $\bar{\bar{S}}(E^-$ in Cu$) = -1.94$ $\mu$vF/deg $= -0.045$ cal/deg. The electronic term could then be eliminated completely in [27] by adopting for the nonisothermal terminal arm a metal whose Thomson coefficient is virtually zero, e.g., Pb(30c). In practice, it is more convenient to use copper experimentally. The third-law value for the electrons in Cu is so small that it could, without significant error, be set equal to zero. This we shall do, and we shall thereby adopt a slightly different electronic standard from that of Temkin and Khoroshin. We shall arbitrarily set $\bar{\bar{S}}(E^-$ in Cu) equal to zero at all temperatures. The electronic term in [27] may then be omitted, provided the thermal cell is measured with nonisothermal terminal arms of copper.

Thus for a thermal $Ag/AgNO_3$ cell ($\beta = 1$)

$$\mathbf{F}(dE_{tb}/dT) = S^*_t = S(Ag) - S^*_s(Ag^+) + t_- S^*_s(NO_3^-) - t_+ S^*_s(Ag^+) \qquad [30]$$

and for a thermal $Al/Al_2(SO_4)_3$ cell ($\beta = 6$)

$$6\mathbf{F}(dE_{tb}/dT) = S^*_t = 2S(Al) - 2S^*_s(Al^{+3}) + 3t_- S^*_s(SO_4^{=}) - 2t_+ S^*_s(Al^{+3}) \qquad [31]$$

The initial thermal emf depends on the ion to which the electrodes are reversible, and also on the gegenion. The migration terms in [30] and [31] determine the thermal liquid junction potential (tljp), the other terms the effect of temperature on the electrode potentials. Neither of these quantities is separately measurable, without assumptions. Both are conceptually measurable by the use of two IRE's, as defined above.

The two transport entropies $S^*_{s_i}$ and $S^*_{u_i}$ for an ion do not coincide with one another, and neither do they coincide with its conventional partial molal ionic entropy $S_i$ (based on the standard $S°(H^+) = 0$ at all temperatures). $S^*_{s_i}$ is the entropy transported between heat reservoirs by an ion when it sheds its hydration sheath in being consumed at one electrode and picks up a new hydration sheath in being produced at the other electrode. $S^*_{u_i}$ is the entropy transported by the ion when it drags its hydration sheath with it across the cell. Neither of these entropies is separately determinable for a single ionic species (without assumptions). Neutral combinations are determinable, and also the sum $\bar{\bar{S}}_i = S^*_{s_i} + S^*_{u_i}$ for a single ion (see below).

The standard entropy of electrochemical transport of the hydrogen ion was shown by deBLS (8) to be $S^{*\circ}_s(H^+) = -4.48 \pm 0.5$ cal/deg at 25°C, from the thermal temperature coefficient of the

[9] Comparison of [28] with classical expressions for the thermoelectric power shows that $S^*_t = \mathbf{F}\pi/T$, where $\pi$ is the Peltier heat, i.e., the heat absorbed by the thermocouple when the unit of positive electricity crosses the junction from "Electrode" to Cu. The temperature derivative of the thermoelectric power yields $d^2V/dT^2 = dS^*_t/\mathbf{F}dT = C^*_t/\mathbf{F}T = [\bar{\bar{C}}(E^-$ in Electrode$) - \bar{\bar{C}}(E^-$ in Cu$)]/\mathbf{F}T = -[\sigma(\text{Electrode}) - \sigma(\text{Cu})]/T$, where $C^*_t$ is the heat capacity of electrical transport, $\bar{\bar{C}}$ the heat capacity of the moving electrons, and $\sigma$ the Thomson coefficient. Thus $\bar{\bar{C}}(E^-$ in Cu$) = -\mathbf{F}\sigma(\text{Cu})$. Over wide ranges of temperature, thermocouple emf's satisfy the empirical equation $V = at + \frac{1}{2}bt^2$. $S^*_t$ is then equal to $\mathbf{F}(a + bt)$ and $C^*_t = \mathbf{F}Tb$. Constancy of $b$ implies that $\bar{\bar{C}}/T$ is a constant.

standard hydrogen electrode which is + 0.871 millivolts per degree when measured with a saturated potassium chloride bridge (8, 31). This result is based on the assumption that $S^*_H$ can be set equal to zero in such a bridge ("saturated KCl bridge rule").

The standard entropy of electrochemical transport $S^{*\circ}_{zi}$ of any other ion should then be

$$S^{*\circ}_{zi} = S^\circ_i + z_i\ (-4.48\ \text{cal/deg}) \qquad [32]$$

Concentration effects on thermal emf's (8) indicate that the ionic entropy $S^*_{zi}$ has substantially the same mass-action dependence as the ordinary entropy $S_i$, i.e.,

$$S^*_{zi} = S^{*\circ}_{zi} - R \ln a_i - RT(d \ln a_i/dT) \qquad [33]$$

Ionic entropies of migration transport $S^*_{zi}$ are discussed in greater detail below. For many ions, the values appear to be quite small, about 0-3 cal/deg. For $H^+$ and $OH^-$, they are significantly larger, about 10 cal/deg. For many salts, the tljp's should not exceed a few hundredths of a millivolt per degree and should make only small contributions to total cell emf's of several tenths of a millivolt per degree (see below). In strong acids and bases, the tljp's appear to be large, about − 0.35 and + 0.5 mv/deg, respectively, referred to KCl as zero (8). These two values are qualitatively consistent with the Soret effect (below) in that the cold end of the thermal liquid junction dipole takes on the charge of the faster ion ($H^+$ or $OH^-$).

### Thermal Diffusion (Soret Effect)

Take cell [1] and remove both electrodes. This effectively makes $X_I = 0$. In the steady state of thermal diffusion, $K = 0$, and

$$X_E = -(L_{EJ}/L_{EE})X_J \qquad [34]$$

By the Onsager relations, this becomes

$$X_E/X_J = -L_{JE}/L_{EE} = -(J/K)_{x_1 = x_2 = 0} \qquad [35]$$

Now bring the cell to uniform temperature ($X_J = 0$), and let there be a small chemical potential gradient ($X_E$ positive), such that the solute flux $K = 1/\tau$, if $\tau$ is the time required for 1 mole of solute to diffuse across the liquid boundary from right to left, under the impulsion of $X_E$, in a cell (without convection) so large that this amount of diffusion does not significantly alter the chemical potential gradient. The concurrent flux of entropy is $J = S^*_D/\tau = (\nu_+ S^*_{z+} + \nu_- S^*_{z-})/\tau$, where $S^*_D$, the *entropy of diffusion transport*, is the entropy transported from the right heat reservoir No. 2 to the left heat reservoir No. 1 by the passage of 1 mole of solute through the liquid boundary from right to left. Equation [35] then transforms to

$$X_E/X_J = \nu RT(d \ln a_\pm/dT) = -(J/K)_{x_1 = x_2 = 0} = -S^*_D/1\ \text{mole} \qquad [36]$$

The Soret coefficient can be defined as the relative change in solute activity (or concentration) per degree change in temperature, i.e., either

$$d \ln a_\pm/dT = -S^*_D/\nu RT \qquad [37a]$$

or

$$d \ln m/dT = -S^*_D/\{\nu RT[1 + (d \ln \gamma_\pm/d \ln m)_T]\} \qquad [37b]$$

If the entropy of diffusion transport $S^*_D$ is positive, the Soret coefficient is negative, i.e., strong electrolytes concentrate in the cold region. This is the situation normally observed. Soret coefficients usually amount to minus a few tenths of one per cent per degree, the corresponding values of $S^*_D$ are then a few calories per degree per mole. Values for $S^*_D$ for a number of salts are listed in Table I.

Consider two thermal cells identical in every respect, except in the nature of the gegenion $g$. Then from Eq. [23] and [27], it can be shown that the difference between the initial thermal emf's of the two cells, containing the two electrolytes 1 and 2, is

$$F(dE/dT)_{\text{in},1} - F(dE/dT)_{\text{in},2} = t_{r2} S^*_{zr}/z_r + t_{g2} S^*_{zg}/z_g - t_{r1} S^*_{zr}/z_r - t_{g1} S^*_{zg}/z_g = \pm t_{g1} S^*_{D1}/\beta_1 \mp t_{g2} S^*_{D2}/\beta_2 \quad (\text{if } z_r = \pm) \qquad [38]$$

Equation [38] provides a convenient method of evaluating the entropy $S^*_D$ of one salt relative to that of another salt with which it has a common ion, from observations of initial thermal emf's. The vanishing of electrode terms from Eq. [38] implies

**Table I. Entropies of diffusion transport $S^*_D$ (cal/deg.mole) at 25°C**

KCl: 0.0025 *m*, 2.21[d]; 0.005 *m*, 1.88[d]; 0.01 *m*, 1.72[a], 1.68[d], 3.15(34.7°)[d]; 0.02 *m*, 1.58[d]; 0.05 *m*, 0.91[c]; 1 *m*, 0.37[b], 1.20(35°)[b], 2.02(45°)[b]; 2 *m*, 0.86[b], 0.087(15°)[b], 1.63(35°)[b], 2.31(45°)[b]; 3 *m*, 1.26[b], 0.52(15°)[b], 1.97(35°)[b], 2.61(45°)[b]; 4 *m*, 1.70[b], 1.06(15°)[b], 2.28(35°)[b], 2.86(45°)[b].

KBr: 0.0025 *m*, 2.15[d]; 0.005 *m*, 1.98[d]; 0.01 *m*, 1.87[c], 1.85[d], 3.15(34.7°)[d]; 0.02 *m*, 1.68[d]; 0.05 *m*, 1.05[c].

KI: 0.0025 *m*, 0.27[d]; 0.005 *m*, 0.10[d]; 0.01 *m*, −0.09[c,d], 1.27(34.7°)[d]; 0.02 *m*, −0.27[d]; 0.05 *m*, −0.65[c].

NaCl: 0.0025 *m*, 3.12[d]; 0.005 *m*, 2.62[d]; 0.01 *m*, 2.60[c], 2.58[d], 3.80(34.7°)[d]; 0.02 *m*, 2.08[d]; 0.05 *m*, 1.81[c].

NaBr: 0.0025 *m*, 3.09[d]; 0.005 *m*, 2.82[d]; 0.01 *m*, 2.74[c], 2.70[d]; 0.02 *m*, 2.42[d]; 0.05 *m*, 1.94[c].

$AgNO_3$: 0.01 *m*, 4.20[c], 4.16[d], 5.33(34.7°)[d]; 0.014 *m*, 3.92[d]; 0.1 *m*, 2.90[b], 4.95(45°)[b]; 0.2 *m*, 2.81[b], 4.24(45°)[b]; 0.5 *m*, 2.79[b], 3.99(45°)[b]; 1 *m*, 3.14[b], 3.86(45°)[b].

$\frac{1}{2}CdSO_4$: 0.01*m*, 3.85[c]; 0.033 *m*, 3.08[c]; 0.09 *m*, 2.35[d]; 0.1 *m*, 2.43[c], 2.41[b], 3.36(45°)[b]; 0.18 *m*, 2.08[b], 2.94(45°)[b]; 0.34 *m*, 1.76[c]; 0.37 *m*, 1.69[b], 2.45(45°)[b]; 1 *m*, 1.22[b], 1.86(45°)[b]; 1.04 *m*, 1.32[c]; 2.1 *m*, 1.14[c].

$TlClO_4$: 0.005 *m*, 2.55[d]; 0.01 *m*, 2.35[d]; 0.02 *m*, 2.18[d]; 0.05 *m*, 2.85[c], 1.98[d]; 0.1 *m*, 1.73[c]; 0.15 *m*, 2.18[c]; 0.2 *m*, 1.58[c]; 0.26 *m*, 1.54[c].

$\frac{1}{2}Tl_2SO_4$: 0.04 *m*, 5.22[d]; 0.1 *m*, 4.03[c].

0.1 *m* solutions[c]: $TlNO_3$: 1.69; $TlOCOCH_3$: 6.17; $\frac{1}{2}Tl_2CO_3$: 4.27; $\frac{1}{2}Cd(ClO_4)_2$: 1.1; $\frac{1}{2}Cd(NO_3)_2$: 0.77; $\frac{1}{2}CdCl_2$: 0.70.

0.01 *m* solutions[d]: KF: 4.56; NaF: 5.48, 6.72(34.7°); NaI, 0.77, 2.05(34.7°); LiF: 2.83, 4.13(34.7°); LiCl: −0.067; LiBr: 0.047, 1.10(34.7°); LiI: −1.94, −0.23(34.7°); RbCl: 2.75; CsCl: 2.78; $(C_2H_5)_4NCl$: 10.36; $KNO_3$: 1.66(34.7°); $NaNO_3$: 1.64; $\frac{1}{2}K_2SO_4$: 4.6, 5.9(34.7°).

[a] Agar, conductimetric (21); [b] Longsworth, optical (11); [c] Agar and Breck, initial and final thermal emf (12); [d] Agar and Turner, conductimetric (51).

**Table II. Differences of thermal liquid junction potentials (mv/deg) and entropies of diffusion transport $S^*_p$ (cal/deg. mole) computed from them by Eq. [38]. 0.01 molal or normal electrolytes, except where noted. Reference values in parentheses.**

| Electrolyte | Δtljp | $S^*_p$ | Electrolyte | Δtljp | $S^*_p$ |
|---|---|---|---|---|---|
| KCl | $+0.011 \pm 0.003^{aa}$ | — | $\frac{1}{2}CdCl_2$ | $+0.03^{af}$ | 0.4 |
| KCl(1*M*) | $+0.024 \pm 0.003^{aa}$ | — | $Et_4NCl^e$ | $-0.114^{ak}$ | 11.6 |
| KCl | $(0.000)^a$ | $(1.72)^f$ | KBr | $(+0.0039)^{am}$ | $(1.87)^f$ |
| KCl(1*M*) | $(0.000)^a$ | $(0.37)^g$ | LiBr | $+0.0367^{bn}$ | 0.18 |
| HCl | $-0.340^{ab}$ | 10.5 | NaBr | $-0.0058^{bn}$ | 2.69 |
| HCl(1*m*) | $-0.344^{ab}$ | $9.7^g$ | $NH_4Br$ | $+0.0336^{bn}$ | 0.27 |
| LiCl | $+0.04^{ai}$ | −0.24 | $Me_4NBr^e$ | $-0.072^{bo}$ | 7.32 |
| LiCl(1*M*) | $+0.046^{aj}$ | $-3.0^g$ | $Et_4NBr^e$ | $-0.0985^{bo}$ | 11.9 |
| NaCl | $-0.007^{ak}$ | 2.56 | $n\text{-}Pr_4NBr^e$ | $-0.1024^{bo}$ | 16.6 |
| NaCl (1*m*) | $-0.033^{ak}$ | $2.54^g$ | $n\text{-}Bu_4NBr^e$ | $-0.1019^{bo}$ | 19.5 |
| $NH_4Cl$ | $+0.01^{al}$ | 1.25 | $n\text{-}Am_4NBr^e$ | $-0.1011^{bo}$ | 22.8 |
| $NH_4Cl$(1*m*) | $+0.026^{ak}$ | $-0.86^g$ | KI | $(-0.0405)^{cm}$ | $(-0.12)^f$ |
| RbCl | $-0.016^{ab}$ | 2.42 | LiI | $+0.0275^{cb}$ | −2.12 |
| RbCl(1*m*) | $-0.088^{ak}$ | $4.42^g$ | NaI | $-0.0165^{cb}$ | 0.83 |
| CsCl | $-0.0265^{ak}$ | 2.90 | KOH | $+0.445^{ca}$ | 15.17 |
| CsCl(1*m*) | $-0.078^{ak}$ | $3.96^g$ | LiOH | $+0.0901^{dn}$ | 12.57 |
| $\frac{1}{2}CaCl_2$(1*N*) | $-0.08^{al}$ | $5.8^g$ | NaOH | $+0.0440^{db}$ | 15.46 |
| $\frac{1}{2}SrCl_2$ | $-0.01^{al}$ | 2.5 | $Me_4NOH^e$ | $+0.0252^{db}$ | 20.2 |
| $\frac{1}{2}SrCl_2$(1*N*) | $-0.08^{al}$ | $5.8^g$ | $Et_4NOH^e$ | $+0.0342^{db}$ | 26.8 |
| $\frac{1}{2}BaCl_2$ | $-0.02^{al}$ | 3.0 | $n\text{-}Pr_4NOH^e$ | $+0.0644^{db}$ | 29.7 |
| $\frac{1}{2}BaCl_2$(1*N*) | $-0.08^{al}$ | $5.3^g$ | $n\text{-}Bu_4NOH^e$ | $+0.0748^{db}$ | 33.6 |
| $\frac{1}{2}MgCl_2$ | $+0.02^{al}$ | 0.9 | $n\text{-}Am_4NOH^e$ | $+0.0813^{db}$ | 36.3 |
| $\frac{1}{2}ZnCl_2$ | $+0.01^{al}$ | 1.5 | $KNO_3$ | $(-0.0219)^{cm}$ | $(0.76)^f$ |
| $\frac{1}{2}ZnCl_2$(1*N*) | $+0.02^{al}$ | $-0.8^g$ | $AgNO_3$ | $-0.123^{cm}$ | 5.85 |

[aa] Referred to "saturated KCl," i.e., observed thermal emf's of calomel and silver chloride cells in 1*M* and 0.01*M* KCl, Richards (3), Kolthoff and Tekelenburg (4), Bernhardt and Crockford (41), Salvi (42), Young (43), Goyan (43), and Levin and Bonilla (47), *minus* calculated thermal emf's of deBLS (8), based on "saturated KCl bridge rule."

[a] Referred to KCl of the same concentration.
[b] Referred to KBr of the same concentration.
[c] Referred to KI of the same concentration.
[d] Referred to KOH of the same concentration.
[e] Me, methyl; Et, ethyl; Pr, propyl; Bu, butyl; Am, amyl.
[f] Reference values of $S^*_p$ for 0.01*m* electrolytes from Agar (21), cf. Tables I and III(b).
[g] Referred to Longsworth's (11) $S^*_p = 0.37$ cal/deg for 1 *m* KCl (Table I).
[h] Bernhardt and Crockford (41).
[i] Khoroshin and Temkin (14).
[j] Salvi (42).
[k] Goyan, Young, and Preston (43).
[l] Richards (3).
[m] Computed from reference values of $S^*_p$ via Eq. [38].
[n] Goodrich, *et al.* (44).
[o] Burian (45), Khoroshin and Temkin (14), Lange and Hesse (46).
[q] Observed thermal emf's in KOH and $AgNO_3$ electrolytes, *minus* calculated thermal emf's of deBLS (8), based on "saturated KCl bridge rule," and corrected to KCl of the same concentration by means of [aa] values above.

that the activity of the ion $r$ is the same in the two electrolytes. Clearly, this assumption is valid only for dilute solutions of the two salts, at the same concentration of the ion $r$, and at the same ionic strength. Under this assumption, the difference of the initial thermal emf's given by [38] is simply the difference of the thermal liquid junction potentials (tljp's) of the two salts.

In Table II are listed such differences of tljp's between the electrolytes listed and certain reference electrolytes chosen to be KCl, KBr, KI, and KOH, as determined from observed values of initial thermal emf's (except for values in parentheses which are computed from the reference $S^*_p$ values via Eq. [38]). A positive sign means that the hot end of the thermal liquid junction dipole is more positively charged than that of the reference electrolyte.

The transference numbers utilized in Eq. [38] have been taken, or estimated, from MacInnes (48), Harned and Owen (20), or from the sources of the thermal emf data. The $S^*_p$ values listed in Table II have then been computed from observed Δtljp's and from certain reference $S^*_p$ values (in parentheses) taken from Tables I and III(b).

While the accuracy of the method is limited, as discussed by Tyrrell, *et al.* (49), *e.g.*, an uncertainty of ± 0.01 mv/deg in the Δtljp yields uncertainties in $S^*_p$ ranging from ± 0.5 cal/deg when the relevant transference number is ½, up to ± 2 cal/deg when the transference number drops to 1/10th, nevertheless, the results are in fair agreement with those of other methods [Tables I and III(a)(b)], and are of interest since they yield a number of new values of $S^*_p$ for electrolytes not previously determined.

In dilute solutions, the entropy $S^*_p$ of diffusion transport behaves as an additive ionic property (21). This permits the evaluation of the entropy of migration transport of an ion, relative to that of some standard ion. Such conventional single ion values of $S^*_{ir}$ are given in Table III, relative to $S^*_{ir}(Cl^-) = 0$ at all concentrations. Column (a) gives Eastman's estimates of 1928, intended by him as absolute values. Column (b) is taken from Agar's work. Columns (c) and (d) are based on the values of $S^*_p$ deduced from the Δtljp's in Table II, except for the reference values in parentheses, and for certain values based on Table IV as noted.

The concentration dependence of $S^*_p$ has been

Table III. Conventional single ion entropies of migration transport $S^*_{M_t}$ (cal/deg) at 25°C based on $S^*_M(Cl^-) = 0$.

| Ion | $S^*_{M_t}$ (a) | (b) | (c) | (d) | Ion | $S^*_{M_t}$ (a) | (b) | (c) | (d) |
|---|---|---|---|---|---|---|---|---|---|
| $H^+$ | 9.3 | 10.4 | 10.5 | 9.7 | $OH^-$ | — | — | 13.5 | — |
| $Li^+$ | 0.1 | —0.084 | —0.3 | —3.0 | $F^-$ | — | 2.92 | — | — |
| $Na^+$ | 0.9 | 2.61 | 2.55 | 2.54 | $Cl^-$ | 0.0 | (0) | (0) | (0) |
| $K^+$ | 1.0 | 1.72 | (1.72) | (0.37) | $Br^-$ | — | 0.134 | ).15) | — |
| $Rb^+$ | 1.1 | 2.79 | 2.4 | 4.4 | $I^-$ | — | —1.84 | (—1.84) | — |
| $Cs^+$ | — | 2.82 | 2.9 | 4.0 | $NO_3^-$ | — | —0.96 | (—0.96) | — |
| $Ag^+$ | — | 5.16 | 6.8 | — | $\frac{1}{2}SO_4^=$ | — | 2.925 | 2.7′ | 0.0′ |
| $NH_4^+$ | 0.0 | — | 0.7 | —0.9 | $ClO_4^-$ | — | — | 1.0′ | —3.0′ |
| $\frac{1}{2}Mg^{++}$ | — | — | 0.9 | — | $CH_3COO^-$ | — | — | 3.3(0.1m)′ | |
| $\frac{1}{2}Ca^{++}$ | — | — | — | 5.8 | $\frac{1}{2}CO_3^=$ | — | — | 1.5(0.1m)′ | |
| $\frac{1}{2}Sr^{++}$ | — | — | 2.5 | 5.8 | $Tl^+$ | — | — | 3.1(0.1m)′ | |
| $\frac{1}{2}Ba^{++}$ | — | — | 3.0 | 5.3 | $\frac{1}{2}Cd^{++}$ | — | — | 1.35′ | 1.05′ |
| $\frac{1}{2}Zn^{++}$ | — | — | 1.5 | —0.8 | | | | | |
| $\frac{1}{2}Cd^{++}$ | — | 0.935 | 0.4 | — | | | | | |
| $Me_4N^{+a}$ | — | 6.71 | 7.0 | — | | | | | |
| $Et_4N^{+a}$ | — | 10.44 | 11.7 | — | | | | | |
| $n\text{-}Pr_4N^{+a}$ | — | — | 16.3 | — | | | | | |
| $n\text{-}Bu_4N^{+a}$ | — | — | 19.7 | — | | | | | |
| $n\text{-}Am_4N^{+a}$ | — | — | 22.7 | — | | | | | |

(a) Eastman (32) for 0.02N.
(b) Agar (12, 21) for 0.01m.
(c) This study, estimated from Table II for 0.01m. Reference values in parentheses.
(d) This study, estimated from Table II for 1 M. Reference values in parentheses.
[a] Me, methyl; Et, ethyl; Pr, propyl; Bu, butyl; Am, amyl.
′ Interpolated or extrapolated from data of Table IV; single ion values based on "saturated KCl bridge rule," instead of chloride ion standard.

discussed by Agar (21). It decreases with increasing concentration (Table I) in dilute solutions, but much less rapidly than a normal mass-action dependent entropy would, and it seems to attain a finite limiting value at infinite dilution. In concentrated solutions of KCl and $AgNO_3$, $S^*_D$ increases with increasing concentration! The derivative $dS^*_D/d \ln a_\pm$ is very close to $-R$ in $CdSO_4$ and to $-\frac{1}{2}R$ in $TlClO_4$, instead of the mass-action value $-2R$ for salts with $\nu = 2$.

In very dilute solutions ($m < 0.02$), $S^*_D$ decreases as a linear function of the square root of the molality. The derivative $dS^*_D/d\sqrt{m}$ has values, in cal/deg. (unit of molality)$^{1/2}$, of —6.0 to —6.5 in dilute KCl, NaCl, KBr, NaBr, and KI; and of —26 in $CdSO_4$. These values are discussed again below in connection with the electrostatic interpretation of the ionic entropy of migration.

### Final EMF of Thermal Cells

Restore the two electrodes to cell [1], and allow a Soret steady state to be established. This makes $K = 0$ while $X_E \neq 0$. At potentiometric balance, $I = 0$. Equations [5], [6], and [7] can then be solved, with elimination of $X_E$, to yield

$$(-X_I/X_J)_{I=0} = dV/dT = dE_{I=0}/dT$$
$$= [L_{IJ}/L_{II} - (L_{IE}/L_{II})(L_{EJ}/L_{EE})]/$$
$$[1 - (L_{IE}/L_{II})(L_{EI}/L_{EE})] \quad [39]$$

This expression involves four distinct admittance ratios, three of which have already been evaluated. The fourth admittance ratio is $L_{EI}/L_{EE}$. This can be equated to $L_{IE}/L_{EE} = (I/K)_{X_I=X_J=0}$, i.e., it is equal to the ratio of the flux of electricity to the flux of matter in the liquid boundary, in the absence of any applied emf (no electrodes) and of a temperature gradient. However, the flux of matter under such conditions occurs by diffusion of electroneutral groups of ions and does not give rise to an electric current at all. Therefore $I/K = 0$ in the boundary, and this fourth admittance ratio is zero. Equation [39] simplifies to

$$(-X_I/X_J)_{I=0} = L_{IJ}/L_{II} - (L_{IE}/L_{II})(L_{EJ}/L_{EE}). \quad [40]$$

The validity of Eq. [40] can be confirmed by noting that the admittance ratios can be replaced by driving force ratios, e.g., $L_{ab}/L_{cc} = -(X_a/X_b)_{a=X_c=0}$, so that

$$(-X_I/X_J)_{I=0} = (-X_I/X_J)_{I=X_E=0} + (-X_I/X_E)_{I=X_J=0} \cdot (X_E/X_J)_{E=X_I=0} \quad [41]$$

The latter expression is obviously equivalent to

$$(dV/dT)_{I=0} = (\partial V/\partial T)_{d\ln a=0} + (\partial V/RT\,\partial \ln a)_{dT=0} \cdot (RT\,\partial \ln a/\partial T)_{dT=0} \quad [42]$$

i.e., the final thermal emf is equal to the initial thermal emf $L_{IJ}/L_{II}$ plus a term which is exactly the isothermal emf of the concentration cell that the Soret effect has created.

We have already established that $L_{IJ}/L_{II} = S^*_I/\beta\mathbf{F}$; $L_{IE}/L_{II} = \pm t_e/\beta\mathbf{F}$ (if $z_e = \pm$); and $L_{EJ}/L_{EE} = S^*_D/1$ mole. Therefore Eq. [40] transforms to

$$dE_{I=0}/dT = S^*_I/\beta\mathbf{F} \mp t_e S^*_D/\beta\mathbf{F} \quad (\text{if } z_e = \pm) \quad [43]$$

By introducing values for $S^*_I$ (Eq. [27]) and $S^*_D$, Eq. [43] further transforms to

$$dE_{I=0}/dT = (1/\beta\mathbf{F})\{-\beta\Sigma\omega_s S_s - (\beta/z_r)S^*_{E_r} - \beta\bar{\bar{S}}(E^- \text{ in Cu}) - t_r(\beta/z_r)S^*_{M_r} - t_e(\beta/z_e)S^*_{M_E} \mp t_e\nu_r S^*_{M_r} \mp t_e\nu_e S^*_{M_E}\} \quad (\text{if } z_e = \pm). \quad [44]$$

Since $\mp \nu_r = -\beta/z_r$ and $\mp \nu_e = +\beta/z_e$ for $z_e = \pm$, the terms involving the migration transport

entropy of the gegenion $g$ vanish, while the two corresponding terms for the ion $r$ coalesce to $-(\beta/z_r)S^*_{w,r}$. The final emf therefore reduces to

$$dE_{t_{1a}}/dT = (1/\beta\mathbf{F})\{-\beta\Sigma\omega_s S_s - \beta\bar{\bar{S}}(E^- \text{ in Cu}) - (\beta/z_r)\bar{\bar{S}}_r\} \quad [45]$$

All properties of the gegenion have vanished from Eq. [44] and [45], while the ion $r$ contributes the sum $S^*_{s,r} + S^*_{w,r} = \bar{\bar{S}}_r$, denoted by Temkin and Khoroshin (14) as the "entropy of the moving ion." This sum thus becomes a measurable thermodynamic property of a single ion, provided a value can be assigned to the electronic term, as discussed above.

For example, for a thermal Ag/Ag$^+$ cell, the final emf, with the electronic term neglected is given by $dE_{t_{1a}}/dT = (1/\mathbf{F})\ [S(\text{Ag}) - \bar{\bar{S}}\ (\text{Ag}^+)]$. For a thermal $\text{Hg/Hg}_2\text{SO}_4/\text{Al}_2(\text{SO}_4)_3$ cell, it is $dE_{t_{1a}}/dT = (1/6\mathbf{F})[6S(\text{Hg}) - 3S(\text{Hg}_2\text{SO}_4) + 3\bar{\bar{S}}(\text{SO}_4^=)]$.

A comparison of Eq. [43] and [23] show that the *final* minus the *initial* thermal emf of a cell is equal to $\mp\ t_+S^*_D/\beta\mathbf{F}$ (if $z_+ = \pm$). This provides an electrochemical method of measuring the entropy $S^*_D$ of diffusion transport, and the associated Soret coefficient (12).

It is of theoretical interest to decompose the measurable final thermal cell emf [45] into formal expressions for the electrode potential difference and the liquid junction potential, since these two quantities are at least conceptually measurable by the use of two IRE's, as defined above. The liquid junction potential in the final state of the thermal cell can be formally expressed by evaluating Eq. [40] for the liquid boundary processes only. In the boundary $L_{12}/L_{11} = L_{21}/L_{11} = (J/I)_{x_2=x_{2'}=0} = -\Sigma t_i(\beta/z_i)S^*_{w,i}/\beta\mathbf{F} = (t_+\nu_-S^*_{w,-} - t_-\nu_+S^*_{w,+})/\beta\mathbf{F}$; and $L_{12}/L_{11} = L_{32}/L_{11} = (K/I)_{x_2=x_{2'}=0} = -t_i(\beta/z_i)/\nu\beta\mathbf{F} = (t_+\nu_- - t_-\nu_+)/\nu\beta\mathbf{F}$, provided $K$ is taken as $(K_+ + K_-)/\nu$; while $L_{33}/L_{33}$ as evaluated above is already a boundary quantity equal to $S^*_D/1$ mole $= (\nu_+S^*_{w,+} + \nu_-S^*_{w,-})/1$ mole. The substitution of these expressions into Eq. [40] gives, for the final thermal liquid junction potential,

$$dE_{lj,\ t_{1a}}/dT = \nu_+\nu_-(S^*_{w,-} - S^*_{w,+})/\nu\beta\mathbf{F} \quad [46a]$$

For example, in sodium chloride electrolyte, this becomes $(1/2\mathbf{F})[S^*_w(\text{Cl}^-) - S^*_w(\text{Na}^+)]$, and in aluminum sulfate $(3\cdot 2/5\cdot 6\mathbf{F})[S^*_w(\text{SO}_4^=) - S^*_w(\text{Al}^{+++})]$.

By subtracting [46a] from [45], neglecting the electronic term, one obtains the difference of the electrode potentials for the final state of the thermal cell in the form

$$dE_{e,\ t_{1a}}/dT = S^*_w/\beta\mathbf{F} - S^*_D/\nu z_+\mathbf{F} \quad [46b]$$

The first term in [46b] gives the effect of temperature on the electrode potentials, without liquid junction potential and without thermal diffusion. The second term gives the further effect of the thermal diffusion concentration gradient on the electrode potentials. This second term takes the form, in a thermal Ag/AgCl/NaCl cell, $(1/2\mathbf{F})[S^*_w(\text{Na}^+) + S^*_w(\text{Cl}^-)]$; in a thermal $\text{Al/Al}_2(\text{SO}_4)_3$ cell, $-(1/5\cdot 3\mathbf{F})[2S^*_w(\text{Al}^{+++}) + 3S^*_w(\text{SO}_4^=)]$.

**Table IV. Transport entropies of $Tl^+$ and $Cd^{++}$ ions and gegenions (cal/mole.deg) from the data of Agar and Breck (12)**

$S^*(Tl^+) = 30.4$; $S^*(Cd^{++}) = -14.6$ (33)

| Electrolyte | $\bar{\bar{S}}_+$ | $pa_+$ | $S^*_{s,+}$ | $S^*_{w,+}$ | $S^*_{w,-}$ |
|---|---|---|---|---|---|
| $TlClO_4$, 0.05$m$ | 35.8 | 1.403 | 32.3 | 3.5 | −0.6 |
| $TlClO_4$, 0.1$m$ | 33.9 | 1.132 | 31.1 | 2.8 | −1.1 |
| $TlClO_4$, 0.15$m$ | 34.0 | 0.982 | 30.4 | 3.6 | −1.4 |
| $TlClO_4$, 0.20$m$ | 33.3 | 0.879 | 29.9 | 3.4 | −1.8 |
| $TlClO_4$, 0.26$m$ | 32.5 | 0.800 | 29.6 | 2.9 | −1.4 |
| $TlNO_3$, 0.1$m$ | 34.0 | 1.151 | 31.2 | 2.8 | −1.1 |
| $TlOCOCH_3$, 0.1$m$ | 34.0 | 1.131 | 31.1 | 2.9 | 3.3 |
| $Tl_2CO_3$, 0.05$m$ | 33.9 | 1.138 | 31.1 | 2.8 | 3.0 |
| $Tl_2SO_4$, 0.05$m$ | 34.0 | 1.138 | 31.1 | 2.9 | 2.3 |
| $CdSO_4$, 0.005$m$ | −8.96 | 2.602 | −11.7 | 2.7 | 5.0 |
| $CdSO_4$, 0.017$m$ | −10.99 | 2.248 | −13.3 | 2.3 | 3.9 |
| $CdSO_4$, 0.05$m$ | −12.47 | 1.973 | −14.6 | 2.1 | 2.8 |
| $CdSO_4$, 0.17$m$ | −13.93 | 1.684 | −15.9 | 2.0 | 1.6 |
| $CdSO_4$, 0.52$m$ | −14.78 | 1.458 | −16.9 | 2.1 | 0.6 |
| $CdSO_4$, 1.05$m$ | −14.64 | 1.327 | −17.5 | 2.9 | −0.6 |
| $Cd(ClO_4)_2$, 0.05$m$ | −12.27 | 1.835 | −15.2 | 2.9 | −0.4 |
| $Cd(NO_3)_2$, 0.05$m$ | −11.87 | 1.842 | −15.2 | 3.4 | −0.9 |
| $CdCl_2$, 0.05$m$ | −10.07 | 2.406 | −12.6 | 2.5 | −0.5 |

### Values of the Ionic Transport Entropies

Values of the entropy $\bar{\bar{S}}_+$ of the moving ion have been obtained for $Cd^{++}$ and $Tl^+$ by Agar and Breck (12) from measured final thermal emf's, and are listed in Table IV. The corresponding entropies $S^*_D$ of diffusion transport, from the difference of final and initial thermal emf's, are given in Table I. In Table IV, $pa_+ = -\log a_+$ where $a_+ = \nu_+m\gamma_\pm$, $\gamma_\pm$ is calculated by the rule $\gamma_+ = \gamma_\pm^{-\nu_-/\nu_+}$, and $\gamma_\pm$ is interpolated from Latimer (33). The entropy of electrochemical transport $S^*_{s,+}$ is computed from entropy data (33) via the "saturated KCl bridge rule" of deBLS (8), Eq. [32] and [33], neglecting the third term in $d$ ln $a_\pm/dT$. The entropies of migration transport for the two ions are then computed from $\bar{\bar{S}}_+$ and $S^*_{s,+}$ (Table IV), and $S^*_D$ (Table I).

For both $Cd^{++}$ and $Tl^+$ ions, the mass-action dependence of $\bar{\bar{S}}_+$ parallels that of $S^*_{s,+}$, so that $S^*_{w,+}$ is apparently independent of concentration: $S^*_w(Tl^+) = 3.1 \pm 0.3$ cal/deg; $S^*_w(Cd^{++}) = 2.5 \pm 0.4$ cal/deg. The migration transport entropies of the anions do vary with concentration, and can be expressed within the range of concentrations studied by the approximate relations: $S^*_w(ClO_4^-) = -3.7 + (\frac{1}{2}R')pa(ClO_4^-)$; $S^*_w(SO_4^=) = -6.6 + R'pa(SO_4^=)$, where $R' = 2.303\ R$ and $pa_- = -\log a_-$. The mass-action dependence for sulfate is normal, while that for perchlorate contains the surprising coefficient $\frac{1}{2}R'$ instead of $R'$. Thus the concentration effect on $S^*_{w,+}$ ranges from apparently no dependence for $Tl^+$ and $Cd^{++}$, to half mass-action dependence for $ClO_4^-$, to full mass-action dependence for $SO_4^=$. Values of $S^*_{w,-}$ for other anions are as follows: 0.1 $m$ $NO_3^-$, −1.1, −0.9; 0.1 $m$ $CH_3COO^-$, 3.3; 0.05 $m$ $CO_3^=$, 3.0; 0.1 $m$ $Cl^-$ (in $CdCl_2$), −0.5. The several anion values, calculated above from the KCl bridge rule, show reasonable agreement between the $Tl^+$ and

Table V. Transport entropies of various ions (cal/deg) from the data of Khoroshin and Temkin (14)

| Ion | $\bar{S}^\circ_i$ | $S^{*\circ}_{\pi i}$ | $S^{*\circ}_{\mu i}$ |
|---|---|---|---|
| $H^+$ | 5.2 | −4.48 | 9.7 |
| $Li^+$ | −1.4 | −1.1 | −0.3 |
| $Na^+$ | 10.8 | 7.7 | 3.1 |
| $K^+$ | 20.0 | 20.0 | 0.0 |
| $NH_4^+$ | 21.4 | 22.49 | −1.1 |
| $Ag^+$ | 20.8 | 13.19 | 7.6 |
| $\frac{1}{2}Mg^{++}$ | −18.15 | −18.6 | 0.45 |
| $\frac{1}{2}Ca^{++}$ | −7.75 | −11.1 | 3.35 |
| $\frac{1}{2}Sr^{++}$ | −4.95 | −9.2 | 4.25 |
| $\frac{1}{2}Ba^{++}$ | −0.15 | −3 | 2.85 |
| $\frac{1}{2}Zn^{++}$ | −15.95 | −17.20 | 1.25 |
| $F^-$ | 7.8 | 2.2 | 5.6 |
| $Cl^-$ | 19.5 | 17.7 | 1.8 |
| $Br^-$ | 23.4 | 23.77 | −0.4 |
| $NO_3^-$ | 42.0 | 39.5 | 2.5 |
| $ClO_4^-$ | 46.8 | 47.7 | −0.9 |
| $\frac{1}{2}SO_4^=$ | 3.2 | 6.53 | −3.3 |

the $Cd^{++}$ series and are not inconsistent with the conventional values of Table III (referred to chloride as zero).

Values of the moving ion entropies $\bar{\bar{S}}_i$ have also been deduced by Khoroshin and Temkin (14) from the ingenious suggestion that initial thermal emf's measured in aqueous LiCl should be virtually the same as final thermal emf's, since $S^*_p$ for dilute LiCl is virtually zero (Table III). This led them to a value of 19.5 cal/deg for $\bar{\bar{S}}^\circ(Cl^-)$. From this, they deduced values for other ions from the relation

$$\Sigma\nu_i\bar{\bar{S}}_i = \Sigma\nu_i S_i + \Sigma\nu_i S^*_{\pi i} \qquad [47]$$

where $S_i$ is the conventional ionic entropy. Equation [47] is valid for any neutral ion combination for which $\Sigma\nu_i S_i = \Sigma\nu_i S^*_{\pi i}$. The final summation in [47] is, of course, $S^*_p$ for a neutral electrolyte. By taking $S_i$ and $S^*_p$ data from various sources, Khoroshin and Temkin obtained the values of $\bar{\bar{S}}^\circ_i$ given in Table V. Standard entropies of electrochemical transport $S^{*\circ}_{\pi i}$ have been computed from conventional entropy data (33) by means of the "saturated KCl bridge rule," Eq. [32]. The migration transport entropy $S^{*\circ}_{\mu i}$ is then obtained by difference. The values given in Table V are only approximate, but, on the whole, they are fairly consistent with data given in Tables I through IV.

### Ionic Transport Entropies

To distinguish between the ionic entropies of electrochemical transport $S^*_{\pi i}$ and of migration transport $S^*_{\mu i}$, it is necessary to consider the interaction between an ion and its environment. Eastman (34) divides the vicinity of an ion "into three concentric regions of gradually differing properties. First, there is the 'ion-cavity,' within which there are no solvent molecules." The thickness of the ion-cavity has been estimated (35) as 0.10Å for anions and 0.85Å for cations, in addition to the crystallographic ionic radius. Next comes the hydration (solvation) layer, described by Eastman in these words: "immediately outside of the ion cavity the (polar) molecules of solvent are strongly attracted and oriented. The inner layers of solvent molecules in this second region, and those extending out from it to varying distances in different cases, are held so strongly by the central ion as to form a complex with it, acting in processes of diffusion, as a single molecule. The third region comprises all the rest of the outer space. In this [third] sphere the solvent molecules are still subject to forces of compression and orientation, diminishing with distance from the center of the complex, and not sufficiently strong to bind these molecules to the ion."

Let one mole of the ion $i$ be associated with $n_2$ moles of bound solvent (in Eastman's second region) and $n_3$ moles comprising the remainder of the (unbound) solvent (Eastman's third region). Let $S_2$ and $S_3$ be the partial molal entropies of the solvent in these second and third regions, and $S_1$ the molal entropy of the solvent in the absence of any ions. The compression and orientation of solvent molecules by electrostatic attraction between the ion and the dipoles of the solvent result in $S_2$ being significantly less, and $S_3$ somewhat less, than $S_1$.

When one mole of an ion is transferred from the right to the left electrolyte compartment by the agency of the two electrode reactions, the entropy transported from the right (No. 2) to the left (No. 1) heat reservoir includes the quantity $(n_2 + n_3)S_1 - n_2S_2 - n_3S_3$, *i.e.*, the gain in entropy of the solvent upon its release from the ordering influence of the electric field of the ion, corresponding to the absorption of heat in the breaking of ion-solvent bonds in the second region and in the relaxation of compression and orientation forces in the third region. The entropy of transport for one molal unit of the electrode reaction might therefore be expressed as $S^*_\pi = S(M) - S_{ic}(M^+) + (n_2 + n_3)S_1 - n_2S_2 - n_3S_3$, where $S_{ic}(M^+)$ is the partial molal entropy of the ion-cavities of $M^+$. The entropy of electrochemical transport of the ion $M^+$ becomes $S^*_\pi(M^+) = S_{ic}(M^+) + n_2(S_2 - S_1) + n_3(S_3 - S_1)$, *i.e.*, it includes entropy terms pertaining to the binding of solvent molecules in the second region and to the orientation and compression of the solvent in the third region.

When one mole of an ion is transferred from the right to the left electrolyte compartment by migration, "the aggregate comprising the first and second regions above remains mostly intact and takes part in no . . . entropy changes. But as the ion moves it leaves behind material which had been under its influence in the third sphere, and brings under its influence solvent molecules not previously so strongly affected. A relaxation occurs, therefore, in the region from which it goes, with an attendant increase of entropy and absorption of heat. The reverse effects appear in the region into which it moves. It is, therefore, these changes in the third sphere that give rise" (Eastman, 34) to the ionic entropy of migration transport $S^*_\mu(M^+)$ which may be equated to $n_2S_1 - n_3S_3$, i.e., to the gain in entropy of the solvent in the third region upon its release from the electric field of the ion. On this model, the entropy of the moving ion $\bar{\bar{S}}(M^+)$ becomes

$S_{i,c}(M^+) + n_s(S_s - S_1)$, i.e., it includes the solvent entropy terms of the second region only, the region that moves with the ion.

The total entropy of the solvent $n_sS_s$ in the third region in the presence of the ion, relative to its entropy $n_sS_1$ in the absence of the ion, can be calculated at infinite dilution from a simple electrostatic model, on the assumption that the solvent in the third region can be treated as a continuous medium of dielectric constant $\epsilon$. Consider a charge $q$ located in a dielectric $\epsilon$ and a concentric sphere of radius $r$ so chosen that the surface of the sphere lies well into the dielectric region. The total electrostatic potential energy of the electric field outside the sphere is $q^2/2\epsilon\, k_s r$ where $k_s$ is a constant equal to 1 esu or $10^{-5}/8.988$ amp.sec.volt$^{-1}$.m$^{-1}$ (36). This energy may be equated to the electrostatic free enthalpy $G$ of the polarized dielectric outside the sphere, whose entropy therefore becomes $-dG/dT = -(q^2/2k_s r)d(1/\epsilon)/dT$. The latter may be taken equal to $n_s(S_s - S_1)$ and therefore to $-S^*_{tr,i}$. Gurney (37) suggests that the dielectric constant may be represented by the empirical formula $\epsilon = \epsilon_0 \exp(-T/\theta)$ where $\epsilon_0 = 305.7$ and $\theta = 219°K$ for water. The derivative $d(1/\epsilon)/dT = 1/\epsilon\theta = 5.83 \times 10^{-5}$ deg$^{-1}$ for water at 25°C. Upon substitution of appropriate numerical values, the ionic entropy of migration is calculated as

$$S^*_{tr,i} = +(9.68\ z_i^2/r_A)\ \text{cal/deg.mole} \quad [48]$$

at infinite dilution. Taking the crystal radius (38) of $K^+$ at 1.33Å, plus 0.85Å for the ion cavity, plus 2.80Å as the approximate diameter of one water molecule, a total radius of 5.0Å is estimated for the sphere "bounding" the second from the third regions. $S^*_{tr,i}$ can then be calculated as 1.94 cal/deg for $K^+$ ion at infinite dilution, a value which is of the right order as compared with the conventional single ion value of Table III. However, Eq. [48] cannot be used for any accurate calculation of $S^*_{tr,i}$ since the appropriate third region radius, and the short range dielectric constant, are uncertain. Agar (21) has shown that little correlation exists between conventional values of $S^*_{tr,i}$ and ionic crystal radii.

At finite concentration, the potential surrounding an ion is reduced by multiplication by the Debye-Hückel factor, $\exp(-\kappa r)$, and Eq. [48] should be multiplied by the same factor. The derivative $dS^*_{tr,i}/d\kappa$ becomes $-9.68\ z_i^2\exp(-\kappa r)$ cal.Å/deg. For 1, 1-salts in water at 25°C, and very dilute solutions where $\exp(-\kappa r) \approx 1$, the derivative $dS^*_{tr,i}/d\sqrt{m}$, in cal/deg. (unit of molality)$^{1/2}$, $= -3.18$. For both ions of the salt, $dS^*_{tr}/d\sqrt{m}$ is twice this or $-6.36$ in satisfactory agreement with observed values of $-6.0$ to $-6.5$ reported above for several 1, 1-salts. For $CdSO_4$, the limiting slope should be $2^5 \cdot 2$ or 8 times this, about $-51$. The observed slope in the most dilute solutions for which there are data, $-26$, appears to be rapidly approaching this limiting value.

Thus Eastman's interpretation of the entropy of migration $S^*_{tr,i}$ as being primarily the entropy of relaxation of the polarized dielectric of the solvent in the third region, when the ion departs, appears to be well founded. On this basis, the migration transport entropy of an ion should always be positive, and, according to Eq. [48], multiplied if necessary by the Debye-Hückel factor to take care of interionic attractions, it should always be small, around 1 to 3 cal/deg for univalent ions.

However, electrostatics does not tell the whole story. Agar (21) points out that where an ion breaks up the structure of the water, its presence may actually increase the entropy of the solvent in the third region, and this would lead to negative migration entropies as reported above for several ions (Tables III to V).

To quote Eastman once more: "The conception of solvated ions . . . takes into account only the electrical effects . . . . Several factors . . . neglected . . . may be of importance in certain cases. Any sort of chemical bonding in the ion aggregate may greatly affect the spheres of influence about the central charge, and so alter the heat [entropy] effects attending its diffusion. This kind of thing may differentiate, for example, between positive and negative ions in their orienting and bonding effects on water molecules. The hydrogen nuclei of the solvent may form a sort of hydrogen bond (39) with electrons of the outer shell of negative ions, a type which is not possible between oxygen atoms and most positive ions. The effect of such bonds, if extensively formed, would be to increase region two at the expense of three, with consequent lessening of the heat of transfer [and of the entropy of migration]. The possibility that either ion of the solvent [$H^+$ or $OH^-$] may be transferred, in effect, by a chain mechanism, must also be considered in solutions of acids and bases. For if this occurs, not only the energy represented in the third sphere above, but that of the second as well, a very much larger quantity, would be involved in the heat of transfer." There is evidence that $S^*_{tr,i}$ for $H^+$ and $OH^-$ is considerably larger (about 10 cal/deg) than for other ions, as discussed above.

The large values obtained for the conventional entropy of migration $S^*_{tr,i}$ of the tetraalkylammonium ions (Table III) appear surprising at first, since Eastman's students (44) had speculatively expected values close to zero, and had even used this hypothesis as a basis for evaluating a set of $S^*_{tr,i}$ values, which proved inconsistent with known values of $S^*_p$ from the Soret effect (Table I). The large values actually obtained point to another mechanism than just the electrostatic one discussed above. The hydrocarbon chains must exert some ordering influence on the neighboring water structure, perhaps by the formation of "icebergs" (44). The removal of the alkyl chains by migration of the ions then allows a disordering of the water structure left behind, i.e., a "melting of the icebergs" (44), with a consequent absorption of heat and a positive entropy of migration. The increment in $S^*_{tr,i}$ for every

four $CH_2$ groups added to the ion appears to be around 4 cal/deg, in going from methyl to amyl, i.e., about 1 cal/deg/$CH_2$ group added. This entropy effect is still small as compared with the intrinsic molal entropies of the materials involved, i.e., about 8.1 cal/deg for $CH_2$ (from the entropy difference between ethanol and methanol) and 16.7 cal/deg for $H_2O$. Thus Eastman's students speculations regarding the smallness of the entropy of migration of the tetraalkylammonium ions may still be justified as regards an individual linkage within the ion, even though it is not justified for the huge ion as a whole.

If one attributes the same value of 1 cal/deg to the migration of the methyl ($CH_3$) group, as well as to $CH_2$, a residual conventional value of about 3 cal/deg is obtained for the migration entropy of the $N^+$ core of the $R_4N^+$ ions, i.e., a value which is quite consistent with that of other simple ions such as $Na^+$, $K^+$, $Rb^+$, and with the electrostatic values, Eq. [48], as well.

The values for divalent ions (Tables III to V) are considerably smaller than what one would expect from the electrostatic relation [48] alone. Undoubtedly, the Debye-Hückel drop-off at finite concentration is already much more significant in this case, as may be the structure-breaking properties of the ion on the solvent, which would tend to lead to negative values of the migration transport entropy.

## Summary

The application of the Onsager thermodynamics to electrochemical systems out of equilibrium permits a unified approach to the problems of concentration cells with transference, thermal diffusion in electrolytes, initial and final emf's of thermal cells. For isothermal concentration cells, the method confirms the classical results of Nernst derived from equilibrium considerations of free energy. For non-isothermal systems, the method brings out the entropy $S^*$ transported from hot to cold heat reservoirs (in the limit of equal temperatures), multiplied by the applied temperature differential $dT$, as the characteristic thermodynamic driving force of a process. For an ion, the entropy transported is different when the ion is transported by electrode reactions and when it is transported by migration. This gives rise to the ionic entropies of electrochemical transport $S^*_{Ei}$ and of migration transport $S^*_{Mi}$, respectively. Values of the ionic transport entropies can be estimated from data on initial and final thermal emf's and Soret coefficients. For an ion, the standard value of $S^{*\circ}_{Ei} = S^\circ_i - z_i(4.48$ cal/deg) while the nonstandard values of $S^*_{Ei}$ show a normal mass action dependence on concentration. For many ions, except $H^+$ and $OH^-$, $S^*_{Mi}$ appears to be small and positive, i.e., about 0-3 cal/deg. Such values are in semi-quantitative agreement with calculations based on Eastman's model of the ionic entropy of migration as the electrostatic entropy of depolarization of the solvent dielectric when the ion moves out. The concentration dependence of $S^*_{Mi}$ does not follow the law of mass action, but it appears to follow the Debye-Hückel relations in dilute solutions. The establishment of better values for the ionic transport entropies remains a challenging task.

Ionic transport across biological membranes is an important process in the release of energy by living systems (18, 40). Holtan (17b) has shown by qualitative experiments that large thermal emf's (of the order of $10^{-6}$ volts per degree) can be developed in colloidal mixtures and in nerve fibers. He has suggested that such thermal emf's may contribute to the initiation of nerve impulses. The role of ionic transports arising from possible local thermal gradients resulting from metabolic energy release in living systems, needs to be explored, and may be hoped to shed some light on the mechanism of the living cell as a thermodynamic engine. "Where is the way to the dwelling of light?" (Job 38: 19).

## Acknowledgment

The author wishes to expre s his gratitude to the International Nickel Company, Inc., of New York, for a Grant-in-Aid in support of this work.

Manuscript received Dec. 28, 1959.

Any discussion of this paper will appear in a Discussion Section to be published in the June 1961 JOURNAL.

## APPENDIX I

*Glossary of Transport Entropies Used in This Paper*

$S^*$: the entropy of transport, the entropy transported reversibly from the right heat reservoir No. 2 (normally the hot one) to the left heat reservoir No. 1 (normally the cold one) by the occurrence of some reversible process in the cell (system), in the limiting case of a vanishing temperature difference between the heat reservoirs.

$S^*_I$: the entropy of electrical transport, i.e., the entropy transported between heat reservoirs, as above, by the flow of a positive current through the cell from left to right.

$S^*_E$: the entropy of electrochemical transport, i.e., the contribution to $S^*_I$ of the two equal and opposite electrode reactions.

$S^*_M$: the entropy of migration transport, i.e., the contribution to $S^*_I$ of the current transported by ionic migration through the solution.

$S^*_D$: the entropy of diffusion transport, i.e., the entropy transported between heat reservoirs, as above, by the flow of solute across the liquid junction from right to left.

$S^*_{Ei}$: the ionic entropy of electrochemical transport, i.e., the contribution of an ion (or electron) to $S^*_E$.

$S^*_{Mi}$: the ionic entropy of migration transport, i.e., the contribution of migration (or diffusion) of an ion (or electron) to $S^*_M$ or to $S^*_D$.

$\overline{\overline{S}}_i$: the entropy of the moving ion, i.e., the sum $S^*_{Ei} + S^*_{Mi}$.

Ionic index $r$: the ion to which the electrodes are reversible; $\rho$: the gegenion of $r$.

## APPENDIX II

*Comparative Nomenclature for the Three Ionic Transport Entropies Appearing in the Equation* $\bar{\bar{S}}_i = S^*_{Ei} + S^*_{Mi}$

| Author | $\bar{\bar{S}}_i$ | $S^*_{Ei}$,[1] | $S^*_{Mi}$ |
|---|---|---|---|
| This paper | Entropy of moving ion $\bar{\bar{S}}_i$ | Ionic entropy of electrochemical transport $S^*_{Ei}$ | Ionic entropy of migration transport $S^*_{Mi}$ |
| Eastman (13a) | — | Absolute partial molal ionic entropy $\bar{S}_i$ | Ionic entropy of transfer $S^*_i$ (= heat of transfer $Q^*_i/T$) |
| Temkin and Khoroshin (14) | Entropy of moving ion $\bar{\bar{S}}_i$ (Entropiya dvizhushchikhsya iona) | Entropy of a single ion $S_i$ | Ionic entropy of transfer $S^*_i$ (= heat of transfer $Q^*_i/T$) |
| Agar (12, 21) | Transported entropy $\bar{\bar{S}}_i$ | Partial molal ionic entropy $S_i$ | Ionic entropy of transport $S^*_i$ (= heat of transport $Q^*_i/T$) |
| deGroot (17a)[2] | Entropy of transfer $S^*_i$ | Ionic entropy $S_i$ | Reduced heat of transfer $Q^{**}_i/T$ |
| Haase (19b) | Überführungsentropie $S^*_i$ | Partielle molare Entropie der solvatisierten ionenart $S_i$ | Überführungswärme $Q^*_i/T$ |
| Domenicali (50)[2] | Transport entropy per particle $S^*$ | — | — |

[1] $S^*_{Ei} = S_i + z_i(-4.48$ cal/deg) where $S_i$ is the conventional partial molal ionic entropy, Latimer (33), and $z_i$ is the ionic charge (with sign).

[2] de Groot defines a "heat of transfer" $Q^*_i$, and Domenicali a "transport heat" $Q^*_i$, where $Q^*_i = T\bar{\bar{S}}_i + \mu_i$.

## REFERENCES


1. W. Nernst, *Z. physik. Chem.*, **4**, 129 (1889).
2. E. Bouty, *J. Phys.*, **8**, 289, 341 (1879); **9**, 306 (1880); **10**, 241 (1881).
3. Th. W. Richards, *Z. physik Chem.*, **24**, 39 (1897).
4. I. M. Kolthoff and F. Tekelenburg, *Rec. trav. chim.*, **46**, 18 (1927).
5. S. P. L. Sorensen and K. Linderstrom-Lang, *Compt. rend. trav. lab. Carlsberg*, **15**, [6], 1 (1925).
6. E. Lange and Th. Hesse, *Z. Elektrochem.*, **37**, 238 (1933).
7. E. Lange, Handbuch Experimental Physik, **12**, 327 (1932); *Z. physik. Chem.*, **209**, 162 (1958).
8. A. J. deBethune, T. S. Licht, and N. Swendeman, *This Journal*, **106**, 616 (1959).
9. Ch. Soret, *Ann. chim. phys.*, [5], **22**, 293 (1881).
10. E. D. Eastman, *J. Am. Chem. Soc.*, **50**, 289 (1928).
11. L. G. Longsworth, "Soret Coefficients of Electrolytes," pp. 183-199 in "Structure of Electrolytic Solutions," W. J. Hamer, Editor, John Wiley & Sons, Inc., New York (1959).
12. J. N. Agar and W. G. Breck, *Trans. Faraday Soc.*, **53**, 167 (1957); W. G. Breck and J. N. Agar, *ibid.*, **53**, 179 (1957).
13. (a) E. D. Eastman, *J. Am. Chem. Soc.*, **48**, 1482 (1926); **50**, 283, 292 (1928). (b) C. Wagner, *Ann. Physik*, [5] **3**, 629 (1929); **6**, 370 (1930).
14. M. I. Temkin and A. V. Khoroshin, *Zhurn. fiz. khimii*, **26**, 500 (1952); A. V. Khoroshin and M. I. Temkin, *ibid.*, **26**, 773 (1952).
15. L. Onsager, *Phys. Rev.*, **37**, 405 (1931); **38**, 2265 (1931).
16. I. Prigogine, "Etude Thermodynamique des Phenomenes Irreversibles," Chap. XII, Desoer, Liege (1947).
17. (a) S. R. deGroot, "Thermodynamics of Irreversible Processes," North Holland Publishing Co., Amsterdam (1951); (b) H. Holtan, Jr., "Electric Potentials in Thermocouples and Thermocells," Thesis, Utrecht (1953).
18. J. G. Kirkwood, "Transport of Ions through Biological Membranes," pp. 119-127, in "Ion Transport across Membranes," H. T. Clarke and David Nachmansohn, Editors, Academic Press, New York (1954.)
19. (a) P. van Rysselberghe, *J. Phys. Chem.*, **57**, 275 (1953); "Electrochemical Affinity," Hermann, Paris (1955); (b) R. Haase, *Z. physik. Chem., N. F.*, **11**, 379 (1957).
20. H. S. Harned and B. B. Owen, "Physical Chemistry of Electrolytic Solutions," 3d ed., Reinhold Publishing Co., New York (1958).
21. J. N. Agar, "Thermal Diffusion in Electrolyte Solutions," pp. 200-223 in *op. cit.*, W. J. Hamer, editor, reference (11); J. N. Agar, *Rev. Pure Applied Chem.* (*Roy. Aust. Chem. Inst.*), **8**, 1 (1958).
22. R. J. E. Clausius, "Mechanische Wärmetheorie," Chap. 10, Vieweg und Sohn, Braunschweig (1876).
23. A. J. deBethune, *Ind. Eng. Chem.*, **50**, 129 (1958).
24. G. N. Lewis and M. Randall, "Thermodynamics and the Free Energy of Chemical Substances," McGraw-Hill Book Co., New York (1923). J. A. Christiansen and M. Pourbaix, *Compt. rend. 17th Conf. I.U.P.A.C.* (Stockholm 1953), pp. 82-84, Maison de la Chimie, Paris (1954). T. S. Licht and A. J. deBethune, *J. Chem. Education*, **34**, 433 (1957).
25. E. A. Guggenheim, "Thermodynamics," North Holland Publishing Co., Amsterdam (1949).
26. P. Debye and E. Hückel, *Physik. Z.*, **24**, 185, 305 (1923).
27. G. Scatchard and R. C. Breckenridge, *J. Phys. Chem.*, **58**, 602 (1954); G. Scatchard, *Science*, **95**, 30 (1942); *Rev. Sci. Instruments*, **26**, 395 (1955).
28. R. G. Bates, "Electrometric pH Determinations," John Wiley & Sons, Inc., New York (1954).
29. M. Stern, H. Shwachman, T. S. Licht, and A. J. deBethune, *Anal Chem.*, **30**, 1506 (1958).
30. (a) D. S. Carr and C. F. Bonilla, *This Journal*, **99**, 475 (1952); (b) G. Borelius, W. H. Keesom, C. H. Johansson, and J. O. Linde, *Proc. Acd. Sci. Amsterdam*, **33**, 1, 17 (1930); **35**, 10, 25 (1932); (c) G. P. Harnwell, "Principles of Electricity and Electromagnetism," McGraw-Hill Book Co., New York (1939).
31. H. A. Fales and W. A. Mudge, *J. Am. Chem. Soc.*, **42**, 2434 (1920).
32. E. D. Eastman, *ibid.*, **50**, 295 (1928).
33. W. M. Latimer, "Oxidation Potentials—The Oxidation States of the Elements and their Potentials in Aqueous Solutions," 2nd Ed., Prentice Hall, New York (1952). National Bureau of Standards, "Selected Values of Chemical Thermodynamic Properties," Circular 500 (1952).

34. E. D. Eastman, *J. Am. Chem. Soc.*, **50**, 285 (1928).
35. W. M. Latimer, K. S. Pitzer, and C. M. Slansky, *J. Chem. Phys.*, **7**, 108 (1939); A. J. deBethune, *ibid.*, **29**, 616 (1958); **31**, 847 (1959).
36. A. J. deBethune and J. J. Perez, *Am. J. Phys.*, **24**, 584 (1956).
37. R. W. Gurney, "Ionic Processes in Solution," McGraw-Hill Book Co., New York (1953).
38. L. Pauling, "Nature of the Chemical Bond," 2nd Ed., Cornell University Press, Ithaca (1942).
39. W. H. Rodebush and W. M. Latimer, *J. Am. Chem. Soc.*, **42**, 1419 (1920).
40. H. T. Clarke and D. Nachmansohn, Editors, "Ion Transport across Membranes," Academic Press, New York (1954).
41. H. A. Bernhardt and H. D. Crockford, *J. Phys. Chem.*, **46**, 473 (1942).
42. G. R. Salvi, Thesis, Boston College (1960).
43. University of California Theses: M. B. Young (1935); F. M. Goyan (1937); R. G. Preston (1941).
44. J. C. Goodrich, F. M. Goyan, E. E. Morse, R. G. Preston, and M. B. Young, *J. Am. Chem. Soc.*, **72**, 4411 (1950).
45. R. Burian, *Z. Elektrochem.*, **37**, 238 (1931).
46. E. Lange and Th. Hesse, *ibid.*, **38**, 428 (1932).
47. H. Levin and C. F. Bonilla, *This Journal*, **98**, 388 (1951).
48. D. A. MacInnes, "Principles of Electrochemistry," Reinhold Publishing Co., New York (1939).
49. H. J. V. Tyrrell and G. L. Hollis, *Trans. Faraday Soc.*, **48**, 893 (1952); H. J. V. Tyrrell and R. Colledge, *ibid.*, **50**, 1056 (1954).
50. C. A. Domenicali, *Rev. Modern Physics*, **26**, 237 (1954).
51. J. N. Agar and J. C. N. Turner, *Proc. Roy. Soc.*, **A255**, 307 (1960).

# Entropy of the Moving Cuprous Ion in Molten Cuprous Chloride from Thermogalvanic Potentials

**Ambrose R. Nichols, Jr.[1] and Cecil T. Langford**

*Scientific Research Laboratory, Convair Division of General Dynamics Corporation, San Diego, California*

ABSTRACT

Potentiometric measurements have been made on a thermogalvanic cell consisting of copper electrodes immersed in molten cuprous chloride in which there was a temperature gradient. The difference in temperature $\Delta T$ between the electrodes was varied from 30° to 70°C and the average temperature of the cell $T_{av_g}$ was varied from 462° to 588°C. Over these ranges the emf was proportional to $\Delta T$, and $\Delta E/\Delta T = -0.436$ mv/°C, the hot electrode being the (—) terminal of the cell. From this value, the entropy of the moving cuprous ion in the melt was calculated for three different temperatures.

Thermogalvanic potentials in aqueous solutions have been studied rather extensively beginning with the work of Richards (1) who measured the temperature coefficient of the calomel electrode. It was not until about 1930 that studies were initiated in the electrochemistry of fused salts, but very little work was done in the field for the next twenty years. In the early 1950's there was a resurgence of interest, and as is evident from a recent bibliography compiled by Janz (2), an enormous amount of work has been done during the past eight years on the electrochemistry of fused salts. As is also evident from this same bibliography, practically all of the investigations in this field have been made with systems at uniform temperature throughout.

Much of the recent work with fused salts has been concerned with the development of reference electrodes constructed in such a manner that liquid junction potentials are practically eliminated. Senderoff and Brenner (3) used a coarse asbestos plug in the tube connecting the two half-cells, but apparently sufficient diffusion took place to introduce an unknown boundary potential into their measurements. Others, including Delimarskii (4), and Bockris, *et al.* (5), have used thin diaphragms of soda glass or Pyrex, but these are not suitable for use at high temperatures and, except in the case of concentration cells, do not lend themselves to exact thermodynamic analysis. Some very precise recent work in this field is described in a series of papers by Flengas and Ingraham (6) who developed a reversible silver-silver chloride reference electrode for use at high temperatures. The side-arm tube of the silica half-cell contains a single asbestos fiber (as opposed to a coarse plug) carefully sealed into the tube in a specified manner (6a). By using the same solvent (an equimolar mixture of NaCl-KCl) in the two half-cells with very low concentrations of the solutes (AgCl in the standard, and $MCl_n$ in the other half-cell) the measured emf is, for all practical purposes, free from any liquid junction potential. In their most recent paper (6f) these authors give an emf series for several metals with corresponding standard electrode potentials referred to their standard Ag-AgCl electrode. Throughout their work they have determined the effect of temperature on the emf of each cell studied. The emf measurements, however, are made under isothermal conditions. It would be possible to calculate reaction entropies from their results but impossible to determine entropies of transport.

Many investigators have studied thermogalvanic potentials in aqueous solutions, but the most comprehensive treatment of the subject is given in a

[1] Professor of Chemistry, San Diego State College, San Diego, California.

recent paper by deBethune, Licht, and Swendeman (7) who give references to 28 earlier contributions, clarify the concepts of isothermal and thermal temperature coefficients of standard electrode potentials, and compute values for both of these, at 25°C, for nearly 300 electrodes. Their treatment of the thermodynamics of thermocells is applicable to fused electrolytes and we shall utilize their notations later in discussing our own results.

Reinhold (8) has measured the emf of a large number of thermocells with solid electrolytes. Among them was a cell analogous to ours and we shall compare his results with those obtained in this study. He also found (8c) that the temperature coefficient of the emf of an isothermal cell could be calculated from the thermal coefficients of related thermocells. Holtan (9), who reinvestigated and extended some of Reinhold's work, found a theoretical basis for the correspondence between thermocells and isothermal cells observed by Reinhold.

The present investigation involved measurements of the emf of a thermogalvanic cell consisting of copper electrodes immersed in molten cuprous chloride in which there was a temperature gradient. It was observed experimentally that the *hotter electrode* was the *negative* (−) *terminal*. The cell may be represented diagramatically as

$$(+)\mathrm{Cu(s)} \mid \underset{T_1}{\mathrm{CuCl(l)}} \mid \underset{T_2}{\mathrm{Cu(s)}} (-) \qquad [1]$$

where $T_2 > T_1$. Following the customary convention in thermocells, where a positive emf means that the hot electrode is the (+) terminal (7-9, 12, 14, 15), the sign of the emf of cell [1] is negative. It will be noted that this sign convention agrees with that of the I.U.P.A.C. (10) when the thermocell is diagrammed with the hot electrode on the right. When the outside circuit is closed and the cell operates spontaneously, the electrode reactions are

at the hot electrode: $\mathrm{Cu(s,}T_2\mathrm{)} = \mathrm{Cu^+}(T_2) + e^-(T_2)$, [2]

at the cold electrode: $e^-(T_1) + \mathrm{Cu^+}(T_1) = \mathrm{Cu(s,}T_1\mathrm{)}$. [3]

If the temperature difference is neglected there is no net over-all chemical reaction but, physically, cuprous ions are transported from the hot electrode to the cooler one inside the cell, and electrons are transported from the hot to the cooler electrode in the outside circuit. Such a cell is analogous to a metallic thermocouple in that the molten electrolyte may be regarded as having replaced one of the dissimilar metals. For this reason some investigators have referred to cells of this type as galvanic thermocouples.

## Experimental

A cell, made of Vycor glass, was placed inside a stainless steel container that fitted snugly in an electrically heated muffle furnace from which the door had been removed. The arrangement is shown in Fig. 1; Fig 2 is a sketch of the thermogalvanic cell. The container protruded 12.7 cm beyond the front of the furnace, and a temperature gradient

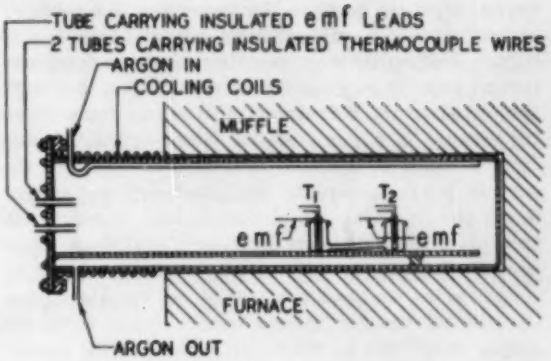


Fig. 1. Thermogalvanic cell assembly

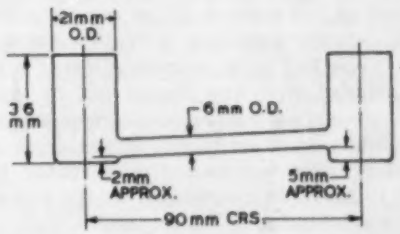


Fig. 2. Thermogalvanic cell made of Vycor glass. Hotter compartment on the right.

was maintained inside it by passing cooling water through coils that surrounded the front parts of the vessel. The tube connecting the two cell compartments was placed at a slight angle to the horizontal to minimize convection currents in the molten salt when the right hand compartment was made the hotter one by placing it toward the rear of the furnace. Powdered cuprous chloride was added to the cell until the connecting tube was full and each of the electrode compartments was about half full. The cuprous chloride was Baker and Adamson's Reagent, A.C.S. grade, dried to constant weight at 110°C without further purification. Preliminary experiments in which vacuum dried, freshly precipitated, cuprous chloride was used gave identical results with those reported here.[2] Electrodes were made from 5-cm lengths of 0.635-cm copper rod. A 0.318-cm hole was drilled from one end of the rod to within 0.16-cm of the other end, giving an open cylinder into which an insulated Pt-Pt + 10% Rh thermocouple was inserted. The junction rested on a single "fish-spine" insulator at the bottom of the cylinder. The cell compartments were covered with crucible lids. A copper electrode for each compartment was inserted through a hole in the center of the lid. When the bottom of the electrode rested on the bottom of the cell compartment the electrode protruded above the lid about 1.3 cm.

The thermocouple wires passed from the electrode through the face-plate of the container and protruded for a distance of 5 cm beyond it. Platinum and platinum + 10% rhodium lead wires ex-

[2] Apparently any $Cu^{++}$ present in the Reagent grade CuCl is reduced by the metallic Cu electrodes, as reported by Flengas and Ingraham (6f).

tended from the front of the face-plate to a near-by Dewar flask where junctions between them and copper lead wires were maintained at the temperature of melting ice. The noble metal lead wires were connected to the corresponding thermocouple wires by means of a compression connector fabricated from a block of micarta that was attached to the outside of the face-plate. Insulated external copper leads passed from the potentiometer through the face-plate for a distance of about 5 cm. These were joined with copper connectors to short lengths of copper wire that were attached to the electrodes. Because of the continuous copper leads from the copper electrodes to the binding posts of the potentiometer, the observed emf was free from any metallic thermocouple voltage. Three double-pole, double-throw switches permitted the three circuits from inside the furnace to be passed either to a 6-point Brown recording potentiometer or to a L & N Type K-2 potentiometer. During a run, air was excluded from the heated cell by passing a stream of oxygen-free argon continuously through the stainless steel container. Argon from a commercial cylinder was passed over copper turnings heated to 350°C in a combustion tube furnace, before it was admitted to the furnace.

At the start of a run, a temperature controller in the heating circuit of the muffle furnace was set to bring the cell to a temperature considerably above the melting point of cuprous chloride. When the first "temperature plateau" was reached, two or three sets of voltages were measured at 10-min intervals, by means of the L & N Type K-2 potentiometer. The Type K-2 readings to the nearest microvolt were recorded and used in the calculations. The controller was then set for the next desired temperature plateau which would be attained in about 30 min. A particular set of voltages was obtained quite rapidly by manipulating the three double-pole, double-throw switches so that the circuit from the thermocouple in the hotter electrode, that from the cooler electrode, and the circuit from the thermogalvanic cell were switched, in turn, from the recording potentiometer to the Type K-2 instrument. Prior to the switching operation each of the three voltages was being printed on the strip chart at intervals of 27 sec and the values could be estimated to 0.01 mv. It was possible, therefore, to preset the Type K-2 potentiometer to a value quite near the actual voltage so that the final balancing required only a few seconds. Indeed, the three voltages could be determined on the Type K-2 in less than 2 min.

It will be observed from Table 1 that the temperature of the electrodes did not remain entirely constant during the two or three sets of readings that were taken at each so-called temperature plateau. During the ascending part of the temperature cycle the furnace cooled slightly at a plateau, while the reverse was true during the descending part of the cycle. It was not deemed necessary to obtain closer temperature control since, for a given set of readings, the actual temperatures of the electrodes and the corresponding emf of the thermogalvanic cell were measured essentially simultaneously.

Table I. Thermogalvanic potentials for the Cell Cu | CuCl(*l*) | Cu ($T_1$ $T_2$) in run No. 1. Hotter electrode ($T_2$) observed to be the negative (—) terminal

| Temp. Plateau No. | $\Delta t$, °C | Avg $t = (t_2 + t_1)/2$, °C | $\Delta E/\Delta t$, mv/°C |
|---|---|---|---|
| 1 | 29.5 | 509.1 | —0.436 |
| 1 | 30.0 | 507.6 | —0.431 |
| 1 | 29.5 | 506.7 | —0.440 |
| 2 | 31.5 | 528.9 | —0.443 |
| 2 | 31.6 | 528.4 | —0.441 |
| 3 | 33.8 | 551.8 | —0.431 |
| 3 | 34.1 | 551.6 | —0.428 |
| 3 | 33.6 | 550.7 | —0.435 |
| 4 | 35.4 | 581.9 | —0.427 |
| 4 | 34.9 | 581.6 | —0.434 |
| 5 | 36.4 | 550.9 | —0.434 |
| 5 | 36.4 | 551.4 | —0.434 |
| 6 | 37.8 | 523.8 | —0.428 |
| 6 | 38.2 | 524.4 | —0.423 |
| 7 | 36.9 | 495.5 | —0.443 |
| 7 | 37.1 | 495.7 | —0.441 |
| | | Average | —0.434 |
| | | Standard deviation of the set | 0.006 |

## Results and Discussion

If an aqueous solution of a substance is placed in a temperature gradient, a gradual change in concentration will, in general, take place because of thermal diffusion of the solute. This phenomenon is known as the Soret (11) effect, and the steady state finally attained is the so-called Soret equilibrium. When a solution of an ionic material constitutes the electrolyte of a thermogalvanic cell the emf will, in general, vary from an initial value $E_i$ before the composition of the solution has had time to alter appreciably, to a final value $E_f$ corresponding to the Soret equilibrium or steady state, as shown experimentally by Agar and Breck (12). In a series of papers, Eastman (13) suggested that the emf of such a cell is related to certain entropy changes that occur when it operates, and he introduced the concepts of entropy of transfer $S^*$ and heat of transfer $Q^*$ for those species that move between the electrodes. He proposed the following equation (13c) for the initial emf,

$$-\mathbf{F}(dE_i/dT) = \Delta S_R + \Delta S^*, \qquad [4]$$

where $\Delta S_R$ is the entropy gained by the electrode system at the higher temperature in the electrode reaction caused by one Faraday of positive electricity passing reversibly from the electrode to the electrolyte, and $\Delta S^*$ is the net entropy of transfer of the ions. $\Delta S^* = t_+S^*_+ - t_-S^*_-$, where $t_+$ and $t_-$ are the transport numbers for the cation and anion, respectively.

More recently Temkin and Khoroshin (14), in a theoretical study of thermogalvanic cells, have developed an equation for the steady-state emf $E_f$. They show that, in so far as the ions are concerned, the heat of transfer of the potential-determining ion only is involved and the effects of the other ions

contained in the solution may be neglected. Their equation [24], with minor changes in symbols, is, for electrodes reversible to positive ions of valence $n$

$$-n\mathbf{F}(dE_r/dT) = \Delta S_R + Q^*_+/T + nQ^*_-/T \quad [5]$$

$Q^*_+$ is the heat of transfer of 1 mole of the positive ion with respect to which the electrode is reversible, and $Q^*_-$ is the heat of transfer of one equivalent of electrons from the electrode. $\Delta S_R$ is the change in entropy during the transfer of the ion from the electrode into the solution and is identical with Eastman's $\Delta S_R$ in Eq. [4], i.e., it is the increase in entropy for the chemical reaction that occurs reversibly at the hotter electrode when $n$ Faradays of positive electricity pass from electrode to electrolyte. Thus, for reaction [2], the above authors would write

$$\Delta S_R = \overline{S}(\mathrm{Cu^+}) - S(\mathrm{Cu}) \quad [6]$$

where, in the general case, $\overline{S}$ is the partial molal entropy of the positive ion in the solution to which the electrode is reversible. As pointed out by deBethune, *et al.* (7) the ionic entropy involved in this reaction is also an entropy of transport, and is not equal to the conventional $\overline{S}$ for a single ion. They suggest that it be called the ionic entropy of electrochemical transport and be designated by the symbol $S^*_{R'}$. Also, they suggest that the entropy $\Delta S_R$ absorbed by the reaction at the hot electrode be referred to as the entropy of electrochemical transport and designated $S^*_R$. For the entropy transported through the cell by electrolytic migration, *i.e.*, the net entropy of transfer $\Delta S^*$, they propose the term entropy of migration transport represented by $S^*_M$.

In terms of the latter concepts, we write for reaction [2]

$$S^*_R = S^*_R(\mathrm{Cu^+}) - S(\mathrm{Cu}) \quad [7]$$

an expression which is equivalent to $\Delta S_R$ in Eq. [4] and [5]. Also, $S^*_M$ is identical with Eastman's $\Delta S^*$ in Eq. [4] and $S^*_{M'}$ is the same as Temkin and Khoroshin's $Q^*_+/T$ in Eq. [5].

Temkin and Khoroshin (14) introduced a quantity $\overline{\overline{S}}$, which they called the entropy of the moving ion, and defined it by the equation

$$\overline{\overline{S}} = \overline{S} + S^* \quad [8]$$

where $S^* = Q^*/T$. In terms of the newer concepts and nomenclature discussed above, $\overline{S}$ should be replaced by $S^*_{R'}$, and $S^*$ by $S^*_{M'}$, hence for the ionic processes occurring in cell [1] (electrochemical transport and migration transport) Eq. [8] should be written,

$$\overline{\overline{S}}(\mathrm{Cu^+}) = S^*_R(\mathrm{Cu^+}) + S^*_M(\mathrm{Cu^+}) \quad [9]$$

According to Khoroshin and Temkin (15), when the Soret effect is zero $E_1 = E_2$. In cell [1] the molten electrolyte consists of only one component, hence no concentration gradient can develop. The measured thermal emf, therefore, is an initial one which is also indefinitely stable, and should be given by both the Eastman Eq. [4], and by the Temkin-Khoroshin Eq. [5]. If we rewrite Eq. [4] in terms of the newer concepts as discussed above, and add a term for the entropy of the moving electron, which Eastman (13c) neglected, we have,

$$-\mathbf{F}(dE_r/dT) = S^*_R + S^*_M + \overline{\overline{S}}_{e^-(\mathrm{Cu})} \quad [10]$$

or

$$-\mathbf{F}(dE_r/dT) = S^*_R(\mathrm{Cu^+}) - \overline{\overline{S}}(\mathrm{Cu}) + t_+ S^*_M(\mathrm{Cu^+}) - t_- S^*_M(\mathrm{Cl^-}) + \overline{\overline{S}}_{e^-(\mathrm{Cu})} \quad [11]$$

Similarly, for Temkin and Khoroshin's Eq. [5], for the passage of one faraday, we have

$$-\mathbf{F}(dE_r/dT) = S^*_R(\mathrm{Cu^+}) - S(\mathrm{Cu}) + S^*_M(\mathrm{Cu^+}) + \overline{\overline{S}}_{e^-(\mathrm{Cu})} \quad [12]$$

For copper electrodes in molten cuprous chloride $t_+ = 0$ and $t_- = 1$, hence Eq. [11] reduces to Eq. [12] and either may be used with the temperature coefficient of the thermopotential of cell [1]. Upon combining Eq. [9] with Eq. [12] and rearranging, the following equation for the entropy of the moving cuprous ion is obtained

$$\overline{\overline{S}}(\mathrm{Cu^+}) = -\mathbf{F}(dE_r/dT) + S(\mathrm{Cu}) - \overline{\overline{S}}_{e^-(\mathrm{Cu})} \quad [13]$$

Table I gives detailed results for run number 1, and Table II summarizes the results of three separate runs comprising 56 measurements of electrode temperatures and corresponding cell potentials. It was thought the $\Delta E/\Delta T$ might vary with the average temperature of the cell or with the magnitude of $\Delta T$, or with both, but no such variations were observed. In a particular run, $\Delta T$ was changed only slightly but the temperature of the furnace was raised through 40°-80°C and then lowered through 80°-120°C during which cycle the values for $\Delta E/\Delta T$ fluctuated around the average shown in the last column with no detectable trend. In run No. 3 the temperature difference between the electrodes was deliberately increased by placing the cell farther toward the front of the furnace where the temperature gradient was greater. Although $\Delta T$ was about doubled, $\Delta E/\Delta T$ remained constant over the temperature cycle shown. The average value for $\Delta E/\Delta T$, for all 56 measurements, is $-0.436$ mv/deg C and may be used for $dE_r/dT$ giving a value of 10.05 cal/deg for the first term on the right of Eq. [13].

The average temperature of the melt varied from about 462° to 588°C (15° below 477° in run No. 2,

**Table II. Summary of thermogalvanic potentials for the cell Cu | CuCl(*l*) | Cu for three runs. Hotter electrode ($T_2$) observed to be the negative (—) terminal**

| Run No. | No. temp plateaus | No. of measurements | Temp cycle for hotter electrode $t_2$, °C | Variation in $\Delta t = t_2 - t_1$, °C | Average $\Delta E/\Delta T$, mv/°C | Standard deviation (set), mv/°C |
|---|---|---|---|---|---|---|
| 1 | 7 | 16 | 522-600-514 | 30-38 | —0.434 | 0.006 |
| 2 | 7 | 18 | 555-596-477 | 30-33 | —0.437 | 0.006 |
| 3 | 7 | 22 | 530-618-519 | 63-70 | —0.437 | 0.005 |

Average $\Delta E/\Delta T$ for 56 observations = $-0.436$ mv/°C

Standard deviation of the set = 0.006 mv/°C

Table III. Effect of temperature on the entropy of the moving cuprous ion as calculated by Eq. [13]

| Avg. temp of cell, °K | $F(dE/dT)_{T_1}$, cal/deg mole $Cu^+$ | $\bar{S}(Cu)$, cal/deg g-atom | $\bar{\bar{S}}_{e^-(Cu)}$, cal/deg equiv | $\bar{\bar{S}}(Cu^+)$, cal/deg mole $Cu^+$ |
|---|---|---|---|---|
| 735 | −10.05 | 13.50 | −0.095 | 23.65 |
| 798 | −10.05 | 14.04 | −0.102 | 24.19 |
| 861 | −10.05 | 14.55 | −0.109 | 24.71 |

to 30° below 618° in run No. 3) and the average of these values is 525°C. The last two terms on the right of Eq. [13] are evaluated from the literature for a temperature of the melt of 525°C. Temkin and Khoroshin (14) give the following equation for the entropy of the moving electrons in copper:

$$\bar{\bar{S}}_{e^-(Cu)} = -[1.95 + 0.005\,(T\text{-}300)] \text{ microvolt-faradays/degree-equiv, } T \geqq 240°K. \quad [14]$$

This yields $\bar{\bar{S}}_{e^-(Cu)} = -0.102$ cal/deg at 798°K. Giauque and Meads (16) have determined the molal entropy of copper and give the value $S(Cu, 298.1°) = 7.961$ cal/deg. Kelley (17) gives the following equation for the molal heat capacity of copper from 298° to 1357°K,

$$C_p = 5.41 + 1.50 \times 10^{-3} T \text{ cal/deg} \quad [15]$$

from which we calculate $S(Cu, 798) - S(Cu, 298) = 6.08$ cal/deg. This gives $S(Cu, 798) = 14.04$ cal/deg.

If the above values are substituted in Eq. [13] we have, at 525°C,

$$\bar{\bar{S}}(Cu^+, 798°K) = 10.05 + 14.04 + 0.10 = 24.19 \text{ cal/deg} \quad [16]$$

Similar calculations for the lowest (462°C) and the highest (588°C) average temperatures of the melt have been made. These results and the above are summarized in Table III.

The following thermocell with solid electrolyte was studied by Reinhold (8c):

$$(+)Cu(s) \,|\, \underset{T_1}{} \, CuCl(s) \,|\, \underset{T_2}{} \, Cu(s)(-) \quad [17]$$

$T_2$ was kept constant at 400°C and $T_1$ was varied from 113° to 400°C. From his equation for $dE/dT$ as a function of $\Delta T$ we calculate, for $\Delta T = 30°C$, $dE/dT = -0.846$ mv/deg. From theoretical considerations applicable only to solid electrolytes, Holtan (9) calculates, for the same cell with $T_1$ between 300° and 400°C, $\Delta E/\Delta T = -0.82$ mv/deg. These values are about double our value of −0.436 mv/deg obtained for cell [1] with molten CuCl. In this connection it is interesting to note that Holtan (9) obtained similar results for the cell,

$$(+)Ag \,|\, \underset{T_1}{} \, AgCl \,|\, \underset{T_2}{} \, Ag(-) \quad [18]$$

thermopotentials for which he measured with both solid and molten AgCl. His observed temperature coefficient of the thermopotential for molten AgCl was approximately half that for the solid electrolyte.

It is possible, by the relationship observed by Reinhold (8c) and confirmed theoretically by Holtan (9), to calculate the temperature coefficient of the thermopotential of the cell,

$$(+)Cl_2(g) \,|\, \underset{T_1}{} \, CuCl(l) \,|\, \underset{T_2}{} \, Cl_2(g)(-) \quad [19]$$

which we may designate as $(\Delta E_m/\Delta T)_{T_1}$. The measured coefficient of cell [1], $(\Delta E_1/\Delta T)_{T_1} = -0.436$ mv/deg, and the temperature coefficient of the emf of the isothermal cell

$$(-)Cu(s)\,|\,CuCl(l)\,|\,Cl_2(g)(+) \quad [20]$$

can be derived from results of Hamer, Malmberg, and Rubin (18), who calculated the emf of cell [20] at several temperatures up to 1500°C. From a plot of their values of $E$ vs. $T$ we have obtained, by graphical methods, the slope of the curve at $T = 525°C$ and find $(\Delta E_m/\Delta T)_{525°K} = -0.220$ mv/deg at 525°C. By Reinhold's rule, which has been demonstrated by deBethune, *et al.* (7) and by Holtan and Krogh-Moe (19), these coefficients are related as follows

$$(\Delta E_m/\Delta T)_{525°K} = (\Delta E_m/\Delta T)_{T_1} - (\Delta E_1/\Delta T)_{T_1} \quad [21]$$

Upon substituting in Eq. [21] the measured value for cell [1] and the derived value for cell [20] we find,

$$(\Delta E_m/\Delta T)_{T_1} = -0.656 \text{ mv/deg at } 525°C \quad [22]$$

The result obtained in Eq. [22] is probably only approximate since it depends not only on the accuracy of our measurements for cell [1], and the reliability of the thermodynamic data used by Hamer, *et al.* in calculating emf's for cell [20], but also on the errors inherent in the graphical differentiation of their results.

Manuscript received Dec. 15, 1959.

Any discussion of this paper will appear in a Discussion Section to be published in the June 1961 JOURNAL.

## REFERENCES

1. T. Richards, *Z. Physik. Chem.*, **24**, 39 (1897).
2. G. J. Janz, "Electrode Processes, E.M.F." in "Bibliography on Molten Salts," pp. 24-30, Rensselaer Polytechnic Institute, Troy, N. Y. (1958).
3. S. Senderoff and A. Brenner, *This Journal*, **101**, 31 (1954).
4. Yu. K. Delimarskii, *Zhur. Fiz. Khim.*, **29**, 28 (1955).
5. J. O'M. Bockris, G. J. Hills, D. Inman, and L. Young, *J. Sci. Instr.*, **33**, 438 (1956).
6. S. N. Flengas and T. R. Ingraham, (a) *Can. J. Chem.*, **35**, 1139 (1957); (b) **35**, 1254 (1957); (c) **36**, 780 (1958); (d) **36**, 1103 (1958); (e) **36**, 1063 (1958); (f) *This Journal*, **106**, 714 (1959).
7. A. J. deBethune, T. S. Licht, and N. Swendeman, *This Journal*, **106**, 616 (1959); A. J. deBethune, *ibid.*, **107**, 829 (1960).
8. H. Reinhold, (a) *Z. anorg. Chem.*, **171**, 181 (1928); (b) *Z. phys. Chem.* (B), **11**, 321 (1931); (c) H. Reinhold and A. Blachny, *Z. Electrochem.*, **39**, 290 (1933).
9. H. Holtan, Jr., Electric Potentials in Thermocouples and Thermocells, Thesis, Utrecht, (1953).
10. T. S. Licht and A. J. deBethune, *J. Chem. Education*, **34**, 433 (1957).
11. C. Soret, *Ann. chem. phys.*, [5] **22**, 293 (1881).
12. J. N. Agar and W. G. Breck, *Trans. Faraday Soc.*, **53**, 167 (1957).
13. E. D. Eastman, (a) *J. Am. Chem. Soc.*, **48**, 1482 (1926); (b) **50**, 283 (1928); (c) **50**, 292 (1928).

14. M. I. Temkin and A. V. Khoroshin, *Zhur. Fiz. Khim.*, **26**, 500 (1952).
15. A. V. Khoroshin and M. I. Temkin, *ibid.*, **26**, 773 (1952).
16. F. W. Giauque and P. F. Meads, *J. Am. Chem. Soc.*, **63**, 1897 (1941).
17. K. K. Kelley, Bull. 476, U. S. Bureau of Mines, p. 63 (1949).
18. W. J. Hamer, M. S. Malmberg, and B. Rubin, *This Journal*, **103**, 8 (1956).
19. H. Holtan, Jr., and J. Krogh-Moe, *Acta Chem. Scand.*, **9**, 1022 (1955).

# Cathodic Processes on Passive Zirconium

**Robert E. Meyer**

*Chemistry Division, Oak Ridge National Laboratory, Oak Ridge, Tennessee*[1]

ABSTRACT

Measurements were made of the rates of reduction of various oxidizing agents on passive zirconium in acid solutions of sodium sulfate at temperatures ranging from 25° to 85°C. The oxidizing agents included in these experiments were oxygen, hydrogen ion, and cupric ion and hydrogen peroxide in the presence of oxygen. The kinetic orders of reduction were determined from potentiostatic experiments in which the current was determined as a function of concentration. Unit and fractional orders were observed with oxygen reduction, and fractional orders from about 0.5 to 0.65 were observed for $Cu^{++}$ and $H_2O_2$. Possible mechanisms are suggested in which charge transfer through the film is assumed to play a predominant role.

The study of electrochemical reduction on the surface of film-covered electrodes has received comparatively little attention. The usual goal in studies of reduction processes is to measure rates on bare metals, and therefore care is taken to remove any films that may be present. It is clear, however, that the presence of a film can markedly influence the reduction processes at the surface by affecting the energetics of the reaction at the double layer, or by imposing a barrier to charge transfer through the film, or both. The study of reduction processes on film-covered electrodes is important to the field of corrosion for the corrosion of metals that form surface films over the entire surface of the metal must necessarily involve the reduction of the oxidizing agent on the surface of the film.

Zirconium is known to form a film, presumably of $ZrO_2$, when in contact with $O_2$ in aqueous solution. The standard potential (1) for the half-reaction $Zr + 2H_2O = ZrO_2 + 4H^+ + 4e^-$ is $-1.43$ v. It is evident from this potential that $ZrO_2$ is thermodynamically stable under potentials at which such oxidizing agents as $O_2$, $H_2O_2$, and $H^+$ are easily reduced. Furthermore, measurements made in $O_2$-saturated 0.1*M* $Na_2SO_4$ (pH ~ 4) showed that the rate of formation of $ZrO_2$ at potentials in the vicinity of SCE falls off to values on the order of $10^{-8}$ to $10^{-9}$ amp/cm$^2$ after a few days (2). Therefore it should be possible to study reduction processes on film-covered zirconium without significant interference from the film-forming reactions. It is found, in practice, that determinations of reduction rates are reasonably reproducible on a given sample, and therefore it is safe to conclude that the effect of reduction experiments on the surface of the electrode is slight.

In the experiments described here, attention was centered on the reduction of $H^+$, $O_2$, and $Cu^{++}$ and $H_2O_2$ in the presence of $O_2$. It was found that reasonable steady states could not be achieved with $Cu^{++}$ and $H_2O_2$ if attempts were made to remove $O_2$. All measurements were made on electrodes after the corrosion reaction had decayed to a negligible rate.

## *Theory*

For the present purposes the following equation will be assumed as representing the reduction current at an electrode:

$$i_c = K \pi_i (a_i^{p_i}) \exp \frac{-\alpha_c z_c EF}{RT} \qquad [1]$$

where $i_c$ is the reduction current density, $\pi (a_i^{p_i})$ is the product of the activities of the reactants raised to the appropriate orders $p_i$, $\alpha_c z_c$ is the product of the transfer coefficient and the charge number, and $E$ is the potential of the electrode measured with respect to the reference electrode. The value of $K$ will depend on the particular reference electrode chosen. From experimental data, one can determine $K$, the orders, and the product $\alpha_c z_c$, and therefore determine information of mechanistic significance.

The product $\alpha_c z_c$ is determined from the slope of the log-current density vs. potential plot and is calculated from the derivative:

$$\frac{\partial \log i_c}{\partial E} = \frac{-\alpha_c z_c F}{2.303\,RT} \qquad [2]$$

The orders are determined in experiments in which the electrode is held at constant potential and the activity of a reactant is increased by progressive additions of concentrated solutions. The orders are calculated from the derivative (3):

[1] Operated by Union Carbide Corporation for the U. S. Atomic Energy Commission.

$$\frac{\partial \log (i_c - i_{c,o})}{\partial \log a_i} = p_i \qquad [3]$$

where $i_{c,o}$ is the initial current density before additions of the reactant. Actually all of the desired information can be obtained either from a series of galvanostatic (constant $i$) experiments at various activities or by a series of potentiostatic experiments at various potentials. However, if the electrodes vary somewhat in their properties from day to day, it is better to do both types of experiments since $\alpha z$ factors can be obtained more accurately from galvanostatic experiments and orders can be determined more precisely from potentiostatic experiments.

## Experimental

Preliminary experiments showed that great precautions had to be taken in order to obtain reproducible data. In particular, the electrodes had to be prepared carefully and the solution and cells thoroughly freed from impurities.

The electrodes were cylinders machined from ¼ in. crystal-bar zirconium and had an area of 2.2 cm². Before use they were cleaned, chemically polished in $H_2O$-$HNO_3$-HF solution, rinsed in boiling triply distilled water, and vacuum annealed for several hours at 750°-800°C. Immediately before use they were removed from vacuum, mounted on Teflon holders, and placed in the cell. Such a procedure involved a few minutes' exposure to air, and therefore the electrodes undoubtedly had a thin oxide film on their surface before being introduced into the cell.

All solutions were made from triply distilled water, one distillation of which was made from alkaline permanganate. The sodium sulfate used was doubly recrystallized and the sulfuric acid was prepared by dilution of the C.P. grade. Solutions were pre-electrolyzed for at least 24 hr before use between platinum electrodes with a current of 5-10 ma. The potential of the platinum cathode was well below the lowest potential used on the zirconium electrodes.

The cells were made from Pyrex and Teflon and no greases, waxes, or other sources of surface-active impurities were used in the cell. The cells were thoroughly cleaned before use, and in most of the experiments the final rinse water and the water used for the solutions was distilled directly into the cell.

Potentials were measured by a L&N model 7664 pH and emf meter coupled to a 10-mv Brown recorder. This apparatus was calibrated periodically with a potentiometer and had an accuracy of ± 1 mv on a 1000-mv scale and ± 0.5 mv on a 100-mv scale. Currents were measured by this same unit by measuring the potential drop across precision resistors. In the constant-potential determinations of the orders, an electronic potentiostat developed at this laboratory was used.

## Results

*Oxygen reduction.*—All measurements of oxygen reduction were made in 0.1*M* $Na_2SO_4$ of varying pH at temperatures in the interval 25°-88°C. Measurements at the lower temperatures were sluggish, and therefore most of the galvanostatic work was done at 75° and 85°C (Fig. 1). In all cases steady-state values only were used in calculating Tafel slopes. In general, points were taken after the potential showed no drift (< 1 mv) in a period of 5-20 min, depending on the current densities. Slow drifting occurred occasionally but was usually eliminated if the solution were changed and freshly pre-electrolyzed solution admitted. In preliminary experiments, almost all of the samples gave values of $\alpha z$ between 0.18 and 0.35 with 0.25 being an approximate average. In order to obtain a better estimate of $\alpha_c z_c$, three electrodes were prepared under carefully reproduced conditions. These samples showed $\alpha_c z_c$ values of 0.28, 0.32, and 0.33 one day after initial immersion at 75°. There was evidence that at very low current densities, i.e., below ~ $10^{-7}$ amp/cm², the Tafel slope changed to give a somewhat higher $\alpha_c z_c$. The exact value could not be determined precisely because the potentials at these current densities were too close to the rest potential.

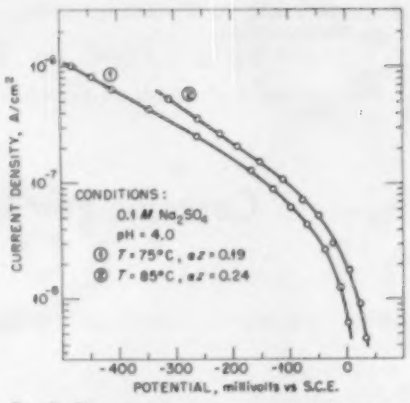


Fig. 1. Oxygen reduction on passive zirconium

The determination of the reaction order at high concentration of $O_2$ was carried out potentiostatically by passing pure He, mixtures of He and $O_2$, and pure $O_2$ through the cell. At low concentrations of $O_2$, varying quantities of $O_2$ were introduced into the cell by anodic evolution on Pt with a closed cell (using an external cathode). Constant current density was used so that the total amount of oxygen present was proportional to the total charge passed. Some of the results are shown in Fig. 2 and 3. In

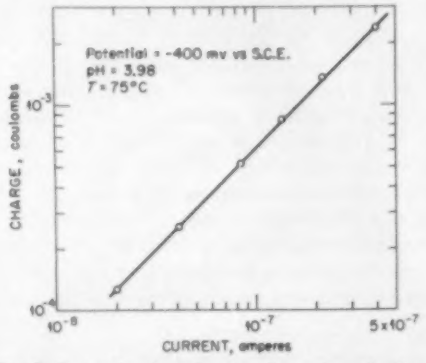


Fig. 2. Determination of order of oxygen reduction

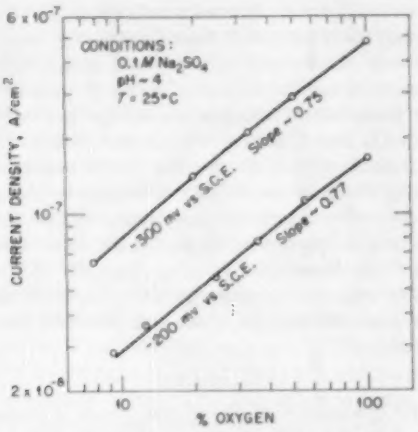


Fig. 3. Determination of order of reduction of oxygen

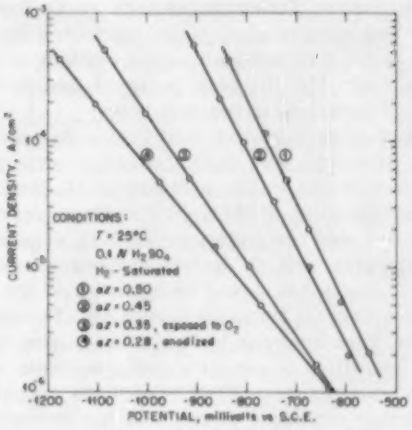


Fig. 4. $H^+$ reduction on zirconium

Fig. 2, current density is obtained by dividing by 2.2 $cm^2$, the electrode area. All of the results taken together showed that, for a given electrode under constant conditions, fractional orders of from 0.7 to 0.8 were obtained at high current densities and unit orders were observed at low current densities. For an electrode at 75°, the order slopes changed from unity to fractional in the region 2-5 x $10^{-7}$ amp/$cm^2$.

The effect of changing the pH at low current densities was to increase the potential by approximately $RT/F$ for every pH unit decrease in the pH range 2-5. At higher current densities the change was complicated by drifting, but the change seemed to be less than $RT/F$. The application of Eq. [3] did not give reproducible orders.

An attempt was made to determine the limiting current due to diffusion with a sample that was unusually stable. By limiting polarization at high current densities to a few minutes, it was possible to estimate roughly the limiting current density as 150 $\mu a/cm^2$ for $O_2$ saturated solutions at 75° (concentration ~ 5 x $10^{-4}M$ and pH = 2.75).

In order to check for any possible $IR$ drop during polarization, current decay measurements were made with an oscilloscope (Tektronix 536). Using a sensitivity of 1 mv/cm and a current density of about 5 x $10^{-7}$ amp/cm, no detectable $IR$ drop was observed when the current was interrupted.

*Hydrogen ion reduction.*—The reduction of hydrogen ions was carried out in hydrogen-saturated solutions on electrodes treated in various ways as described below. Unless otherwise mentioned all experiments were carried out at 25°C in $H_2$-saturated 0.1$N$ $H_2SO_4$. Most of the electrodes were introduced directly into $H_2$-filled solution-free cells and solution was added only after $H_2$ was passed through the cell for several hours.[2] When $H_2$-saturated solution was admitted to the cell, the initial potentials of the zirconium electrode were well below the reversible $H_2$ potential because of the corrosion reaction $Zr + 2H_2O \rightarrow ZrO_2 + 2H_2$. However, the rate of this reaction decreased rapidly with time and, after an hour, polarization measurements were begun. Usually linear Tafel plots were obtainable with electrodes treated this way and two examples are shown as curve No. 1 and 2 in Fig. 4. In general, the slopes were such as to give $\alpha z$ factors of 0.4-0.5, which is frequently observed in hydrogen-evolution experiments on other metals.

If oxygen were admitted to the cell, the potential would rise rapidly before leveling off. After several days the $O_2$ was removed and Tafel plots such as is shown as No. 3 of Fig. 4 were obtained. A similar effect was produced by anodizing in the absence of $O_2$ as shown by curve No. 4. Both of these curves show linear Tafel plots but low $\alpha z$ factors (0.35 and 0.28, respectively).

The effect of pH was investigated by preparing an alkaline 0.1$M$ $Na_2SO_4$ solution and decreasing the pH by the progressive addition of small quantities of $H_2$-saturated 2$N$ $H_2SO_4$. The temperature was 25°C and the electrodes were exposed only to $H_2$-saturated solution before the effect of pH was investigated. The electrode therefore had only that small amount of film that would be formed by reaction with hydrogen ions. Results are shown in Fig. 5. In alkaline solution there was no change in current at constant potential with change in pH and in acid solution a change of about 60 mv/pH unit was observed at constant current. The pH was measured by forcing out several milliliters of solu-

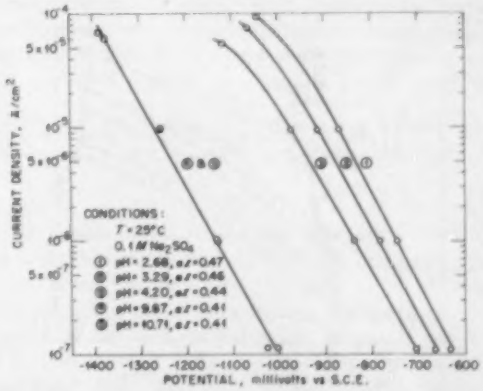
CONDITIONS:
T = 25°C
0.1 M Na2SO4
① pH = 2.68, αz = 0.47
② pH = 3.29, αz = 0.46
③ pH = 4.20, αz = 0.44
④ pH = 9.87, αz = 0.41
⑤ pH = 10.71, αz = 0.41
CURRENT DENSITY, A/cm²
POTENTIAL, millivolts vs S.C.E.

Fig. 5. pH Dependence of $H^+$ reduction on zirconium

[2] The $H_2$ was purified with an all Pyrex train containing Drierite, Hopcalite (for CO removal), Ascarite, liquid nitrogen traps, and hot catalyst (either Pd or Cu).

tion through a Teflon valve into an $O_2$-free container and using a glass electrode with a Beckman Model G pH meter. Results are consistent with discharge from $H_2O$ in basic solution and discharge from hydrogen ions in acid solution.

*Reduction of Copper II and* $H_2O_2$.—As mentioned above, the $Cu^{++}$ and $H_2O_2$ reduction experiments were carried out in the presence of $O_2$. Because of the decomposition of $H_2O_2$ at 66°C, the oxygen could not be removed completely in the $H_2O_2$ experiments. Temperatures had to be maintained at 66°C or higher because at lower temperatures the rates were too slow to measure accurately. The concentrations were changed by precisely measuring out small quantities of concentrated stock solutions of known concentration. Electrodes were prepared in the manner described above, and the corrosion reaction was allowed to decay for several days before measurements were made. All experiments were carried out at constant ionic strength (0.1*M* $Na_2SO_4$).

Results are shown in Fig. 6 and 7. The order of reduction of $Cu^{++}$ as determined from the slope $\partial \log (i—i_a)/\partial \log a$ varied from 0.66 to 0.61. The orders with respect to $H_2O_2$ reduction were also fractional, but the slopes varied from about 0.40 to 0.66 as shown in Fig. 7. A possible explanation for these unusual orders is presented below. Tafel slopes could not be measured directly in this case since reasonable steady states were not attained in the absence of oxygen. Potential-current curves taken in the presence of oxygen represent the reduction of both $O_2$ and $Cu^{++}$ (or $H_2O_2$) and there may be interaction between them. The Tafel slope can be estimated roughly by taking current-potential points from lines of constant concentration in Fig. 6 and 7. Using this method the slope for copper reduction varied from somewhat greater than $RT/F$ ($a_c z_c \approx 1$) at low current densities to almost $3RT/F$ ($a_c z_c \approx 1/3$) at high current densities and for $H_2O_2$ the slope was about $4RT/F$.

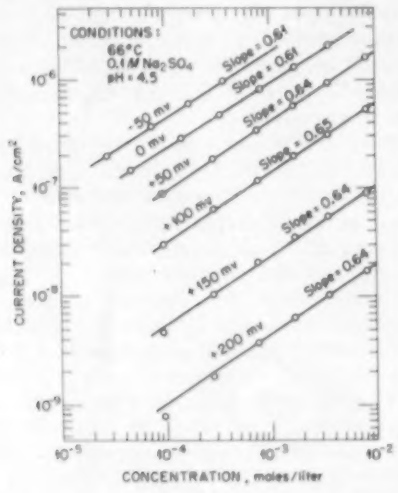


Fig. 6. Reduction of copper(II) on passive zirconium

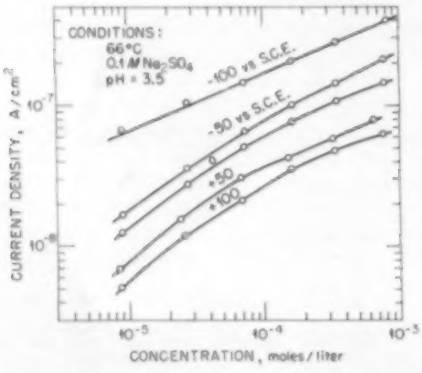


Fig. 7. Reduction of $H_2O_2$ on passive zirconium

## Discussion

In the discussion of these results, it is important to keep in mind that the results described here may be valid only for films prepared as described above. Films which are prepared by higher temperature gaseous oxidation or by anodizing to high voltages are not necessarily similar in kinetic properties to those described here.

The films formed in these experiments are not assumed to be uniform, since the various inhomogeneities at the surface should cause local variations in the nature and amount of the film. This lack of uniformity may cause large variations in current density across the surface of the electrode[a] but it does not invalidate the use of Eq. [1]. This point has been discussed in detail by Posey (3).

Pores or cracks are sometimes suggested as being present in films of this sort. However, at the potentials of these experiments any exposure of bare metal through defects of this type is unlikely. It must be remembered that these potentials are almost 2 v above the equilibrium potential of the reaction $Zr + 2H_2O \rightarrow ZrO_2 + 4H^+ + 4e^-$ and that zirconium is an extremely reactive metal. The arguments against the existence of pores in passive films on iron have been given by Vetter (4) and similar arguments apply to zirconium. Further, the limiting current measurements show that the effective area of the electrode is not significantly smaller than the apparent area. Thus, the experimental figure of 150 $\mu a/cm^2$ should be compared to values of from 80 $\mu a/cm^2$ to $4 \times 10^5$ $\mu a/cm^2$ calculated from the well-known equation, $i_l = zFDC/l$ where $D$ is the diffusion coefficient, $C$ is the concentration in moles/cm³, and $l$ is the thickness of the diffusion layer. Values of $D = 2 \times 10^{-5}$ cm²/sec, $z = 4$, $C = 5 \times 10^{-7}$ moles/cm³, and $l$ varying from 0.05 to $10^{-4}$ cm were taken. Since the experimental measurement was taken under conditions of slight stirring (a slow stream of gas bubbles at the side of the cell), it is clear that the effective area is of the same order of magnitude as the apparent area. This observation is difficult to reconcile with any hypothesis which suggests that only a few pores or singularities are responsible for charge transfer through the film.

Any mechanism of reduction must however take into account the fact that the presence of this film may cause charge transfer through the film to affect

[a] This may also be a cause of the difference observed in different specimens since it is clearly impossible to duplicate the surface of a given specimen.

the over-all kinetics. For very thick films of high resistivity, the film barrier can simply be regarded as *IR* drop, but for the thin films considered here (20-100Å) such an explanation cannot be used. For the reasons described below, it seems better to interpret the data given here on the basis of a potential barrier within the film such that the current, which is assumed to be electron current, is given by the exponential expression, $I \sim \exp -\alpha V/kT$.

According to the original Mott-Cabrera (5) theory of thin film formation on metals, an electric field is formed across the film by electrons which leave the metal surface and find their way to $O_2$ adsorbed on the surface. The rate-determining step is assumed to be the movement of metal ions through the metal-oxide interface under the influence of the field. However, as Cabrera points out later (6) the transport of electrons through film will also be under the influence of this field, and for all but the thinnest films, the transport of the electrons should also affect the rate.

In the case of zirconium it was shown by the author (2) that a rate law in reasonable agreement with experiment can be derived under the assumption that both ion transport (an anodic process) and the reduction of oxygen were rate-determining. The assumption was made that the reduction current was proportional to $\exp(-\alpha_c z_c V_f/kT)$ where $V_f$ is the potential across the film. The resulting rate-time expression is roughly hyperbolic in rate and time but does not permit a simple exact analytical expression. The important point here is that a fit of the data is obtained if the reduction process is considered a function of the potential across the film and that it too is rate-determining.

Because of the above considerations it is felt that a reduction process on these zirconium electrodes involves charge transfer through the film as well as the usual charge transfer process at the interface. Furthermore, the fractional orders and the unusually low $\alpha z$ factors obtained from the reduction experiments can be best explained from the above assumptions. Before this can be explained the formal mathematics must be stated.

For the purpose of describing these kinetics two cases of a dual-barrier model are used. Case I assumes that, if a reduction process is occurring at a steady-state, two potential-dependent reactions occur at equal rates, the one corresponding to the film reaction and the other to the surface double layer reaction. The rates of the individual reactions can be represented by the two equations:[4]

$$i = K_f \pi_i (a_{i,f}^{p_{i,f}}) \exp(-\alpha_f z_f V_f/kT) \qquad [4]$$

$$i = K_s \pi_j (a_{j,s}^{p_{j,s}}) \exp(-\alpha_s z_s V_s/kT) \qquad [5]$$

where $V_f$ and $V_s$ are the separate potential drops affecting the two different barriers. The activities for the solution reaction are to be taken as the ordinary solution activities. Depending on the nature of the film reaction, the activities in Eq. [4] may represent the effective concentration of electrons, holes, etc., or in some cases may represent the concentration of adsorbed species on the surface of the electrode. Thus, if the film reaction were the transfer of an electron over the potential barrier to adsorbed oxygen, the reaction rate would depend on the number of electrons striking the barrier, the number of $O_2$ molecules adsorbed, and the probability of electron transport across the barrier.

The over-all measured potential $E$ will be equal to $V_f + V_s + V_b$ where $V_b$ is the constant sum of all of the other potential drops occurring in the measuring circuit. Combining this relation with Eq. [4] and [5] by eliminating $V_f$ and $V_s$ one obtains:

$$i = K_i \left[\pi_{i,f}(a_{i,f}^{p_{i,f}})^{\frac{\alpha_s z_s}{\alpha_f z_f + \alpha_s z_s}}\right] \left[\pi_{j,s}(a_{j,s}^{p_{j,s}})^{\frac{\alpha_f z_f}{\alpha_f z_f + \alpha_s z_s}}\right] \exp \frac{-\alpha_i z_i E}{kT} \qquad [6]$$

where

$$\alpha_i z_i = \frac{\alpha_f z_f \alpha_s z_s}{\alpha_f z_f + \alpha_s z_s}$$

and

$$K_i = \left(\exp \frac{\alpha_f z_f \alpha_s z_s V_b}{(\alpha_f z_f + \alpha_s z_s) kT}\right) K_f^{\frac{\alpha_s z_s}{\alpha_s z_s + \alpha_f z_f}} K_s^{\frac{\alpha_f z_f}{\alpha_s z_s + \alpha_f z_f}}$$

Therefore

$$\frac{\partial \ln i}{\partial E} = \left(\frac{-\alpha_f z_f \alpha_s z_s}{\alpha_f z_f + \alpha_s z_s}\right) \times \frac{1}{kT} \qquad [7]$$

and

$$\frac{\partial \log i}{\partial \log a_{i,f}} = \frac{p_{i,f} \alpha_s z_s}{\alpha_f z_f + \alpha_s z_s} \qquad [8]$$

and

$$\frac{\partial \log i}{\partial \log a_{j,s}} = \frac{p_{j,s} \alpha_f z_f}{\alpha_f z_f + \alpha_s z_s} \qquad [8a]$$

Equation [6] predicts that the apparent orders as measured by $\partial \log i/\partial \log a$ will be the true order $p$ multiplied by a fraction. This will be true only if all activities are completely independent of each other so that the activity in question can be varied without affecting the values of the activities at either of the barriers. If an activity affecting one barrier is a function of the activity of a reactant of the other, i.e., if $a_s = f(a_f)$, then

$$\left(\frac{\partial \log i}{\partial \log a_f}\right)_s = \frac{p_i \alpha_s z_s}{\alpha_f z_f + \alpha_s z_s} + \frac{p_j \alpha_f z_f}{\alpha_f z_f + \alpha_s z_s} \left(\frac{\partial \log a_s}{\partial \log a_f}\right)_s \qquad [9]$$

If $a_s$ is proportional to $a_f$, the derivative $\partial \log a_s/\partial \log a_f$ will be unity and, if both p's are unity, the over-all order will be unity.

Although the order determinations were carried out at constant over-all potential, it is still possible that $V_f$ and $V_s$ may have varied, subject to the condition that their sum is constant. If the solution concentration of the oxidizing agent is increased,

[4] One might justifiably object to the use of this rate equation for the film reaction. In this derivation, it is to be regarded purely as a formal equation giving the current as a function of the activities and the potential for a film at constant thickness. The constants $K_f$ and $\alpha_f$ are not necessarily analogous in their theoretical interpretation to $K_s$ and $\alpha_s$ in the rate equation representing the surface reaction.

this will cause an increase in current at the double layer (or through the film if it is adsorbed and affects the film barrier). In order that a steady state be maintained, the potentials $V_f$ and $V_s$ must readjust. The effect of this is described mathematically by Eq. [8], in which it is shown that the apparent order will be $p$ multiplied by a fraction.

Using Eq. [8a], it is possible to predict that lowering $\alpha_f z_f$ will lower the apparent order. Since it was observed experimentally that the thicker the film the lower the $\alpha_s z_s$ coefficient for $H^+$ and $O_2$ reduction, it was assumed that this was due to a decrease of $\alpha_f z_f$. Therefore a specimen was anodized to a light blue color (16 v) and reduction of $Cu^{++}$ was carried out with this electrode. The log $a$ vs. log $(i-i_o)$ slope was not linear, but in no portion of the curve was the slope greater than 0.3, as would be predicted qualitatively from Eq. [8a].

Alternatively the fractional orders may be explained by the assumption of an adsorption isotherm such that the activity at the surface is not directly proportional to the activity in the bulk of the solution. This however seems somewhat more arbitrary than the explanation involving the dual barrier. Also, one would have to assume that the same adsorption isotherm holds for $H_2O_2$ and $Cu^{++}$ since they both give about the same order.

Equation [7] also predicts that the observed $\alpha_f z_f$ will generally be smaller than either $\alpha_s z_s$ or $\alpha_f z_f$. The unusually low transfer coefficients observed in these experiments may be explained on this basis. Thus, if $\alpha_f z_f = \alpha_s z_s = 0.5$, $\alpha_f z_f$ will be 0.25. For $O_2$ reduction, it is possible to calculate that $\alpha_s z_s = 1.2$ and $\alpha_f z_f = 0.4$, using the fact that the observed order, 0.75, $= \alpha_s z_s/(\alpha_s z_s+\alpha_f z_f)$ and the observed $\alpha_f z_f$, 0.31, $= (\alpha_s z_s \alpha_f z_f)/(\alpha_f z_f+\alpha_s z_s)$. Here it is arbitrarily assumed that oxygen affects the film barrier. The experimental determinations of the apparent order and the apparent Tafel slope are, however, not considered precise enough to warrant accurate calculations of $\alpha_f z_f$ and $\alpha_s z_s$.

The second case that might occur in this system is that which occurs when one of the reactions is essentially at equilibrium. In this case a Nernst-like expression may be used for the potential of the barrier at equilibrium and the normal rate equation for the other. A steady potential across the barrier at equilibrium will be achieved if the activities affecting this barrier remain constant. For the barrier at equilibrium, we may write

$$V_1 = V_{1,0} + \frac{RT}{nF} \ln \frac{\pi a'_{1,ox}}{\pi a'_{1,red}} \qquad [10]$$

The standard rate equation, e.g., Eq. [4] or [5], along with the relation $V_1 + V_2 = V_t$ gives:

$$i = K_2(\pi_f a_2^{p_2}) \left( \frac{\pi a'_{1,ox}}{\pi a'_{1,red}} \right)^{\frac{a}{n}} \exp \frac{+\alpha z V_{1,0}}{kT} \exp \frac{-\alpha z V_t}{kT} \qquad [11]$$

The following derivatives are obtained from Eq. [11]:

$$\frac{\partial \log i}{\partial \log a_2} = p_2 \qquad [12]$$

$$\frac{\partial \log i}{\partial \log a_{1,ox}} = \tau \frac{a}{n} \qquad [13]$$

and

$$\frac{\partial \ln i}{\partial V_t} = -\frac{\alpha z}{kT} \qquad [14]$$

Thus it is possible to obtain either unit or fractional orders in this case depending on whether the added constituent affects the barrier at equilibrium or not. It must be emphasized that the added constituent cannot affect any of the other activities; otherwise Eq. [12] and [13] are not valid.

It is therefore possible for the models proposed here to account for the fractional orders and low values of $\alpha z$ without resorting to unusual adsorption isotherms. Furthermore, the postulate of two barriers seems quite reasonable on film-covered electrodes of this type. There is not enough experimental evidence, however, to say fairly conclusively that these models are valid, or further to give explicit mechanisms for the reduction of the various oxidizing agents. The primary purpose of the presentation was to show that it is possible to obtain these effects from the two-barrier model.

It should be pointed out that two of the effects that do not seem to conform to Case I can be explained by assuming that Case II applies at low current densities. Thus, the fact that unit order is observed with oxygen reduction at low current densities can be explained by assuming that oxygen is adsorbed at the interface and that the rate-determining step is the transfer of electrons through the film barrier to the $O_2$ at the surface with the ultimate formation of a negatively charged oxygen-containing species, perhaps $OH^-$. Charge transfer through the surface is effected by a slight perturbation of the equilibrium $OH^-$ (ads.) + $H_3O^+ \rightleftarrows 2H_2O$. The amount of $OH^-$ adsorbed would probably be relatively constant since most of the oxide ions exposed to solution would probably react to form $OH^-$. At high current densities this equilibrium would be polarized and Case I would apply. This equilibrium also agrees with the observed pH dependence.

Similarly the change of the Tafel slope of $Cu^{++}$ reduction may indicate a change from Case I to Case II with the difference that $Cu^{++}$ (aq.) may not be adsorbed but may affect only the outer barrier. In both of these cases there is not enough experimental evidence to propose specific mechanisms.

The precise mechanism of charge transfer through the film is open to speculation since little is known concerning the structure and semiconducting properties of these films. For the reasons described above, cracks or pores were rejected as a mechanism for charge transfer. Tunnel effect should be extremely dependent on thickness and its effects are probably slight for the stable films present after a day's exposure to $O_2$. The data on $H_2$ evolution, however, show large changes in current at constant potential. It is suggested, therefore, that the initial

film present on the samples used in the $H_2$ overvoltage work is relatively transparent to electrons because of the tunnel effect. The growth of the oxide on the surface then causes a sharp reduction in the rate of tunneling.

In order for electrons to be transferred through the stable films formed by anodizing or exposure to $O_2$, electrons must *surmount* the barrier imposed by the field in the film. This of course results in very low rates at room temperature and even at 88°C the electrodes will reach rates of about $10^{-8}$ amp/cm$^2$ at open circuit after several days. The important parameter here is therefore the height of the potential energy barrier and the rate of transfer should therefore not be so sensitive to changes in thickness. To a good approximation therefore, the rate of transfer will be given by $i = K \exp - eV/kT$ where $eV$ represents the height of the potential energy barrier.

**Acknowledgment**

The kind encouragement and helpful discussions of Dr. G. H. Cartledge, Dr. F. A. Posey, and Dr. A. L. Bacarella, all of this Laboratory, are gratefully acknowledged.

Manuscript received Jan. 18, 1960. This paper was prepared for delivery before the Chicago Meeting, May 1-5, 1960.

Any discussion of this paper will appear in a Discussion Section to be published in the June 1961 JOURNAL.

REFERENCES

1. W. M. Latimer, "Oxidation Potentials," p. 271, Prentice-Hall, New York (1952).
2. R. E. Meyer, *This Journal*, **106**, 930 (1959).
3. F. A. Posey, *ibid.*, **106**, 571 (1959).
4. K. J. Vetter, *Z. Elektrochem.*, **55**, 274 (1951).
5. N. Cabrera and N. F. Mott, *Repts. Prog. Phys.*, **12**, 163 (1948-49).
6. N. Cabrera, "The Oxidation of Metals," in "Semiconductor Surface Physics," p. 327, University of Pennsylvania Press, Philadelphia (1957).

## Manuscripts and Abstracts for Spring 1961 Meeting

Papers are now being solicited for the Spring Meeting of the Society, to be held at the Claypool Hotel in Indianapolis, Ind., April 30, May 1, 2, 3, and 4, 1961. Technical sessions probably will be scheduled on Electric Insulation, Electronics (including Luminescence and Semiconductors), Electrothermics and Metallurgy, Industrial Electrolytics, and Theoretical Electrochemistry.

To be considered for this meeting, triplicate copies of abstracts (*not exceeding 75 words in length*) must be received at Society Headquarters, 1860 Broadway, New York 23, N. Y., *not later than January 2, 1961. Please indicate on abstract for which Division's symposium the paper is to be scheduled and underline the name of the author who will present the paper.* Complete manuscripts should be sent in triplicate to the Managing Editor of the JOURNAL at the same address.

Presentation of a paper at a technical meeting of the Society does not guarantee publication in the JOURNAL. However, all papers so presented become the property of The Electrochemical Society, and may not be published elsewhere, either in whole or in part, unless permission for release is requested of and granted by the Editor. Papers already published elsewhere, or submitted for publication elsewhere, are not acceptable for oral presentation except on invitation by a Divisional program Chairman.

# Technical Note

## Crystallographic Data on Beta-$Sr_2P_2O_7$

C. W. W. Hoffman and R. W. Mooney

*Chemical and Metallurgical Division, Sylvania Electric Products Inc., Towanda, Pennsylvania*

The tin-activated alkaline-earth pyrophosphates have been studied by three groups of workers (1-3) with the discovery of several phosphors. Calcium, strontium, and barium pyrophosphate occur in polymorphic modifications and Ranby and co-workers (1) showed that α-modifications were orthorhombic and probably isomorphous. It was also suggested that β-$Ca_2P_2O_7$ and β-$Sr_2P_2O_7$ were probably isomorphous although no crystallographic data were given. Recent work (3) has shown that there is a relationship between the emission and perhaps the excitation spectra of the three tin-activated α-modifications as well as a marked similarity between the excitation and emission spectra of β-$Ca_2P_2O_7$:Sn and β-$Sr_2P_2O_7$:Sn.

In a recent publication, Corbridge (4) working with single crystals of β-$Ca_2P_2O_7$ showed that it was tetrahedral with space group $P4_1$, and cell dimensions: a = 6.66Å and c = 23.86Å. Assuming a similar tetrahedral unit cell for β-$Sr_2P_2O_7$, it turned out to be a straightforward task to index its Debye-Scherrer pattern resulting in a = 6.920Å and c = 24.79Å. Table I lists the observed intensities and the slightly refined d-spacings, (omitting a very weak line at d = 3.30 which has been found to be in error), from a recent publication (5). It is evident that the calculated d-spacings based on the proposed unit cell account very well for the pattern.

Table I. X-ray powder data for β-$Sr_2P_2O_7$

| I | d (obs) | d (calc.) | hkl |
|---|---|---|---|
| 12 | 4.86 | 4.89 | 1 1 0 |
| | | 4.80 | 1 1 1 |
| 5 | 4.54 | 4.55 | 1 1 2 |
| 9 | 4.20 | 4.21 | 1 1 3 |
| 8 | 3.544 | 3.548 | 1 0 6 |
| 32 | 3.460 | 3.460 | 2 0 0 |
| 44 | 3.427 | 3.427 | 2 0 1 |
| 60 | 3.333 | 3.333 | 2 0 2 |
| 25 | 3.193 | 3.192 | 2 0 3 |
| 20 | 3.156 | 3.157 | 1 1 6 |
| | | 3.153 | 1 0 7 |
| 100 | 3.099 | 3.099 | 5 0 8 |
| | | 3.095 | 2 1 0 |
| 45 | 3.076 | 3.071 | 2 1 1 |
| 35 | 3.023 | 3.021 | 2 0 4 |
| | 3.006 | 3.003 | 2 1 2 |
| 25 | 2.902 | 2.898 | 2 1 3 |
| 22 | 2.870 | 2.869 | 1 1 7 |
| 20 | 2.839 | 2.838 | 2 0 5 |
| 11 | 2.772 | 2.769 | 2 1 4 |
| 11 | 2.652 | 2.653 | 2 0 6 |
| 15 | 2.626 | 2.625 | 2 1 5 |
| 10 | 2.475 | 2.477 | 2 1 6 |
| | | 2.475 | 2 0 7 |
| 15 | 2.439 | 2.435 | 2 2 1 |
| 12 | 2.403 | 2.400 | 2 2 2 |
| 6 | 2.344 | 2.346 | 2 2 3 |
| 17 | 2.307 | 2.307 | 3 0 0 |
| 6 | 2.278 | 2.276 | 2 2 4 |
| 9 | 2.225 | 2.222 | 3 0 3 |
| 12 | 2.186 | 2.188 | 3 1 0 |
| 26 | 2.161 | 2.162 | 3 0 4 |
| | | 2.155 | 3 1 2 |
| | | 2.155 | 2 0 9 |
| 8 | 2.110 | 2.115 | 3 1 3 |
| | | 2.105 | 2 2 6 |
| 25 | 2.063 | 2.066 | 5 1 2 |
| | | 2.064 | 3 1 4 |
| 23 | 2.016 | 2.015 | 2 0 10 |
| | | 2.014 | 3 0 6 |
| | | 2.013 | 2 2 7 |
| 8 | 1.937 | 1.935 | 2 1 10 |
| | | 1.934 | 3 1 6 |
| | | 1.933 | 3 0 7 |
| 12 | 1.924 | 1.920 | 2 2 8 |
| | 1.918 | 1.919 | 3 2 0 |
| 8 | 1.901 | 1.903 | 1 1 12 |
| | | 1.897 | 3 2 2 |
| 11 | 1.824 | 1.833 | 3 2 4 |
| | | 1.829 | 2 2 9 |
| | | 1.822 | 2 1 11 |
| 10 | 1.791 | 1.790 | 3 2 5 |
| | | 1.788 | 3 1 8 |
| 10 | 1.743 | 1.741 | 3 2 6 |
| 11 | 1.678 | 1.678 | 4 1 0 |
| | | 1.675 | 4 1 1 |
| 12 | 1.667 | 1.666 | 4 0 4 |
| 5 | 1.634 | 1.634 | 4 0 5 |
| | | 1.632 | 3 2 8 |
| 6 | 1.594 | 1.596 | 4 0 6 |
| 6 | 1.557 | 1.555 | 4 1 6 |
| | | 1.554 | 4 0 7 |
| 6 | 1.521 | 1.521 | 4 2 3 |

The sample of β-$Sr_2P_2O_7$ had been prepared by heating $SrHPO_4$ for several hours at 650°C giving a material whose analysis agreed generally with the theoretical composition of $Sr_2P_2O_7$ (5). Assuming, as

with $\beta$-$Ca_2P_2O_7$, 8 $Sr_2P_2O_7$ groups per unit cell a theoretical density of 3.91 g/cm³ results, in good agreement with the experimental value of 3.86 g/cm³ (5). In view of the marked similarities between the $\beta$-$Ca_2P_2O_7$ and $\beta$-$Sr_2P_2O_7$ powder patterns, it is likely that the compounds have the same space group, namely $P4_1$, although single crystal work would be required to definitely establish the space group of $\beta$-$Sr_2P_2O_7$.

**Acknowledgment**

The authors are indebted to Mr. R. C. Ropp for the preparations of several $\beta$-$Sr_2P_2O_7$ samples.

Manuscript received May 18, 1960.

Any discussion of this paper will appear in a Discussion Section to be published in the June 1961 JOURNAL.

**REFERENCES**

1. P. W. Ranby, D. H. Mash, and S. T. Henderson, *Brit. J. Appl. Phys.*, Supplement #4, 518 (1955).
2. A. H. McKeog and E. G. Steward, *ibid.*, Supplement #4, 526 (1955).
3. R. C. Ropp and R. W. Mooney, *This Journal*, **107**, 15 (1960).
4. D. E. C. Corbridge, *Acta Cryst.*, **10**, 85 (1957).
5. R. C. Ropp, M. Aia, C. W. W. Hoffman, T. J. Veleker, and R. W. Mooney, *Anal. Chem.*, **31**, 1163 (1959).

# Technical Review

## The Structure and Relaxation of Dielectrics

**Charles P. Smyth**

*Frick Chemical Laboratory, Princeton University, Princeton, New Jersey*

It is the aim of this paper to examine the reasons for the behavior of simple dielectric materials at high frequencies, in particular, in relation to their structures. It is a well-known fact that the dielectric constant and loss of a simple dielectric material depends on its polarizability. For molecular materials, nonpolar molecules give low dielectric constant and zero loss, and molecules with permanent dipole moments give dielectric constants to liquids which are larger, the larger their moments, and the greater their number per unit volume. The loss, which normally occurs only in a certain frequency region, depends on the same quantities, as well as on the frequency. In the region of loss, the dielectric constant falls off rapidly with increasing frequency. This behavior has been described and explained by the familiar Debye theory (1).

In order that these simple relationships may hold, the molecules must have freedom to orient in the alternating electric field used to measure the dielectric constant and loss. It is for this reason that most molecular solids have low dielectric constants and zero losses. However, many crystalline solids composed of symmetrical molecules have been found (2) to behave much like liquids for some distance below the melting point in a so-called "rotator state," and the orientational freedom of the polar segments of large molecules and polymers may result in similar behavior.

The static or low-frequency dielectric constant is observed when the dielectric material is in equilibrium with the applied field. Under the influence of the field, the polar molecules or segments rotate toward an equilibrium distribution of molecular orientation with a resultant polarization of the dielectric. When the polar molecules are very large, or the viscosity of the material is very great, or the frequency of the alternating field is very high, the rotary motion of the molecules is not sufficiently rapid for the attainment of equilibrium with the field. The displacement current then acquires a conductance component in phase with the field, and dielectric loss occurs. The lag in the attainment of the equilibrium is termed dielectric relaxation, which may be defined as the exponential decay with time of the polarization when the applied field is removed. The phenomenon may be treated in terms of a relaxation time, defined as the time in which polarization is reduced to $1/e$ times its value at the instant the field was removed, $e$ being the natural logarithmic base. This definition leads to the relationship that the relaxation time is the reciprocal of the critical angular frequency at which the loss is a maximum. The lag of the molecular dipoles behind the field increases with increasing frequency until the dielectric constant has decreased to a value which receives no contribution from dipole orientation.

The formal relationships between dielectric constant, loss, relaxation time, and frequency of field are largely independent of the mechanism of relaxation. The dielectric relaxation time is obtained by various methods from the measured values of dielectric constant and loss (1). If the dielectric is a dilute solution of polar molecules in a nonpolar solvent, the macroscopic relaxation time thus obtained may be regarded as the molecular relaxation time. If, however, each polar molecule is surrounded immediately by other polar molecules, the change in local internal field caused by the turning of one molecule requires the neighboring molecules to assume new orientations, with consequent longer relaxation time for the dielectric as a whole, the

macroscopic relaxation time. No generally satisfactory relationship between the two relaxation times has as yet been obtained, but an approximate relationship derived independently by O'Dwyer and Sack (3) and by Powles (4) requires the ratio of the macroscopic to the molecular relaxation time to lie between 1 and 1.5. Experiment has shown (5) that the ratio lies within this range for a large number of molecules, while an extension of the range to 0.9-2.0 would include most of the molecules which have been examined. For approximate consideration of the magnitudes of the relaxation times, the difference between the macroscopic and the molecular values can evidently be neglected in most cases, but, in detailed consideration of structural effects, account should be taken as far as possible of the difference. In his early treatment (1) Debye derived a much used and abused equation for the relaxation time $\tau$ on the assumption that the orienting dipole was in a spherical molecule of radius $a$ moving in a continuous viscous fluid of internal friction coefficient $\eta$:

$$\tau = \frac{4\pi\eta a^3}{kT}$$

where $k$ is the gas constant per molecule and $T$ is the absolute temperature.

When, in early work, several observed values of the relaxation time and the macroscopic viscosity were substituted in this equation, molecular radius values of the right order of magnitude were obtained, the apparent agreement being facilitated by the cube root relationship involved. The development of the equation by Perrin (6) and others in more elaborate form to make it applicable to ellipsoidal molecules gave good agreement with measurements on aqueous solutions of proteins (7). It is to be noted that, in these solutions, the solvent molecules are so small in comparison with the solute as to give an approximation to the continuous viscous fluid assumed by Debye. The full significance of these results for protein solutions is, however, uncertain because it has been shown (8) that proton fluctuations, rather than molecular orientation may be at least partially responsible for the observed behavior (7). When the relaxation times of small, nearly spherical molecules of known radius were measured and used to calculate the coefficient of internal friction or microscopic viscosity, the values found for the latter were only 0.008-0.06 of the macroscopic viscosity, and little parallelism was observed between the internal friction coefficient and the macroscopic viscosity (9). The extreme departure from predicted behavior was observed for $t$-butyl chloride and dibromodichloroethane in the "rotator" crystalline state, in which the apparent coefficient of internal friction was lower than that of the substance in the liquid state (10). In these cases, the orienting polar molecules are surrounded by molecules of the same or nearly the same size and not by the continuous fluid postulated by Debye.

This behavior may be further illustrated by some recent measurements and calculations (11) on solutions of several polar molecules, which, for the present purpose, may be regarded as rigid. The relaxation times were calculated from the molecular dimensions and the macroscopic viscosity by Fischer's (12) modification of the Perrin equation (6). The calculated value for $t$-butyl chloride in heptane solution is 25 times the observed at 20°, while, for the solution in Nujol, which has a macroscopic viscosity 257 times that of heptane, the calculated value is 3870 times the observed. For the slightly larger camphor molecule, the ratio is 10.5 in heptane and 2110 in Nujol solution while, for the large and somewhat flat molecule of 1-chloronaphthalene the ratio is 4.4 in heptane and 188 in Nujol solution. The macroscopic viscosity is almost without significance when the polar molecule is spherical and can rotate without displacement of its neighbors, but increase in molecular asymmetry and size increases the extent to which the polar molecule must displace its neighbors in order to rotate and so increases the dependence on viscosity. The long molecule of 4-bromobiphenyl, which has the dipole in its long axis, has a relaxation time in Nujol solution so long that, when measured at a wave length of 1.2 cm, the loss is very small and the dielectric constant is close to the optical dielectric constant, which receives no contributions from the permanent molecular moment. For the Nujol solutions of this molecule, the calculated relaxation time is 19.5 times the observed while, for those in heptane, the ratio is down to 2.1. For all these solutions, the departure of the calculated from the observed relaxation times is less wide, the lower the viscosity and the higher the temperature, which causes the viscosity to be lower. These results indicate that the larger the solute molecules and the smaller the solvent, the better the agreement between the calculated and the observed relaxation times.

Meakins (13) has recently concluded from a number of measurements that, when the polar solute molecule is at least three times as large as the solvent molecule, the solutions give good agreement with the unmodified Debye theory. Measurements (14) on benzene solutions of a large disk-shaped porphyrazine molecule having about 10 times the volume of the solute molecule give fair agreement with the unmodified Debye theory, but a shift of the molecular dipole from the plane of the disk to a direction perpendicular to it increases the relaxation time to 2.5 times the value, an increase not predicted by the unmodified Debye relation. It appears, therefore, that the relaxation times of molecules at least three times as large as the molecules surrounding them may be roughly proportional to the macroscopic viscosity, but dipole direction within the molecule and molecular shape must be taken into account (5, 14). The use of mutual viscosity instead of macroscopic viscosity gives much worse agreement for these solutions of large molecules, although it has been found to lessen the discrepancies between theoretical and observed behavior for some solutions of smaller molecules (15).

Although dielectric loss is proportional to the square of the permanent dipole moment of the

molecule (1), the dipole moment does not occur in the simple Debye equation for the relaxation time. However, the dipole moment affects the relaxation time indirectly through its effect on the intermolecular forces which influence the viscosity. Atomic and molecular polarizability exert somewhat similar effects upon the viscosity and, hence, upon the relaxation time. The Debye equation requires proportionality of the relaxation time to the molecular volume, and a very rough proportionality has been observed (16). The actual effect of change in molecular volume may be large because of its effect on viscosity, in addition to its direct effect on the relaxation time. In spite of the extreme departures of relaxation times of solutions from proportionality to viscosity which have been pointed out, a very definite tendency of the relaxation times of pure liquids to increase with viscosity has been observed (17, 18), so much so that it is frequent practice in comparing relaxation times to use a so-called reduced relaxation time, $\tau/\eta$, the ratio of the relaxation time to the viscosity.

The specific effects of molecular structure and shape may be illustrated by examples (18). As shown by the Stuart-Briegleb atomic models, fluorobenzene and pyridine depart only a little from the form of the symmetrical benzene molecule, fluorobenzene showing a slight protusion at the fluorine atom and pyridine a slight indentation at the nitrogen atom. The relaxation times of these molecules are nearly the same, although the measured viscosity of pyridine is 47% larger than that of fluorobenzene. Attachment of a methyl group to benzene lowers the viscosity slightly from 0.65 to 0.59 centipoise, while a similar substitution in the 4-position of pyridine lowers the viscosity still less. The protrusion of the methyl group raises the molecular relaxation time of 4-methylpyridine 83% above that of pyridine. It is higher than that of the similarly shaped toluene molecule by 56%, as compared to a difference of 59% in the viscosities. The substitution of methyl groups on the pyridine molecule in the 2- and 6- and in the 2-, 4-, and 6-positions alters the viscosity only slightly but raises the relaxation time greatly, so that 2,4,6-trimethylpyridine has a molecular relaxation time about 6 times that of pyridine. Substitution on the side chain of the toluene molecule raises the viscosity by 15% and doubles the relaxation time, but substitution of a second methyl group in the ortho position of toluene raises the viscosity by 37% and the relaxation time by 59%. The viscosity of i-propylbenzene is 16% higher than that of ethylbenzene, while the relaxation time is 42% higher.

In the monohalogenated benzenes, increasing size of the halogen and consequent increase in its polarizability and in the intermolecular forces increase both the viscosity and the molecular relaxation time. Benzonitrile and nitrobenzene, when compared to the monohalogenated benzenes, show somewhat longer relaxation times than would be expected on the basis of their viscosities and molecular volumes. Their larger dipole moments, 4.39 x $10^{-18}$ for benzonitrile and 4.21 x $10^{-18}$ for nitrobenzene, may account for this through increased intermolecular action not adequately taken into account in the calculation of the molecular relaxation time. In dilute solution in benzene, relaxation times ($10^{-11}$ sec.) have been found as follows: chlorobenzene, 0.75; bromobenzene, 1.02; nitrobenzene, 1.15. The comparatively small differences between these values and between them and the value for toluene show the importance of the liquid viscosities and the dipole-dipole interactions in causing the much larger differences between the pure liquids which are observed (19).

It is natural to expect that a nonspherical molecule should have different relaxation times around different axes of rotation. Perrin (6) has calculated that, for an ellipsoidal molecule with its permanent moment along one axis, the dispersion is the same as if the molecule were spherical, although the value of the relaxation time is different, while, for an elongated ellipsoid of revolution having a moment perpendicular to the axis of revolution, the single relaxation time is almost the same as that for a sphere of the same volume. If, however, the permanent moment does not lie in an axis of symmetry, more than one relaxation time results. The loss peaks associated with the different relaxation times are normally so close together that a single somewhat broadened and flattened loss maximum is observed. It has been common practice to represent the dependence of the dielectric loss on the frequency by an equation giving a distribution of relaxation times around a most probable value (1). In the equation of Cole (20) and Cole the extent of the distribution is represented by an empirical constant, which is 0 when there is but a single relaxation time and 1 when the number of different relaxation times approaches infinity. For nearly spherical molecules, the constant is zero or close to it. Variation in the environment of the polar molecules may result in some distribution of relaxation times. However, in the mixed solvent, Nujol, the roughly ellipsoidal molecule of 4-bromobiphenyl shows (11) but one relaxation time, in conformity with the Perrin theory, which is frequently not obeyed so well.

It is usually impossible to distinguish experimentally between the different distribution functions. The dielectric losses of the pure alkyl bromides were satisfactorily analyzed in terms of a Cole-Cole distribution (20) of relaxation times around a most probable value for each liquid (21). Recently, however, Professor K. Higasi in the writer's laboratory has carried out an analysis in terms of a distribution of relaxation times between two limiting values (22), one corresponding to the rotation of the terminal $CH_2Br$ group around its C-C bond and the other to the end-over-end rotation of the entire molecule in its extended form. The intermediate relaxation times correspond to orientation by twisting of segments around the other C-C bonds of the molecular chain. This method of analysis is an equally good representation of the experimental results and, for these molecules, is much more logical from the point of view of struc-

ture than the Cole-Cole distribution. Dipole orientation in polymers may occur by mechanisms resembling those just discussed for the alkyl bromides, but the much greater sizes of the molecules provide a greater variety of possible segmental orientation with consequent distribution of relaxation times, so that the loss-frequency curves commonly extend over very wide frequency ranges and have extremely flat maxima.

The presence of movable polar groups, such as $CH_2O$, $CH_2Cl$, and $NH_2$ in otherwise rigid molecules provides a possibility of dipole orientation by a single intramolecular rotation as well as by molecular rotation. The relaxation times observed for such substances are normally the result of two overlapping absorption regions, which can be clearly distinguished only by measurements at several frequencies extending into the region of millimeter waves. Measurements at 3 mm have been combined with those at longer wave lengths to show the existence of only one dielectric absorption region for rigid polar molecules, such as methylquinolines, while alcohols show additional absorption regions (23). Water shows but a single value of the relaxation time in this region with no distribution, but the high value, 6.0, of the apparent optical dielectric constant proves the presence of further considerable absorption at shorter wave-lengths, a conclusion at least qualitatively consistent with the infrared absorption spectrum.

From the practical point of view, it is evident that the dielectric loss of a material, like the dielectric constant, is greater, the greater the number of polar molecules per unit volume and the larger their polarities, provided that the molecules are free to orient in an applied electric field. The frequency region within which the loss is considerable lies within a hundredfold range of frequency or two logarithmic decades when the material has a single relaxation time. When there is a distribution of relaxation times, the frequency region of loss is extended and the maximum loss is lowered. The location of the region of loss is moved to higher frequency, the higher the temperature, the smaller the molecules, and the lower the resistance to molecular or polar group rotation. For large molecules surrounded by small, the measured macroscopic viscosity may give a fair measure of this resistance to orientation, but, for small molecules, the resistance is much lower than indicated by the viscosity, which, in such cases, frequently has little significance. Loss then occurs at higher frequencies than those predicted from the viscosity.

Manuscript received March 2, 1960

Any discussion of this paper will appear in a Discussion Section to be published in the June 1961 JOURNAL.

REFERENCES

1. C. P. Smyth, "Dielectric Behavior and Structure," Chap. I, II, McGraw-Hill Book Co., New York (1955).
2. *Ibid.*, Chap. V.
3. J. J. O'Dwyer and R. A. Sack, *Australian J. Sci. Research*, **A5**, 647 (1952).
4. J. G. Powles, *J. Chem. Phys.*, **21**, 633 (1953).
5. R. C. Miller and C. P. Smyth, *J. Am. Chem. Soc.*, **79**, 3310 (1957).
6. F. Perrin, *J. Phys. Radium*, **5**, 497 (1934).
7. Ref. (1), Chap. XIII.
8. J. G. Kirkwood and J. B. Shumaker, *Proc. Nat. Acad. Sci.*, **38**, 855 (1952).
9. C. P. Smyth, *J. Phys. Chem.*, **58**, 580 (1954).
10. J. G. Powles, D. E. Williams, and C. P. Smyth, *J. Chem. Phys.*, **21**, 136 (1953); D. E. Williams, Thesis, Princeton University (1956).
11. O. F. Kalman and C. P. Smyth, *J. Am. Chem. Soc.*, **82**, 783 (1960).
12. E. Fischer, *Physik. Z.*, **40**, 645 (1939).
13. R. J. Meakins, *Trans. Faraday Soc.*, **54**, 1160 (1958).
14. D. A. Pitt and C. P. Smyth, *J. Am. Chem. Soc.*, **63**, 582 (1959).
15. D. A. Pitt and C. P. Smyth, *J. Phys. Chem.*, **81**, 783 (1959).
16. A. D. Franklin, W. M. Heston, Jr., E. J. Hennelly, and C. P. Smyth, *J. Am. Chem. Soc.*, **72**, 3447 (1950).
17. P. L. McGeer, A. J. Curtis, G. B. Rathmann, and C. P. Smyth, *ibid.*, **74**, 3541 (1952).
18. C. P. Smyth, *Proc. Nat. Acad. Sci.*, **42**, 234 (1956).
19. See also R. W. Rampolla and C. P. Smyth, *J. Am. Chem. Soc.*, **80**, 1057 (1958).
20. K. S. Cole and R. H. Cole, *J. Chem. Phys.*, **9**, 341 (1941).
21. E. J. Hennelly, W M. Heston, Jr., and C. P. Smyth, *J. Am. Chem. Soc.*, **70**, 4102 (1948).
22. Cf. H. Fröhlich, "Theory of Dielectrics," pp. 93-95, Oxford University Press, London (1949).
23. R. W. Rampolla, R. C. Miller, and C. P. Smyth, *J. Chem. Phys.*, **30**, 566 (1959).

## June 1961 Discussion Section

A Discussion Section, covering papers published in the July–December 1960 JOURNALS, is scheduled for publication in the June 1961 issue. Any discussion which did not reach the Editor in time for inclusion in the December 1960 Discussion Section will be included in the June 1961 issue.

Those who plan to contribute remarks for this Discussion Section should submit their comments or questions in triplicate to the Managing Editor of the JOURNAL, 1860 Broadway, New York 23, N. Y., *not later than March 1, 1960*. All discussion will be forwarded to the author(s) for reply before being printed in the JOURNAL.

# Current Affairs

## George W. Heise Honored by Cleveland Section

The George W. Heise Medal of the Cleveland Section of The Electrochemical Society.

The Cleveland Section has established a George W. Heise Medal, the awarding of which expresses respect and appreciation to those members of the Section who in the past have contributed conspicuously to its continued progress, or may do so in the future. A Medal Committee, which began its function in the spring of 1959 under the Chairmanship of Dr. H. P. Coats, is deeply indebted to Mrs. George W. Heise for her skill as sculptress. At the request of the Committee, she executed in plaster the Heise head in bas-relief. Her art work was reproduced in the three-inch natural-finish bronze medal by the Medallic Art Company, makers of the Society's Acheson and Palladium Medals.

The obverse of the medal bears the name and likeness of George W. Heise, and a tribute to his services to the Section and the Society. The reverse, engraved with the name of the recipient, is inscribed: "For Meritorious Service to Cleveland Section Electrochemical Society."

The Section has felt the need, on a local basis, for a tangible expression of thanks to those founders, officers, and others who have contributed to its success over the years. In addition, there was a desire to honor George W. Heise, a Co-Founder of the Cleveland Section, whose contributions have extended far beyond local bounds. These sentiments came to fruition on May 20, 1960, with the first presentations of the George W. Heise Medal.

The ceremony was held in conjunction with the Ladies' Night dinner of the Section in downtown Cleveland. Mr. Heise received the first medal from the hands of H. P. Coats. J. R. Brown and J. D. Ceader, two of the earliest members whom the Section had not seen for several years, were present to receive their medals from Mr. Heise himself, as were A. C. Zachlin and H. P. Coats. Other early members receiving the medal were L. R. Westbrook, R. S. Mackie, and C. E. Heil. Further awards were made to R. W. Erwin, A. G. Gray, M. Janes, H. R. Schoenfeldt, M. E. Sibert, and W. H. Stoll. The Cleveland Section plans to hold an annual Heise Night for future presentations.

Mr. Heise also has the distinction of being selected by Cleveland's Fenn College as one of four men to whom were given honorary doctorates on June 12, 1960. His degree of Doctor of Science was in recognition of his contributions in the field of electrochemistry.

## D. M. Smyth to Receive Battery Division Research Award for 1958-1959

The Battery Division has selected Dr. Donald M. Smyth of the Sprague Electric Co. as the recipient of its Research Award for the period 1958-1959. The basis of Dr. Smyth's selection was his paper entitled "Silver / Silver Chloride / Chlorine Solid Electrolyte Cell" which appeared in the August 1959 issue of this JOURNAL, pp. 635-639. It is expected that the award will be presented to Dr. Smyth at the Battery Division Luncheon to be held on Tuesday, October 11, 1960, during the Fall Meeting of the Society in Houston, Texas.

Dr. Smyth was born in Bangor, Maine, in 1930; received his B.S. degree in chemistry from the University of Maine in 1951 and his Ph.D. degree in inorganic chemistry from the Massachusetts Institute of Technology in 1954. Since that time, he has been employed at the Sprague Electric Co. at North Adams, Mass. He is, at present, a section head in the Research and Engineering Division. During this time, he has published several papers which have appeared in the *Journal of the American Chemical Society* and this JOURNAL, and has been granted two patents in the battery field. He is a member of The Electrochemical Society and the American Chemical Society.

He is married to the former Elisabeth Luce of Hermon, Maine, and is the father of two daughters, Carolyn, five years old, and Joanne, one year old.

The Research Award of the Battery Division was first established in 1958 for the purpose of stimulating battery research and encouraging the preparation of high-quality papers for the JOURNAL of The Electrochemical Society. It is expected that a selection will be made every two years of an author, or authors, of a recent paper relating to electrochemical cells or batteries which has been published in the JOURNAL. The paper is selected primarily on the basis of scientific merit and importance. This includes originality of concept and experimental approach, the thoroughness of experiments, and the logic of conclusions.

D. M. Smyth

Clarity of presentation also is considered to be an important aspect. The Research Award consists of an engraved scroll to each author of the chosen paper, along with a prepaid membership in the Society and subscription to the JOURNAL as follows: single author—life membership and subscription; two authors—ten years' prepaid membership and subscription to each; three authors—seven years' prepaid membership and subscription to each.

A Research Award winner is chosen by a committee of five appointed by the Battery Division Chairman. The selection is approved by the Battery Division Executive Committee and the recommendation is submitted to the Society's Board of Directors for final approval. The Award Committee for this second selection for the Battery Division Research Award consisted of N. C. Cahoon, Chairman, W. S. Herbert, J. J. Lander, E. B. Yeager, and W. J. Hamer.

## Section News

### News from India

*Indian Aluminium's Expansion Project.*—The Indian Aluminium Co. will carry out a substantial expansion of its bauxite, alumina, aluminum ingot, rolling mill, and extrusion facilities. The plans will cost about $17,000,000. The largest segment of the project is the addition of 12,000 tons of primary ingot capacity, doubling to 22,400 tons the present capacity of the company's Hirakud smelter. Established in 1938, the company has since become a fully integrated enterprise with smelters in Orissa and Kerala States, and fabricating facilities in Calcutta, Bombay, and Kerala. Aluminium Ltd. of Canada has a majority interest in the concern. The rolling mill at Belur, West Bengal, will be expanded from 10,000 tons of rolled products to 18,500 tons a year. There are also proposals to install an additional modern extrusion press at Alupuram, Kerala, with a ram pressure of 3300 tons.

*Seminar in Electrochemistry at Karaikudi.*—The Central Electrochemical Research Institute, Karaikudi, held a Seminar in Electrochemistry from April 23 to 25, 1960. Sixty-seven papers were presented in six sections: electrode kinetics and polarography, metal finishing and growth of electrodeposits, electrolytic equilibria, corrosion, electrolytic preparations, experimental techniques, and miscellaneous. Scientists from Belgium, Ceylon, East Germany, England, Poland, and the U.S.S.R. participated in the Seminar. Abstracts of the papers presented have been published as a booklet by the CECRI.

*Corrosion and the ISI.*—Popularization of the use of cold-formed light-gauge sections in structures is an important item of the Steel Economy Programme which the Indian Standards Institution (ISI) has undertaken on the recommendation of the Planning Commission and at the request of the Government of India.

In recent years, the use of light-gauge steel, both strip and sheet, as a structural material has developed considerably in the U.K., U.S.A., and the countries of Western Europe.

In structural engineering, hot-rolled steel sections used are usually of thicknesses of more than 3/16 in. The use of thinner material is specifically prohibited in many specifications and codes due to the possibility of corrosion. The progressive and rapid development, in other countries, of the use of thin sections in structures has been possible only through a corresponding improvement in the standards for the corrosion protection and maintenance of the structures. In India also, the use of cold-formed light-gauge sections as a structural material could be popularized if suitable corrosion protection schemes can be developed to suit Indian conditions.

With this object in view, the Structural Steel Research Subcommittee set up a Panel in 1956 for investigations relating to Corrosion Protection of Light-Gauge Steel Sections. Later, in August 1957, the work was transferred to the Panel for Corrosion Research of Light-Gauge Steel Structures, SMDC 1/P3, under the Metal Standards Sectional Committee, SMDC 1, of the Structural and Metals Division Council. A brief description of the scope of work of this Panel follows: (*a*) Investigations and research for formulation of standard specifications for corrosion protection of light-gauge steel structures; (*b*) Investigations and research for formulation of standard specifications for performance tests for protective schemes used in corrosion protection of light-gauge steel; and (*c*) Investigations and research relating to corrosion protection of steel transmission towers and steel work in foundation.

At present, the work on the following items is in progress: (*a*) Classification of areas in India on the basis of intensity of corrosiveness; (*b*) Procedure with regard to preparation of test specimens, surface preparation, and exposure tests; (*c*) Details with regard to protective schemes to be tried; and (*d*) Development of accelerated tests to assess the corrosiveness of various environments and testing characteristics of corrosion protection schemes established now or hereafter. Exposure tests for this purpose are being conducted at certain selected sites, viz., Mandapam Camp, Madras, Karaikudi, Calcutta, Bombay, Jodhpur, Hyderabad, Kanpur, Cochin, and Pandu.

*New Patrons, India Section.*—The following industries have become Patrons of the India Section: (*a*) Atoz Private Ltd., Bombay, and (*b*) Hind Cycles Ltd., Bombay.

T. L. Rama Char,
*India Correspondent*

## Division News

### Electro-Organic Division Business Meeting in Houston

A business meeting of the Electro-Organic Division will be held during the Society's Houston Convention, October 9-13. The time and place of the meeting will be on display by the registration desk at the Shamrock-Hilton Hotel.

G. W. Thiessen, *Chairman*

### Battery Division

The Nominating Committee for the Battery Division fall meeting has completed its selection of candidates for officers to serve during the next two years (1960-1962). All candidates have agreed to serve if elected. The Nominating Committee consisted of W. C. Vosburgh of Duke University Samuel Eidensohn of the Electric Storage Battery Co., and R. C. Kirk of the Dow Metal Products Co. as Chairman. The election will take place during the annual meeting of the Battery Division in Houston this month.

The list of candidates is as follows:

*Chairman*—E. J. Ritchie, Eagle-Picher Co., Joplin, Mo.

*Vice-Chairman*—Arthur Fleischer, McGraw-Edison Co., West Orange, N. J.

W. S. Herbert, Electric Storage Battery Co., Yardley, Pa.

C. K. Morehouse, Radio Corp. of America, Somerville, N. J.

*Secretary-Treasurer*—C. H. Clark, U. S. Army Signal R & D Labs., Fort Monmouth, N. J.

*Members-at-Large (two to be elected*—Jeanne B. Burbank, U. S. Naval Research Lab., Washington, D. C.; T. P. Dirkse, Calvin College, Grand Rapids, Mich.; D. T. Ferrell, Electric Storage Battery Co., Raleigh, N. C.; P. L. Howard, Yardney Electric Corp., New York, N. Y.; Ernest Yeager, Western Reserve University, Cleveland, Ohio.

R. C. Kirk, *Chairman*
*Nominating Committee, 1960*

### Electronics Division Enlarged Abstracts

Copies of past issues of the Electronics Division Enlarged Abstracts booklets are available as follows::

**1956**—Vol. 5, No. 1, at $2.50
**1959**—Vol. 8, No. 1, at $3.00
**1960**—Vol. 9, No. 1, at $3.50

Please send order and check directly to:

Austin E. Hardy
Secretary-Treasurer
Electronics Division
Electrochemical Society
c/o RCA
Lancaster, Pa.

## Personals

**J. Balachandra** has been appointed research officer, Metallurgy Div., Atomic Energy Establishment, Bombay, India.

**Bruce E. Deal,** research chemist in the field of surface chemistry of metals, formerly with Kaiser Aluminum & Chemical Corp., Spokane, Wash., has joined Rheem Semiconductor Corp., Mountain View, Calif., as a member of the technical staff. Dr. Deal will continue to study the kinetics of surface reactions, with particular emphasis on the surfaces of semiconductor materials. In addition, he will develop techniques and processes to aid in improving the performance and reliability of semiconductor diodes and transistors.

**K. S. G. Doss, S. Krishnamurthy, and S. Panchapakesan** have been nominated as members of the Expert Committee for the Effluent Treatment Plant, Heavy Electricals Ltd., Bhopal, India.

**Andrew Gemant,** widely known research scientist and staff physicist for the Detroit Edison Co.'s engineering research department, Detroit, Mich., retired on August 1 after 20 years of service with the company. Dr. Gemant has won distinction in the engineering research field as well as the electric power industry for his basic research activities concerning the physical chemistry of insulating materials.

Before coming to the United States in 1938 to accept a post as research associate at the University of Wisconsin in Madison, he was a physicist for the Siemens-Schuckert Cable Co., Berlin, Germany, a lecturer at the Technical University of Berlin, and a research associate at Oxford University, Oxford, England.

Dr. Gemant was retained by Detroit Edison as a consultant in 1939 and joined the company the following year as staff physicist for the engineering research department.

In addition to The Electrochemical Society, he is a member of the German Physical Society and the National Research Council, and a Fellow of the American Physical Society and the American Association for the Advancement of Science.

**Julian Glasser and William E. F.w,** formerly associated as consultants, Chattanooga, Tenn., in chemical and metallurgical activities, are now associated as president and vice-president, respectively, in a new corporation, Chemical and Metallurgical Research, Inc., with offices located in the Volunteer Bldg., Chattanooga. This organization was set up to own and operate facilities for chemical and metallurgical research, particularly in the field of material sciences, including laboratory, pilot plant, and other types of activities incident to the operation of progressive research organization.

**Ralph J. Hovey** has been appointed plant superintendent of the Packaged Electronics Div. of Amphenol-Borg Electronics Corp., Broadview, Ill. Mr. Hovey joined Amphenol-Borg in August 1959 as staff engineer in material research at the Broadview plant. Prior to that time, he had been associated with Fansteel Metallurgical Corp.

**Byung J. Kim,** formerly of Brooklyn, N. Y., has moved to Los Angeles, Calif., to take a position as metallurgist with the Michael-Rand Plating Co., Van Nuys.

**H. A. Liebhafsky, H. G. Pfeiffer, E. H. Winslow, and P. D. Zemany,** scientists of the General Electric Research Lab., Schenectady, N. Y., are authors of the new book, "X-Ray Absorption and Emission in Analytical Chemistry," published in June by John Wiley & Sons, Inc., New York City. This volume opens up a vital and important scientific field, that of x-ray spectrochemical analysis.

**Hugh L. Logan,** a physicist with the Corrosion Section of the National Bureau of Standards, Washington, D. C., has received a U. S. Dept. of Commerce Silver Medal for Meritorious Service. He was cited for "exceptional achievement in metallurgy, particularly in researches into the stress-corrosion cracking of metals and for meritorious authorship." Mr. Logan supervises investigation of the mechanism of stress-corrosion cracking and of

high-temperature oil ash corrosion. Prior to 1950, his research was in stress corrosion of aluminum and magnesium alloys and beryllium, and the mechanical properties of aircraft steels.

**E. E. Nelson** has been transferred by his company, Socony Mobil Oil Co. Inc., to their corrosion and metallurgy group, Research Dept., Paulsboro, N. J. Since 1956, he had worked at the Brooklyn, N. Y., laboratory on various corrosion problems, principally in the field of tanker corrosion. He will continue with similar activities at the Paulsboro laboratory.

**S. K. Panikkar** has joined Hind Cycles Ltd., Bombay, as chief chemist.

**John K. Taylor,** a chemist with the Analytical Chemistry Section of the National Bureau of Standards, Washington, D. C., has received a U. S. Dept. of Commerce Silver Medal for Meritorious Service. The citation was in "recognition of his contributions to accurate electrochemical methods of analysis." Dr. Taylor's present work is in the application of physical methods to analytical chemical research. He directs a program of electroanalytical chemistry concerned with high-precision coulometric methods of analysis. He also is in charge of a program for providing a series of uranium isotopic standards. This involves high-precision analysis of uranium compounds and the blending of highly purified isotopic species for mass spectrographic analysis.

**T. J. Varkey** has joined the Regional Engineering College, Bangalore, as assistant professor in the Dept. of Chemistry.

## Book Reviews

**The Dynamic Behavior of Thermoelectric Devices,** by Paul E. Gray. Published by Technology Press, Massachusetts Institute of Technology, Cambridge, Mass., and John Wiley & Sons, Inc., New York City, 1960. $3.50.

With available semiconductors, it is possible to design practical thermoelectric devices, both heat pumps which provide refrigeration for individual electronic components, and small-scale generators which convert heat directly into electricity. An important example of a heat pumping application is a thermostatic device which maintains a fixed inside temperature when the ambient varies above or below this temperature. In designing such a device, it is necessary to understand the transient behavior of the thermocouples to achieve accurate control.

It is to such problems that this publication provides partial answers. Described as "larger in scope than a journal article but less ambitious than a finished book," it is based on an M.I.T. Electrical Engineering doctoral thesis. The differential equations involved in a complete analysis were found to be too complex for exact solution and, therefore, approximate solutions are given for the case of small changes, either abrupt or periodic, in the current, temperature, or load for both heat pumps and generators. The heat pump results are in good agreement with the experiments to which one of the seven chapters is devoted. Many of the theoretical results are presented in useful graphical form.

This monograph will be useful not so much for the materials scientist who is concerned with finding improved semiconductors for the individual thermoelements as for the engineer who is concerned with the design of controlled devices.

Raymond Wolfe

**Direct Conversion of Heat to Electricity.** Edited by Joseph Kaye and John A. Welsh. Published by John Wiley & Sons, Inc., New York City, 1960. $8.75.

The direct conversion of heat into useful electrical energy is receiving considerable attention, and a substantial amount of work now is being done in various universities and industries to develop static and reliable techniques which show promise of being employed in practical engineering devices. The July 1959 Special Summer Program in "Direct Conversion of Heat to Electricity" held at the Massachusetts Institute of Technology treated a major aspect of this field.

The 23 papers presented at this program and which make up this volume are of high quality. They are divided into five general sections: A—Thermionic Engines-High Vacuum B—Thermionic Engines-Low Pressure, C—Magnetohydrodynamic Converters, D—Semiconductor Devices, E—Fuel Cells. The papers on thermionic engines or converters and the papers on thermoelectric effects in semiconductors constitute all but three of the published papers. As a result, Magnetohydrodynamics and Fuel Cells are given inadequate coverage. While this appears as a weakness in the book, its organization and technical material make it of considerable value as a reference work in this field.

The investigations and analysis in Section A of high-vacuum thermionic converters by Hatsopoulos, Kaye, and Nottingham, *et al.*, include fine treatments of the requirements of anode and cathode materials, the effects of space charge, and the thermodynamics of the vacuum diode. The papers in Section B adequately describe some of the important work on the gaseous thermionic diode. Nottingham's paper discusses the ionization of cesium following the work of Langmuir and Taylor, the effects of nonuniform cathode work functions, and, in addition, presents some useful empirical equations. The paper by Pidd, *et al.*, presents some results dealing with the effects of cesium pressure, and emitter material and temperature on the open-circuit voltage and short-circuit current of an experimental cell. The paper by Steel shows some interesting results of experiments to determine the rate at which cesium atoms are ionized at the cathode surface.

Section D includes a very fine survey paper on thermoelectric effects by Jaumot which provides an excellent list of references. Papers by Fritts and Bollmeir present some elementary design and device information concerning thermoelectric generation. A paper by Hatsopoulos and Keenan and one by Somers and Swanson deal with the thermodynamics of thermoelectric generators and the conditions for optimizing thermal efficiency in generators. Several papers also are included which describe the effects of impurities on bismuth, antimony, and tellurium alloys, along with methods for measuring thermoelectric parameters.

**Notice to Members and Subscribers**
**(Re Changes of Address)**

To insure receipt of each issue of the JOURNAL, please be sure to give us your old address, as well as your new one, when you move. Our records are filed by states and cities, not by individual names. The Post Office does not forward magazines.

This book will be appreciated by specialists and new workers in this field of energy conversion, for the papers are basic and significant. A reasonable balance exists among the papers with sufficient emphasis on theoretical analysis, experimental results, and engineering considerations.

D. Feldman

**Properties and Structure of Polymers,** by Arthur V. Tobolsky. Published by John Wiley & Sons, Inc., New York City, 1960. 331 + IX pages; $14.50.

The increasing use of polymers as structural materials during the last two decades has led to an exuberant interest in understanding how the mechanical properties of plastics arise from the more fundamental properties of macromolecules. Professor Tobolsky has been one of the leading investigators in this field and has developed a posture in this area which is sometimes called the "Princeton School."

This book is essentially a compendium of the writings of Tobolsky and his students; in fact, in order not to overburden the index, the author's name has been omitted. The book was needed to concatenate and distill the 125 articles which they have published in the last 18 years.

The work is a monument to Professor Tobolsky's intellectual commitment to understanding why polymers act the way they do. He has not used the elegant tools of nuclear magnetic resonance, dynamic shear equipment, nor electromagnetic spectroscopy. His work has been distinguished by the simplicity of his techniques and the depth of his conclusions. He has been particularly concerned with the properties of hydrocarbon elastomers; these include the relaxation of stress, the generation of heat, and the birefringence of light in natural and synthetic rubbers. In his interpretations, he has espoused the viscoelastic models of Maxwell and Voigt.

This book is not as broad in scope as its title, "The Properties and Structure of Polymers," would indicate, nor is it an exposition of the physical properties of polymers. While certain of the properties of the polar polymers are mentioned, the detailed studies and interpretations are based generally on the nonpolar aliphatic and aromatic hydrocarbons. Because of this, many of the subtleties of this science involving electronegativity, dipole-dipole bonding, and proton transfer do not enter into the general tone of the book. Perhaps it is because of this that the relationships which exist between the mechanical and electrical properties of polymers receive only glancing notice.

The book consists of an introductory section on elasticity and viscosity, and the contribution of molecular architecture to the properties of polymers. This is followed by a detailed mathematical and experimental exposition of the viscoelastic behavior of polymers, and climaxed with a study of transformations in cross-linked elastomers. There is an extensive appendix where such concepts as the Partition function, the equation of state for molecular crystals, and size distribution in linear polymers are developed.

The work is presented in a series of vignettes, each in itself an interesting facet or aspect of polymer properties, and to each are appended the references thought to be of particular value to the reader. Tobolsky has indicated the importance he puts on reading the original manuscript by listing them in full print at the end of each section instead of as footnotes. Many of these essays are short and pithy such as the one entitled "Stress Relaxation of Amorphous Polymers" (pp. 137-143), which consists of only 300 words of text, six graphs, and a photograph of a relaxation balance.

The book is, then, a compendium of Tobolsky's work and as such is a recording of the experiments of a specialist in the field of polymers. It is recommended to other specialists.

Thomas D. Callinan


# FUEL CELL RESEARCH

**We have immediate openings for physical or electro chemists with experience in FUEL CELLS. Work consists of laboratory research and development on FUEL CELLS.**

**Recognition of achievement is readily attained in our small development group of 20 men. New air-conditioned laboratories are in the process of completion. Location is in Minnesota, famous for its year-round beauty and recreational opportunities.**

***Résumé should include educational background and complete details of fuel cell experience.***

**Reply to Box A-284,**
**c/o The Electrochemical Society, Inc.,**
**1860 Broadway, New York 23, N. Y.**


## News Items

### 1961 Palladium Medal Award, ECS

The sixth Palladium Medal of The Electrochemical Society will be awarded at the Fall Meeting of the Society to be held in Detroit, Mich., October 1-5, 1961.

The medal was established in 1951 by the Corrosion Division for distinguished contributions to fundamental knowledge of theoretical electrochemistry and of corrosion processes. It is awarded biennially to a candidate selected by a committee appointed by the Society's Board of Directors.

Sections, Divisions, and members of the Society are invited to send suggestions for candidates, accom-

panied by supporting information, to the National Office of the Society, 1860 Broadway, New York 23, N. Y., attention of Robert K. Shannon, Executive Secretary, for forwarding to the committee Chairman. *Deadline for submission of suggestions is March 15, 1961.*

Candidates may be citizens of any country and need not be members of the Society. Previous medalists have been: Carl Wagner, Max Planck Institut für Physikalische Chemie; N. H. Furman, Princeton University; U. R. Evans, Cambridge University; K. F. Bonhoeffer, Max Planck Institut für Physikalische Chemie (posthumous award); and A. N. Frumkin, Electrochemical Institute of the U.S.S.R.

### C. L. Faust and A. K. Graham Honored at AES Convention

The American Electroplaters' Society, Inc., (AES) launched its four-day 47th Annual Convention at the Statler Hilton Hotel in Los Angeles on July 25.

At the Grand Opening Session, the distinguished scientist Dr. Charles L. Faust, Battelle Memorial Institute, Columbus, Ohio, was proclaimed winner of this year's AES Scientific Achievement Award, the society's highest scientific annual honor. In consequence, he will deliver the annual "William Blum Lecture" at the Society's 48th Annual Convention to be held in Boston in June 1961.

The Grand Opening Session was the morning forerunner of the Opening Educational Session conducted early in the afternoon before a packed audience composed of the leaders and rank and file of the electroplating and metal finishing industry. The session featured the "William Blum Lecture" delivered on the subject of "Faraday's Laws Applied to Cleaning" by Dr. A. Kenneth Graham, 1959 AES Scientific Achievement Award winner. Dr. William Blum presided. After the delivery of his address, Dr. Graham was presented with a $500 honorarium and an attendant scroll by AES National President Wysong in behalf of the American Electroplaters' Society, Inc.

### Patents Granted to G.E. on Diamond-Making Process and Apparatus

The U. S. Patent Office recently granted patents to the General Electric Co. on the process and apparatus for making diamonds and other high-pressure products. Based on work performed at the General Electric Research Lab. in Schenectady, N. Y., where man-made diamonds were first announced in February 1955, the patents cover the basic high-pressure equipment used in making diamonds, as well as later improvements on such equipment. Also included are processes for making garnet and Borazon, the cubic form of boron nitride.

Because of a secrecy order of the Federal Government, General Electric was unable to file patent applications in many foreign countries on its diamond-making process until 1959 because industrial diamonds are of strategic importance to the national defense.

General Electric diamonds have proved to be superior in many respects to natural diamonds for a variety of industrial uses. Their manufacture and sale in commercial quantities was announced in October 1957. These diamonds are of the proper size for most industrial uses —less than a tenth of a carat. After more than two years of large-scale production of man-made industrial diamonds, the secrecy order on the diamond process was rescinded in the fall of 1959.

At that time, General Electric published details of its diamond process. The long-sought transformation of common graphite into diamond was accomplished, the company revealed, by the action of a molten metal catalyst and the simultaneous application of pressures of from 1.5 to 2 million pounds per square inch, and temperatures ranging from 2200° to 4400°F.

The shape and color of man-made diamonds can be controlled by varying the temperature of formation. The best starting material was identified as substantially pure graphite, although other carbonaceous materials, such as carbon black, sugar, charcoal, or carburizing compound may be used. The catalyst metal may be chromium, manganese, iron, cobalt, nickel, ruthenium, rhodium, palladium, osmium, iridium, tantalum, or platinum.

### Western Reserve University Science Center

Western Reserve University held a ground-breaking ceremony for its $6,270,000 Science Center on the University Circle campus on July 14.

Heading the program was John A. Greene, chairman of the WRU board of trustees. Others on the program were WRU president John S. Millis


# ELECTROCHEMIST

**Doctor's Degree—5 to 10 Years' Experience**

To head a newly organized group of electrochemists and physical chemists devoted to research on fuel cells.

This is a challenging position in a new field. It requires considerable theoretical background, experimental skill and inventive talent.

Work is strongly supported by the Corporation and directed at commercial exploitation. The position has excellent potential for growth.

A new laboratory building has been erected in our plant at East Hartford, Connecticut.

***Send resume and minimum salary requirements to Mr. P. R. Smith, Office 61,***

**PRATT & WHITNEY AIRCRAFT**
**Division of United Aircraft Corporation**
**East Hartford 8, Connecticut**

and Neil J. Carothers, president of the University Circle Foundation.

The basic science building will be named the John Schoff Millis Science Center honoring the university's ninth president, according to a resolution adopted by the board of trustees, it was announced by Greene. Millis became president of Reserve in September 1949. He is the first president of Western Reserve whose educational and teaching background is in the field of science.

This building represents the first phase in the development of a new WRU Science Center. It will provide new laboratories, a library, auditorium, and teaching and research facilities for the departments of biology, chemistry, physics, geology, geography, astronomy, and mathematics.

The first part of the building, which will be for the chemistry department, is expected to be completed by fall of 1961 with the remainder ready for occupancy by the spring of 1962.

### RCA Enters Electroluminescent Lighting Field

The Radio Corp. of America announced recently that it had entered the electroluminescent lighting field and was manufacturing light-emitting panels for consumer, industrial, and military uses.

The panels give off a soft glow of light in any one of five colors and are designed for use in decorative lighting, and for illuminating dials, control panels, highway signs, signals, and safety devices. They will be merchandised under the trade name "Panelray."

Full-scale manufacturing of panels at the company's Lancaster, Pa., plant was slated for early fall. Pilot production already was under way during the summer.

### Pennsalt Chemicals Completes Modernization of Chlorine-Caustic Facilities

Modernization of its largest chlorine-caustic plant in Wyandotte, Mich., has been completed on schedule by Pennsalt Chemicals Corp. The largest single modernization project undertaken by Pennsalt, it included the replacement of some 5000 old diaphragm-type electrolytic cells with 200 large, modern, 30,000-amp cells.

Installation of the new cells, the last series of which was put into operation on June 30, was preceded earlier this year by the installation of modern caustic evaporating and brine treatment facilities. The total program cost $6,000,000.

In addition to providing increased output of chlorine, caustic soda, and hydrogen, the new cells will afford considerably greater operating economies.

### Leasing Plan for Scientific Instruments Announced by RCA

A broad-scale leasing plan, under which educational institutions, laboratories, and other users may rent scientific instruments, has been announced by the Radio Corp. of America.

The plan is expected to make such RCA scientific aids as the electron microscope available to an increased number of organizations, regardless of size.

"One of the plan's more significant benefits will be in the educational field. Schools and colleges depending on funds available on a year-to-year grant basis now will be able to incorporate electron microscope and x-ray diffraction equipment into their research and training programs," according to an RCA spokesman.

## Announcements from Publishers

"Gmelins Handbuch der Anorganischen Chemie, 8th Edition." Systems: 29—Strontium, 306 pages; 30—Barium, 572 pages; 33—Cadmium, 802 pages. Published by Verlag Chemie, GmbH., Weinheim/Bergstrasse, West Germany, 1960.

All three of these volumes are organized in the familiar Gmelin fashion, and all have the extremely useful English-German table of contents, together with the marginal translation of paragraph titles. Also, the inside back covers have a paragraph, in English, giving directions for use of the classification system. Even for the student, information on any particular topic is accessible almost instantly.

The volume on Strontium covers the period 1931-1949, with individual references as late as 1953. The Barium volume covers the period 1932-1949, with some references as late as 1957. This volume contains a new chapter on oxide-coated cathodes. It starts with a review of the subject and then goes into a discussion of forming oxide-coated cathodes, their activation, composition, temperature dependence, etc. The chapter ends with an alphabetical index of 334 patents which have been ab-

**PHYSICAL CHEMISTS**

**ELECTRO-CHEMISTS**

**CHEMICAL ENGINEERS**

Important research positions are available in the Electrochemistry Laboratory at Lockheed Missiles and Space Division, located 40 miles south of San Francisco.

The laboratory is engaged in the field of electrochemical energy conversion such as fuel cell systems, and requires outstanding personnel qualified by extensive experience or academic background in the following areas:

**CHEMICAL ENGINEERS**
PROCESS & EQUIPMENT DESIGN
MASS TRANSFER
PILOT OPERATIONS

**CHEMISTS**
SOLID STATE CHEMISTRY
SURFACE CHEMISTRY
HETEROGENEOUS KINETICS
CATALYSIS
ELECTROCHEMISTRY
PHOTOCHEMISTRY

These positions provide an excellent opportunity in a young and growing new technology with an assured future. If you are experienced in work related to the above areas, you are invited to write: Research and Development Staff, Dept. J-26, 962 W. El Camino Real, Sunnyvale, Calif. U.S. citizenship or existing Department of Defense industrial security clearance required.

**Lockheed**
**MISSILES AND SPACE DIVISION**

Sunnyvale, Palo Alto,
Van Nuys, Santa Cruz,
Santa Maria, California
Cape Canaveral, Florida
Hawaii

stracted to give the practical information contained in the chapter. The Cadmium volume covers the period 1925-1949, with references up to 1958 on the topic of the cadmium-nickel battery. ECS members will be especially interested in a 127-page section on the electrochemical behavior of cadmium, 18 pages of which are on the Weston cell, 6 pages on the nickel-cadmium cell, 38 pages on electrolytic deposition of cadmium, and 9 pages on the polarography of cadmium. There also is an 80-page section on addition compounds and complexes of cadmium with neutral ligands. This is arranged systematically, according to ligand, and is followed by a formula index of the compounds formed and an alphabetical index of the ligands.

"Instability Constants of Complex Compounds," by K. B. Yatsimirskii and V. P. Vasil'ev. Published by Consultants Bureau Enterprises, Inc., 227 W. 17 St., New York 11, N. Y., 1960. Clothbound, 214 pages; $6.75.

This translation from the Russian presents the instability constants of 1381 complex compounds, and provides complete literary references through 1956.

"An Experimental Investigation on the Chemistry and Interconversion of Boron Hydrides," R. Schaeffer, Indiana University, for Wright Air Development Center, U. S. Air Force, July 1959. Report PB 161479,* 51 pages; $1.50.

"Study of Ultra High Temperatures," A. V. Grosse and C. S. Stokes, Research Institute of Temple University, for Wright Air Development Center, U. S. Air Force, April 1959. Report PB 161460,* 26 pages; $1.00.

* Order from Office of Technical Services, U. S. Dept. of Commerce, Washington 25, D. C.

## Advertiser's Index


American Brass Company ..... 238C
General Motors Research Laboratories ..... 232C
Great Lakes Carbon Corp., Electrode Division ..... Cover 2
Lockheed Missiles & Space Division ..... 245C
Pratt & Whitney Aircraft ..... 244C
E. H. Sargent & Company ..... 236C
Stackpole Carbon Company ..... 233C
Sylvania Electric Products Inc. ..... 235C


## New Products

**Lightweight Mirrors for Space Telescope.** New lightweight mirrors of fused silica have been developed for use in missile, satellite, and airborne telescope systems. Corning Glass Works is producing mirror blanks made by an unusual sandwich construction that reduces size and weight of mounting and auxiliary equipment, vital considerations in aerospace telescopes.

The telescope mirror blanks are made at Corning's Fused Silica plant, Bradford, Pa., and are marketed by the company's Optical Sales Dept., Corning, N. Y.

**Trimmer Capacitors for Printed Circuits.** Miniature trimmer capacitors, introduced this spring by Corning Electric Components, a department of Corning Glass Works, Bradford, Pa., for panel mounting, are now being made also for printed circuit mounting; they are trademarked Corning Mini-Trimmers. Fixed cavity tuning with an 0-80 nontraversing screw is smooth and linear; change in capacitance is 0.4 $\mu\mu$f per turn.

**Pyroceram Cement 89.** A new glass-ceramic cement for the electronics industry has been developed by Corning Glass Works to seal glasses and other materials with thermal expansions between 80 and 92 x $10^{-7}$ cm/cm°C. The new cement fires at approximately 450°C. The resulting seal is serviceable up to about 425°C.

Additional information can be obtained from Corning's Industrial Bulb or Receiver Bulb Sales Depts., both in Corning, N. Y.

**Entek CU-56,** a rinse-water additive which inhibits corrosion of copper and brass, has been introduced by Enthone, Inc., of New Haven, Conn. The product produces an invisible film which prevents tarnishing, staining, spotting-out, green salt formation, pit corrosion, and finger marking of copper and its alloys. It is designed to preserve freshly plated or cleaned metal surfaces during storage.

Literature on Entek CU-56 is available from the manufacturer.

## Employment Situations

### Positions Available

**Research Chemist**—Research Associate for American Electroplaters' Society Research Project No. 19, Galvanic Effects Associated with Coating Failure. To work at the National Bureau of Standards in Washington, D. C. Post-graduate work or research experience required. Reply to Fielding Ogburn, National Bureau of Standards, Washington 25, D. C.

**Research Chemists**—Research and development group seeks chemist or chemical physicist for solid-state work on cathodoluminescent and electroluminescent materials, photoconductors, and chemicals for electronic applications. Candidates should have Ph.D. or equivalent and be capable of independent work. Modern and well-equipped laboratories in Northeastern Pennsylvania. Publication of work encouraged.

Send résumé to: Dr. J. S. Smith, Manager of Chemical Research and Development, Chemical and Metallurgical Division, Sylvania Electric Products Inc., Towanda, Pa.

**Four challenging research positions** for experienced surface chemists, in fully-equipped laboratory devoted to research and development on aluminum and copper alloys, involving: A. Electrochemical kinetics, adsorption, and oxide film structure investigations related to finishing processes. B. Studies of interfacial surface reactions between polymeric resins and metal oxide surfaces relating to strength and permanence of joints in the adhesive bonding of metals. C. Mechanisms relating to surface phenomena, associated with liquid metal-solid metal inter-action as applied to soldering and brazing. D. Surface and electrochemical reactions effecting the kinetics of general, localized, and stress corrosion processes. Pleasant living, with access to major university. Interviews may be arranged for October ECS meeting in Houston, Texas. Send reply to R. H. Endriss, Personnel Manager, Olin Mathieson Chemical Corp., 125 Munson St., New Haven, Conn.

### Position Wanted

**Chemical Engineer, B.S.**—Thirteen years of electrolytic background in development and production work. Supervisory experience. Desires responsible position in either process engineering or production. *Reply to Box No. 370, c/o The Electrochemical Society, 1860 Broadway, New York 23, N. Y.*

# The Electrochemical Society

**Patron Members**

Aluminum Co. of Canada, Ltd., Montreal, Que., Canada

International Nickel Co., Inc., New York, N. Y.

Olin Mathieson Chemical Corp., Niagara Falls, N. Y.
- Industrial Chemicals Div., Research and Development Dept.

Union Carbide Corp.
Divisions:
- Union Carbide Metals Co., New York, N. Y.
- National Carbon Co., New York, N. Y.

Westinghouse Electric Corp., Pittsburgh, Pa.

**Sustaining Members**

Air Reduction Co., Inc., New York, N. Y.

Ajax Electro Metallurgical Corp., Philadelphia, Pa.

Allen-Bradley Co., Milwaukee, Wis.

Allied Chemical & Dye Corp.
- General Chemical Div., Morristown, N. J.
- Solvay Process Div., Syracuse, N. Y. (3 memberships)

Allied Research Products, Inc., Detroit, Mich.

Alloy Steel Products Co., Inc., Linden, N. J.

Aluminum Co. of America, New Kensington, Pa.

American Metal Climax, Inc., New York, N. Y.

American Potash & Chemical Corp., Los Angeles, Calif. (2 memberships)

American Smelting and Refining Co., South Plainfield, N. J.

American Zinc Co. of Illinois, East St. Louis, Ill.

American Zinc, Lead & Smelting Co., St. Louis, Mo.

American Zinc Oxide Co., Columbus, Ohio

M. Ames Chemical Works, Inc., Glens Falls, N. Y.

Basic Inc., Maple Grove, Ohio

Bell Telephone Laboratories, Inc., New York, N. Y. (2 memberships)

Bethlehem Steel Co., Bethlehem, Pa. (2 memberships)

Boeing Airplane Co., Seattle, Wash.

Burgess Battery Co., Freeport, Ill. (4 memberships)

Canadian Industries Ltd., Montreal, Que., Canada

Carborundum Co., Niagara Falls, N. Y.

Catalyst Research Corp., Baltimore, Md.

Ciba Pharmaceutical Products, Inc., Summit, N. J.

Columbian Carbon Co., New York, N. Y.

Columbia-Southern Chemical Corp., Pittsburgh, Pa.

Consolidated Mining & Smelting Co. of Canada, Ltd., Trail, B. C., Canada (2 memberships)

Continental Can Co., Inc., Chicago, Ill.

Cooper Metallurgical Associates, Cleveland, Ohio

Corning Glass Works, Corning, N. Y.

Diamond Alkali Co., Painesville, Ohio (2 memberships)

Dow Chemical Co., Midland, Mich.

Wilbur B. Driver Co., Newark, N. J. (2 memberships)

E. I. du Pont de Nemours & Co., Inc., Wilmington, Del.

Eagle-Picher Co., Chemical Div., Joplin, Mo.

Eastman Kodak Co., Rochester, N. Y.

Thomas A. Edison Research Laboratory, Div. of McGraw-Edison Co., West Orange, N. J.

Electric Auto-Lite Co., Toledo, Ohio
- C & D Division, Conshohocken, Pa.

Electric Storage Battery Co., Yardley, Pa.

Englehard Industries, Inc., Newark, N. J. (2 memberships)

The Eppley Laboratory, Inc., Newport, R. I. (2 memberships)

Erie Resistor Corp., Erie, Pa.

Exmet Corp., Tuckahoe, N. Y.

Fairchild Semiconductor Corp., Palo Alto, Calif.

Food Machinery & Chemical Corp.
- Becco Chemical Div., Buffalo, N. Y.
- Westvaco Chlor-Alkali Div., South Charleston, W. Va.

Foote Mineral Co., Paoli, Pa.

Ford Motor Co., Dearborn, Mich.

General Electric Co., Schenectady, N. Y.
- Chemistry & Chemical Engineering Component, General Engineering Laboratory
- Chemistry Research Dept.
- General Physics Research Dept.
- Metallurgy & Ceramics Research Dept.
- Aircraft Accessory Turbine Dept., West Lynn, Mass.

General Instrument Corp., Newark, N. J.

## (Sustaining Members cont'd)

General Motors Corp.
Delco-Remy Div., Anderson, Ind.
Guide Lamp Div., Anderson, Ind.
Research Laboratories Div., Detroit, Mich.
General Transistor Corp., Jamaica, N. Y.
Gillette Safety Razor Co., Boston, Mass.
Globe-Union, Inc., Milwaukee, Wis.
Gould-National Batteries, Inc.,
Minneapolis, Minn.
Grace Electronic Chemicals, Inc.,
Baltimore, Md.
Great Lakes Carbon Corp., New York, N. Y.
Hanson-Van Winkle-Munning Co.,
Matawan, N. J. (2 memberships)
Harshaw Chemical Co., Cleveland, Ohio
(2 memberships)
Hercules Powder Co., Wilmington, Del.
Hill Cross Co., Inc., New York, N. Y.
Hoffman Electronics Corp., El Monte, Calif.
Hooker Chemical Corp., Niagara
Falls, N. Y. (3 memberships)
Hughes Aircraft Co., Culver City, Calif.
Industro Transistor Corp.,
Long Island City, N. Y.
International Business Machines Corp.,
Poughkeepsie, N. Y.
International Minerals & Chemical
Corp., Skokie, Ill.
ITT Laboratories, Nutley, N. J.
Jones & Laughlin Steel Corp.,
Pittsburgh, Pa.
K. W. Battery Co., Skokie, Ill.
Kaiser Aluminum & Chemical Corp.
Div. of Chemical Research,
Permanente, Calif.
Div. of Metallurgical Research,
Spokane, Wash.
Kennecott Copper Corp., New York, N. Y.
Keokuk Electro-Metals Co., Keokuk, Iowa
Libbey-Owens-Ford Glass Co., Toledo, Ohio
M. & C. Nuclear, Inc., Attleboro, Mass.
Mallinckrodt Chemical Works, St. Louis, Mo.
P. R. Mallory & Co., Indianapolis, Ind.
McGean Chemical Co., Cleveland, Ohio
Merck & Co., Inc., Rahway, N. J.
Metal & Thermit Corp., Detroit, Mich.
Minnesota Mining & Manufacturing Co.,
St. Paul, Minn.
Monsanto Chemical Co., St. Louis, Mo.
Motorola, Inc., Chicago, Ill.
National Cash Register Co., Dayton, Ohio
National Lead Co., New York, N. Y.
National Research Corp., Cambridge, Mass.
National Steel Corp., Weirton, W. Va.
New York Air Brake Co., Kinney Vacuum
Div., Boston, Mass.
Northern Electric Co., Montreal, Que.,
Canada
Norton Co., Worcester, Mass.
Olin Mathieson Chemical Corp.,
Research & Engineering Operations,
Energy Div., New Haven, Conn.
Ovitron Corp., Long Island City, N. Y.
Peerless Roll Leaf Co., Inc., Union City, N. J.
Pennsalt Chemicals Corp.,
Philadelphia, Pa.
Phelps Dodge Refining Corp., Maspeth, N. Y.
Philco Corp., Philadelphia, Pa.
Philips Laboratories, Inc., Irvington-on-
Hudson, N. Y.
Pittsburgh Metallurgical Co., Inc.,
Niagara Falls, N. Y.
Poor & Co., Promat Div., Waukegan, Ill.
Potash Co. of America,
Carlsbad, N. Mex.
Radio Corp. of America
Tube Div., Harrison, N. J.
RCA Victor Record Div., Indianapolis,
Ind.
Ray-O-Vac Co., Madison, Wis.
Raytheon Manufacturing Co.,
Waltham, Mass.
Reynolds Metals Co., Richmond, Va.
(2 memberships)
Rheem Semiconductor Corp.,
Mountain View, Calif.
Schering Corporation, Bloomfield, N. J.
Shawinigan Chemicals Ltd., Montreal, Que.,
Canada
Speer Carbon Co.
International Graphite & Electrode
Div., St. Marys, Pa. (2 memberships)
Sprague Electric Co., North Adams, Mass.
Stackpole Carbon Co., St. Marys, Pa.
Stauffer Chemical Co., New York, N. Y.
Sumner Chemical Co., Div. of
Miles Laboratories, Inc., Elkhart, Ind.
Sylvania Electric Products Inc., Bayside,
N. Y. (2 memberships)
Tennessee Products & Chemical Corp.,
Nashville, Tenn.
Texas Instruments, Inc., Dallas, Texas
Three Point Four Corp., Yonkers, N. Y.
Titanium Metals Corp. of America,
Henderson, Nev.
Tung-Sol Electric Inc.,
Newark, N. J.
Udylite Corp., Detroit, Mich.
(4 memberships)
Universal-Cyclops Steel Corp.,
Bridgeville, Pa.
Upjohn Co., Kalamazoo, Mich.
Victor Chemical Works, Chicago, Ill.
Western Electric Co., Inc., Chicago, Ill.
Wyandotte Chemicals Corp.,
Wyandotte, Mich.
Yardney Electric Corp., New York, N. Y.